Hydrodynamic Modeling of Effects of Flow Reduction on Salinity and Thermal Habitats in the Homosassa River

XinJian Chen, Ph.D., P.E

Southwest Florida Water Management District

7601 US 301 North
Tampa, Florida 33637

May 2019

(Final Draft)

Table of Contents

Summary

The Homosassa River is a spring-fed estuary located in Citrus County, on the Gulf coast of central Florida. The river is about 13 kilometers (8 miles) long, from its headwaters, the Homosassa Springs, to the Gulf of Mexico, and receives a small amount of freshwater runoff from its 145 square kilometers of watershed. Most of the hydrologic loading to the Homosassa River comes from its 700 square kilometer springshed, in forms of submarine groundwater discharges (SGDs) mainly from Homosassa Springs, SE Fork, and Halls River.

In order to evaluate minimum flows and levels (MFLs) for this relatively small and narrow estuarine system, a laterally averaged hydrodynamic model has been applied to study how reductions of SGD would affect salinity and thermal conditions and transport time scales in the Homosassa River. The hydrodynamic model, named LAMFE, is a flux-based finite difference model that uses z-level in the vertical direction and fits bottom elevation with a cut-cell method. It is a semi-implicit model that uses a free-surface correction method, a very efficient numerical scheme that is unconditionally stable with respect to gravity waves, wind and bottom shear stresses, and vertical eddy viscosity terms. The LAMFE model is especially effective in simulating hydrodynamics in narrow and meandering rivers or estuaries such as the Homosassa River.

The simulation domain extends from the mouth of the Homosassa River to the Southeast Fork of the Homosassa River, with the actual longitudinal length of 13.11 kilometers for the main stem. All major branches of the Homosassa River were included in the simulation domain. The model was driven by measured real-time data of water elevation, salinity, and temperature at its mouth, measured meteorological data in the region, and measured and estimated SGDs entering the estuarine system. Based on the availability of these data at the time when the model was developed, the LAMFE model for the Homosassa River was calibrated and verified against real-time water elevations, salinities, and temperatures measured at three locations within the simulation domain during 11/4/2014 – 8/31/2017. The period prior to 6/1/2016 was for model calibration, while the period between 6/1/2016 – 8/31/2017 was for model verification.

Following calibration and verification of the LAMFE model for the Homosassa River, the model was used to simulate hydrodynamics, salinity transport, and thermal dynamics in the estuary for over 10 years, from October 9, 2007 to March 12, 2018, to evaluate effects of the SGD reduction to salinity and thermal habitats in the river. Impacts of the existing groundwater withdrawal were estimated to cause roughly 1.85% SGD reductions, based on a groundwater modeling effort. As such, the baseline flow scenario was determined to be 1/(1-0.0185) times of the existing flow condition. A series of model runs were conducted to simulate salinity and temperature in the estuary for various flow reductions from the baseline flow scenario, including 2.5%, 5%, 7.5%, 10%, …, 27.5%, and 30% reductions. Simulated salinity results were post-processed, with water volumes, bottom areas, and shoreline lengths for salinities less than or equal to 1, 2, 3, 5, 10, 15 psu being calculated based on known bathymetry. For temperature, water

volumes and surface areas for temperature ≤ 15 ºC, 15 – 20 ºC, and ≥ 20 ºC were calculated. Manatees and Common Snook (*Centropomus undecimalis*) are the primary animals to be considered in the thermal analysis. Because an adult manatee needs up to 3.8 ft (1.158 m) of a water layer to be totally submerged in, water volume and surface area of 15 – 20 ºC and ≥ 20 ºC with a constraint of a minimum of 1.158 m of water layer were also calculated.

Salinity habitats (water volumes, bottom areas and shoreline lengths for ≤ 1, 2, 3, 5, 10, 15 psu) and thermal habitats (water volume and surface area for ≤ 15 ºC, 15 ºC – 20 ºC, and ≥ 20 ºC) for various flow reduction scenarios were analyzed to obtain allowable flow reduction percentages based on a criterion that favorable salinity and/or thermal habitats should not suffer a loss of 15% or more from their baseline conditions. The most sensitive salinity habitat to flow reduction is ≤ 2 psu bottom area, which will be reduced by 15% with a 11.09% SGD reduction. The most sensitive manatee thermal habitat to the flow reduction is the 4-hour average of ≥ 15 ºC surface area, which can be reduced by 15% with a 6.44% reduction of SGD when the thermal habitat under the acute condition is low. For Common Snook, the most sensitive thermal habitat is the single cold day average of ≥ 15 ºC surface area, which can be reduced 15% with a 5.03% SGD reduction. Based on model results of the scenario simulations, the MFL for the Homosassa River was proposed to be 95% of the baseline flow condition, or a maximum of 5% reduction from the baseline condition.

The proposed MFL was evaluated for sea level rises in 2035. Three SLRs at the mouth of the Homosassa River were estimated based on data obtained at the NOAA St. Petersburg and Cedar Key stations from the USACE web site http://www.corpsclimate.us/ccaceslcurves.cfm. Estimated low, intermediate, and high SLRs that could occur during 2012 – 2035 were 4.741, 8.588, and 20.990 cm, respectively. These SLRs were added to the mouth of the Homosassa River, Salt River, and Mason Creek to drive the hydrodynamic model in simulating the baseline flow and the MFL conditions. Habitat reductions caused by the proposed MFL with a SLR relative to those for the baseline flow condition with the same SLR were calculated and analyzed. Model results suggest that a sea level rise could significantly change salinity and thermal characteristics in the Homosassa River. Although the proposed MFL does not cross the threshold for salinity habitats and manatee thermal habitats when the three SLRs are concerned, it could cause thermal habitats for Common Snook to be reduced by more than 15% when any one of the three SLRs occurs.

1. Introduction

The Homosassa River is a spring-fed estuary located in Citrus County, on the Gulf coast of central Florida (Fig. 1). The river is about 8 miles long from its headspring to the Gulf of Mexico, and receives an insignificant amount of freshwater runoff from its 145 square kilometers of watershed. Most of the hydrologic loading to the Homosassa River comes from its 699 square kilometer springshed, in forms of submarine groundwater discharges out of numerous spring vents in its headspring area and in several of its tributaries.

Like some other estuaries along the Gulf coast of Florida, the Homosassa River estuary is generally well or partially mixed. The system is ecologically important for many marine species, including Florida manatees (*Trichechus manatus latirostris*) and Common Snook (*Centropomus undecimalis*), which use the spring-fed estuaries as thermal refuges in winters because a large amount of spring water with a relatively constant temperature of 22.0 ºC or higher flows to the river. In order to protect this ecologically valuable springs/estuarine system, a regulatory minimum spring water flow rate was established in 2013. The adoption of the MFL rule for the Homosassa River in 2013 required that the MFL is to be re-evaluated in 2019.

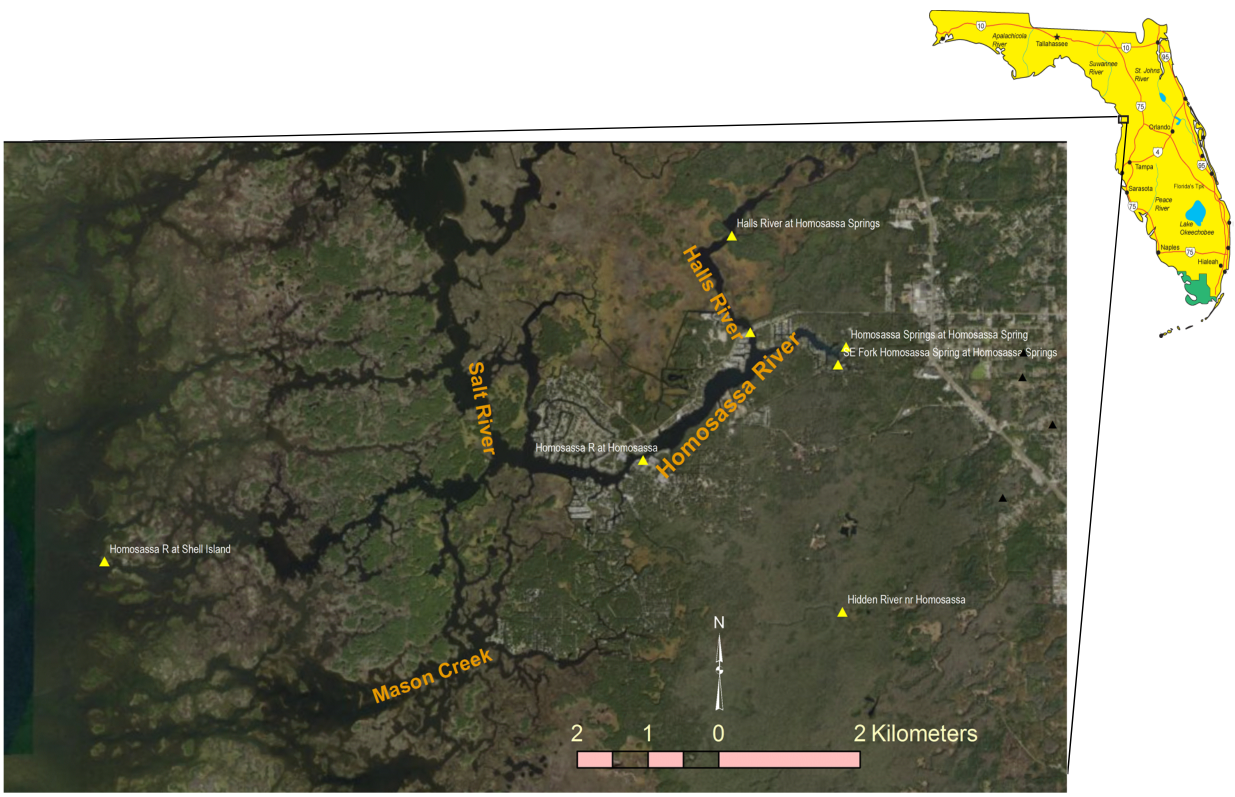

Figure 1. Aerial view of the Homosassa River on the Gulf coast of Florida. Triangles mark locations of USGS real-time data stations along the river.

The objective of this modeling study is to support the MFL re-evaluation for the Homosassa River. For this purpose, efforts have been made to improve model simulations for circulations, salinity transport processes, and thermal transport processes in the estuary. Improvement of the current modeling study over the previous one includes: the use of a more suitable hydrodynamic model for the river than that used in the 2013 MFL establishment, a much longer calibration/verification period, more recent flow data, and a much longer simulation period for scenario runs.

In 2011, HSW Engineering, Inc. applied the Environmental Fluid Dynamics Code (EFDC), originally developed by Hamrick (1992) to the Homosassa River, with the downstream area of the river being expanded and deepened to form a funnel to artificially force salt wedge to migrate upstream (HSW, 2011). Because the Homosassa River is a narrow and meandering estuary, its circulation pattern and salinity and temperature distributions are normally vertically two-dimensional, which is typical for narrow estuaries (Prandle, 1985; Jay and Smith, 1990; Chen, 2004a). Therefore, the most suitable hydrodynamic model for the Homosassa River is the Laterally Averaged Model for Estuaries, or LAMFE, developed by the author. The LAMFE model has been used in several previous MFL studies and has been extensively reviewed by numerous external experts over the last two decades. Examples of the LAMFE model application in the MFL evaluation include the lower Hillsborough River (Chen 1997; Chen, 1999; and Chen, 2004a), the lower Alafia River (Chen, 2005; Flannery et al., 2007), the lower Peace and Myakka Rivers (Chen, 2007a; Chen, 2008a; and Chen, 2010), and the lower Manatee/Braden Rivers (Chen, 2012a). Numerous peer-reviewed, LAMFE-related papers have been published in reputable journals (e.g., Chen, et al., 2000; Chen, 2003a; Chen, 2004b; Chen, 2004c; Chen, 2007b; Chen, 2007c; Chen, 2008b; Chen, 2012b) and international conference proceedings (e.g., Chen and Flannery, 1997; Chen, 2003b; Chen, 2006; Chen, 2008c; Chen, 2012c). Some of these peer-reviewed papers include validations of the LAMFE code. A user manual of the LAMFE model is also available (Chen, 2011) and contains all the details of testing of the LAMFE code.

As mentioned in Chen (2017), most previous coastal and estuarine hydrodynamic modeling studies did not consider effects of SGDs (Johnson et al, 1991; Blumberg and Kim, 2000), partly because SGDs are much lower than river flows and precipitations for these estuaries and partly because SGDs are very difficult to quantify in many cases. There are only very limited estuarine and coastal hydrodynamic modeling studies which considered SGDs. Ganju et al. (2011) applied the 3D model ROMS (Warner et al., 2008) to West Falmouth Harbor, Massachusetts to verify their tidal and groundwater flux estimates to the estuary based on velocity and salinity measurements. Chen (2017) estimated and considered SGDs in the hydrodynamic simulations for Crystal River/Kings Bay using the 3D model UnLESS3D for the MFL evaluation of the estuarine system.

Because SGDs constitute a majority of the hydrologic loading to the Homosassa River, a good quantification of SGDs for the estuarine system is important for a successful simulation of the Homosassa River. Although there are much more flow data available for the estuary now than several years ago when the previous MFL evaluation was conducted, a high-quality dataset for all the SGDs to the spring-fed estuarine system still does not exist at this moment. As a result, some of the SGD data had to be estimated based on limited data available to this modeling study.

In the following, a discussion of the physical characteristics of the Homosassa River estuary is provided in Section 2, which also contains available field data collected in the estuary. Section 3 describes model setup and model calibration and verification, including comparisons of modeled water levels, salinities, and temperatures to measured real-time data, with a skill assessment of the model performance. Section 4 presents scenario simulations and analyses of model results of these scenario runs, while Section 5 considers effects of the sea level rise on the MFL evaluation results. Conclusions of this modeling effort for the MFL re-evaluation of the Homosassa River are summarized at the end of the report in Section 6.

2. Physical Characteristics of the Estuary and Field Data

2.1 Physical characteristics of the Homosassa River

The Homosassa River (Figure 1) is a short and narrow estuary, which originates in Citrus County and flows to the Gulf of Mexico. The river is about 13 km long, with a width varying from about 60 m in the upstream reach to about 305 m near the mouth (Yobbi and Knochemus, 1989). Based on available survey data, the mean depth of the Homosassa River is found to be about 1.55 meters.

Although the river has a watershed of about 145 square kilometers, most of the watershed is self-percolating and barely contributes any quantifiable surface water runoff. The majority of its hydrologic loading comes from spring flows out of numerous spring vents located in the headspring area and in several of its tributaries, mainly the SE Fork and the Halls River. Submarine groundwater discharges from these spring vents are from the Upper Floridan aquifer, with a contributing springshed estimated at about 700 square kilometers.

Figure 2 shows locations of the springs that discharge groundwater flows to the Homosassa River. The Homosassa Springs, and several other springs consist of the headwaters.

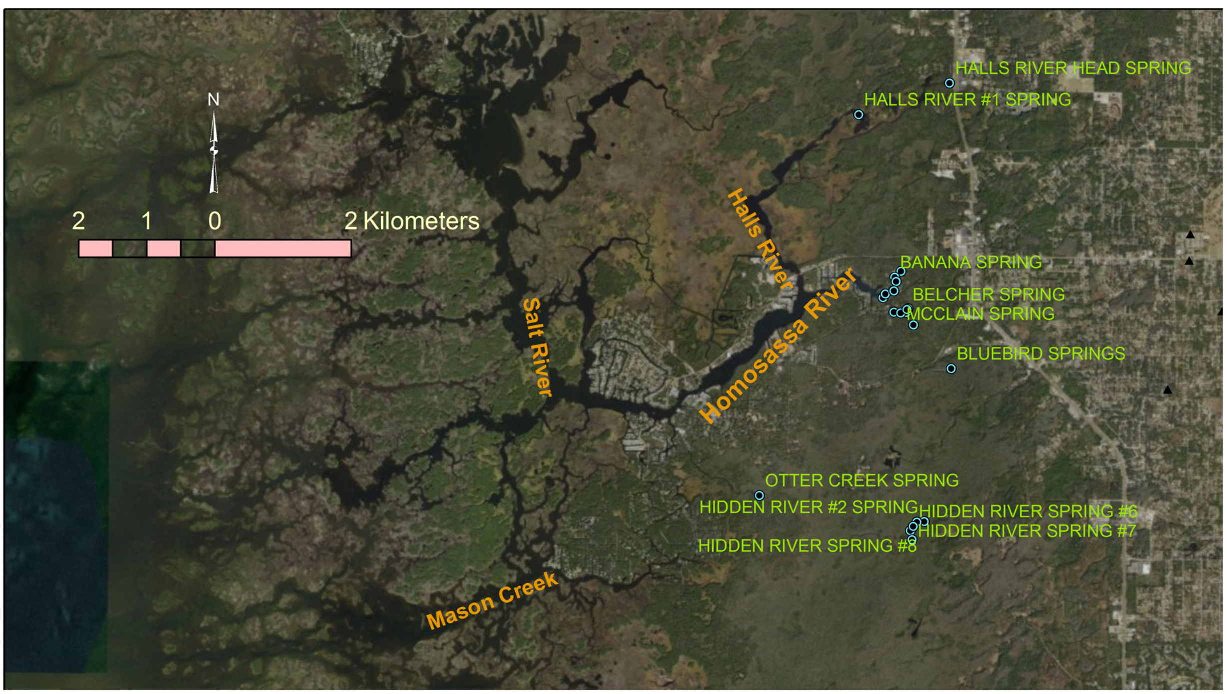

Figure 2. Spring locations of the Homosassa River estuarine system.

3.2 Field data

Available field data for the hydrodynamic modeling of the Homosassa River system using the LAMFE model included bathymetry survey and real-time data of water elevation, salinity (measured in the form of specific conductance), and/or temperature at United States Geological Survey (USGS) stations in the estuary. Bathymetry survey was conducted by the University of South Florida (Wang, 2007). Figure 3 is a plot of Homosassa River bathymetry directly from Wang (2007). In addition to the bathymetry survey, there are also Light Detection and Ranging (LIDAR) data available for the Homosassa River system in this study.

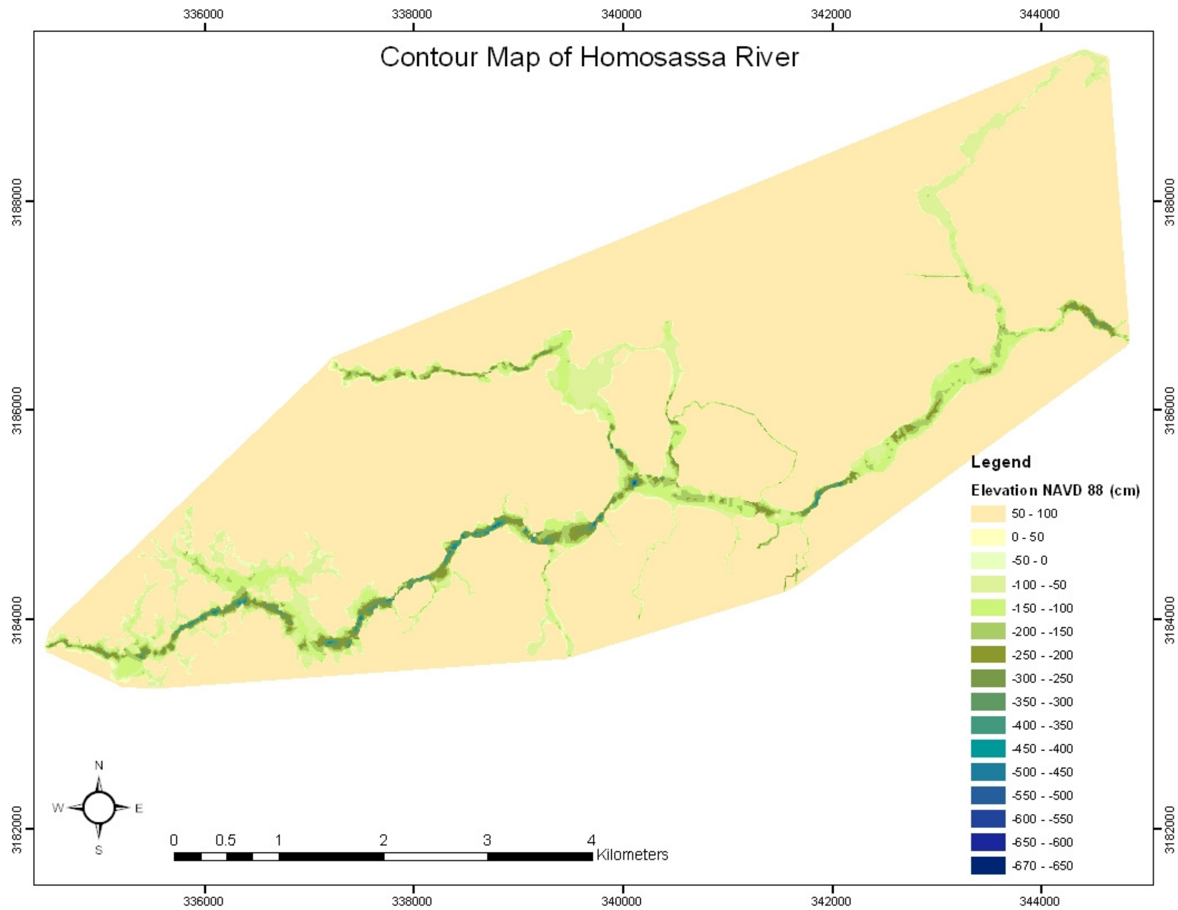

Figure 3. Bathymetry surveyed by Wang (2007) in the Homosassa River system

With funds provided by the Southwest Florida Water Management District (SWFWMD), the USGS collects and reports real-time data at seven stations in the Homosassa River system, showing with triangles in Figure 1. These USGS stations include: (1) Homosassa River at Shell Island near Homosassa (#02310712), (2) Homosassa River at Homosassa (#02310700), (3) Halls River near Homosassa (#02310690), (4) Halls River at Homosassa Springs (#02310689), (5) Homosassa Springs at Homosassa Springs (#02310678), (6) SE Fork Homosassa Spring at Homosassa Springs (#02310688), and (7) Hidden River near Homosassa (#02310675). Table 1 shows some general information about these USGS stations, including station name, station number, longitude, latitude, starting date of the data collection, datum, and sensor elevations for conductance and temperature. At the Hidden River near Homosassa station, no CTD (conductivity, temperature, depth) data were collected and only discharge data are available. CTD data at all other six stations were collected, with CTD sensor elevations being listed in the bottom row of Table 1. At the Homosassa River at Shell Island and Homosassa River at Homosassa stations, conductance and temperature were collected at multiple depths, while at other four CTD stations, conductance and temperature data were collected at only one depth.

Table 1. General information about the USGS data collection stations in the Homosassa River system.

Station Name	Homosassa River		Halls River		Homosassa Springs at Homosassa Springs	SE Fork Homosassa Spring	Hidden River near Homosassa
	at Shell Island	at Homosassa	near Homosassa	at Homosassa Springs			
Station #	02310712	02310700	02310690	02310689	02310678	02310688	02310675
Longitude	-82.69583	-82.61806	-82.60278	-82.60564	-82.58889	-82.59000	-82.58889
Latitude	28.77139	28.78500	28.80111	28.81311	28.79944	28.79722	28.76639
Available since	10/1/2007	10/1/2006	10/1/2007	3/9/2012	10/1/2007	10/1/2007	10/1/2007
Datum	NAVD88	1.49 ft, NGVD29	NAVD88	NAVD88	-2.99 ft, NAVD88	-0.62 ft, NAVD88	
Sensor Elevation (ft, NAVD88)	-0.5 -1.4 -4.8	-3.10 -6.00	-4.99	-2.58	-0.10	-2.62	

In addition to the discharge data at the Hidden River near Homosassa station, discharges are also available for the SE Fork Homosassa Spring, Homosassa Springs at Homosassa Springs, Halls River at Homosassa Springs, and Homosassa River at Homosassa stations. The discharge data for the Homosassa Springs were calculated from a regression equation, which relates the discharge with the water level at the site and the groundwater level measured in a well in Weeki Wachee. This regression equation was updated several times over the years. The most recent version takes the following form

$$Q_{hs} = 76.863 - 20.7636h + 5.3139W \tag{1}$$

where Q_{hs} (in cfs) is the flow rate for Homosassa Springs at Homosassa Springs, h is water level (feet, NGVD29) and W is Weeki Wachee well level (feet, NGVD29). This regression equation is valid from October 1, 2013 to present.

For the SE Fork discharge, the following USGS regression equation was used

$$Q_{se} = 18.6293 - 10.3114h - 418.139\Delta h + 3.31029W \tag{2}$$

where Q_{se} (in cfs) is the flow rate through the SE Fork Homosassa station, h is water level (feet, NGVD29), Δh is the water level change over the data collection interval (15 minutes), and W is Weeki Wachee well level (feet, NGVD29). This regression equation is valid for the period from October 1, 2001 to September 30, 2011. From October 1, 2011 on, the USGS started to provide discharge data calculated using index velocity ratings.

At the Homosassa River at Homosassa and Halls River at Homosassa Springs stations, no regression equations are available from the USGS. Discharges based on the index velocity method can be obtained from the USGS website, with the available periods of 10/1/2006 – present for Homosassa River at Homosassa and 3/10/2012 – present for Halls River at Homosassa Springs.

Figure 4 shows plots of available discharge data at all the stations in the Homosassa River system, including the Hidden River station (top panel), the SE Fork Homosassa Spring and Homosassa Springs at Homosassa Springs stations (middle panel), and then Halls River at Homosassa Spring and Homosassa River at Homosassa stations (bottom panel). As can be seen from the figure, most discharge data contain significant tidal signals, mainly due to the existence of tidal prisms upstream of these stations. The Homosassa River at Homosassa has the biggest upstream tidal prism, resulting in the biggest tidal flux varying between about -1,000 cfs to about 1,000 cfs. The Hidden River discharge has only insignificant tidal signals but has a large seasonal variability, which is especially obvious after 2012.

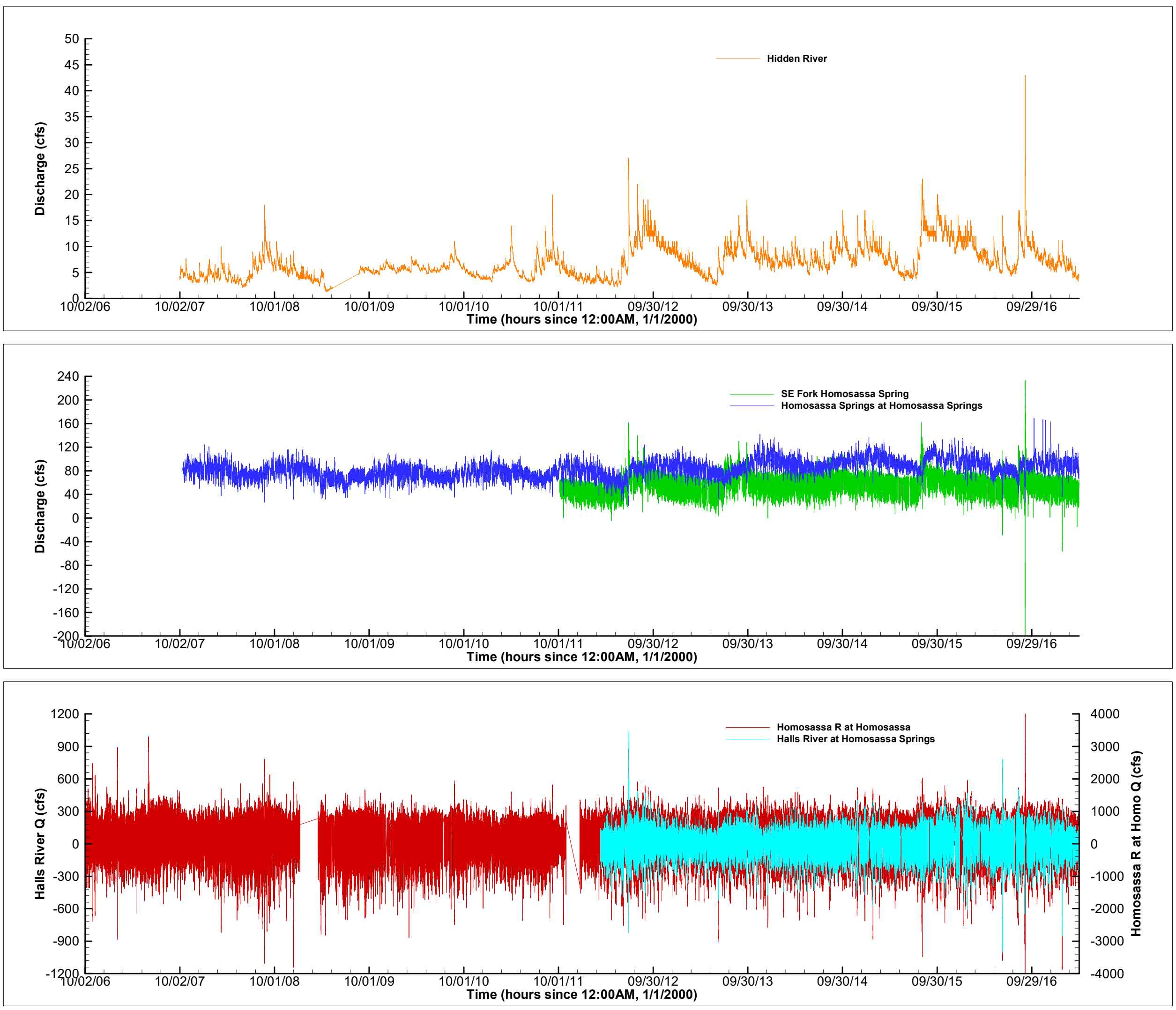

Figure 4. Available discharge data in the Homosassa River system since October 2, 2006.

The big positive/negative peaks shown in Figure 4 were during days of Hurricane Hermine in 2016. Hermine developed in the Florida Straits on August 28, 2016 and made landfall in the Florida Panhandle on September 2, 2016. Figure 5 shows discharge data during a 50-day period from 8/5/2016 to 9/24/2016. During the hurricane days, the SE Fork Homosassa Spring station had a negative discharge peak of more than 400 cfs, while the Homosassa River at Homosassa station had a negative discharge peak of almost 10, 000 cfs. There were unfortunately no discharge data available at the Halls River at Homosassa Springs and Homosassa Springs at Homosassa Springs stations during Hurricane Hermine. It is likely that discharges at these two stations had big negative peaks, too.

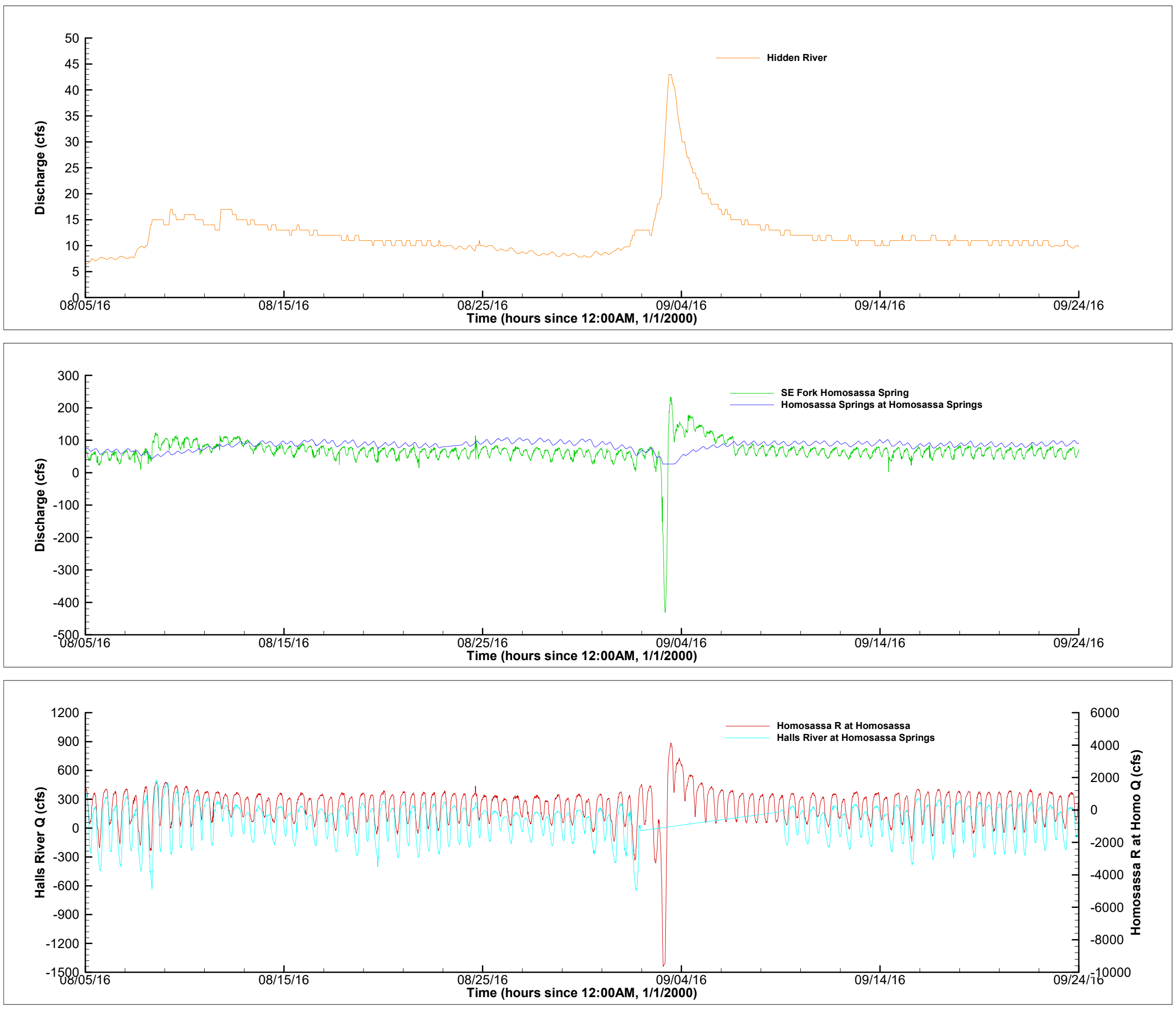

Figure 5. Discharge data in the Homosassa River system during a 50-day period from 8/5/2016 to 9/24/2016. Hurricane Hermine made landfall on September 2, 2016.

Because discharge gaged at the Homosassa River at Homosassa station includes those at the SE Fork Homosassa Spring, Homosassa Springs at Homosassa Springs, and Halls River at Homosassa Spring stations, it is meaningful to compare long-term averages of discharge at these stations to check if there is any ungaged flow upstream of the Homosassa River at Homosassa station. An analysis of discharge data shows that the average discharges during September 30, 2016 through March 13, 2018 were 177.09 cfs, 56.77 cfs, 90.90 cfs, and 30.58 cfs at the Homosassa River at Homosassa, SE Fork Homosassa Spring, Homosassa Springs at Homosassa Springs, and Halls River at Homosassa Springs stations, respectively. The three upstream stations had a total of 178.25 cfs, which was very close to the average discharge of 177.09 cfs at the Homosassa River at Homosassa station. This suggests that it is unlikely that there is not a significant ungaged flow upstream of the Homosassa River at Homosassa station.

Figure 6 shows measured water elevations at SE Fork Homosassa Spring (red lines), Homosassa Springs at Homosassa Springs (green lines), Halls River near Homosassa (blue dashed lines), Halls River at Homosassa Springs (gray dashed lines), Homosassa River at Homosassa (cyan lines), and Homosassa River at Shell Island during a 270-day period: 2/22/2015 – 5/23/2015 (top panel), 5/23/2015 – 8/21/2015 (middle panel) and 8/21/2015 – 11/19/2015 (bottom panel).

The top panel of Figure 7 shows measured salinities at the SE Fork Homosassa Spring (pink line), Homosassa Springs at Homosassa Springs (orange line), Halls River near Homosassa (blue line), and Halls River at Homosassa Springs (green line) stations during a 90-day period: 2/21/2015 – 5/21/2015. The middle panel in Figure 7 shows measured salinities at the top (orange line) and bottom (pink line) layers of the Homosassa River at Homosassa station during the same 90-day period. In the bottom panel of the figure, measured salinities at the top, middle, and bottom layers of the Homosassa River at Shell Island station are plotted with red, green, and blue lines, respectively. Figure 8 shows measured temperatures at the six USGS stations during the same 90-day period between 2/21/2015 and 5/21/2015 in the same format as that for salinity data shown Figure 7.

Graphics of time series plots of water elevation, salinity, and temperature at the six USGS stations for other time periods are similar and not presented here. These plots are included in Appendixes A – C. Although Figures 6 - 8 only show several months of real-time data measured in the Homosassa River, they display that tidal signals are evident in water level, salinity, and temperature in the estuarine system. The high-frequency tidal variability includes both diurnal and semi-diurnal variations. There are also some non-tidal, low frequency signals in the real-time data, which are mainly influenced by meteorological and hydrological characteristics of the region.

From Figure 6, it can be seen that tides lose their energy quite significantly as they propagate from the mouth of at the Homosassa River at Shell Island to the Homosassa River at Homosassa station. As tidal waves at the Homosassa River at Homosassa are less than half of that at the mouth, the tides lose more than 75% of their energy along the way. In the tidal reach upstream of the Homosassa River at Homosassa station, up to the headwaters of the river, the tidal energy attenuation becomes very small, as tidal waves attenuate only slightly while propagating further upstream.

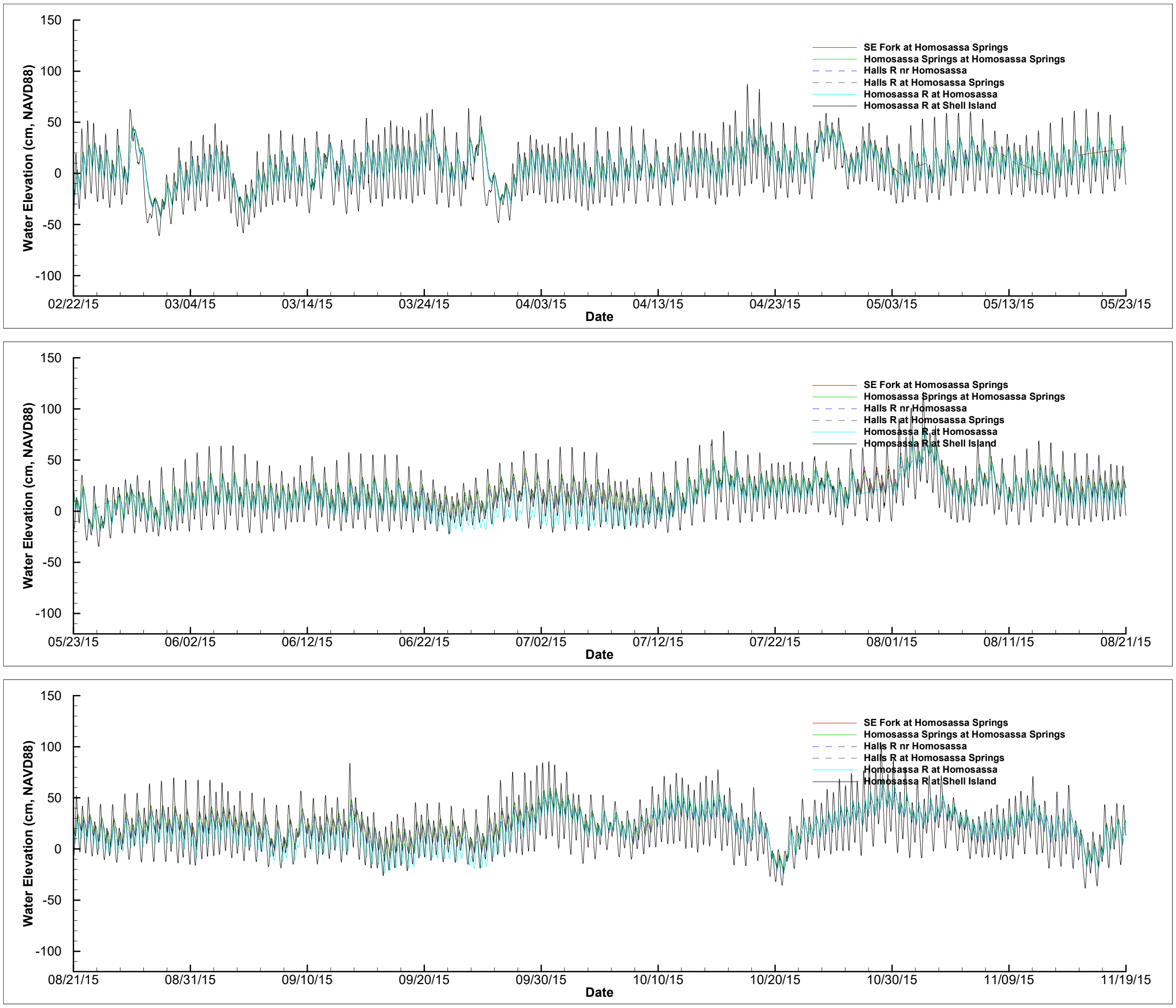

Figure 6. Measured water elevations at SE Fork Homosassa Spring (red lines), Homosassa Springs at Homosassa Springs (green lines), Halls River near Homosassa (blue dashed lines), Halls River at Homosassa Springs (gray dashed lines), Homosassa River at Homosassa (cyan lines), and Homosassa River at Shell Island during 2/22/2015 –11/19/2015.

One of the reasons for this phenomenon of different tidal energy losses is that the downstream reach is almost two times of the length of the upstream reach, causing the tidal energy to lose more in the downstream reach than in the upstream reach. Another reason is that the tidal currents in the downstream part are stronger than these in the upstream part of the estuary. Nevertheless, a major reason for the large tidal energy loss in the downstream reach may be caused by a few narrow segments in the downstream portion of the river, especially the one at around the half way between the Homosassa River at Shell Island and Homosassa River at Homosassa stations, which is about 2 km long and greatly restricts the passage of tidal energy through it.

Figure 7. Measured salinities at the SE Fork Homosassa Spring (top panel), Homosassa Springs at Homosassa Springs (top panel), Halls River near Homosassa (top panel), Halls River at Homosassa Springs (top panel), Homosassa River at Homosassa (middle panel), and Homosassa River at Shell Island (bottom panel) during a 90-day period between 2/22/2015 and 5/23/2015.

Figure 7 demonstrates a few important characteristics of salinity distribution in the Homosassa River system. Firstly, although the SE Fork Homosassa Spring station is only about 130 meters to the confluence with the Homosassa River, which is roughly the same distance to the Homosassa Springs at Homosassa Springs, salinity measured at the SE Fork is mostly fresh (< 0.5 psu), while salinity measured at the Homosassa Spring at Homosassa Springs is barely below 1 psu. This suggests that SGDs from SE Fork springs, including Belcher Spring, Trotter Springs, McClain Spring, and Pumphouse Spring are fresh and the occasional peaks up to less than 2 psu are caused by high tides. Under the normal condition, the freshwater-salt water interface moves back and forth around the SE Fork station, with its location being downstream of the station most of the time. As salinity at the SE Fork station comes from the estuarine part of the river, not from the SGD, it can be concluded that SGD gaged at the SE Fork is fresh. It is not expected that a reduction of SGD would cause any salinity increases in SGD.

Secondly, although the Halls River at Homosassa Springs station is located upstream of the Halls River near Homosassa station, salinity measured at the upstream station is about 2 psu higher than that measured at the downstream station. Obviously, SGD entering the upstream of the Halls River is brackish. The relatively flat salinity peaks suggest that the upstream SGD is a salinity source for the Halls River and salinity in the SGD is quite stable under various discharge conditions. The relatively lower salinity at the downstream station is caused by the relatively fresher SGDs from SE Fork and Homosassa headwaters, because the Halls River near Homosassa station is close to the confluence of the Halls River with the Homosassa River. The tidal currents transport relatively fresher water upstream to dilute the brackish SGD in the upstream portion of the Halls River. From Figure 7, it can be seen that the relatively flat salinity peaks generally varied at around 5 psu and it is possible that salinity in the upstream SGD of the Halls River is the same or slightly higher than that measured at the Halls River at Homosassa Springs station.

Thirdly, salinities measured at the Homosassa River at Homosassa do not correlate well with these measured at the mouth of the river. In addition to the fact that salinities measured at the Homosassa River at Homosassa station have relatively smaller variabilities than these measured at the mouth of the river do, a regression between salinities at the two stations has a R^2 of less than 0.5, even when various time leads/lags were considered. As can be seen in the bottom panel in Figure 7, there were 3 low salinity periods, each lasted only a couple of days, in measured salinities at the Homosassa River at Shell Island station during the first 45 days. However, these three low salinity periods were not evident at the Homosassa River at Homosassa station (middle panel of Fig. 7). On the other hand, there were a couple of high salinity periods with relatively strong tidal variations at around 12:00 AM, 4/22/2015 at the Homosassa River at Homosassa station but these tidal variations in the salinity data collected at the mouth of the river were relatively weak during the two periods. More discussions about correlating measured salinities at these two stations are provided in the next section.

In the 90-day period shown in Figure 8, the first couple of days were cold, with water temperature at the mouth dropping to 10 ºC or lower. The upstream area near Homosassa Springs and the SE Fork were warm with water temperature higher than 20 ºC during these cold days. Further downstream in the Homosassa River and in Halls River, the low water temperature was about 15 ºC, which was still roughly 5 ºC higher that at the river mouth for these cold days, mainly because of the warm SGDs flowing to the estuarine system. In early 2010, there were more than 10 consecutive days when the air temperature in the Homosassa region dropped to below 0 ºC every day. Unfortunately, no real-time temperature data are available for 2010 at the Homosassa River at Shell Island, Halls River near Homosassa, and Halls River at Homosassa Springs stations. Otherwise, one could exam water temperature data for all the six stations during these days to get a picture about the temperature distribution in the Homosassa River system during this extreme weather condition.

Figure 8. Measured temperatures at the SE Fork Homosassa Spring (top panel), Homosassa Springs at Homosassa Springs (top panel), Halls River near Homosassa (top panel), Halls River at Homosassa Springs (top panel), Homosassa River at Homosassa (middle panel), and Homosassa River at Shell Island (bottom panel) during 2/22/2015 – 5/23/2015.

As can be seen from Figure 2, the Salt River and Mason Creek at the downstream portion of the Homosassa River are two tributaries. To provide boundary conditions of salinity, temperature and water elevation in the Salt River and Mason Creek, CTD data were collected by SWFWMD in 2017 at two locations shown in Figure 9. Because of the limited time available, only a little more than 4 months of data during March – August were collected (VHB, 2017).

Figures 10 and 11 are plots of water level, salinity, and temperature data collected during March – August 2017 at the Salt River and Mason Creek stations, respectively. As can be seen from the figures, because the Mason Creek station was a little closer to the Gulf of Mexico than the Salt River station, tidal variations in Mason Creek are stronger that those in the Salt River. Although the Mason Creek at the data collection station is deeper than the Salt Creek station, the

Mason Creek has less salinity and temperature stratification. For a reason that yet to be verified, the Salt River receives certain amount of low salinity flow, which appears to come from a channel on its east connecting to Halls River. As a result, there is a significant salinity stratification at the Salt River station, which reduces the vertical mixing and causes temperature to be a little more stratified in Salt River than in Mason River too.

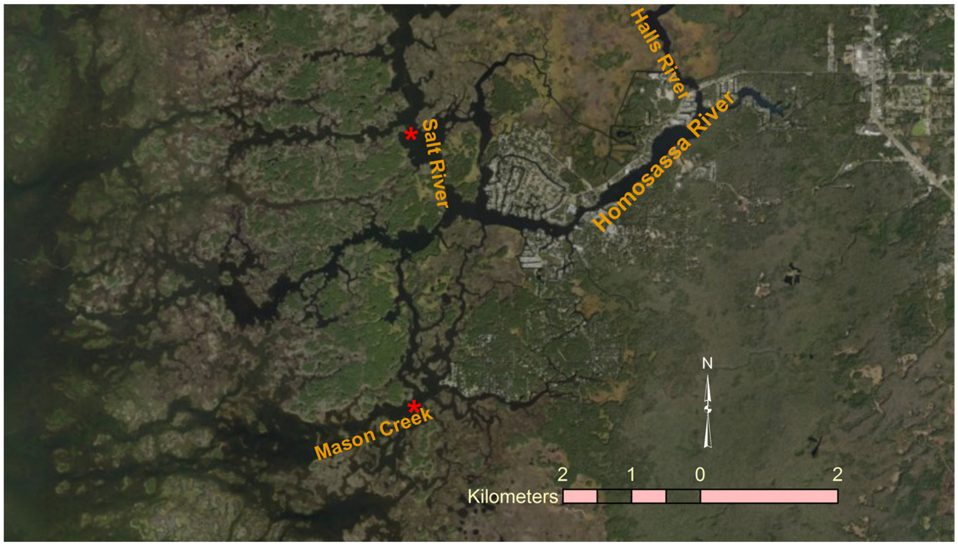

Figure 9. Locations of data collection in the Salt River and the Mason Creek in 2017.

Meteorological data (wind speed, wind direction, air temperature, air humidity, and solar radiation) used for this modeling study were hourly readings at a SWFWMD weather station near Inglis, Florida for days prior to 7/2/2013. For days since 7/2/2013, meteorological data collected with a 15-minute interval at a Florida Automated Weather Network (FAWN) station by the University of Florida's Institute of Food and Agricultural Science (UF/IFAS) were used. The Inglis station is about 16 miles north of the Homosassa River, while the FAWN station of UF/IFAS is located at the Lecanto High School, about 6 miles northeast of the Homosassa River.

Similar to the Crystal River/Kings Bay system (Chen, 2017), the climatology in the region has distinct winter and summer patterns. Winter is characterized by frequent frontal incursions and extratropical cyclones that can produce large shifts in wind speed and wind direction in response to rapidly changing atmospheric pressure and thermal gradients. In the summer, the weather is generally characterized by light and variable winds originating from the northeast trade wind circulation. Sea/land breezes are typical due to the strong differential heating of the land and adjacent waters along the coast during the summer months. Occasional tropical storms can move to the area during summer, causing a temporal but sometimes intense modification to the meteorological conditions of the region.

Figure 12 shows time series of vector plot of wind measured at 10 m above the ground at a FAWN station at the Lecanto High School during a 270-day period, from November 19, 2015 to August 15, 2016. Solar radiation, air temperature, and air humidity measured at the Lecanto High

School station during the same 270-day period are shown in Figure 13. Time series plots of these meteorological parameters for other time periods are available but not included in the report, because the temporal variabilities of wind, solar radiation, air temperature, and air humidity during other periods are mostly similar to those during the 270-day period displayed in Figures 12 and 13.

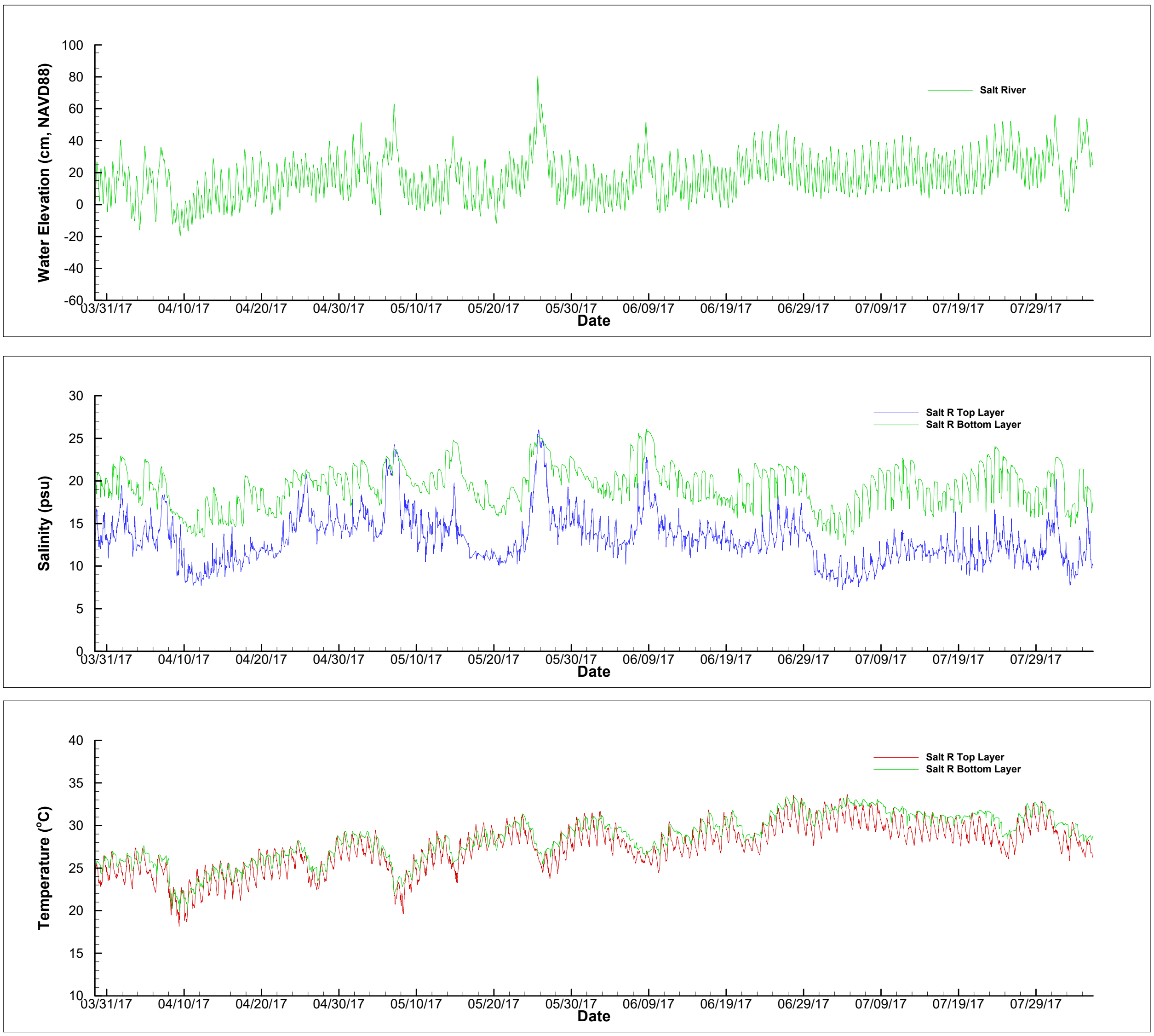

Figure 10. Measured water elevation (top panel), top- and bottom layer salinities (middle panel), and top- and bottom-layer temperatures (bottom panel) at the Salt River station in March – August 2017.

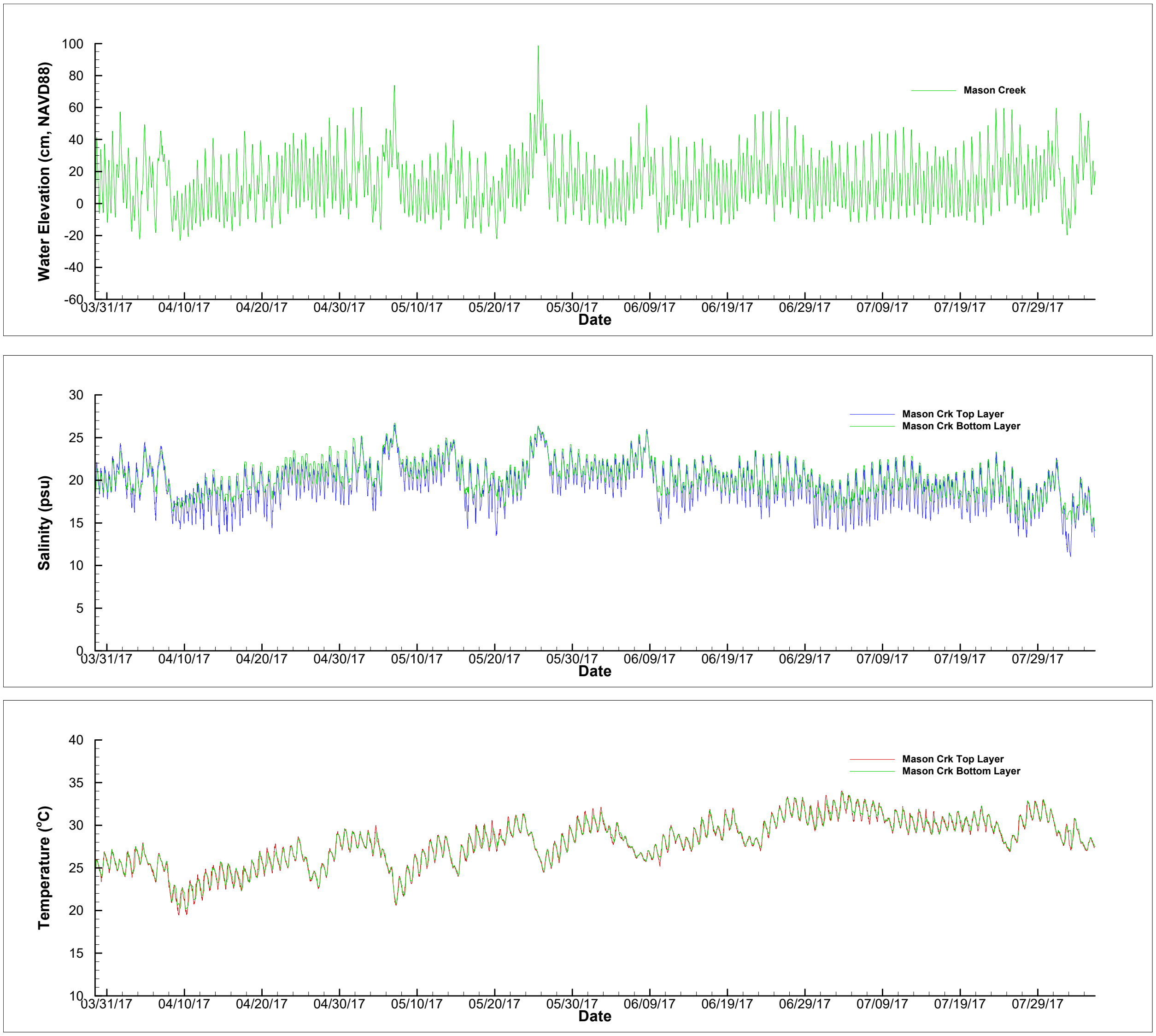

Figure 11. Measured water elevation (top panel), top- and bottom layer salinities (middle panel), and top- and bottom-layer temperatures (bottom panel) at the Mason Creek station in March – August 2017.

Overall, real-time data of water elevation, salinity, temperature, and discharge measured by the USGS and SWFWMD on the Homosassa River are of good quality, despite the fact that there are a few missing data periods and a number of problematic data points in the dataset. The meteorological data collected by the SWFWMD at the Inglis station and by the FAWN at the Lecanto High are good enough for a successful application of the LAMFE model to the Homosassa River.

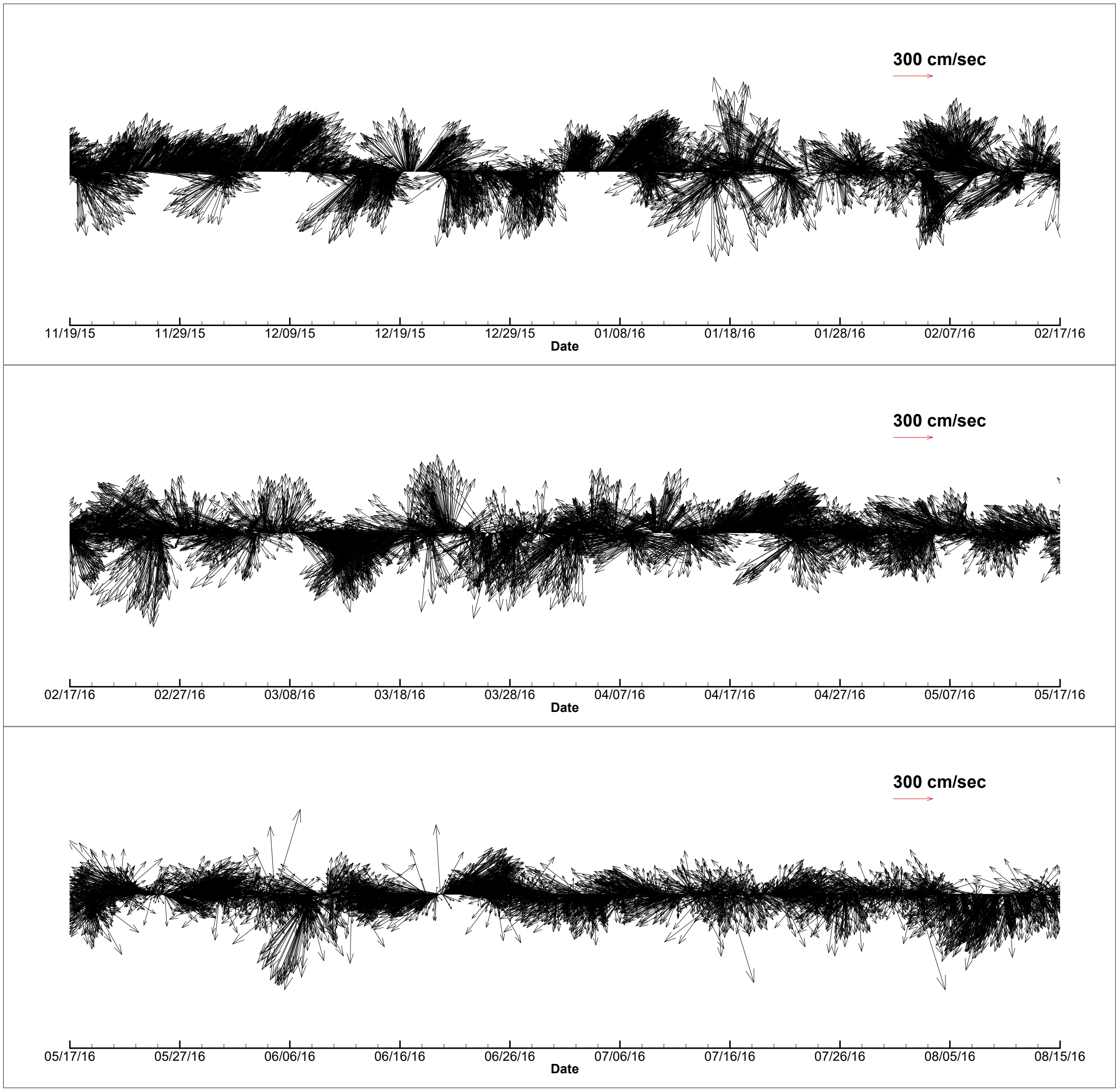

Figure 12 Vector plots of measure wind at a FAWN station at the Lecanto High School during 11/19/2015 – 8/15/2016.

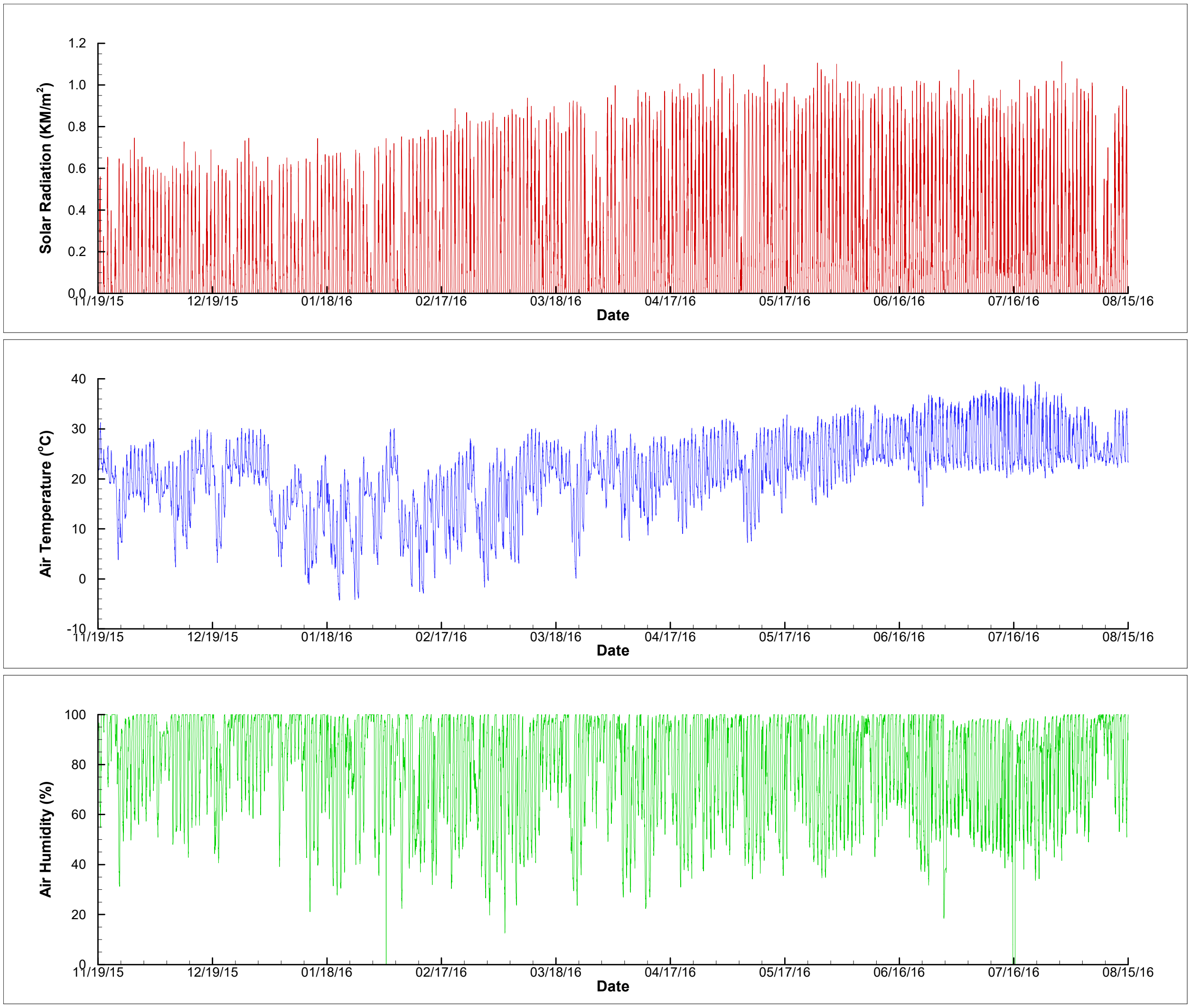

Figure 13 Measured solar radiation, air temperature, and air humidity at a FAWN station at the Lecanto High School during 11/19/2015 – 8/15/2016.

3. Model Development

This section is a brief description of the LAMFE model development for the MFL re-evaluation of the Homosassa River system. The model theory and numerical methods used in the model are not included here but can be found in several previous publications (e.g., Chen, 2003a; Chen, 2004c).

3.1 Model Setup

Based on its physical characteristics, the Homosassa River system was discretized with 406 grids along the river main stem and its 21 branches. The horizontal spacing of the grids varies between 29 m to 277 m. Figure 14 shows cross sections that form the 406 LAMFE grids along the main stem of the Homosassa River and its branches. The water body was discretized with 15 layers between -6.56 m, NAVD88 to 3.0 m, NAVD88, with the layer thickness varying from 0.3 m to 1.76 m.

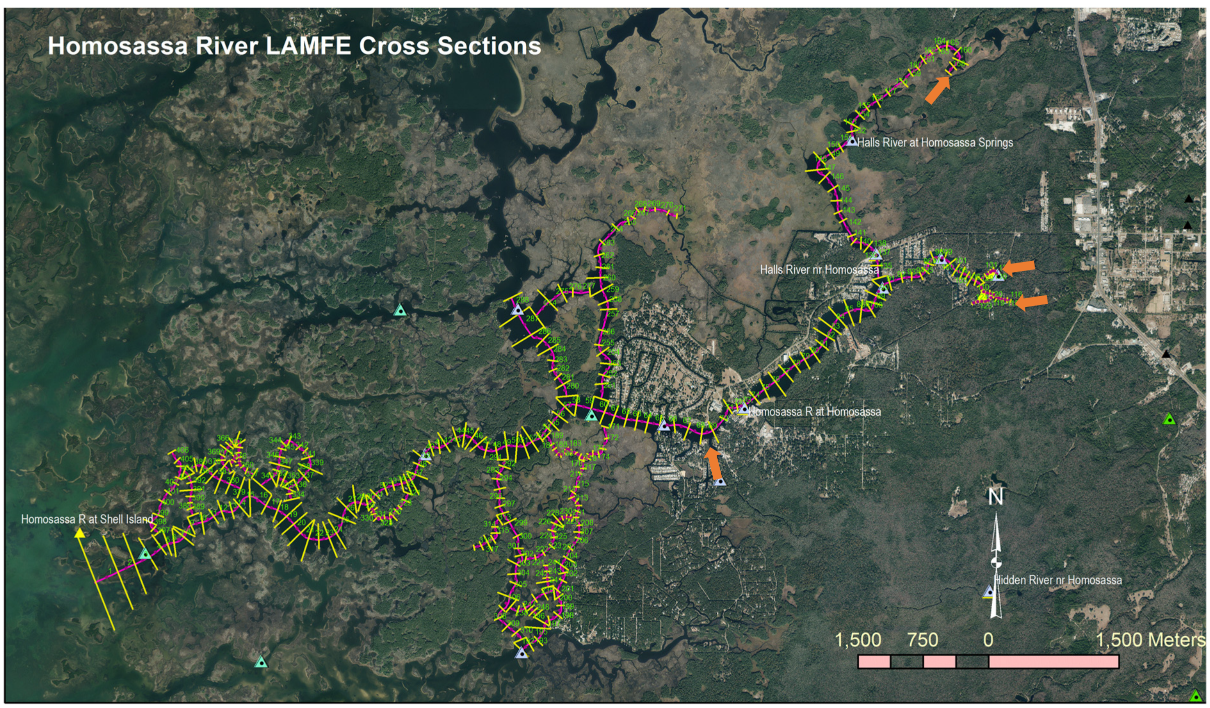

Figure 14. Cross sections (yellow segments) that form the LAMFE grids for the Homosassa River and its branches. Numbers in green are grid numbers in the longitudinal direction. Orange arrows are locations where SGDs enter the model domain.

Based on the availability of measured data which were used to drive the model at the time of the model development, a 34-month period between 11/4/2014 and 8/31/2017 was chosen for model calibration and verification. During this 34-month period, SGDs and meteorological data were available. Water elevation, salinity, and temperature data at the mouth of the Homosassa River were also available. However, there were no water elevation, salinity, and temperature data for the open boundaries in the Salt River and the Mason Creek for the entire 34 months, except for the 4 months of SWFWMD data collection activity in 2017, as mentioned in the previous section.

To obtain boundary conditions of water elevation, salinity, and temperature in the Salt River and Mason Creek for the entire 34 months, an effort was made to correlate water elevations, salinities, and temperatures measured at the Salt River and Mason Creek stations with those at other data collection stations with longer period of record. It was found that water level, salinity, and temperature data in the Salt River and Mason Creek are best correlated with those measured at the mouth of the Homosassa River.

A trial and error approach with various time lags or leads was used to find the best correlations between measured water elevations, salinities, and temperatures at the Homosassa River at Shell Island station with those measured during the 4-month period in 2017 at the Salt River and Mason Creek stations. Table 2 lists the best regression relationships with the mouth of Homosassa for the Salt River and the Mason Creek. In the table, y is a dependent variable (water elevation, salinity, or temperature) in the Salt River or the Mason Creek, x is the independent variable of the same parameter at the mouth of the Homosassa River, h is water level (in ft, NAVD88) at the mouth of the Homosassa River, r is residual depth-average salinity (in psu) at the river mouth (after taking out tidal effects), Y is 24-hour running average of top- or bottom-layer salinity (in psu) in the Salt River, and H and R are 24-hour running averages of h and r, respectively. The regression relationships for temperatures have the highest R^2 values, ranging from 0.94 to 0.98, while the salinity regression relationships have the lowest R^2 values, which are between 0.59 and 0.65. The water elevation has a R^2 of 0.77 between Salt River and mouth of the Homosassa River and a R^2 of 0.88 for Mason Creek and the Homosassa mouth. The time lag (ΔT) of the dependable variable behind the independent variable is in hours (a negative ΔT means that the dependable variable leads independent variable.)

Table 2. Regression relationships between measured water elevations, salinities, and temperatures at the mouth of the Homosassa River with those measured at the Salt River and Mason Creek.

	Salt River			Mason Creek		
Variable	Regression Equations	R^2	ΔT	Regression Equations	R^2	ΔT
Water Elevation	$y = 0.4373x + 0.5577$	0.77	2.75	$y = 0.7419x + 0.0852$	0.88	1.75
Salinity (top)	$Y = 10.096+5.782H-0.237R$ $Y=1.028H^2+4.113H+10.524$	0.62 0.61	14.50 14.50	$y = 18.255+2.405h+0.295r$	0.60	2.25
Salinity (bottom)	$Y=16.951+4.583H+0.526R$	0.65	14.25	$y = 19.324+2.011h+0.237r$	0.59	2.75
Temp (top)	$y=0.9240x+1.5069$	0.94	-1.25	$y=0.9613x+1.0561$	0.98	-1.00
Temp (bottom)	$y=0.9469x+2.0064$	0.97	1.75	$y=0.9547x+1.2558$	0.98	0.00

Figure 15 compares estimated water elevations at the Salt River and Mason Creek stations (blue lines) using the corresponding regression equations listed in the above table with measured water elevations at the two stations during the 4-month period in 2017. Comparisons of estimated top- and bottom-layer salinities at the Salt River (left panels) and Mason Creek (right panels) stations using the corresponding salinity regression equations with measured salinities were shown in Figure 15. Estimated top- and bottom-layer temperatures at the Salt River and Mason Creek were compared with measured data in Figure 17 in the same way as that in Figure 16.

From Figures 15 - 17, it can be seen that estimated water elevations, salinities, and temperatures at both the Salt River and Mason Creek stations match with measured data well. Although the salinity regression relationships listed in Table 2 have relatively low R^2 values, the overall long-term and short-term variations of the estimated salinities are similar to these of measured data in the Salt River and the Mason Creek. The mismatch for the Salt River water elevation estimation prior to 9:00 AM, 6/19/2017 appeared to be caused by a possible datum shift in the field data.

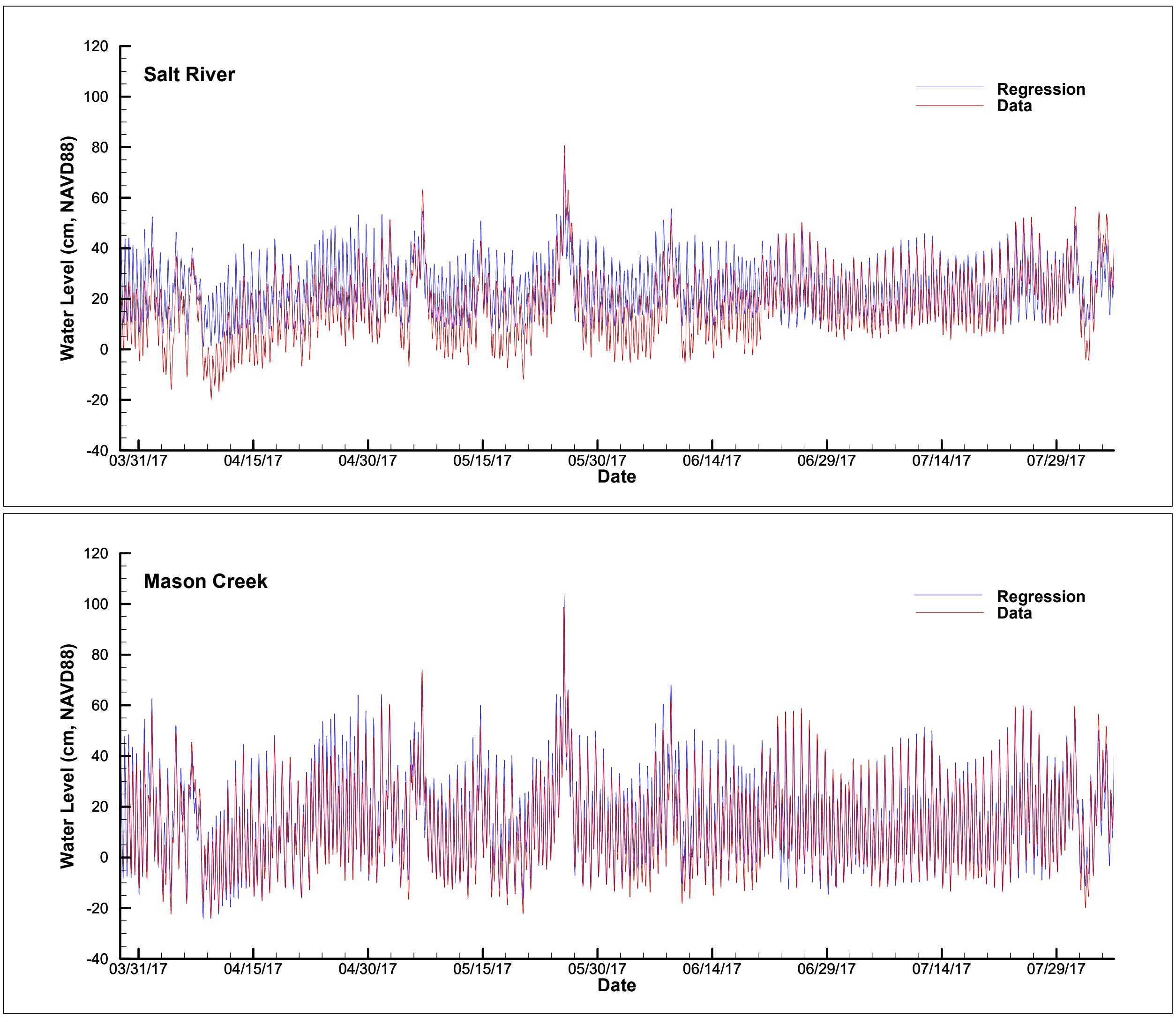

Figure 15. Comparisons of estimated water elevations at the Salt River and Mason Creek stations using regression equations listed in Table 2 with measured water elevations during the 4-month data collection period in 2017.

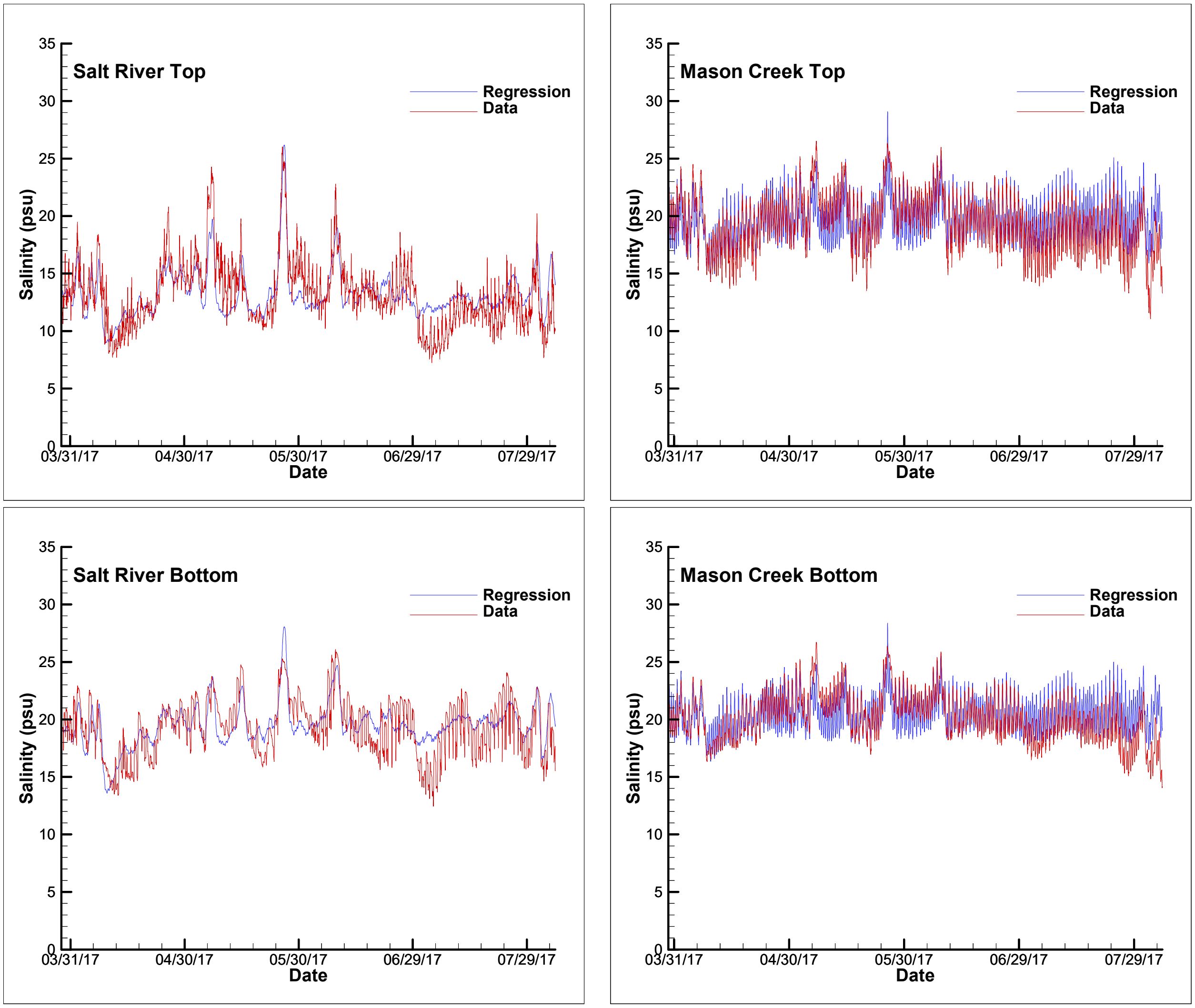

Figure 16. Comparisons of estimated salinities at the top and bottom layers at the Salt River and Mason Creek stations using regression equations listed in Table 2 with measured top- and bottom-layer salinities during the 4-month data collection period in 2017.

Using the regression relationships listed in Table 2, water elevations, salinities, and temperatures at the open boundaries in the Salt River and the Mason Creek can be hindcasted for other 30 months during November 4, 2014 to August 31, 2017. Together with the SGD data, meteorological data, and water elevation, salinity, and temperature data at the mouth of the Homosassa River, all the necessary input data which drive the model are available for a successful simulation of the Homosassa River estuary.

The 34 months were divided into a model calibration period and a model verification period. The former was 11/4/2014 – 5/31/2016, while the latter was 6/1/2016 – 8/31/2017. A variable time step (Δt) between 45 and 60 seconds was used in model runs, with Δt = 75 sec being used 95.56% for the 34-month simulation period.

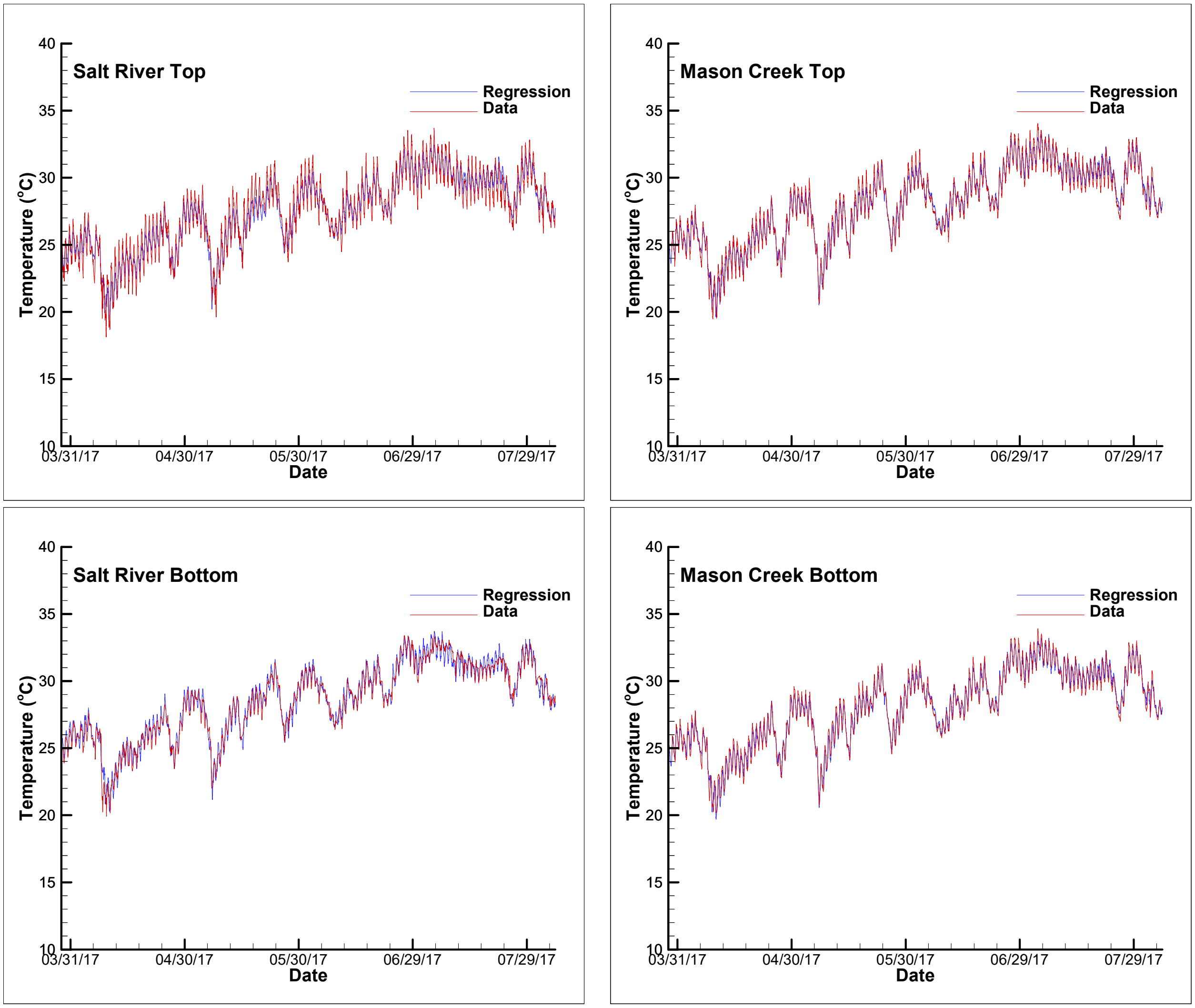

Figure 17. Comparisons of estimated temperatures at the top and bottom layers at the Salt River and Mason Creek stations using regression equations listed in Table 2 with measured top- and bottom-layer temperatures during the 4-month data collection period in 2017.

It should be noted that net SGDs were used as input data for the model. Because the discharge measurements at the SE Fork Homosassa Spring station and the Halls River at Homosassa Springs station contains tidal fluxes through the cross sections, they normally have higher tidal variabilities than the net SGDs do. To obtain net SGDs entering the upstream reaches of the cross sections, tidal fluxes were estimated through the following formula and taken away from the reported discharge data.

$$q_t = -A \frac{\partial \eta}{\partial t} \tag{3}$$

where q_t is the tidal flow, with the positive flow pointing toward downstream, η is measured water level, t is time, and A is the surface water area upstream of the cross section.

Net SGDs were added to the model domain at the most upstream grids of the main stem and branches of the estuarine system, instead of at the stations where discharges were measured or estimated. Orange arrows in Figure 14 indicate locations where SGDs enter the model domain.

Because no direct measurements of salinity in the spring vents were available for this modeling study, salinity in SGD was an unknown and needed to be reasonably estimated. This study used a trial and error approach to estimate salinities in all the SGDs. Based on measured salinity at the SE Fork Homosassa Spring station, the Homosassa Springs at Homosassa Springs station, and the Halls River at Homosassa Springs station, a large number of salinity estimates were tested in model runs. After a careful analysis of simulated salinity results for all salinity estimates for SGDs, it was found that it is suitable to use measured salinity at the Homosassa Springs at Homosassa Spring for the Homosassa Main SGD and measured salinity at the Halls River at Homosassa Springs station for the Halls River SGD. For the SE Fork, the best SGD salinity estimate takes the following form

$$\boldsymbol{s_{se} = max\left(s_{sef}/1.05, 0.3\right)} \tag{4}$$

where s_{sef} represents measured salinity at the SE Fork Homosassa Spring station and s_{se} is the estimated salinity in SGD entering the SE Fork.

For the Hidden River, because no CTD data were measured, no information was available and could be used for a reasonable estimation of salinity boundary condition. A few options were tested, including 0 psu, measured salinity at the Homosassa Springs at Homosassa Springs station, measured salinity at the Halls River at Homosassa Springs station, as well as adding 1 – 2 psu to measured upstream salinities. All these model runs showed that only a couple of grids in both the upstream and downstream directions of the Hidden River flow input location are slightly affected by the choice of the Hidden River salinity boundary condition. Because the Hidden River flow is added to the main stem of the Homosassa River in the model, it is very small compared to the tidal flow and other flow from upstream spring vents. As a result, it only affects a little on model results near its confluence with the Homosassa River but has almost no effects on the overall model results for the entire Homosassa River. To be a little conservative for the scenario simulations described in the next section, the final salinity boundary condition for Hidden River used was measured salinity at the Halls River at Homosassa Springs station plus 2 psu.

Similarly, information about temperatures in spring vents is also needed as the boundary condition for the LAMFE model. Generally, SGD temperature is very stable and barely contains any tidal variations. From temperature data collected in springs vents in Kings Bay, it was found that spring water is slightly colder in winter than in other seasons. This kind of seasonal variability is also expected to exist for SGD temperature in the Homosassa River system and contained in the temperature data collected in at the upstream stations of the Homosassa River system. This study used a combination of measured temperature and a constant temperature value as the estimate of water temperature in SGDs for the Homosassa River system, as follows:

$$T_{se} = \alpha T_{sef} + (1 - \alpha) T_0 \tag{5}$$

$$T_{hs} = \alpha T_{homo} + (1 - \alpha) T_0 \tag{6}$$

$$T_{hr} = \alpha T_{hall} + (1 - \alpha) T_0 \tag{7}$$

$$\boldsymbol{T_{hd} = T_{hs}} \tag{8}$$

where T_{sef}, T_{homo}, and T_{hall} are measured temperatures at the SE Fork Homosassa Spring, Homosassa Springs at Homosassa Springs, and Halls River at Homosassa Springs stations, respectively. T_{se} , T_{hs}, T_{hr}, $and\ T_{hd}$ are estimated temperatures in SGDs for SE Fork, Homosassa Spring, Halls River, and Hidden River respectively. T_0 is a constant value of 23.5 °C and α is a model parameter, which was determined to be 0.5 during the model calibration process.

While Figure 4 shows available discharge data at the USGS stations, the top panel of Figure 23 in the next section shows time series of discharges entering the simulation domain at the locations marked in Figure 14. Except for that entering the Halls River, discharges shown in Figure 23 are SGDs, with tidal fluxes being removed. For the Halls River, there exists an area upstream of the upper end of the river, which is not included in the simulation domain. As such, the tidal flow entering to and coming out of this area is contained in the Halls River discharge shown in Figure 23 for the period after March 10, 2012, when the USGS started to gage Halls River discharge using the index-velocity method. Halls River discharge prior to March 10, 2012 was estimated using Equation (12) and had no tidal signals (see next section for details.) Salinities and temperatures in the upstream discharges are shown in the middle and bottom panels of the figure, respectively. High variabilities seen in salinity and temperature of Halls River discharge are due to the tidal prism upstream of the river. Because Figure 23 are plots for a 125-month period, from October 9, 2007 to March 12, 2018, the 34-month simulation period for model calibration and verification is included in the figure.

3.2 Model Calibration and Verification

Model calibration involves a series of adjustment of model parameters within certain allowable ranges to obtain the best match of simulated water levels, salinities, and temperatures with measured data collected in the field. As mentioned above, the LAMFE model for the Homosassa River was mainly calibrated against measured real-time data at the USGS SE Fork Homosassa Spring, Homosassa Springs at Homosassa Springs, Halls River at Homosassa Spring, Halls River near Homosassa, and Homosassa River at Homosassa stations.

Only limited model parameters had to be tuned in the calibration process, including the bottom roughness, ambient vertical eddy viscosity and diffusivity, and light attenuation. Among them, ambient vertical eddy viscosity is the most sensitive parameter for salinity simulation and light attenuation is the most sensitive parameter for temperature simulation.

Comparisons of model results with measured field data at the five measurement stations in the Homosassa River estuarine system are presented in Figures 18 - 20. In these three time series plots, red lines are model results, while dashed green lines are measured data. For simplicity and clarity, only 60 days of model results and field data of water level, salinity, and temperature between 1/4/2015 and 3/5/2015, are shown in Figures 18 - 20. The choice of these 60-day period is arbitrary. Comparisons of model results with real-time field data during other time periods are similar, with some having a slightly better match and a slightly worse match. Time series plots showing comparisons of model results with field data of water level, salinity, and temperature during other time periods are included in Appendixes E, F, and G, respectively.

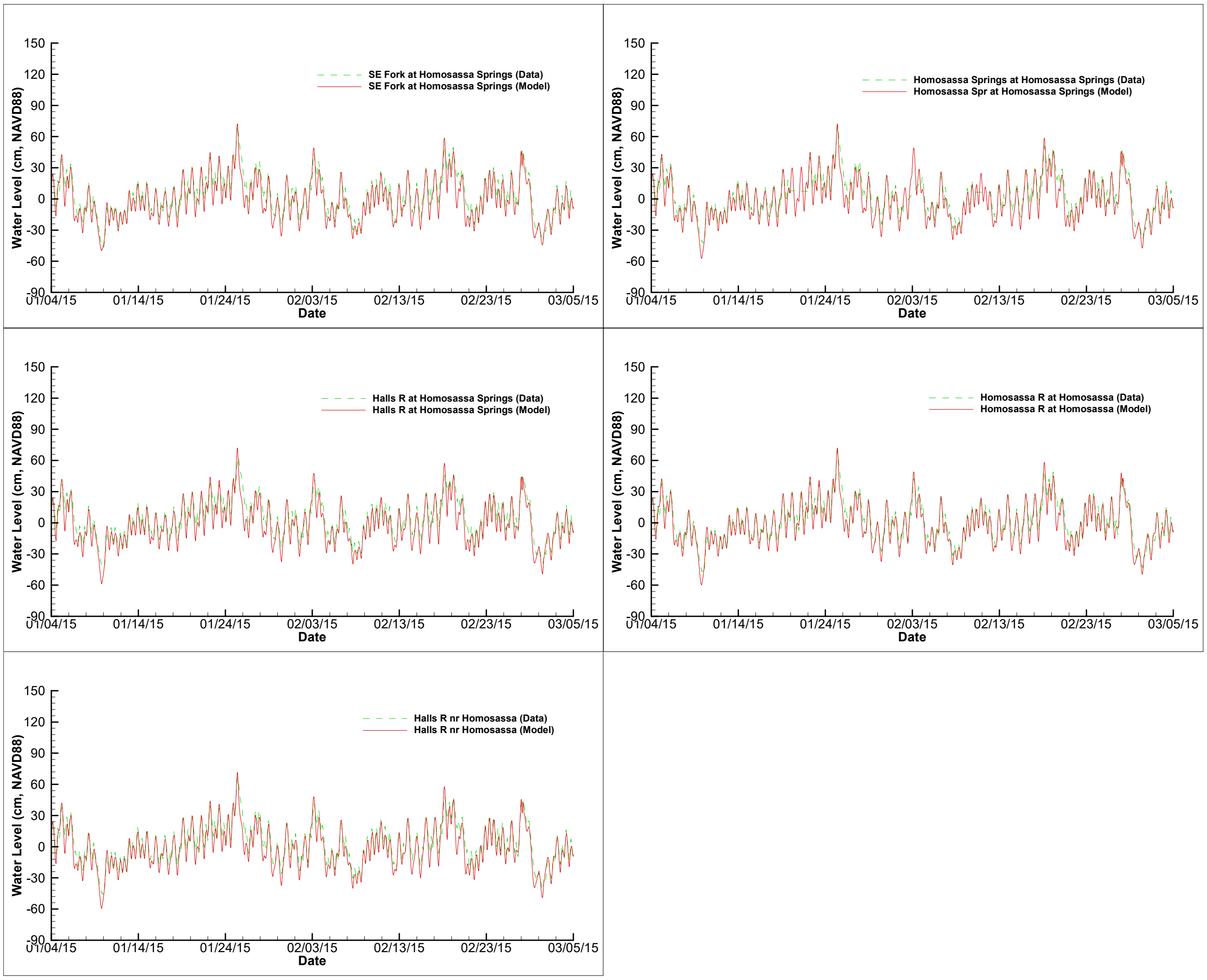

Figure 18. Comparison of measured and simulated water levels at the SE Fork Homosassa Spring, Homosassa Springs at Homosassa Spring, Halls River at Homosassa Spring, Halls River near Homosassa, and Homosassa River at Homosassa stations during 1/4/2015 through 3/5/2015.

As can be seen in Figure 18, simulated water elevations at all five USGS stations agree very well with measured data. Simulated water levels have the same long-term and short-term variations as measured data. Modeled salinity and temperature results also have good agreement with field data (Figures 19 - 20), both in terms of long-term and short-term variations. Because of the uncertainties included in the input data that drive salinity and temperature simulations, it is expected that the match between model results and data for salinity or temperature is not as good as that for water level simulation. Nevertheless, simulated salinity and temperature results are satisfactorily well matched measured real-time data. The reversed salinity distribution in Halls River, where upstream salinity is higher than downstream salinity, was correctly simulated.

More details about comparisons of model results with field are shown in the next subsection, where skill assessment for the model is described.

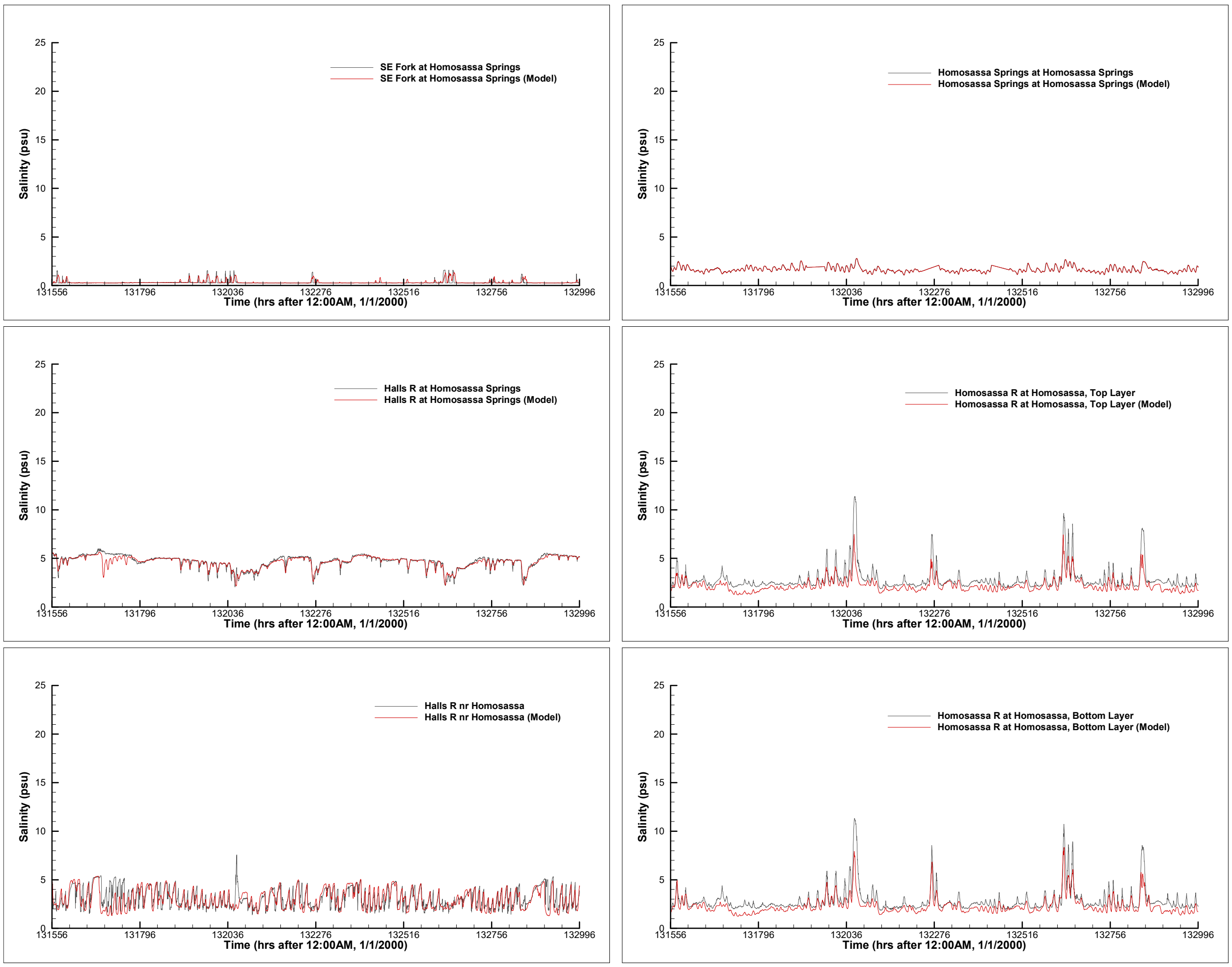

Figure 19. Comparison of measured and simulated salinities at the SE Fork Homosassa Spring, Homosassa Springs at Homosassa Spring, Halls River at Homosassa Spring, Halls River near Homosassa, and Homosassa River at Homosassa stations during 1/3/2015 through 3/4/2015.

3.3 Model Performance Metrics

The performance of the LAMFE model for the Homosassa River is accessed quantitatively with several statistics, including the mean error, mean absolute error, the coefficient of determination (R^2), and a skill assessment parameter introduced by Willmott (1981). The Willmott skill assessment parameter was used by Warner et al. (2005) to assess the performance of a hydrodynamic model for the Hudson River estuary. It also was used by the author to examine performances of the LAMFE model for the Lower Alafia River estuary (Chen, 2005), a multi-block, dynamically coupled 3D-2DV model for the lower Peace River – Lower Myakka River – Upper Charlotte Harbor estuarine system (Chen, 2010,) and an unstructured Cartesian grid model for Crystal River/Kings Bay (Chen, 2012d and 2017.)

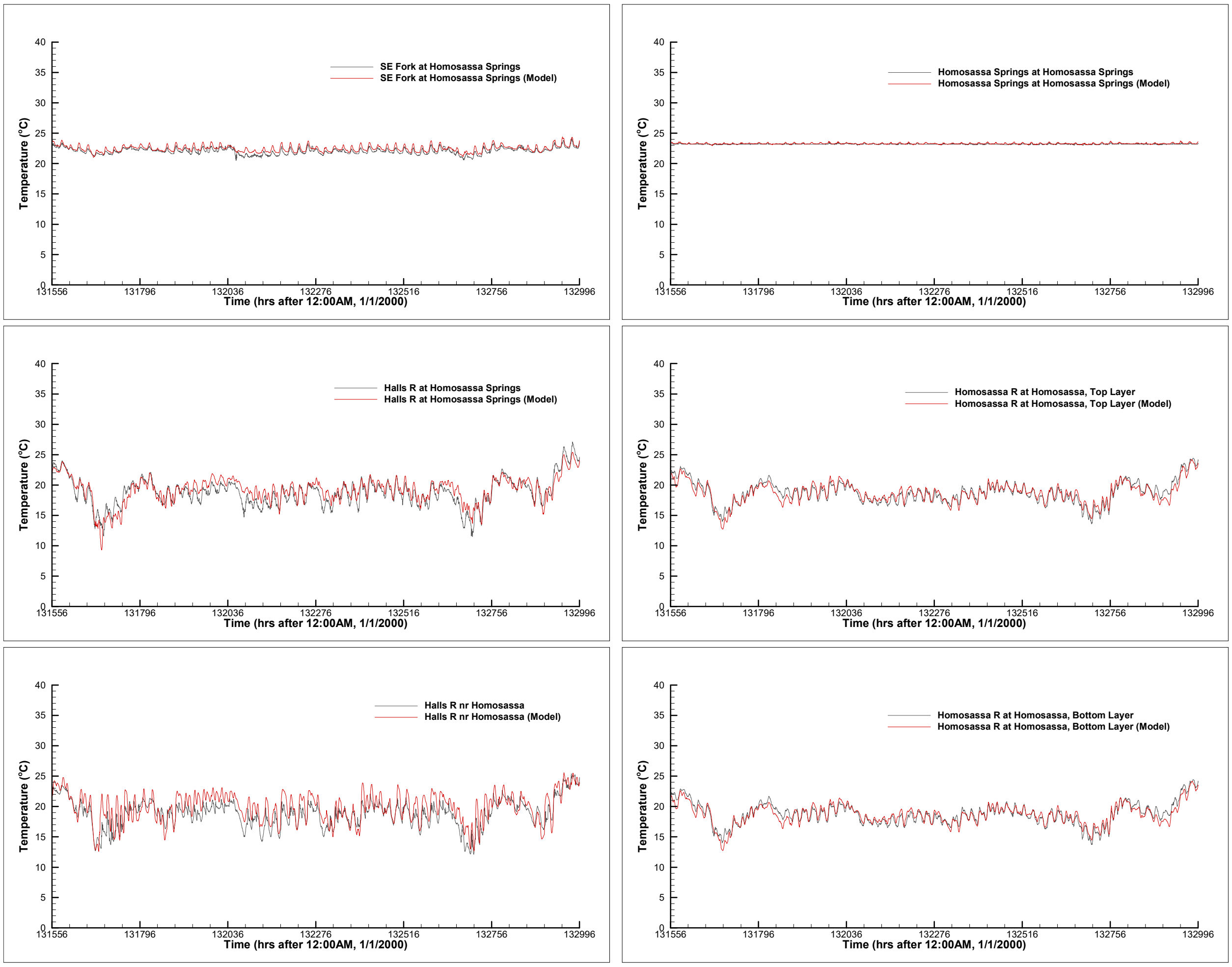

Figure 20. Comparison of measured and simulated temperatures at the SE Fork Homosassa Spring, Homosassa Springs at Homosassa Spring, Halls River at Homosassa Spring, Halls River near Homosassa, and Homosassa River at Homosassa stations during 1/3/2015 through 3/4/2015.

The Willmott skill assessment parameter takes the following form

$$S_k = 1 - \frac{\sum (y^M - y^D)^2}{\sum (|\, y^M - \overline{y^D}\,| + |\, y^D - \overline{y^D}\,|)^2} \tag{9}$$

where S_k is the skill assessment parameter (or simply the skill); y^M and y^D represent simulated and measured variables (water level, salinity, etc.); and $\overline{y^D}$ is the expectation of y^D. S_k in the above equation varies between 0 and 1, with one being a perfect agreement and zero being a complete disagreement between simulated results and measured data.

Mean errors, mean absolute errors, root-mean-square errors, normalized root-mean-square errors, coefficients of determination and Willmott skills for simulated water elevations, salinities, and temperatures are presented in Tables 3, 4, and 5, respectively, during the entire calibration (11/4/2014 - 5/31/2016), verification period (6/1/2016 - 8/31/2017), and the entire simulation (calibration & verification) period (11/4/2014 – 8/31/2017).

As can be seen from Table 3, the mean error between simulated and measured water elevations ranges between -1.66 cm and 0.18 cm among the five USGS stations within the simulation domain in the Homosassa River system during the calibration period, between -0.03 cm and 1.88 cm during the verification period, and between -1.77 cm and 0.63 cm during the entire simulation period. The mean absolute error between simulated and measured water elevations ang the five stations ranges between 4.93 cm and 5.94 cm during the calibration period, between 5.03 cm and 6.21 cm during the verification period, and between 4.96 cm and 6.08 cm during the entire period. The RMSE between simulated and measure water levels varies in the ranges of 6.44 cm – 7.79 cm for the calibration period, 6.99 cm – 7.85 cm for the verification period, and 6.45 cm – 7.82 cm for the entire period. Accordingly, normalized RMSEs are in the ranges of 0.036 – 0.047, 0.040 – 0.067, and 0.035 – 0.047, respectively for the calibration period, the verification period, and the entire period, respectively. The R^2 value and Willmott skill parameter for simulated water elevations are in the ranges of 0.82 - 0.95 and 0.92 – 0.99, respectively for the calibration period. They are in the ranges of 0.85 – 0.88 and 0.96 – 0.97, respectively for the verification period. For the entire simulation period, the R^2 value and Willmott skill parameter for water level simulation in the Homosassa River are in the range of 0.84 – 0.88 and 0.96 – 0.97 respectively. Overall, the ME, MAE, RMSE, NRMSE, R^2, and skill parameter for simulated water elevations are respectively -0.64 cm, 5.54 cm, 7.21 cm, 0.029, 0.86, and 0.96 among the three USGS stations for the entire period.

Table 3. MEs, MAEs, RMSEs, NRMSEs, R^2 values, and Willmott skill assessment parameters for simulated water levels in comparison with real-time field data measured at the SE Fork Homosassa Spring, Homosassa Springs at Homosassa Spring, Halls River at Homosassa Spring, Halls River near Homosassa, and Homosassa River at Homosassa stations during the calibration period, the verification, and the entire simulation period (11/4/2014 – 8/31/2017.)

Water Level (cm)	**ME**	**MAE**	**RMSE**	**NRMSE**	R^2	**Skill**
	Calibration Period					
SE Fork Homosassa	-2.663	5.358	7.073	0.036	0.875	0.961
Homosassa Springs	-2.237	5.208	6.888	0.045	0.874	0.961
Halls R. at Homosassa	-1.239	4.931	6.443	0.047	0.882	0.966
Halls R. near Homosassa	-1.479	5.936	7.789	0.042	0.826	0.948
Homosassa R. at	0.018	5.727	7.478	0.037	0.845	0.958
Overall for all stations	-1.525	5.443	7.165	0.035	0.856	0.959

	Verification Period					
SE Fork Homosassa	-0.025	5.486	6.99	0.053	0.852	0.958
Homosassa Springs	0.598	5.477	7.211	0.04	0.851	0.957
Halls R. at Homosassa	0.174	5.026	6.454	0.053	0.877	0.966
Halls R. near Homosassa	1.013	6.207	7.846	0.067	0.853	0.956
Homosassa R. at	1.878	5.444	7.006	0.053	0.868	0.959
Overall for all stations	0.793	5.684	7.290	0.04	0.861	0.96
	Entire Simulation (Calibration & Verification) Period					
SE Fork Homosassa	-1.767	5.402	7.045	0.036	0.863	0.96
Homosassa Springs	-1.302	5.297	6.997	0.035	0.861	0.96
Halls R. at Homosassa	-0.791	4.961	6.446	0.047	0.879	0.966
Halls R. near Homosassa	-0.169	6.078	7.819	0.042	0.841	0.955
Homosassa R. at	0.627	5.634	7.327	0.036	0.849	0.958
Overall for all stations	-0.639	5.535	7.213	0.029	0.855	0.959

Table 4 show that simulated salinities at the five USGS stations have a mean error between -0,30 psu and 0.15 psu and a mean absolute error in the range of 0.04 to 0.75 psu during the calibration period. During the verification period, ME and MAE range between -0.002 psu and 0.32 psu and between 0.05 psu and 1.12 psu, respectively, while during the entire period, they range between -0.19 psu to 0.21 psu and between 0.04 psu and 0.87 psu, respectively. RMSE and NRMSE between simulated and measured salinities are respectively in the ranges of 0.12 psu – 1.09 psu and 0.011 – 0.053 for the calibration period, 0.09 psu – 1.49 psu and 0.014 – 0.072 for the verification period, and 0.11 psu – 1.24 psu and 0.010 – 0.058 for the entire period. R^2 values of simulated salinities at the five USGS stations vary between 0.66 and 0.87, between 0.54 and 0.96, and between 0.61 and 0.92, respectively for the calibration, verification, and entire periods. Willmott skills for simulated salinities at the five USGS stations range between 0.85 and 0.96 for the calibration period, between 0.85 and 0.99 for the verification period, and between 0.85 and 0.98 for the entire period. Overall, ME, MAE, RMSE, NRMSE, R^2, and skill parameter for simulated salinities are -0.001 psu, 0.46 psu, 0.81 psu, and 0.034, 0.84, and 0.95, respectively among the five USGS stations in the Homosassa River.

Table 4. MEs, MAEs, RMSEs, NRMSEs, R^2 values, and Willmott skill assessment parameters for simulated salinities in comparison with real-time field data measured at the SE Fork Homosassa Spring, Homosassa Springs at Homosassa Spring, Halls River at Homosassa Spring, Halls River near Homosassa, and Homosassa River at Homosassa stations during the calibration period, the verification, and the entire simulation period (11/4/2014 – 8/31/2017.)

Salinity (psu)	**ME**	**MAE**	**RMSE**	**NRMSE**	$\boldsymbol{R^2}$	**Skill**
	Calibration Period					
SE Fork Homosassa Spring	0.107	0.175	0.336	0.025	0.657	0.888

Homosassa Springs	-0.006	0.035	0.119	0.011	0.874	0.964
Halls R. at Homosassa Springs	0.150	0.538	0.729	0.048	0.531	0.848
Halls R. near Homosassa	-0.082	0.185	0.341	0.023	0.869	0.96
Homosassa R. at Homo (top)	-0.275	0.614	0.929	0.046	0.734	0.908
Homosassa R. at Homo (bottom)	-0.300	0.749	1.091	0.053	0.733	0.911
Overall for all stations	-0.067	0.385	0.690	0.032	0.852	0.957
	Verification Period					
SE Fork Homosassa Spring	0.200	0.344	0.58	0.041	0.561	0.846
Homosassa Springs	-0.002	0.045	0.094	0.014	0.956	0.989
Halls R. at Homosassa Springs	0.318	0.694	1.032	0.046	0.543	0.847
Halls R. near Homosassa	0.223	0.462	0.831	0.052	0.577	0.863
Homosassa R. at Homo (top)	0.070	0.959	1.329	0.057	0.715	0.91
Homosassa R. at Homo (bottom)	0.038	1.122	1.493	0.072	0.719	0.915
Overall for all stations	0.141	0.605	1.009	0.043	0.812	0.946
	Entire Simulation (Calibration & Verification) Period					
SE Fork Homosassa Spring	0.138	0.231	0.432	0.03	0.612	0.87
Homosassa Springs	-0.004	0.038	0.112	0.01	0.92	0.979
Halls R. at Homosassa Springs	0.205	0.588	0.84	0.038	0.542	0.851
Halls R. near Homosassa	0.019	0.276	0.553	0.035	0.706	0.915
Homosassa R. at Homo (top)	-0.161	0.727	1.077	0.046	0.736	0.918
Homosassa R. at Homo (bottom)	-0.189	0.871	1.237	0.058	0.742	0.922
Overall for all stations	0.001	0.457	0.809	0.034	0.833	0.953

From Table 5, it can be seen that simulated temperatures at the five USGS stations have a mean error between -0,70 ºC and 0.19 ºC during the calibration period, between -0.60 ºC and 0.46 ºC during the verification period, and between -0.67 ºC and 0.34 ºC during the entire period. The mean absolute error varies in the ranges of 0.12 ºC - 1.30 ºC, 0.12 ºC - 1.07 ºC, and 0.12 ºC - 1.22 ºC for the calibration, verification, and entire periods, respectively. RMSE and NRMSE between simulated and measured temperatures are respectively in the ranges of 0.17 ºC – 1.63 ºC and 0.031 – 0.067 for the calibration period, 0.17 ºC – 1.40 ºC and 0.032 – 0.068 for the verification period, and 0.17 ºC – 1.55 ºC and 0.031 – 0.064 for the entire period. R^2 values of simulated temperatures at the three USGS stations vary between 0.44 and 0.96, between 0.56 and 0.98, and between 0.44 and 0.97, respectively for the calibration, verification, and entire periods. Willmott skills for simulated temperatures at the three stations range between 0.69 and 0.99 for the calibration period, between 0.61 and 0.99 for the verification period, and between 0.67 and 0.99 for the entire period. Overall, ME, MAE, RMSE, NRMSE, R^2, and skill parameter for simulated temperatures are -0.14 ºC, 0.66 ºC, 0.98 ºC, and 0.032, 0.93, and 0.98, respectively among the five USGS stations.

Table 5. MEs, MAEs, RMSEs, NRMSEs, R^2 values, and Willmott skill assessment parameters for simulated temperatures in comparison with real-time field data measured at the SE Fork Homosassa Spring, Homosassa Springs at Homosassa Spring, Halls River at Homosassa Spring, Halls River near Homosassa, and Homosassa River at Homosassa stations during the calibration period, the verification, and the entire simulation period (11/4/2014 – 8/31/2017.)

Temperature (°C)	**ME**	**MAE**	**RMSE**	**NRMSE**	R^2	**Skill**
	Calibration Period					
SE Fork Homosassa Spring	0.196	0.296	0.376	0.036	0.897	0.956
Homosassa Springs	0.115	0.124	0.174	0.031	0.438	0.685
Halls R. at Homosassa Springs	0.285	0.924	1.214	0.053	0.922	0.974
Halls R. near Homosassa	-0.702	1.296	1.626	0.067	0.952	0.959
Homosassa R. at Homo (top)	-0.525	0.807	1.004	0.049	0.964	0.986
Homosassa R. at Homo (bottom)	-0.459	0.769	0.967	0.047	0.964	0.987
Overall for all stations	-0.179	0.701	1.016	0.041	0.934	0.977
	Verification Period					
SE Fork Homosassa Spring	0.176	0.256	0.354	0.058	0.859	0.95
Homosassa Springs	0.108	0.115	0.171	0.068	0.562	0.613
Halls R. at Homosassa Springs	0.463	0.948	1.198	0.058	0.897	0.967
Halls R. near Homosassa	-0.602	1.071	1.397	0.064	0.941	0.966
Homosassa R. at Homo (top)	-0.276	0.593	0.878	0.032	0.956	0.987
Homosassa R. at Homo (bottom)	-0.275	0.536	0.685	0.036	0.975	0.992
Overall for all stations	-0.067	0.586	0.892	0.031	0.926	0.979
	Entire Simulation (Calibration & Verification) Period					
SE Fork Homosassa Spring	0.190	0.283	0.369	0.035	0.883	0.955
Homosassa Springs	0.113	0.121	0.173	0.031	0.437	0.667
Halls R. at Homosassa Springs	0.343	0.932	1.209	0.053	0.914	0.972
Halls R. near Homosassa	-0.669	1.221	1.553	0.064	0.948	0.961
Homosassa R. at Homo (top)	-0.443	0.736	0.964	0.034	0.961	0.986
Homosassa R. at Homo (bottom)	-0.398	0.692	0.885	0.043	0.965	0.989
Overall for all stations	-0.142	0.663	0.977	0.032	0.931	0.978

The R^2 values for temperature prediction at the five USGS stations are all high, except for the Homosassa Springs at Homosassa Springs station, which has a R^2 of 0.44 during the calibration and entire periods and 0.56 during the calibration period. The reason for the low R^2 at the Homosassa Springs at Homosassa Springs station is that water temperature is almost constant and thus has a very small variance. The Homosassa Spring at Homosassa Springs station also has the lowest Willmott skill at 0.67 for the entire simulation period and 0.69 and 0.61 respectively for the calibration and verification periods, because of the very low variance of temperature at the station. As can be seen form Table 5, the Willmott skills are all better than 0.95 for other stations.

While Tables 3 – 5 are statistics measuring how well the model results match field data, they also represent errors or uncertainties of simulated water levels, salinities, and temperature if it is assumed that measured data at the USGS stations at SE Fork Homosassa Spring, Homosassa Spring at Homosassa Spring, Halls River at Homosassa Springs, Halls River near Homosassa, and Homosassa River at Homosassa are all perfectly accurate. These errors or uncertainties are combined results of all uncertainties in input data, model parameters, and numerical schemes used in the LAMFE model. Although uncertainties of certain model parameters are known, uncertainties are generally not quantified for most input data, including measured and estimated SGD from upstream spring vents, measured and estimated water levels at the mouth of the Homosassa River and in Mason Creek and Salt River, and measured and estimated salinities and temperatures at all the open boundaries and in the spring vents. As such, a detailed uncertainty analysis of model results for the Homosassa River is not possible.

As shown in Table 2 and Figures 15 -17, while estimated temperature in Salt River and mason Creek match with measured temperature very well, there are some noticeable errors associated with estimated water levels and salinities at the two open boundaries. In this study, an effort was made to study sensitivities of simulated salinities and temperatures at the five USGS real-time data stations within the simulation domain to estimated water levels and salinities in Mason Creek and Salt River. Response variables selected for the analysis include average salinities and temperatures at the five USGS stations, or a total of 12 variables (at the Homosassa River at Homosassa station, salinity and temperatures were measured at both the top and bottom layers.) Independent variables include water levels and salinities at the open boundaries in the Salt River and Mason Creek.

Similar to the sensitivity analysis presented in Chen (2012b), dimensionless local derivatives (DLDs) are used to define sensitivity of the output space to individual parameters in the input space. The four independent variables constitute an input space of four dimensions, while the 12 response variables make up a 12-dimensional output space. The location (or point) of concern in the input space (X_0) is the estimated water levels and salinities in Salt River and Mason Creek using regression equations listed in Table 2, and the correspond point in the output space (Y_0) is 34-month averages of simulated salinities and temperatures at the five USGS stations of the final model calibration and verification. At (X_0, Y_0), the DLD of the j-th response variable (y_j) with respect to the i-th independent variable (x_i) represents percentage change of y_j for every percent of change in the i-th direction in the input space, or

$$\boldsymbol{DLD_{ij}}|_{X_0} = \frac{x_{i0}}{y_{j0}}\frac{\partial y_j}{\partial x_i} \tag{10}$$

where x_{i0} is the i-th component of X_0 and y_{j0} is the j-th component of Y_0.

With the four independent variables being increased and decreased by 3% independently, eight model runs were conducted. Model results were post-processed and averages of simulated salinities and temperatures at the five USGS stations during the 34-month period of calibration and verification were calculated for the eight model runs. Using central differencing, DLDs were calculated numerically as follows

$$\boldsymbol{DLD_{ij}}|_{\boldsymbol{X_0}} = \frac{\boldsymbol{y_{j+} - y_{j-}}}{\boldsymbol{0.06 y_{j0}}} \tag{11}$$

where y_{j+} and y_{j-} represent model results of the j-th response variable for a 3% increase and a 3% decrease, respectively, of the i-th independent variable.

A total of 48 dimensionless local derivatives can be calculated: 24 DLDs of salinities and 24 DLDs of temperatures at the five stations with respect to each of the four independent variables. As shown in Table 6, the percentage change of average salinities and temperatures per one percent change of water level or salinity in Salt River or Mason Creek is very small at all five USGS stations. The response of the output space to 1% change in any directions of the input space is generally two orders of magnitude smaller than 1%. For example, a 1% of salinity increase in Salt River would cause 0.0021% increase of salinity at the Halls River near Homosassa station, but a 1% decrease of water level in Mason Creek would cause 0.0001% increase of temperature at the top layer of the Homosassa River at Homosassa station. Changes of simulated temperatures at the five stations are all less than 0.0005% for a 1% change of water level or salinity in Salt River or Mason Creek. From Table 6, it is interesting to see that simulated salinity at the SE Fork station is generally more sensitive than those at other stations to a change of any of the four independent variables, with DLDs ranging from -0.025 to 0.014. In other words, a 1% change of any of the four independent variables will cause 0.014% to 0.025% salinity change at the SE Fork station. The reason for the relatively high DLDs for simulated salinity at the SE Fork is that salinity at this station is generally very low, making the relative change a little sensitive to a change at the open boundaries in Salt River or Mason Creek. Salinities at other stations are not sensitive to changes of water levels or salinities in Salt River or Mason Creek, except for those at Halls River near Homosassa and Homosassa River at Homosassa stations, which are very slightly sensitive to water level change in Salt River, with salinities decreasing -0.024% to -0.015% for every percent of water level increase at the open boundary in Salt River.

From Table 6, it can be concluded that although boundary conditions in Salt River and Mason Creek are important input data to the hydrodynamic modeling of the Homosassa River, simulated salinities and temperatures at the five USGS stations inside the simulation domain are not sensitive to the estimated water levels and salinities in Salt River and Mason Creek. It is expected that model results for the entire spring-fed estuary are also not sensitive to the boundary conditions in Salt River and Mason Creek.

Table 6. Dimensionless local derivatives of simulated 34-month averages of salinity and temperature at the five USGS station with respect to estimated salinities and water levels in Salt River and Mason Creek.

Response Variables	Independent Variables			
	Mason Creek Salinity	Salt River Salinity	Mason Creek Water Level	Salt River Water Level
Average Salinities at:				
SE Fork	0.0208	-0.0157	0.0136	-0.0246
Homo Springs	-0.0007	0.0012	0.0005	0.0011
Halls R at Homo Springs	0.0013	0.0009	-0.0020	-0.0010
Halls R nr Homo	0.0025	0.0021	0.0035	-0.0149
Homo R at Homo, Top	0.0079	-0.0015	0.0000	-0.0222
Homo R at Homo, Bottom	0.0042	-0.0006	-0.0013	-0.0238
Average Temperatures at:				
SE Fork	0.0000	0.0000	0.0000	-0.0001
Homo Springs	0.0000	0.0000	0.0000	0.0000
Halls R at Homo Springs	-0.0001	0.0001	0.0000	-0.0001
Halls R nr Homo	-0.0001	-0.0002	-0.0001	0.0004
Homo R at Homo, Top	0.0000	-0.0001	-0.0001	-0.0004
Homo R at Homo, Bottom	0.0000	0.0000	-0.0002	-0.0003

4. Scenario Simulations

4.1 Input Data

It is desirable to run the Homosassa River LAMFE model for various flow reduction conditions for as many years as possible, provided that input data which are used to drive the model are available. In addition to SGD data, the most important data that are needed to drive the model are boundary conditions at the mouth of the Homosassa River and in Salt River and Mason Creek. From Table 1, it can be seen that the USGS started to collect CTD data at the Homosassa River at Shell Island at Homosassa station since 10/1/2007; however, the data collection effort was suspended on October 6, 2009 and did not resume till November 1, 2014. As such, no real-time data of water elevation, salinity, and temperature at the mouth of the Homosassa River were available that can be used as the downstream boundary conditions for the model during October 6, 2009 through October 31, 2014, making a data gap which was almost 61 months long, or a little over five years.

As mentioned in Section 2, there were more than 10 consecutive days when the air temperature in the Homosassa region dropped to below 0 ºC every day in early 2010. It would be ideal if 2010 were included in the scenario simulations to study how flow reduction would affect thermal habitats for manatees and Common Snook during this extremely long period of cold weather. Nevertheless, 2010 was during the 61-month data gap, and to include 2010 in the scenario runs, it is necessary to fill 61-month data gap of the open boundary conditions for the model. For this purpose, available data of water elevation, salinity, and temperature at the mouth of the Homosassa River, at the mouth of Chassahowitzka River, and at the Homosassa River at Homosassa station were analyzed and correlation relationships among the three data stations were studied. It turned out that the mouth of the Homosassa River is better correlated with the mouth of the Chassahowitzka River than with the Homosassa River at Homosassa station for water elevation, salinity, and temperature. For example, the R^2 value of a linear regression between measured water elevations at mouths of the Homosassa and Chassahowitzka Rivers is 0.97, while the R^2 of a linear regression for water elevations at the Homosassa mouth and at the Homosassa River at Homosassa station is 0.83. Table 7 lists regression equations for water elevation, salinity, and temperature between measured data at the mouth of the Homosassa River and those at the mouth of the Chassahowitzka River. In these regression equations, y is the dependent variable (water elevation, salinity, or temperature at the mouth of the Homosassa River), while x is independent variable (water elevation, salinity, or temperature at the mouth of the Chassahowitzka River). It should be noted that the regression equations for salinity and temperature were found with depth-average salinities and temperatures at both the mouth of the Homosassa River and the mouth of the Chassahowitzka River.

Various regression types were tested, and it was found that a simple linear regression is good enough for water elevation and temperature. For salinity, a third order polynomial regression fits the data the best but should be done for the rainy and non-rainy seasons separately. Here, the rainy season is defined as June 11 – October 31.

Table 7. Regression relationships for water elevation, salinity, and temperature between the mouth of the Homosassa River and the mouth of the Chassahowitzka River.

	Regression Equations	R^2
Water Elevation (cm)	$y = 0.9178x+3.9918$	0.974
Salinity (psu, Jun 11 – Oct 31)	$y = 0.0033x^3 - 0.1717x^2 + 3.5969x - 6.1688$	0.802
Salinity (psu, other days)	$y = -0.0008x^3 + 0.0084x^2 + 1.0748x + 6.1196$	0.756
Temperature	$y = 1.0441x - 0.7648$	0.994

Because measured CTD data at the mouths of the Homosassa and Chassahowitzka Rivers are highly correlated, it is possible to estimate water elevations, salinities, and temperatures at the mouth of the Homosassa River from data collected at the mouth of Chassahowitzka using the regression equations listed in Table 7. Because the USGS did collect real-time data at the mouth of the Chassahowitzka River during 10/6/2009 – 10/31/2014, the 61-month data gap at the mouth of the Homosassa River can be filled using estimated water elevations, salinities, and temperatures at the mouth of the Chassahowitzka River.

With the data gap during 10/6/2009 – 10/31/2014 being filled for the mouth of the Homosassa River, the boundary conditions at the downstream open boundary of the simulation domain became available for a period of more than 10 years, from October 1, 2007 to early 2018. Boundary conditions in the Salt River and Mason Creek can also be estimated from data at the Homosassa River at Shell Island station using equations listed in Table 2.

Based on all the available data that could be used to drive the LAMFE model continuously, including data of water elevation, salinity, and temperature at all open boundaries, SGDs, and meteorological data in the region, the longest time span, during that the model can be run for flow reduction scenario runs for the Homosassa River is a 125-month period during October 9, 2007 through March 12, 2018, provided that flows at the Halls River at Homosassa Springs station can be hindcasted back to October 2007. To do so, correlations of the Halls River at Homosassa Spring flow with those of SE Fork and Homosassa Springs were studied. It was found that there is no correlation for flows between the Halls River at Homosassa Springs station and the Homosassa Spring at Homosassa Springs station. However, there is a decent correlation between the Halls River at Homosassa Spring station and the SE Fork station if both flows filtered with a moving average using a time window of one half of the lunar cycle. The regression equation takes the following form

$$\overline{Q_{HR}} = 2.0483\overline{Q_{SE}} - 89.875 \tag{12}$$

where $\overline{Q_{HR}}$ and $\overline{Q_{SE}}$ moving averages of measured flows at the Halls River at Homosassa Springs and SE Fork Homosassa Spring stations, respectively. The above linear regression equation has a coefficient of determination of 0.704. Because of the removal of tidal variations, Halls River discharge hindcasted using the above equation for days prior to the installation of the Halls River at Homosassa Springs station would have a much smaller variability than measured discharge using the index-velocity method would do.

It is reasonable to assume that discharge based on the index-velocity method is a better estimate of the true discharge through the cross section at the SE Fork Homosassa Spring station than that calculated from tidal data and groundwater level data at a Weeki Wachee well using the regression relationship (Equation 2), which the USGS used during October 1, 2001 through September 30, 2011. Because the installation of an acoustic velocity meter (AVM) or an acoustic Doppler velocity meter (ADVM) for the measurement of index-velocity follows a standard operating procedure, which involves a rigorous calibration process (Levesque and Oberg, 2012), it is certain that index-velocity-based discharge reported at the SE Fork Homosassa Spring station was accurate at the time the instrument was installed. It is also expected that the discharge data collected during the first couple of weeks after the installation were also accurate regardless of the maintenance schedule of the USGS, as no storm or episodic events were recorded during this period.

Because the USGS didn't calibrate and verify its discharge regression equation for the SE Fork station after September 30, 2011, it is unknown if the regression equation is valid after September 30, 2011. Nevertheless, it is meaningful to use Equation (2) to estimate SE Fork discharge after September 30, 2011 and compare the regression-based discharge with index-velocity-based discharge. Such a comparison helps one gain confidence in the regression equation, with which one may have a few points of concern. First, the Weeki Wachee well is over 30 KM away from the SE Fork and there could be many things happening in terms of groundwater level between the two locations. There is no evidence that potentiometric surface at the SE Fork has a linear and time-independent relationship with the level in the Weeki Wachee well. Second, the groundwater movement follows Darcy's law, which says that groundwater velocity is proportional to the head gradient. Therefore, it is physically more meaningful to relate SE Fork discharge to the head difference, instead of treating groundwater level and surface water level as separate terms in the regression equation. As shown in Equation (2), the surface water level term has a coefficient with the magnitude being about 3 times of that for the groundwater level term. In other words, the SE Fork discharge is about 2 times more sensitive to the surface water level than to the groundwater level. A rise of 1 foot of groundwater level causes about 3.31 cfs increase of the SE Fork discharge, but a drop of 1 foot of surface water level will cause about 10.31 cfs increase. Third, because of the different magnitudes of coefficients for the surface water and groundwater terms, the regression equation is dependent of the vertical datum. Physically, the groundwater movement does not depend on the choice of the vertical datum. In theory, if the groundwater level and surface water level were measured at a very close proximity, the datum shifts at the two locations would be the same and the head difference would be independent of the use of the datum. Even when the groundwater level and surface water level were measured a few kilometers apart, the use of the regression equation with different datums could only cause a minor difference in estimated discharges because a slight difference between the datum shifts is possible.

Figure 21 shows time series plots of SE Fork discharge estimated using Equation (2) (red line) and that of the index-velocity method (blue line) during December 2005 through December 2017. As can be seen from the figure, there is an overlap for about 600 days, from October 2011 to March 2013. The two discharges differed noticeably, especially during the relatively dry months, during which the regression-based discharge is systematically higher than the index-velocity-based discharge. During wet months, however, there were several spikes of index-velocity-based discharge, which did not exist in the regression-based discharge. These high discharge values during the raining season could be caused by water stored in the upstream area of the SE Fork station during high tides (Yobbi, 2016) and/or during heavy rains. As a result, these high index-velocity based discharges helped to elevate the average discharge during the wet months, making it close to the average regression-based discharges during the wet season.

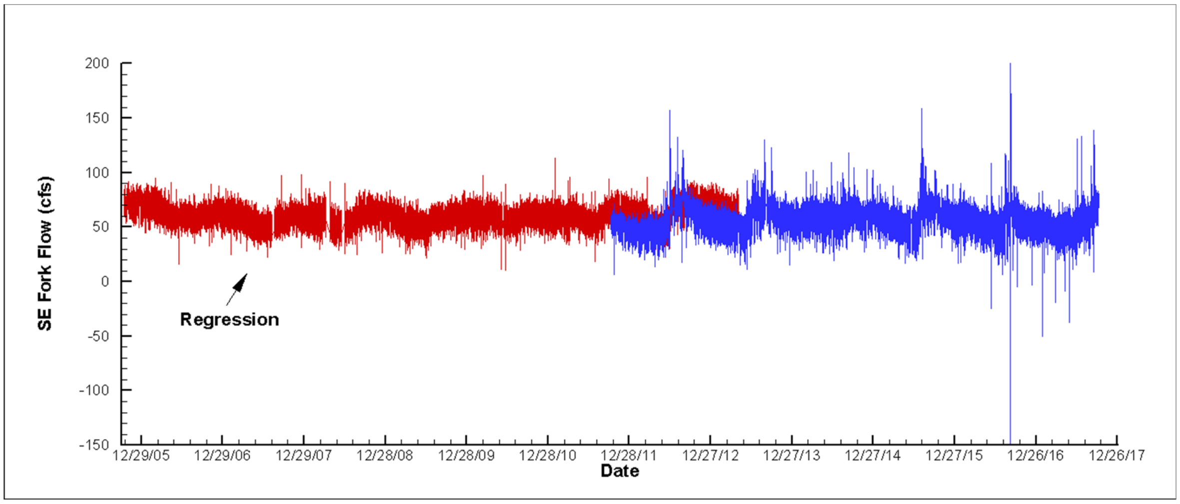

Figure 21. Index-velocity-based discharge (blue line) and regression-based discharge (red line) at the SE Fork Homosassa Spring station. The latter was calculated using Equation (2).

As pointed out by Yobbi (2016), the difference between regression-based and index-velocity-based discharges varies with the season and depend on the time scale used for comparison. On an annual scale, regression-based discharge is about 0 – 4 cfs higher than index-velocity-based discharge. As the time scale becomes smaller and smaller (quarterly, monthly, and daily), the range of difference becomes larger and larger.

Because of the difference between the regression-based discharge and index-velocity-based discharge, it is necessary to adjust the regression-based down a little bit to match index-velocity-based discharge if the latter is considered to be more accurate. Using a higher discharge through the SE Fork without an adjustment obviously suffers a risk of evaluating the MFL for the Homosassa River less conservative. As a comprehensive study on the difference between regression-based discharge and index-velocity-based velocity and a high-order season-dependent modification of the regression equation for the SE Fork Homosassa Spring station are beyond the scope of this modeling effort, a simple zero-order season-independent adjustment was applied to Equation (2). Because the SE Fork Homosassa Spring station is significantly influenced by astronomical tides, tidal cycles of approximately 24.84 hours exist in the discharge data (please see the USGS website https://waterdata.usgs.gov/fl/nwis/current/?type=flow for the note.) To minimize tidal effects on averaging the discharge, seven tidal cycles within the first couple of weeks after the ADVM was installed and calibrated were chosen to calculate average discharges by the regression method and the index-velocity method. The 7-cycle period was between 11:00 AM, 10/5/2011 and 5:00 PM, 10/12/2011 for a total of 174 hours, with 696 pairs of discharge data. It was found that Equation (2) roughly over-estimates 15 cfs (or 11 cfs) of discharge at the SE Fork station if the NAVD88 datum (or the NGVD29 datum) was used for the surface water level and ground water level in Equation (2).

As such, a simple zero-order adjustment of Equation (2) takes the following form:

$$Q_{se} = 3.6293 - 10.3114h - 418.139\Delta h + 3.31029W \tag{13}$$

where units for h and W are feet (NAVD88).

The adjusted regression equation shown above was verified against index-velocity-based discharge during a 30-day period from 1/8/2013 to 2/7/2014. Figure 22 shows the comparison of the estimated discharge using Equation (13) with that derived from the index velocity measurement at the SE Fork Homosassa Spring station during the 30-day verification period. Although the estimated discharge using the modified regression equation misses a couple of peaks during January 8, 2013 through February 7, 2013, it matches with index-velocity based discharge well in terms of both magnitude and phase.

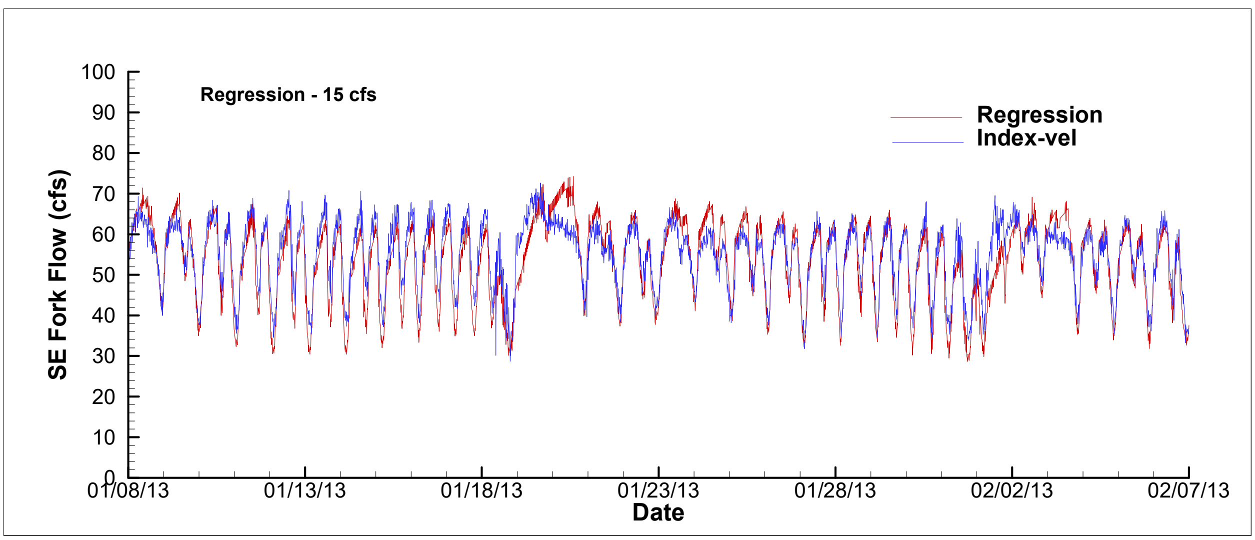

Figure 22. Comparison of estimated discharge using the modified USGS regression relationship (Equation 13) with the index-velocity based discharge at the SE Fork Homosassa Spring station during a 30-day period from 1/8/2013 to 2/7/2013.

Figure 23 shows plots of all upstream submarine groundwater discharges entering the simulation domain as well as salinities and temperatures in these upstream discharges. These time series plots are for the 125-month scenario simulation period from October 9, 2007 to March 12, 2018.

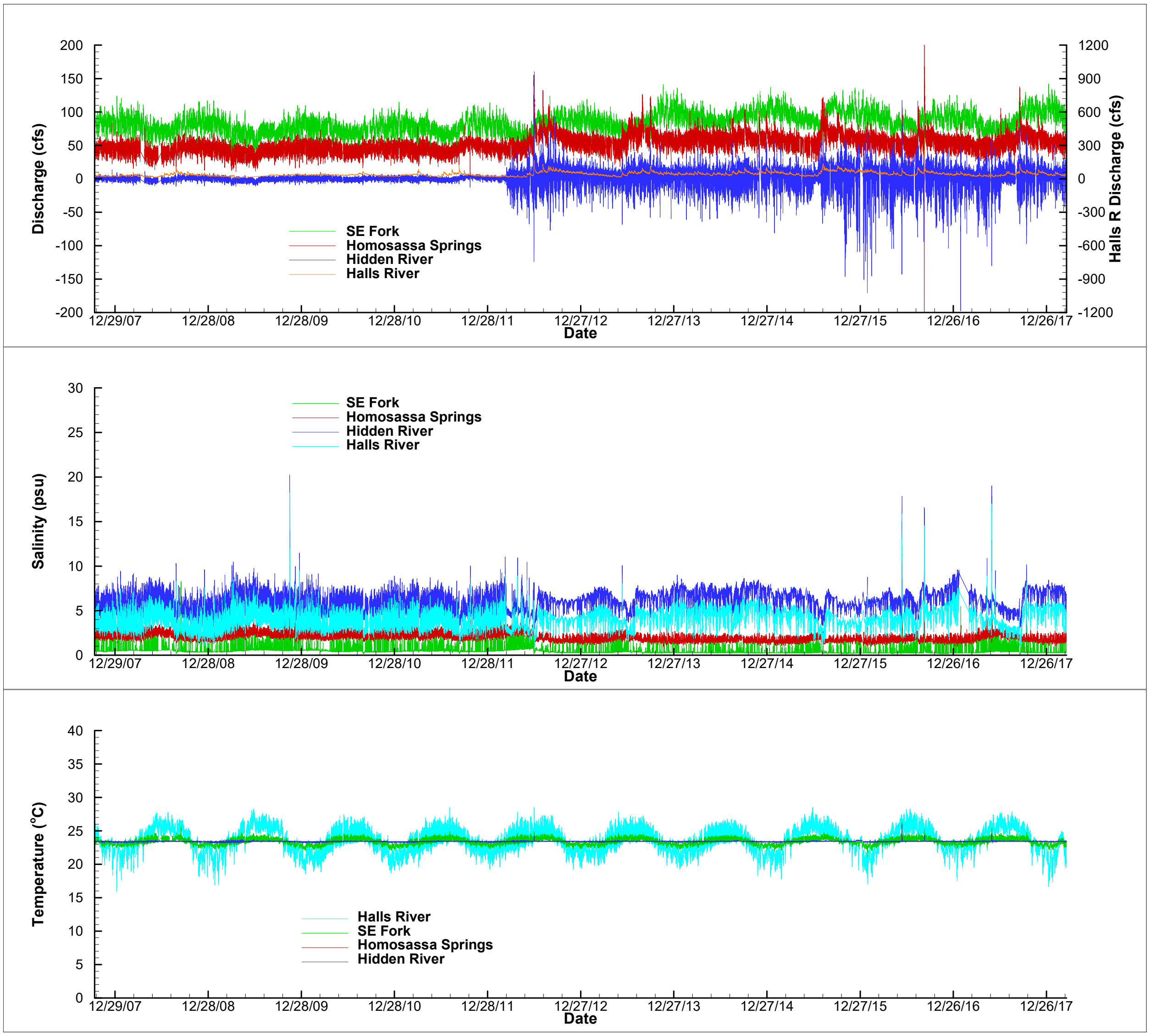

Figure 23. Time series of upstream discharges (top panel) entering the Homosassa River as well as salinities (middle panel) and temperatures (bottom panel) in the upstream discharges during October 9, 2007 through March 12, 2018.

Because the downstream boundary of the model domain for the Homosassa River is at the mouth of the river, it is possible that a flow reduction may cause salinity at the open boundary to slightly increase. To consider this factor in the scenario simulations, a series test runs of the LAMFE model with an extended simulation domain were conducted to figure out how much salinity increase could occur with various flow reductions. The extended simulation domain has five extra grids that cover an offshore area below the mouth of the Homosassa River.

Figure 24 shows the cross sections of the LAMFE model for the extended simulation domain of the Homosassa River. The downstream open boundary in the extended simulation domain is 5.88 km offshore of the mouth of the Homosassa River and it is expected that any flow reductions in the Homosassa River only have very insignificant effect on salinity increase there.

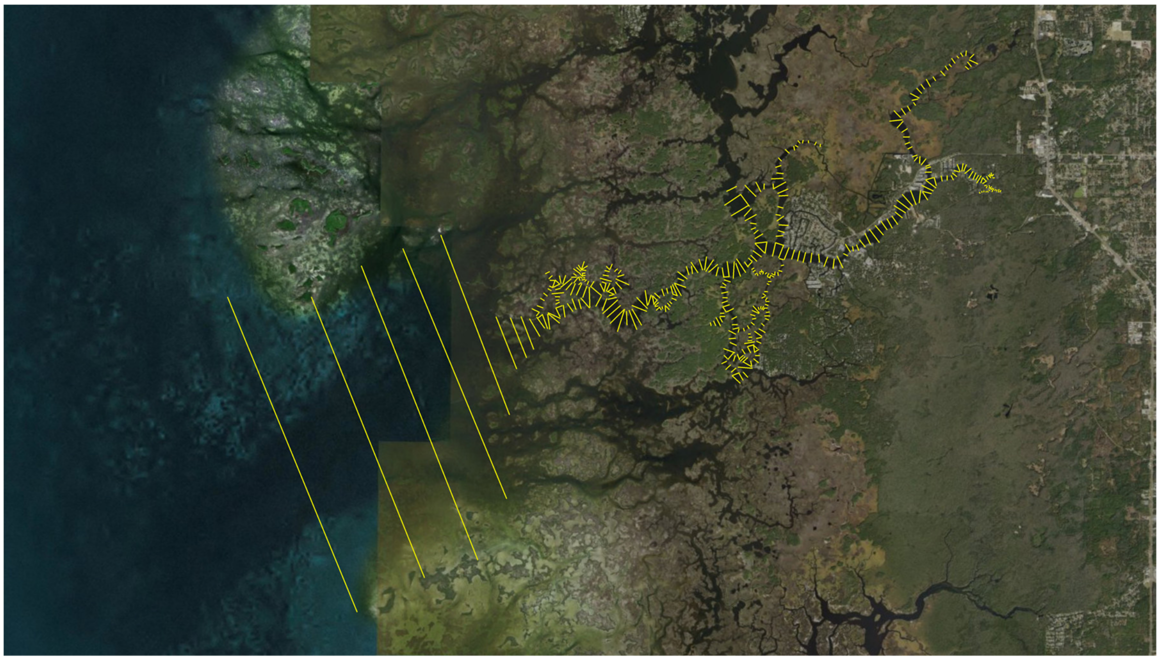

Figure 24. An extended simulation domain for the Homosassa River, which has five extra grids coving an offshore area below the mouth of the river.

Bathymetry data for this offshore area were obtained from the U.S. Coastal Relief Model Vol. 3 – Florida and East Gulf of Mexico of NOAA's National Center for Environmental Information. The following is its website link

https://www.ngdc.noaa.gov/docucomp/page?xml=NOAA/NESDIS/NGDC/MGG/DEM/iso/xml/307.xml&view=getDataView&header=none

In the test runs, it was assumed that the water level and water temperature at the offshore open boundary is the same as these at the mouth of the Homosassa River, but the salinity is a higher than that at the river mouth and roughly takes the following form

$$S_1 = S_0 + \min(\max(0.1(30 - S_0), 0.0), 2.5) \tag{14}$$

where S_0 is measured salinity at the mouth of the Homosassa River and S_1 is estimated salinity at the offshore open boundary. The above equation for estimating S_1 is obtained through a trial and error process with a goal to reach a best match between simulated and measured salinities at the mouth of the Homosassa River for the existing flow scenario. It is interesting to note that the above equation is also valid for the Chassahowitzka LAMFE model, which was developed for the MFL re-evaluation of the Chassahowitzka River (Chen, 2019a).

Figure 25 shows the average salinity increases in different layers of the model for different flow reductions. The low case k on the right side of the figure is an index for vertical layers, counting from the bottom to the top. From the figure, it is clear that salinity increase at the mouth of the Homosassa River due to upstream flow reduction is generally small. A 30% flow reduction causes a salinity increase of about 0.2 psu at the top layer of the mouth but only a < 0.02 psu increase at the bottom layer. At the same depth, the salinity increase at the river mouth is linearly increase with the flow reduction percentage. Near the bottom of the river mouth, flow reduction in the Homosassa has barely any effects on salinity.

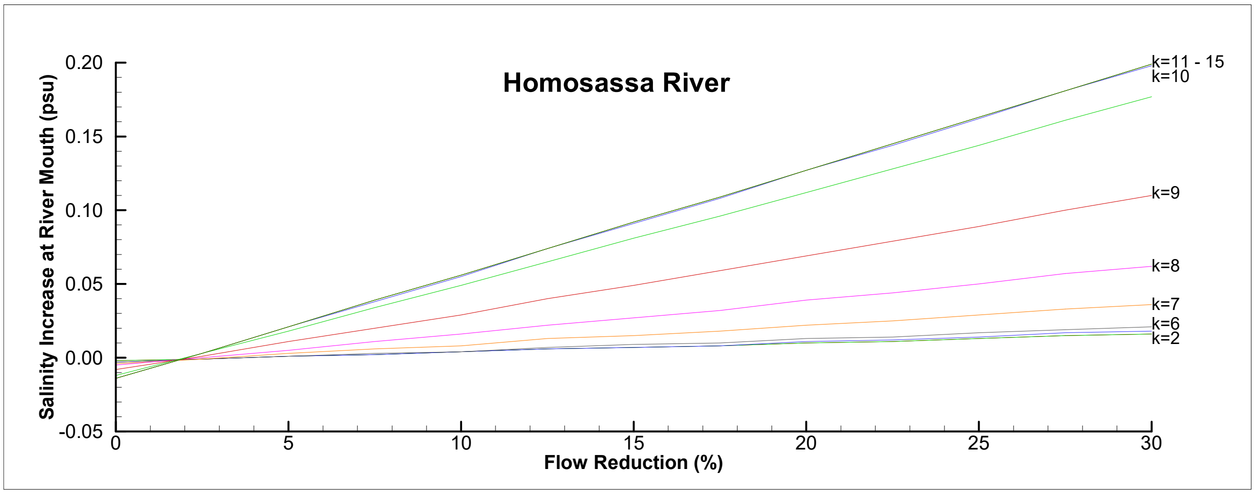

Figure 25. Effects of flow reduction on salinities in different layers at the mouth of the Homosassa River.

With effects of reduced SGD on salinity at the mouth of the Homosassa River being considered, a question was raised if a reduction of SGD will cause a change of salinity in the spring discharge itself. Because there is not a subterranean estuary model available for the region, a comprehensive modeling study on how groundwater withdrawal affects salinity distributions in the groundwater, especially in the proximity of spring vents of the Homosassa River, is impossible. Because both salinity and SGD are affected by tides, it is necessarily to filter out tidal signals in salinity and SGD data before any correlations between them are sought. An analysis of discharge and salinity data measured at the upstream stations (Chen, 2019b) shows that R^2 values for the linear regression between tidally filtered salinity and tidally filtered SGD are only 0.04 and 0.06 at the SE Fork Homosassa Spring and Halls River at Homosassa Springs stations, respectively (Chen, 2019b). As such, it can be concluded that a reduction of SGD will likely not cause salinity in spring discharges to change in the Homosassa River system.

4.2 Flow Reduction Scenarios

A total of 14 flow scenarios were simulated and analyzed, including the baseline flow (BSL) condition, the existing flow condition, and 2.5%, 5%, 7.5%, 10%, 12.5%, 15%, 17.5%. 20%, 22.5%, 25%, 27.5%, and 30% reductions from the baseline flow condition. The baseline flow condition is an imaginary flow condition that would exist if no ground water were withdrawn in the springshed. It is estimated that the existing withdrawal causes about 1.85% reduction of SGDs in Homosassa. As such, the baseline flow is obtained by dividing the existing SGDs by 0.9815. Table 8 lists details on how flow is calculated for each flow scenarios.

Table 8. Flow reduction scenarios conducted for the Homosassa River MFL re-evaluation.

Scenario No.	Scenario Name	Flow Calculation
1	Baseline	(No. 2 SGDs)/0.9815, or 1.0188×(No. 2 SGDs)
2	Existing	Measured and estimated existing SGDs
3	2.5%	0.975×(No. 1 SGDs), or 0.9934(No. 2 SGDs)
4	5%	0.95×(No. 1 SGDs), or 0.9679×(No. 2 SGDs)
5	7.5%	0.925×(No. 1 SGDs), or 0.9424×(No. 2 SGDs)
6	10%	0.9×(No. 1 SGDs), or 0.9170×(No. 2 SGDs)
7	12.5%	0.875×(No. 1 SGDs), or 0.8915×(No. 2 SGDs)
8	15%	0.85×(No. 1 SGDs), or 0.8660×(No. 2 SGDs)
9	17.5%	0.825×(No. 1 SGDs), or 0.8406×(No. 2 SGDs)
10	20%	0.8×(No. 1 SGDs), or 0.8151×(No. 2 SGDs)
11	22.5%	0.775×(No. 1 SGDs), or 0.7896×(No. 2 SGDs)
12	25%	0.75×(No. 1 SGDs), or 0.7641×(No. 2 SGDs)
13	27.5%	0.775×(No. 1 SGDs), or 0.7387×(No. 2 SGDs)
14	30%	0.7×(No. 1 SGDs), or 0.7132×(No. 2 SGDs)

Although the effect of flow reduction on salinity at the river mouth is very small, the scenario runs take these small salinity increases into consideration. Salinity boundary conditions at the open boundary at the mouth of the Homosassa River were adjusted according to the salinity increases shown in Figure 25. For the upstream spring vents, salinities in SGDs were assumed to be independent of the flow reduction and no adjustments were made.

Simulated salinities and temperatures at centers of all grid cells were written out to output files with an interval of 30 minutes for all 14 scenarios. These model results were processed to calculate volumes, bottom areas, and shoreline lengths for various salinity ranges and volumes and surface areas of various temperature ranges at each time point. Salinity and thermal habitats calculated and analyzed are listed in Table 9 below.

Table 9. Salinity and temperature ranges used in the post-processes of model results of the scenario runs.

	Ranges	Habitats
Salinity	1. ≤ 1 psu 2. ≤ 2 psu 3. ≤ 3 psu 4. ≤ 5 psu 5. ≤ 10 psu 6. ≤ 15 psu 7. ≤ 20 psu	Salinity habitats calculated: 1. Water volume, 2. Bottom area, and 3. Shoreline length.
Temperature	1. < 15 ºC 2. ≥ 15 ºC (or 15 ºC < Temp < 20 ºC) 3. ≥ 20 ºC	Thermal habitats for manatees and Common Snook calculated: water volume and surface area. Habitats of ≥ 15 ºC and ≥ 20 ºC were calculated both with and without the 3.8 ft (1.158 m) requirement for depth or layer thickness.

4.3 Results of Salinity Habitats

Direct comparisons and analyses of 30-minute results of water volume, bottom area, and shoreline length for different flow reductions are very tedious and not necessary, because one would easily lose the forest for the trees. Instead, daily mean values of salinity habitats are typically analyzed in the MFL evaluation. Figures 26 & 27 show daily mean volumes, bottom area, and shoreline lengths for salinity ≤ 1, 2, 3, 5, 10, and 15 for the baseline and 10% flow reductions, respectively.

Although salinity habitats for salinity ≤ 20 psu were calculated, they are not included in the following discussion, because they are very similar to salinity habitats of ≤ 15 psu, except that ≤ 20 psu habitats are much less sensitive to flow reduction than ≤ 15 psu habitats. The first 20 days were considered as a spin-up period and model results during these 20 days were excluded in Figures 26 and 27. Time series plots of simulated daily salinity habitats for other flow reduction scenarios have similar temporal variabilities as those shown in Figures 26 & 27 and are thus not included here.

Time series plots of simulated salinity habitats for the baseline scenario and the 10% flow reduction scenario look similar, with low salinity habitats being reduced when all SGDs entering the system are reduced 10%; however, these salinity habitat reductions are only evident when Figures 26 and 27 are overlaid together. To get a better overall picture of the effects of flow reduction on salinity habitats, cumulative distribution functions are plotted. Figures 28 - 30 show CDFs of water volume, bottom area, and shoreline length for various salinity ranges and flow reduction scenarios.

For a better inspection of the differences among different CDFs for different flow reductions, only the baseline, existing, 2.5%, 5%, 10%, 15%, 20%, 25%, and 30% flow reduction scenarios are included in Figures 28 - 30. From these figures, it is apparent that the low salinity habitats for ≤ 1 psu, ≤ 2 psu, or ≤ 3 psu are generally much more sensitive to these for ≤ 10 psu and ≤ 15 psu. This is consistent with many other estuarine systems we've studied in the SWFWMD. To quantify the relative changes of salinity habitats caused by flow reduction, average water volume, bottom area, and shoreline length for different salinity ranges can be calculated. Graphically, these average values equal to areas between the *y*-axis and the corresponding CDF curves in Figures 28 - 30.

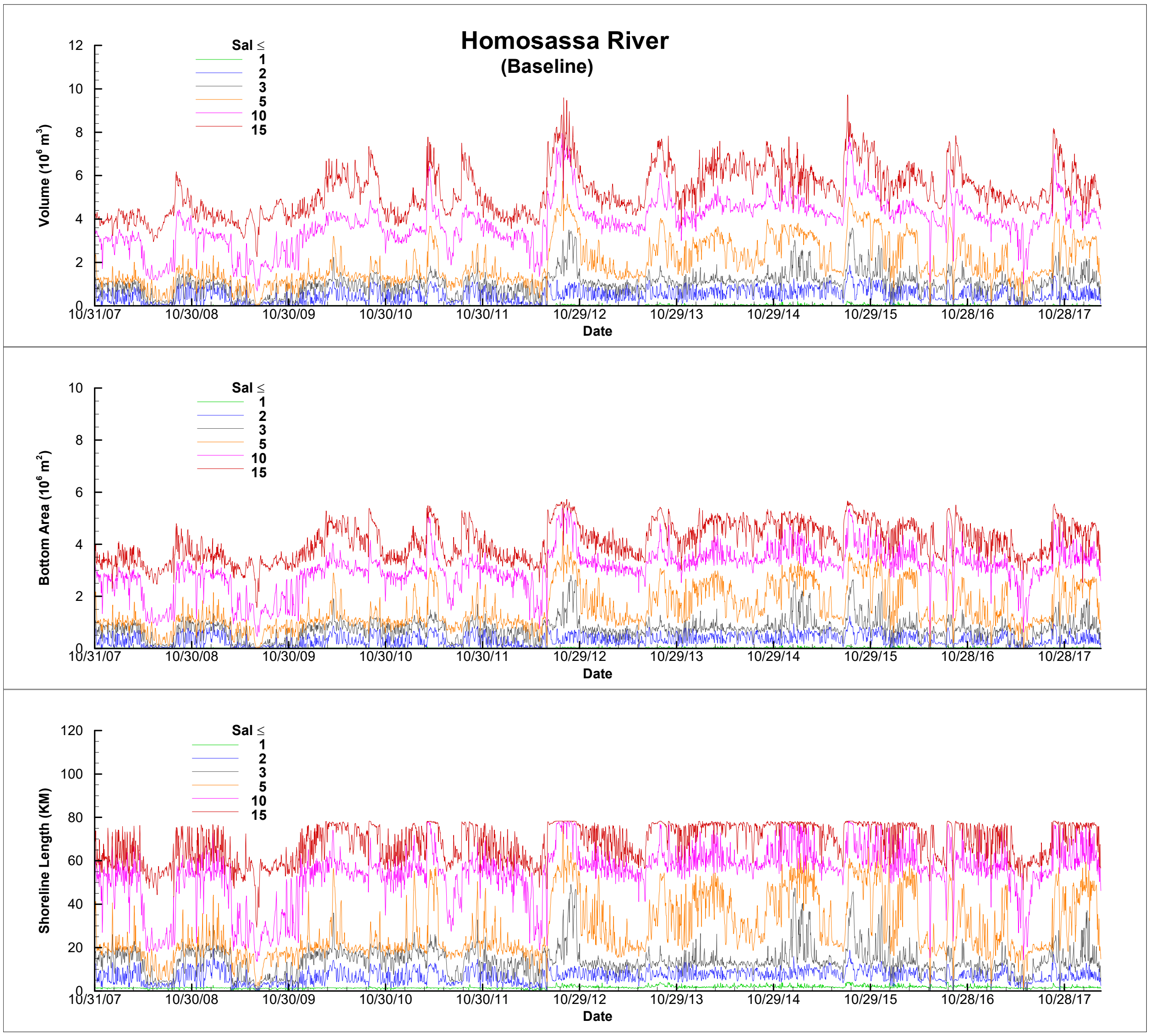

Figure 26. Simulated daily salinity habitats for salinity ≤ 1, 2, 3, 5, 10, and 15 psu for the baseline flow scenario during the 125-month simulation period.

Tables 10 -12 list average salinity volumes, bottom areas, and shoreline lengths, respectively for salinity ≤ 1, 2, 3, 5, 10, and 15 psu under various flow reduction conditions. As can be seen from Table 10, ≤ 1 psu salinity volumes are more than one order of magnitude smaller than ≤ 2 psu volumes, which are roughly less than half of those for ≤ 3 psu, for all the flow reduction scenarios.

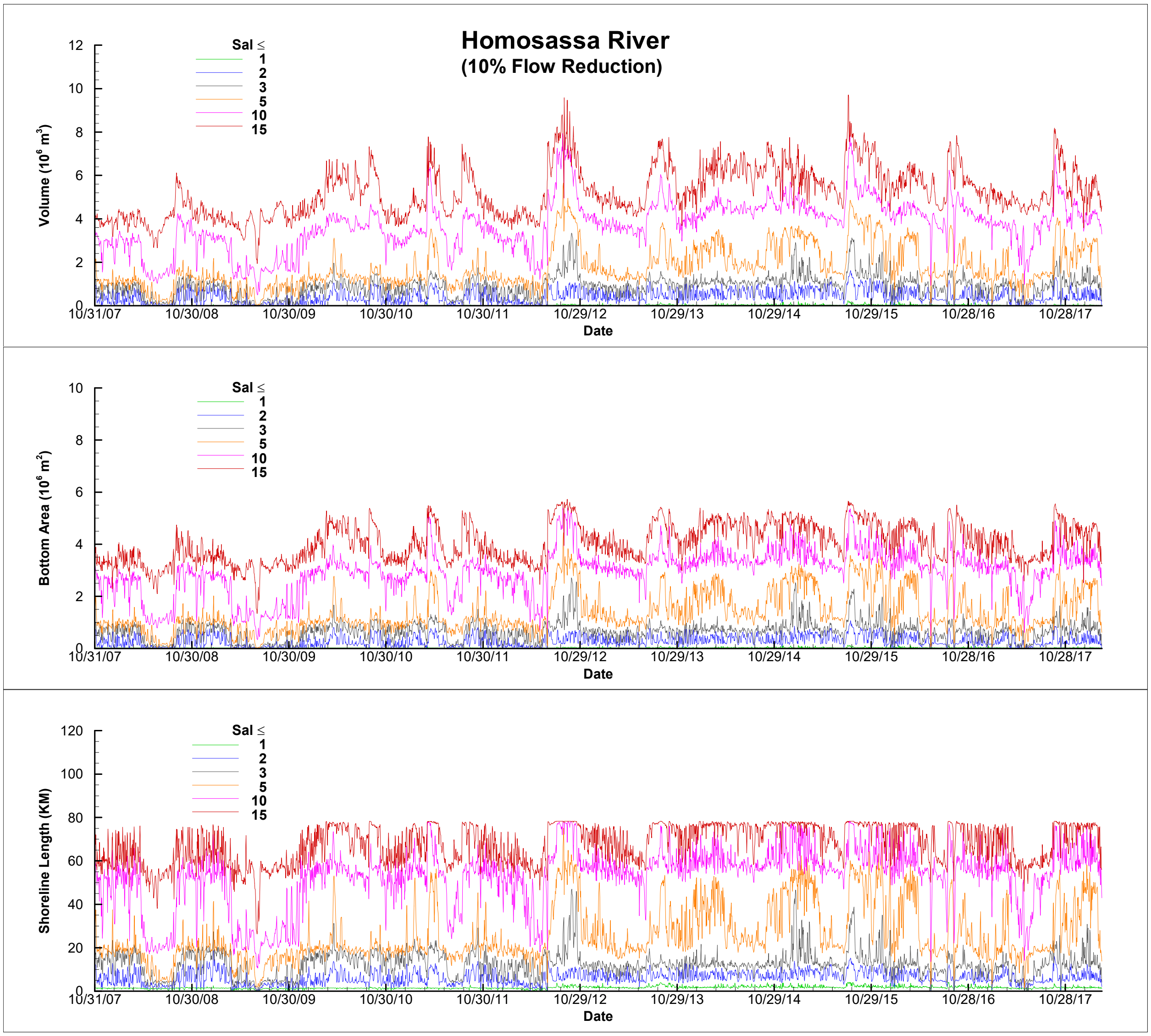

Figure 27. Simulated daily salinity habitats for salinity ≤ 1, 2, 3, 5, 10, and 15 psu for the 10% flow reduction scenario during the 125-month simulation period.

Similar scale differences among bottom areas and shoreline lengths of different salinity ranges can also be seen in Tables 11 &12. Table 11 shows that ≤ 1 psu bottom areas are also about one order of magnitude smaller than ≤ 2 psu bottom areas, which are about 42% of ≤ 3 psu bottom areas. Table 12 shows that ≤ 1 psu shoreline lengths are about 25% of ≤ 2 psu shoreline lengths, which are about 50% of ≤ 3 psu shoreline lengths.

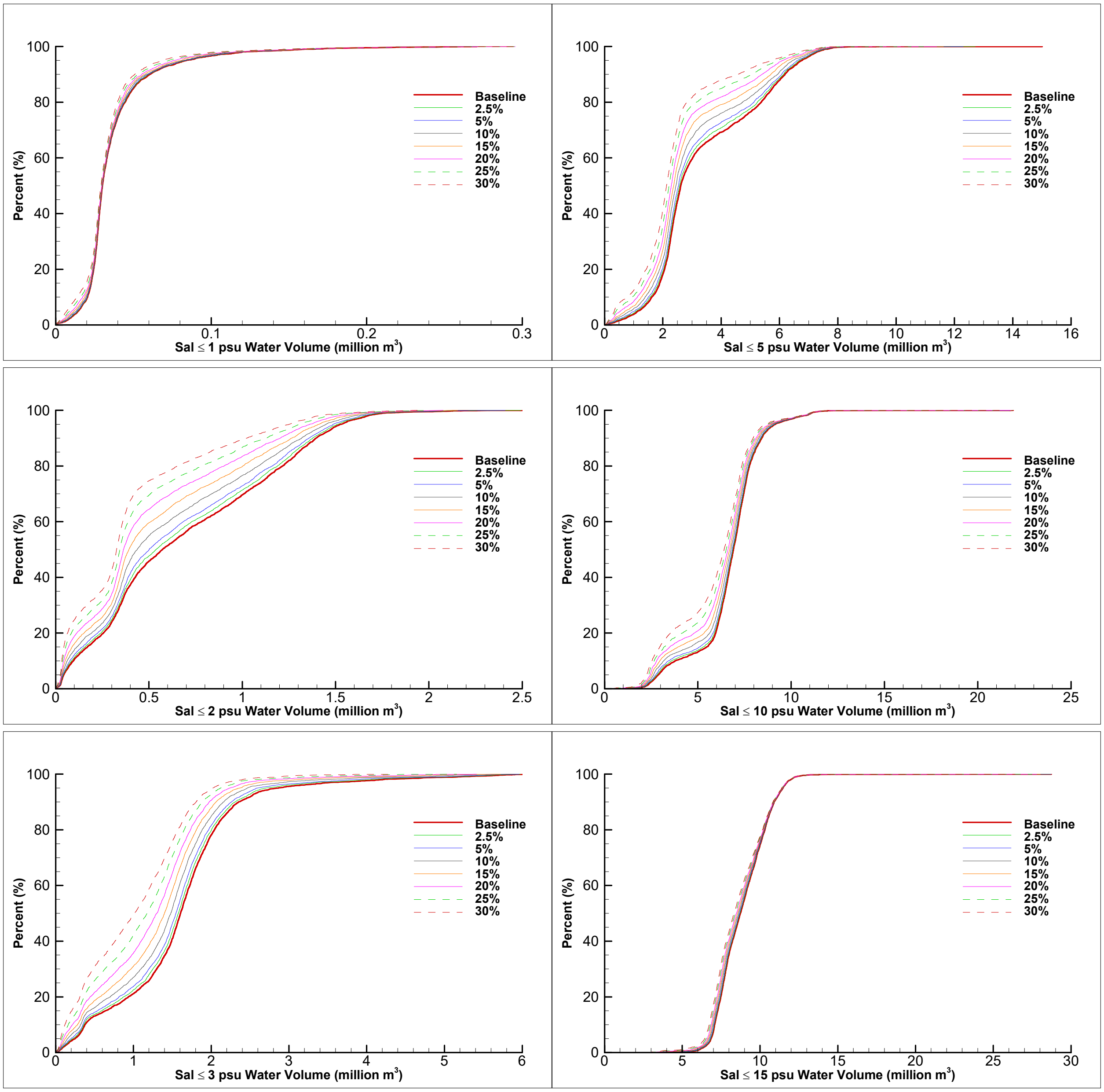

Figure 28. Cumulative distribution functions of simulated water volumes for various flow reductions for salinity ≤ 1, 2, 3, 5, 10, and 15 psu.

From Tables 10 - 12, relative reductions of salinity habitats from these of the BSL condition caused by flow reductions can be easily calculated and are presented in Tables 13 - 15. It can be seen from these tables, the relative reduction of any salinity habitats increases with the increase of flow reduction, with low salinity habitats being more sensitive than those for salinity ≤ 10 psu or higher. The percent flow reduction that would trigger a 15% reduction of each individual salinity habitat is listed at the bottom row of the tables. The most sensitive salinity habitat is ≤ 2 psu bottom area, which has a decline of 15% if SGDs are reduced by 11.09%. In other words, if the flow reduction is not larger than 11.09%, none of the salinity habitats that are considered here will be reduced 15% or more.

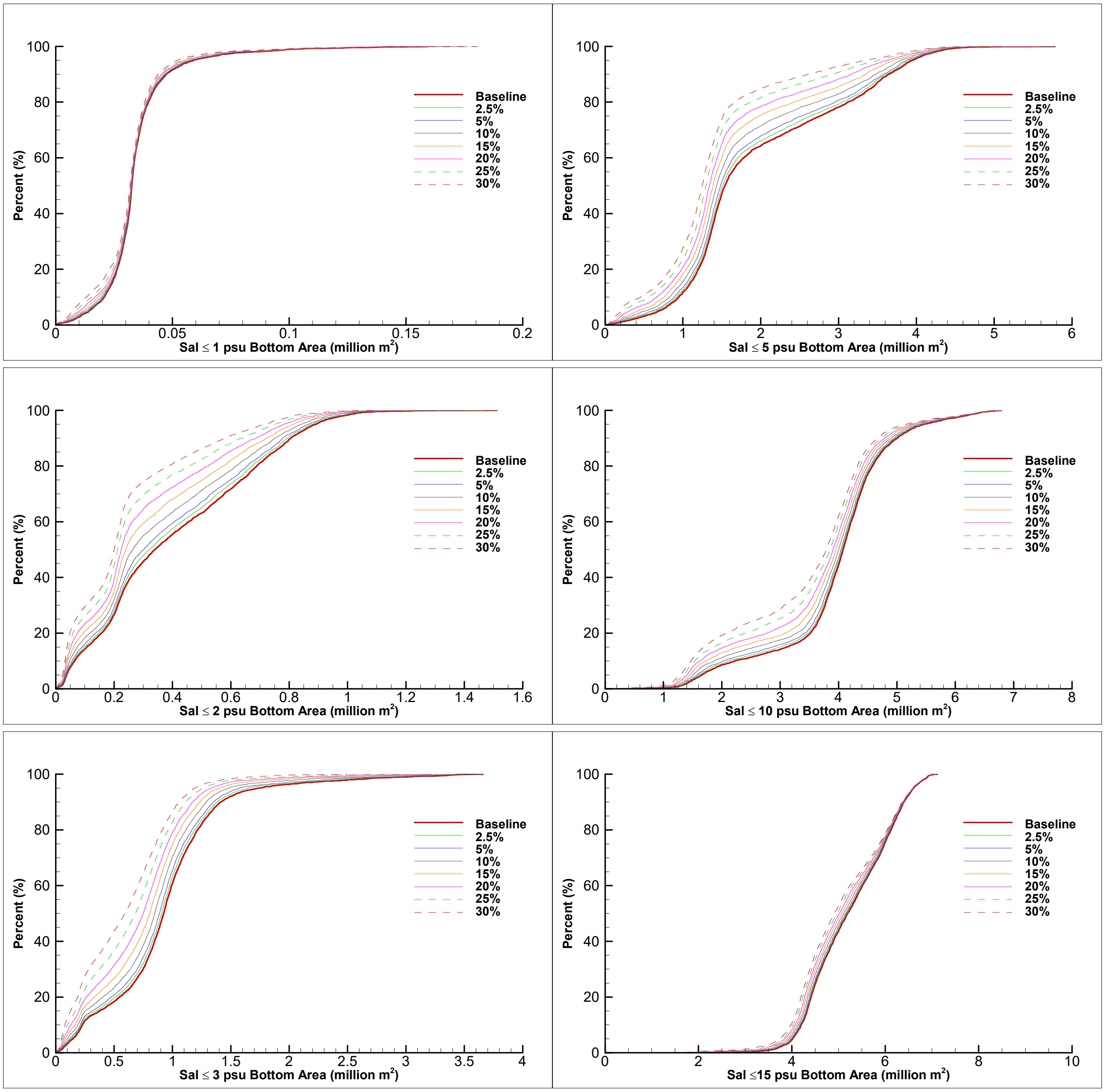

Figure 29. Cumulative distribution functions of simulated bottom areas for various flow reductions for salinity ≤ 1, 2, 3, 5, 10, and 15 psu.

Based on the review comments received for the Crystal River/Kings Bay MFL report, effects of the flow reduction on different types of shoreline should be analyzed separately. Data on Chassahowitzka River shoreline survey was collected by Water & Air Research, Inc. (2018), which found five shore types in the Homosassa River system, including open water, herbaceous, forest, rock/shell, riprap, and seawall. While ripraps and seawalls are altered shores, herbaceous, forest, and rock/shell shores are considered as natural. Analyses of shoreline variations for different salinity ranges under different flow reduction scenarios were done for both altered and natural shores. Tables 16 and 17 shows relative reductions of altered and natural shoreline lengths from these of the BSL condition caused by different flow reductions in the Homosassa River.

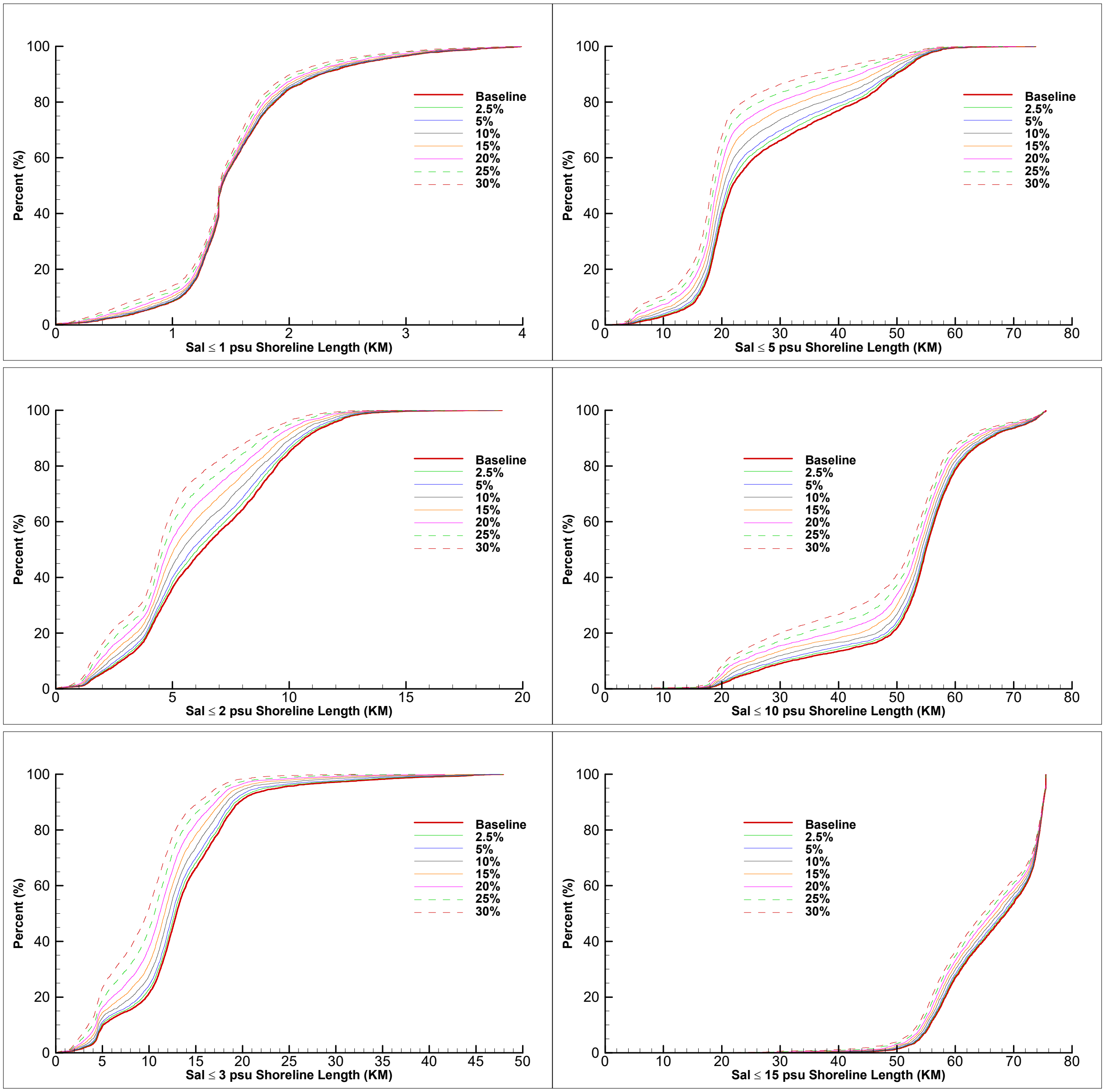

Figure 30. Cumulative distribution functions of simulated shoreline length for various flow reductions for salinity ≤ 1, 2, 3, 5, 10, and 15 psu.

Table 10. Average water volumes of different salinity ranges for 14 flow reduction scenarios.

Reduction Scenario	Average Water Volumes (million m^3)					
	≤ 1	*≤ 2*	*≤ 3*	*≤ 5*	*≤ 10*	*≤ 15*
Baseline	0.024141	0.471965	0.998198	1.947998	3.853637	5.298407
Existing	0.024041	0.460660	0.977017	1.914685	3.829097	5.286259
2.5%	0.024001	0.456731	0.969785	1.903294	3.820637	5.282194
5.0%	0.023850	0.441180	0.941286	1.857378	3.786231	5.265240
7.5%	0.023688	0.425278	0.912393	1.810265	3.750041	5.247493
10.0%	0.023500	0.409306	0.883339	1.762284	3.712853	5.229591
12.5%	0.023283	0.392949	0.853473	1.712752	3.673329	5.210015
15.0%	0.023048	0.376685	0.823623	1.663802	3.633235	5.191329
17.5%	0.022776	0.360324	0.793431	1.614411	3.591322	5.171807
20.0%	0.022470	0.343682	0.761878	1.564456	3.546958	5.150906
22.5%	0.022137	0.327292	0.729756	1.514572	3.501046	5.129846
25.0%	0.021762	0.310942	0.696951	1.463916	3.451607	5.107149
27.5%	0.021352	0.294717	0.663322	1.413711	3.399791	5.084025
30.0%	0.020899	0.278517	0.628256	1.363758	3.346475	5.060391

Table 11. Average bottom areas of different salinity ranges for 14 flow reduction scenarios.

Reduction Scenario	Average Bottom Areas (million m^2)					
	≤ 1	*≤ 2*	*≤ 3*	*≤ 5*	*≤ 10*	*≤ 15*
Baseline	0.022270	0.319397	0.727974	1.522543	3.047483	4.106031
Existing	0.022212	0.311641	0.712305	1.496210	3.029149	4.097350
2.5%	0.022189	0.308945	0.706929	1.487245	3.022782	4.094403
5.0%	0.022104	0.298305	0.685807	1.451241	2.996925	4.082263
7.5%	0.022007	0.287396	0.664377	1.414277	2.969769	4.069547
10.0%	0.021895	0.276428	0.642889	1.376689	2.941914	4.056705
12.5%	0.021762	0.265236	0.620881	1.337702	2.912151	4.042659
15.0%	0.021615	0.254143	0.598935	1.299208	2.881732	4.029256
17.5%	0.021446	0.242977	0.576672	1.260379	2.849834	4.015280
20.0%	0.021255	0.231590	0.553280	1.221207	2.815811	4.000316
22.5%	0.021043	0.220354	0.529229	1.182090	2.780421	3.985182
25.0%	0.020802	0.209174	0.504682	1.142281	2.742265	3.968833
27.5%	0.020534	0.198052	0.479354	1.103114	2.702178	3.952233
30.0%	0.020231	0.186937	0.452827	1.064224	2.660536	3.935134

Table 12. Average shoreline lengths of different salinity ranges for 14 flow reduction scenarios.

Reduction Scenario	Average Shoreline Lengths (KM)					
	≤ 1	*≤ 2*	*≤ 3*	*≤ 5*	*≤ 10*	*≤ 15*
Baseline	1.617573	6.732102	13.846741	28.417436	54.317439	68.618924
Existing	1.613954	6.624073	13.606412	27.965036	54.029596	68.503090
2.5%	1.612526	6.585891	13.523871	27.808646	53.926755	68.461775
5.0%	1.606833	6.435934	13.197298	27.188131	53.516569	68.296217
7.5%	1.600584	6.280540	12.868501	26.546707	53.086580	68.123464
10.0%	1.593385	6.125207	12.542025	25.892627	52.642694	67.948151
12.5%	1.584912	5.966737	12.206605	25.216963	52.168671	67.755073
15.0%	1.575573	5.805734	11.868038	24.552271	51.679470	67.572983
17.5%	1.564862	5.643192	11.522754	23.895091	51.163957	67.380696
20.0%	1.553096	5.475445	11.155612	23.245468	50.609974	67.176481
22.5%	1.539539	5.309125	10.774227	22.598643	50.038339	66.970289
25.0%	1.524200	5.139449	10.387786	21.939389	49.420316	66.744622
27.5%	1.507239	4.970264	9.982925	21.285842	48.772673	66.513079
30.0%	1.488604	4.798092	9.550700	20.639280	48.086547	66.272555

Table 13. Relative reductions of water volume for various salinity ranges under different flow reduction scenarios.

Reduction Scenario	Relative Reduction (Water Volume)					
	≤ 1	*≤ 2*	*≤ 3*	*≤ 5*	*≤ 10*	*≤ 15*
Existing	0.41%	2.40%	2.12%	1.71%	0.64%	0.23%
2.5%	0.58%	3.23%	2.85%	2.29%	0.86%	0.31%
5.0%	1.21%	6.52%	5.70%	4.65%	1.75%	0.63%
7.5%	1.88%	9.89%	8.60%	7.07%	2.69%	0.96%
10.0%	2.66%	13.28%	11.51%	9.53%	3.65%	1.30%
12.5%	3.55%	16.74%	14.50%	12.08%	4.68%	1.67%
15.0%	4.53%	20.19%	17.49%	14.59%	5.72%	2.02%
17.5%	5.65%	23.65%	20.51%	17.12%	6.81%	2.39%
20.0%	6.92%	27.18%	23.67%	19.69%	7.96%	2.78%
22.5%	8.30%	30.65%	26.89%	22.25%	9.15%	3.18%
25.0%	9.85%	34.12%	30.18%	24.85%	10.43%	3.61%
27.5%	11.55%	37.56%	33.55%	27.43%	11.78%	4.05%
30.0%	13.43%	40.99%	37.06%	29.99%	13.16%	4.49%
Trigger (%)	***> 30%***	***11.24%***	***12.92%***	***15.41%***	***> 30%***	***> 30%***

Table 14. Relative reductions of bottom areas for various salinity ranges under different flow reduction scenarios.

Reduction Scenario	**Relative Reduction (Bottom Area)**					
	≤ 1	*≤ 2*	*≤ 3*	*≤ 5*	*≤ 10*	*≤ 15*
Existing	0.26%	2.43%	2.15%	1.73%	0.60%	0.21%
2.5%	0.36%	3.27%	2.89%	2.32%	0.81%	0.28%
5.0%	0.75%	6.60%	5.79%	4.68%	1.66%	0.58%
7.5%	1.18%	10.02%	8.74%	7.11%	2.55%	0.89%
10.0%	1.68%	13.45%	11.69%	9.58%	3.46%	1.20%
12.5%	2.28%	16.96%	14.71%	12.14%	4.44%	1.54%
15.0%	2.94%	20.43%	17.73%	14.67%	5.44%	1.87%
17.5%	3.70%	23.93%	20.78%	17.22%	6.49%	2.21%
20.0%	4.56%	27.49%	24.00%	19.79%	7.60%	2.57%
22.5%	5.51%	31.01%	27.30%	22.36%	8.76%	2.94%
25.0%	6.59%	34.51%	30.67%	24.98%	10.02%	3.34%
27.5%	7.80%	37.99%	34.15%	27.55%	11.33%	3.75%
30.0%	9.16%	41.47%	37.80%	30.10%	12.70%	4.16%
Trigger (%)	***>30%***	***11.10%***	***12.74%***	***15.32%***	***> 30%***	***> 30%***

Table 15. Relative reductions of shoreline length for various salinity ranges under different flow reduction scenarios.

Reduction Scenario	**Relative Reduction (Shoreline Length)**					
	≤ 1	*≤ 2*	*≤ 3*	*≤ 5*	*≤ 10*	*≤ 15*
Existing	0.22%	1.60%	1.74%	1.59%	0.53%	0.17%
2.5%	0.31%	2.17%	2.33%	2.14%	0.72%	0.23%
5.0%	0.66%	4.40%	4.69%	4.33%	1.47%	0.47%
7.5%	1.05%	6.71%	7.06%	6.58%	2.27%	0.72%
10.0%	1.50%	9.01%	9.42%	8.88%	3.08%	0.98%
12.5%	2.02%	11.37%	11.84%	11.26%	3.96%	1.26%
15.0%	2.60%	13.76%	14.29%	13.60%	4.86%	1.52%
17.5%	3.26%	16.17%	16.78%	15.91%	5.81%	1.80%
20.0%	3.99%	18.67%	19.44%	18.20%	6.83%	2.10%
22.5%	4.82%	21.14%	22.19%	20.48%	7.88%	2.40%
25.0%	5.77%	23.66%	24.98%	22.80%	9.02%	2.73%
27.5%	6.82%	26.17%	27.90%	25.10%	10.21%	3.07%
30.0%	7.97%	28.73%	31.03%	27.37%	11.47%	3.42%
Trigger (%)	***> 30%***	***16.28%***	***15.71%***	***16.51%***	***> 30%***	***> 30%***

Table 16. Relative reductions of altered shoreline length for various salinity ranges under different flow reduction scenarios in the Homosassa River.

Reduction Scenario	**Relative Reduction (Altered Shoreline Length)**					
	Sal ≤ 1	*≤ 2*	*≤ 3*	*≤ 5*	*≤ 10*	*≤ 15*
Existing	0.18%	1.37%	1.20%	0.81%	0.21%	0.04%
2.5%	0.25%	1.85%	1.62%	1.10%	0.29%	0.05%
5.0%	0.54%	3.76%	3.28%	2.24%	0.59%	0.10%
7.5%	0.85%	5.73%	4.99%	3.44%	0.91%	0.16%
10.0%	1.20%	7.71%	6.76%	4.69%	1.25%	0.22%
12.5%	1.63%	9.71%	8.58%	6.00%	1.61%	0.29%
15.0%	2.08%	11.74%	10.47%	7.35%	2.00%	0.35%
17.5%	2.61%	13.81%	12.40%	8.74%	2.41%	0.42%
20.0%	3.19%	15.92%	14.43%	10.21%	2.86%	0.50%
22.5%	3.85%	17.99%	16.50%	11.71%	3.34%	0.58%
25.0%	4.61%	20.11%	18.65%	13.28%	3.86%	0.66%
27.5%	5.44%	22.24%	20.83%	14.90%	4.43%	0.76%
30.0%	6.35%	24.39%	23.11%	16.57%	5.02%	0.85%
Trigger (%)	***>30%***	***18.91%***	***20.69%***	***27.65%***	***>30%***	***>30%***

Table 17. Relative reductions of natural shoreline length for various salinity ranges under different flow reduction scenarios in the Homosassa River.

Reduction Scenario	**Relative Reduction (Natural Shoreline Length)**					
	Sal ≤ 1	*≤ 2*	*≤ 3*	*≤ 5*	*≤ 10*	*≤ 15*
Existing	0.10%	1.44%	2.18%	2.07%	0.67%	0.22%
2.5%	0.13%	1.94%	2.91%	2.78%	0.90%	0.29%
5.0%	0.28%	3.93%	5.83%	5.59%	1.85%	0.60%
7.5%	0.47%	5.98%	8.72%	8.48%	2.84%	0.92%
10.0%	0.67%	8.02%	11.51%	11.41%	3.85%	1.25%
12.5%	0.90%	10.11%	14.30%	14.43%	4.93%	1.61%
15.0%	1.19%	12.23%	17.05%	17.36%	6.05%	1.95%
17.5%	1.51%	14.35%	19.81%	20.20%	7.21%	2.30%
20.0%	1.87%	16.55%	22.75%	22.97%	8.46%	2.68%
22.5%	2.27%	18.75%	25.80%	25.68%	9.75%	3.06%
25.0%	2.73%	20.97%	28.83%	28.45%	11.13%	3.48%
27.5%	3.25%	23.17%	32.03%	31.15%	12.57%	3.90%
30.0%	3.83%	25.42%	35.47%	33.78%	14.09%	4.35%
Trigger (%)	***>30%***	***18.24%***	***13.14%***	***12.99%***	***>30%***	***>30%***

4.4 Results of Manatee Thermal Habitats

One of the purposes for considering thermal habitats (water volume and surface area of certain temperature ranges) is to protect manatees during the coldest days in winter by ensuring that the warm-water refuge in the estuary won't be significantly reduced because of SGD reduction. Manatees have hard time to survive in water colder than 20 ºC for a prolonged period, because of their inability to increase their metabolic rates in cold water to compensate the increased rate of body heat loss, as they have a high thermal conductance, or poor insulation (Worthy et al., 2000). Since SGDs have a relatively stable temperature of > 22.0 ºC in winter, they are able to provide a quite big area of warm-water refuge for manatees when water temperature in the Gulf drops to 20 ºC or lower.

Following the similar MFL-evaluation procedure used during the previous MFL evaluations for the Homosassa River and for other spring-fed estuaries in the District (e.g. Weeki Wachee River, Crystal River/Kings, and Chassahowitzka River), water volumes and surface areas of three temperature ranges, namely < 15 ºC, between 15 and 20 ºC, and ≥ 20 ºC, were calculated for various flow reduction scenarios. Figure 31 shows time series (30-minute interval) plots of water volumes and surface areas for temperature < 15 ºC, ≥ 15 ºC but < 20 ºC, and ≥ 20 ºC under the BSL condition. For comparison, time series of < 15 ºC, ≥ 15 ºC but < 20 ºC, and ≥ 20 ºC thermal habits for the 10% flow reduction scenario are shown in Figure 32. Time series plots of thermal habitats for other flow reduction scenarios are similar and omitted here.

It should be noted that the computation of 15 – 20 ºC or ≥ 20 ºC volume and surface area only includes grids containing at least one continuous noncold (15 – 20 ºC) or warm water (≥ 20 ºC) layer with a thickness of 1.158 m (3.8 feet) or more in the water column. This 1.158 m thickness constrain for the warm water layer is determined from the size of an adult manatee to ensure that the animal is fully enclosed in warm water. Any grids that do not meet the 1.158 m criterion are excluded from the computation of 15 – 20 ºC and ≥ 20 ºC volumes and surface areas.

As expected, during the warm months of the year, water temperature in the Homosassa River is ≥ 20 ºC and there exist no water volume and surface area that are < 20 ºC. As a result, 15 – 20 ºC habitats and < 15 ºC habitats are non-existent. During the manatee season, which is defined as November – March in this MFL evaluation, water temperature in the Homosassa River can drop to 10 ºC or lower, a significant amount of < 15 ºC water volume and surface area exist in the estuary. During the coldest days of the year, the total ≥ 20 ºC volume with a layer thickness of 1.158 m or more became significantly smaller than warm days.

Although the manatee season lasts five months long, warm water refuge for manatee are critical only during or right after a cold front event. The Gulf water during the manatee season generally varies between 15 – 25 ºC most of the time; however, during severe cold front days, Gulf water can drop to a couple of degree below 10 ºC. When the Gulf water is only a few degrees warmer or colder than the spring flow temperature, reducing spring flow won't have much an effect on thermal habitats. As such, the only time when thermal habitats are sensitive to SGD reduction would be during the cold days when the Gulf water is much colder than spring flows out of the vents. Clearly, considering the overall warm thermal habitat reduction for the entire manatee season or several manatee seasons is meaningless, because such a parameter barely responds to flow reduction. As a result, thermal analysis in this study considers only short time scales, in the order of several days or several hours when warm water or noncold water thermal habitats become less available to manatees during or right after cold front events.

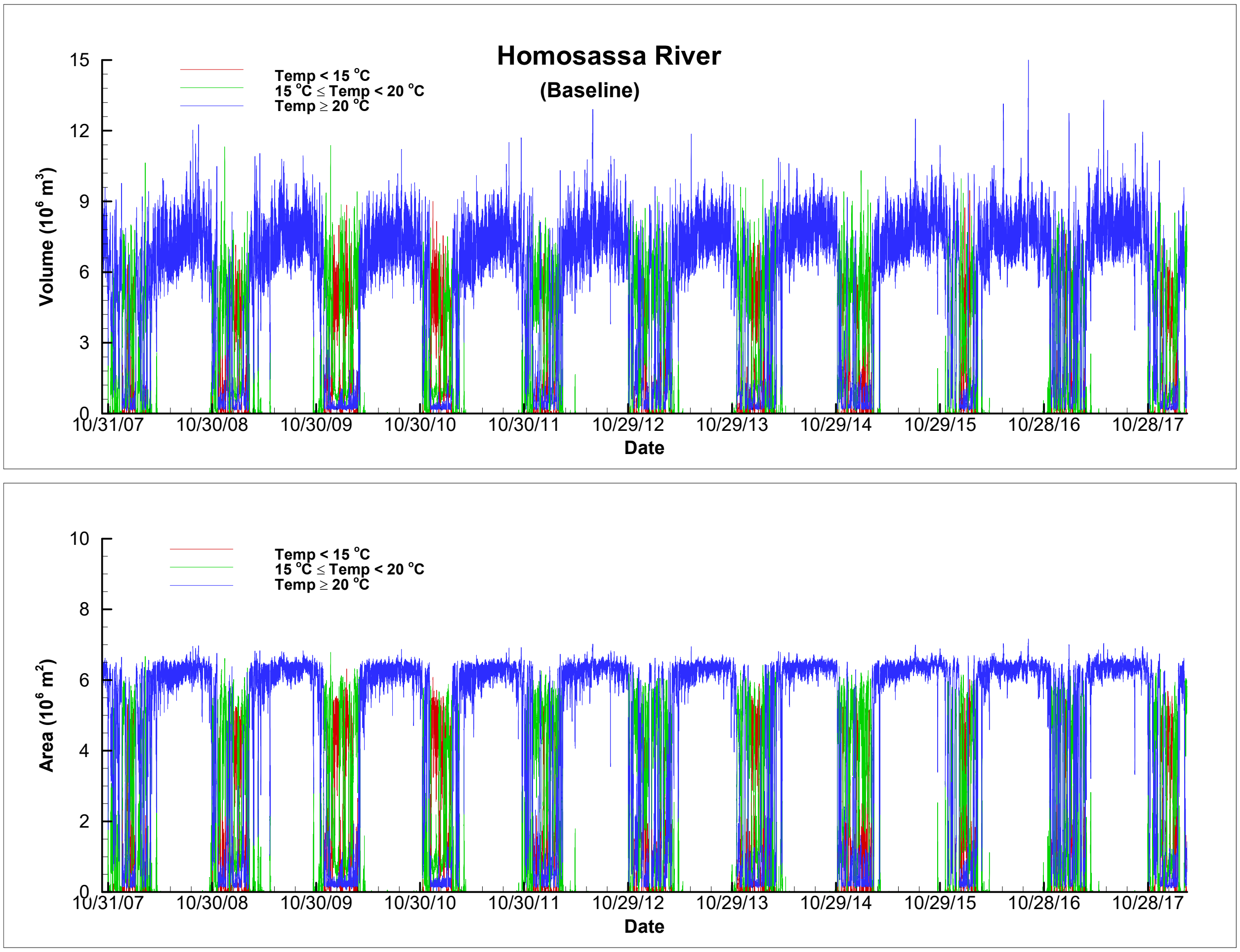

Figure 31. Time series of simulated water volumes (top panel) and surface areas (bottom panel) for temperature < 15 ºC, 15 – 20 ºC, and ≥ 20 ºC under the baseline flow condition during the 125-month simulation period.

There are also physiological reasons for considering a relatively short time scale in studying effects of flow reduction to thermal habitats. Manatees have a low metabolic rate and high thermal conductance, and they have a limited ability to raise their metabolic rate to keep them warm during cold days. Consequently, manatees are not capable of surviving in cold environment for a long time. Any exposure to water below 20 ºC for longer than 4 – 7 days could result in disastrous losses to the manatee population (Rouhani et al., 2007). When water temperature is further drops to below 15 °C, manatees cannot withstand the cold for more than 4 hours (Janicki Environmental and Applied Technology & Management, 2007).

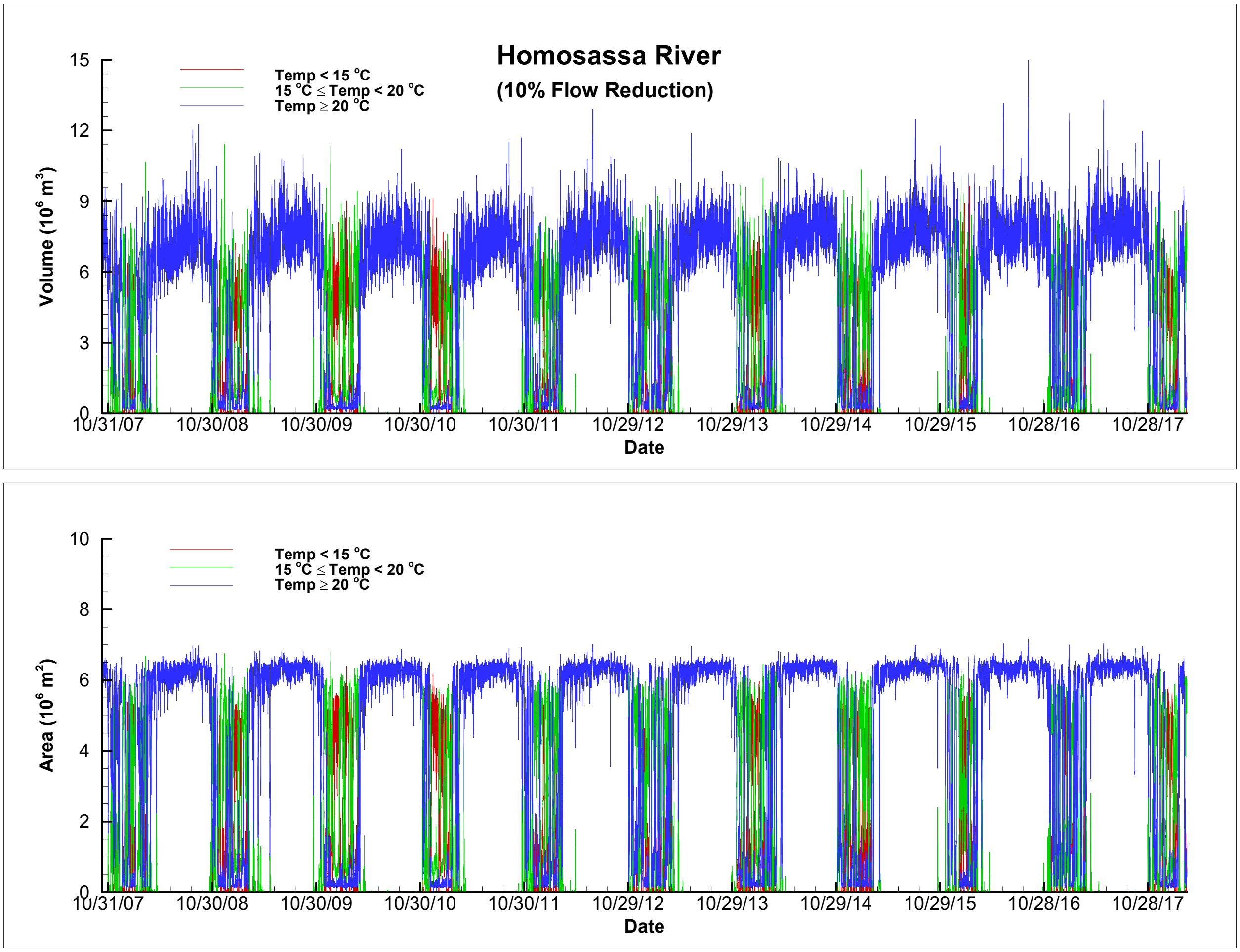

Figure 32. Time series of simulated water volumes (top panel) and surface areas (bottom panel) for temperature < 15 °C, 15 – 20 °C, and ≥ 20 °C under the 10% flow reduction during the 125-month simulation period.

Because of these physiological constraints for manatees, the MFL evaluation generally takes two temporal scales into consideration. One is no longer than 4 days (96 hours) for the warm water habitats with temperature 20 °C or higher, and the other is about 4 hours for the noncold water habitats with temperature 15 °C or higher. The former is considered as a chronic condition for manatees, while the latter is an acute condition for manatee. To be conservative and consistent with previous MFL evaluations (e.g., Rouhani et al., 2007; Janicki Environmental and Applied Technology & Management, 2007; Chen, 2017), the time scale for the chronic condition is further reduced to 72 hours.

In the analysis of thermal habitats for the chronic and acute conditions, 72-hour and 4-hour moving averages of simulated water volumes and surface areas for temperature ≥ 20 °C and ≥ 15 °C, respectively were first calculated. The 72-hour and 4-hour moving averages at a time point t (in hours) were simply calculated as the arithmetic means during [t-36, t+36] and [t-2, t+2], respectively.

Figure 33 shows time series of 72-hour moving averages of volume (top panel) and surface area (bottom panel) for temperature ≥ 20 ºC under various flow conditions, including the baseline, existing, 5%, 10%, 15%, 20%, 25%, and 30% flow reductions. The small inserts are plots showing available warm water (≥ 20 ºC) volumes and areas during and after a typical cold front in early 2011. Time series of 4-hour moving averages of water volume and surface area for temperature ≥ 15 ºC under various flow conditions are shown in Figure 34, in which noncold water habitats during and after a typical cold front are also plotted in small inserts.

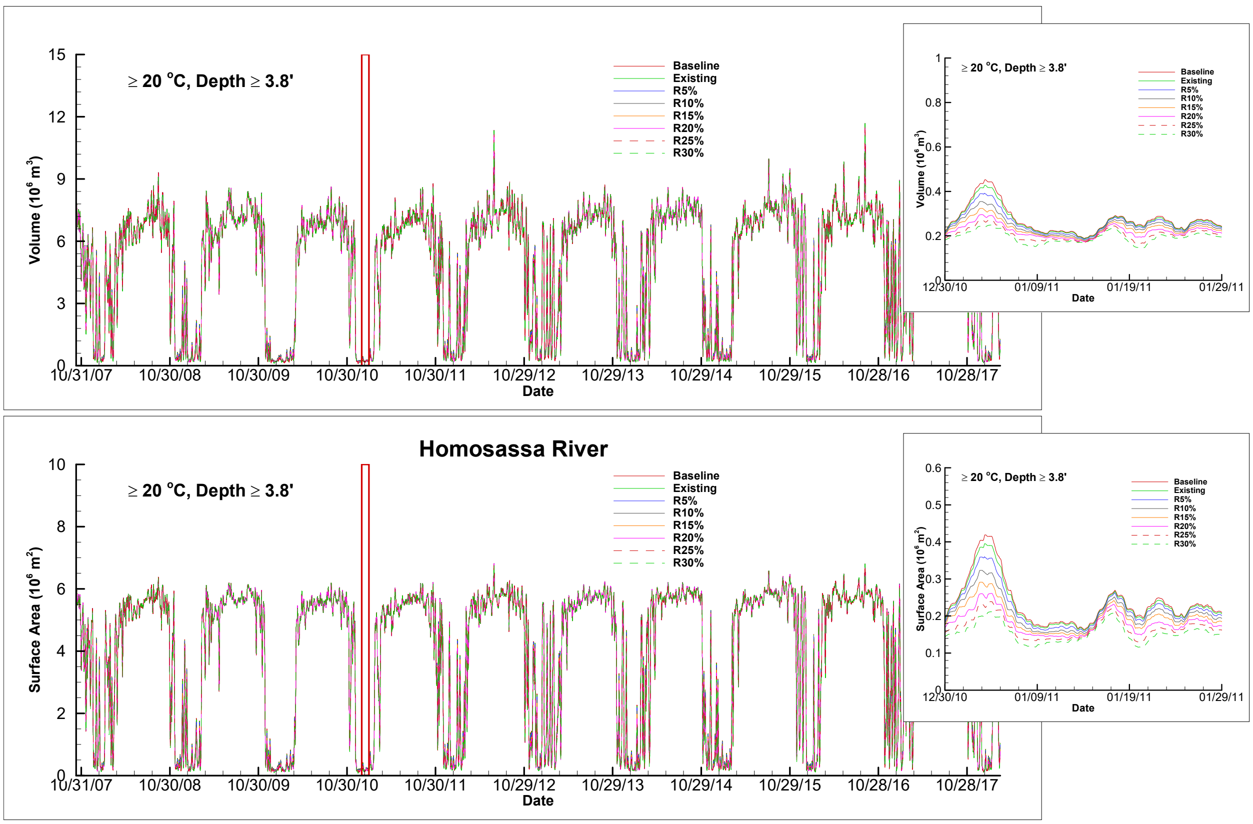

Figure 33. Comparisons of time series of 72-hour moving averages of ≥ 20 ºC volume (top panel) and surface area for the baseline, existing, 5%, 10%, 15%, 20%, 25%, and 30% flow reduction scenarios during the 125-month simulation period.

An analysis of the 72-hour moving averages of warm water volume and surface area for all the time points simulated during manatee season is neither practical nor necessary. Similar to the procedure used in the Crystal River/Kings Bay MFL evaluation (Chen, 2017), 72-hour averages of warm water volume and surface area at several critical time points were chosen to examine the effect of flow reduction on thermal habitats with temperature ≥ 20 ºC. These critical time points included times when the lowest air temperatures were recorded at the weather stations in 2010 and 2018 and the time when the lowest overall water temperature in the Homosassa River occurred. Times at or around which ≥ 20 ºC volume and surface area reached their minima were also examined.

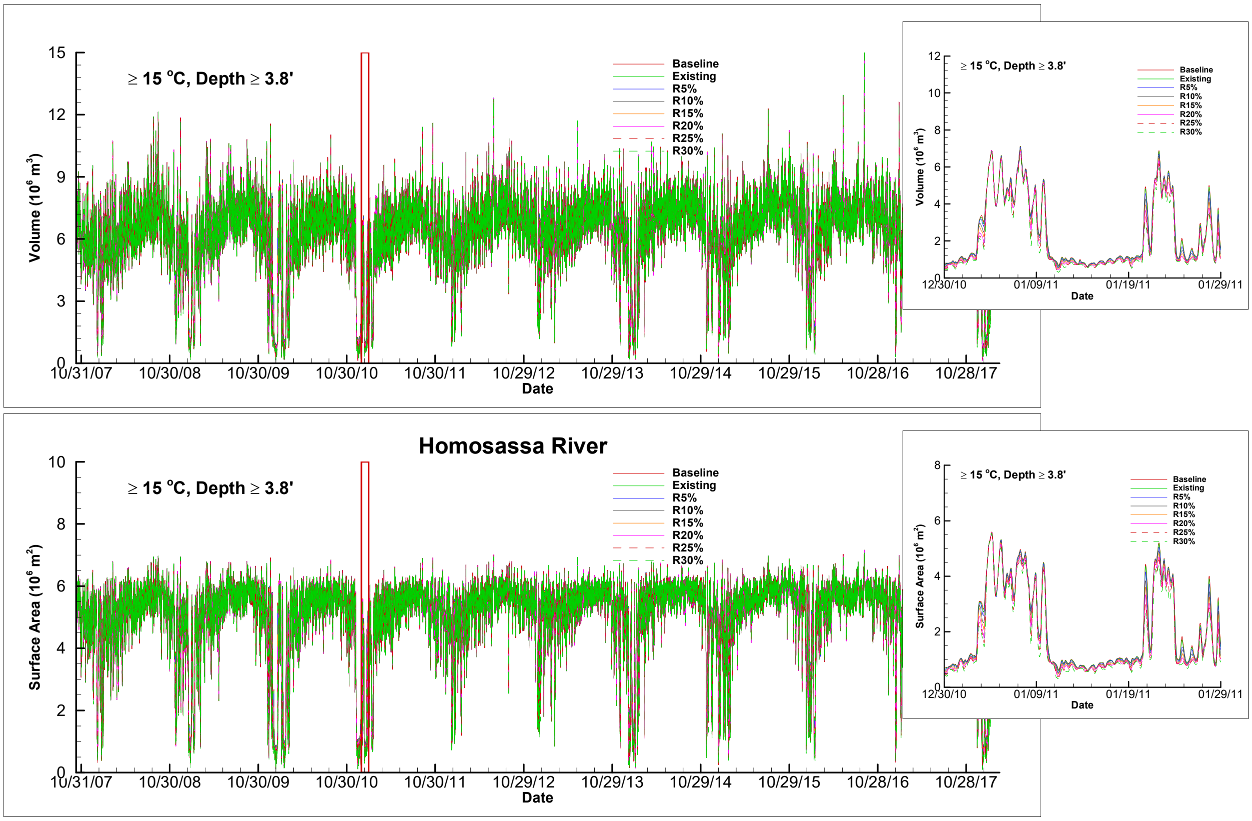

Figure 34. Comparisons of time series of 4-hour moving averages of ≥ 15 ºC volume (top panel) and surface area for the baseline, existing, 5%, 10%, 15%, 20%, 25%, and 30% flow reduction scenarios during the 125-month simulation period.

The coldest air temperature measured in the Homosassa/Chassahowitzka area during the entire 125 months of the simulation period was -9.13 ºC, which was recorded at 7:30 AM on January 18, 2018 at the Lecanto High School. The area also experienced a couple of severe cold fronts during the first couple of months in 2010. The most severe cold front event was during January 4, 2010 - January 15, 2010, when daily lows of air temperature were all below 0 ºC during these 12 days, making the longest period on record for consecutive days with freezing air temperature in the area. The coldest air temperature recorded was -7.78 ºC during these 12 days and recorded at 6:00 AM on January 11, 2010. Although -7.78 ºC is not the coldest air temperature on record for the area, the longevity of the coldness makes this time point and several hours around it to be critical about the availability of the useable thermal habitats for manatees. Figure 35 shows measured air temperatures during the coldest days in 2010 (top panel) and 2018 (bottom panel).

In general, water temperature in the Homosassa River has a delay of response when a cold front moves in. Other factors such as the temperature boundary conditions at the downstream boundary, SGDs, heat fluxes at the free surface, and transport processes within the water body also affect temperature distributions in the river. As a result, water temperature in the Homosassa River does not necessarily correlate well with air temperature. Based on available temperature data, the overall lowest water temperature during the 125-month simulation period in the Homosassa River is found to be at 1:00 AM on January 12, 2010.

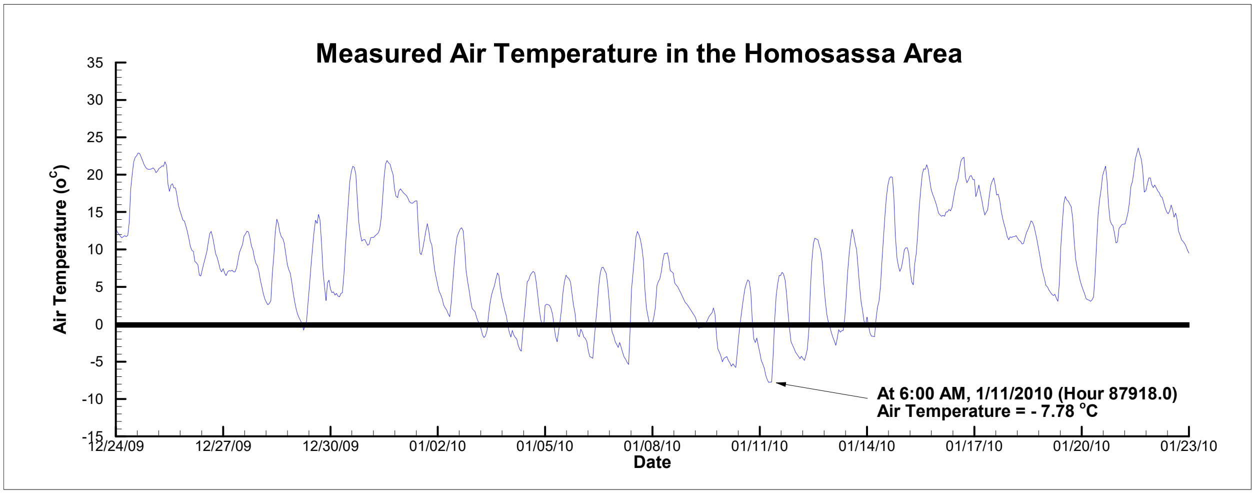

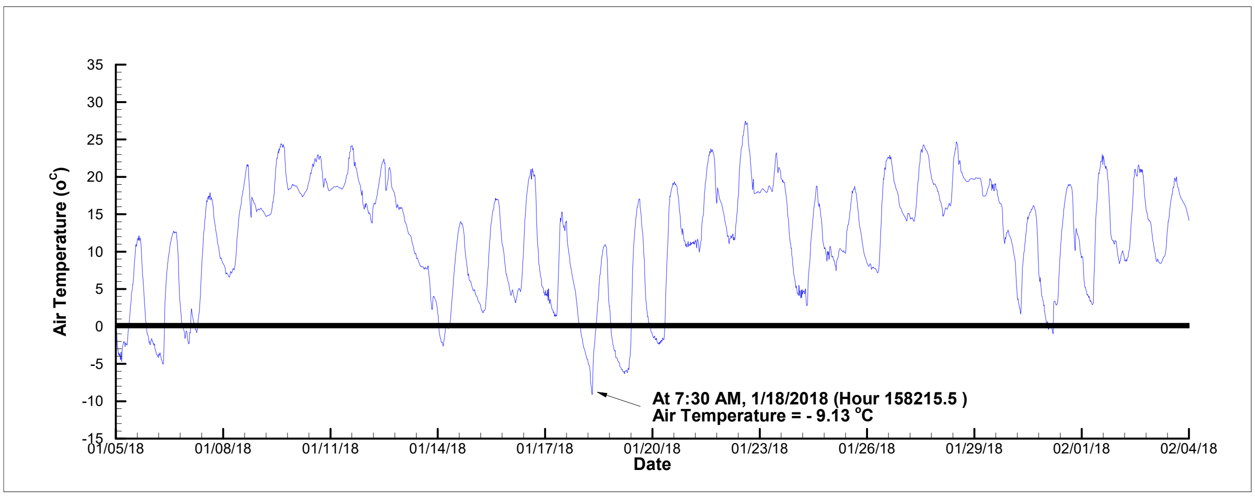

Figure 35. Coldest days with the lowest air temperatures measured in 2010 and 2018 in the Homosassa area.

Table 18 shows 72-hour averages of water volume for the chronic condition for manatees at five critical time points in the Homosassa River. Besides the coldest air in 2010 (6:00 AM, 1/11/2010) and in 2018 (7:30 AM, 1/18/2018) as well as the coldest water in the river (1:00 AM, 1/12/2010), two time points (12:00 AM and 3:00 AM, 12/14/2010) were also included in the table. During the 72-hour period centered at 3:00 AM, 12/14/2010, the river had the smallest amount of 72-hour average of ≥ 20 ºC volume (154,186 m^3) under the BSL condition. Three hours earlier, at 12:00 AM, 12/14/2010, the 72-hour average of ≥ 20 ºC volume had the most sensitive reaction to the SGD reduction among the lowest 0.02% warm water volumes in the river. With a 30% SGD reduction, the lowest 72-hour average of ≥ 20 ºC volume during the 125 months was 94,603 cubic meters, or 3,340,876 cubic feet (24,991,464 gallons).

Because a reduction of SGD not only reduces the amount of warm water entering the estuarine system but also more or less affects other physical processes and parameters (e.g., density distribution, mixing, baroclinic forces, heat exchanges at the free surface, velocities, elevations, etc.) in the river, which eventually affect the temperature distribution in the water body. As the interaction among these processes and parameters are highly nonlinear, the relationship between water temperature and the percentage of the SGD reduction at a fixed spatial location and a fixed time point is not necessarily monotonic. A close examination of Figure 33 shows that due to the nonlinear interactions, an SGD reduction can cause the time series of the 72-hour moving averages of ≥ 20 ºC volume and surface area to have a time drift.

Table 18. Seventy-two-hour averages of warm water volumes (in m^3) under the chronic condition for manatees at five critical time points.

	72-Hour Time Window				
	#1	*#2*	*#3*	*#4*	*#5*
	1/9/10 18:00 - 1/12/10 18:00	*1/10/10 13:00 - 1/13/10 13:00*	*12/12/10 12:00 - 12/15/10 12:00*	*12/12/10 15:00 - 12/15/10 15:00*	*1/16/18 19:30 - 1/19/18 19:30*
Baseline	199944	225165	155472	154186	239217
Existing	197226	221655	152805	151650	234271
2.5%	197347	221816	149624	148513	233811
5.0%	195321	218720	143510	143029	227046
7.5%	194029	215784	139064	138659	223353
10.0%	192927	212867	132013	131632	222071
12.5%	191866	210421	128214	128014	220357
15.0%	190859	207920	122062	121825	217440
17.5%	189297	204984	116885	116501	215315
20.0%	187861	202335	111697	111111	213130
22.5%	186294	198721	107430	106290	210760
25.0%	184506	194494	103674	102373	206857
27.5%	182478	191767	100102	98801	203262
30.0%	179212	186990	95904	94603	200776

Relative changes of the 72-hour average of the ≥ 20 ºC water volume from the baseline volumes at the five critical time points are shown in Table 19, in the form of percentage reduction. From Tables 18 and 19, it can be seen that at the time of the coldest air or water, the 72-hour average of the ≥ 20 ºC water volume is generally not lowest and does not react to the SGD reduction in a most sensitive way either. The most reasonable time frame for examining SGD effects on ≥ 20 ºC water volume is at or near the time point when the thermal habitats reach the lowest values under the chronic condition. As can be seen from Table 19, the 72-hour average of

≥ 20 ºC water volume was most sensitive to the SGD reduction at 12:00 AM, 12/14/2010, or during 12:00 PM, 12/12/2010 – 12:00 PM, 12/15/2010. With a 9.95% SGD reduction, the 72-hour average of ≥ 20 ºC water volume was reduced by 15%.

Table 19. Percentage reductions of the 72-hour average of the ≥ 20 ºC water volume relative to the corresponding baseline volumes at five critical time points.

	72-Hour Time Window				
	#1	*#2*	*#3*	*#4*	*#5*
	1/9/10 18:00 - 1/12/10 18:00	*1/10/10 13:00 - 1/13/10 13:00*	*12/12/10 12:00 - 12/15/10 12:00*	*12/12/10 15:00 - 12/15/10 15:00*	*1/16/18 19:30 - 1/19/18 19:30*
Existing	1.36%	1.56%	1.72%	1.64%	2.07%
2.5%	1.30%	1.49%	3.76%	3.68%	2.26%
5.0%	2.31%	2.86%	7.69%	7.24%	5.09%
7.5%	2.96%	4.17%	10.55%	10.07%	6.63%
10.0%	3.51%	5.46%	15.09%	14.63%	7.17%
12.5%	4.04%	6.55%	17.53%	16.97%	7.88%
15.0%	4.54%	7.66%	21.49%	20.99%	9.10%
17.5%	5.32%	8.96%	24.82%	24.44%	9.99%
20.0%	6.04%	10.14%	28.16%	27.94%	10.91%
22.5%	6.83%	11.74%	30.90%	31.06%	11.90%
25.0%	7.72%	13.62%	33.32%	33.60%	13.53%
27.5%	8.74%	14.83%	35.61%	35.92%	15.03%
30.0%	10.37%	16.95%	38.31%	38.64%	16.07%
Triger	***>30%***	***27.70%***	***9.95%***	***10.40%***	***27.45%***

Like Table 18, Table 20 lists 72-hour averages of surface area for the chronic condition for manatees at five critical time points in the Homosassa River. The time point when the river had the least 72-hour average of ≥ 20 ºC surface area was at 12:00 AM, 12/14/2010 and 30 minutes before this time point at 11:30 PM, 12/13/2010, the 72-hour average of ≥ 20 ºC surface area had the most sensitive reaction to the SGD reduction among the lowest 0.02% warm water surface area. The smallest warm water surface area for the entire 125 months of simulation was 122,057 m^2 under the BSL condition. With a 30% SGD reduction, this amount was reduced to 75,978 m^2, or 817,820 square feet, which is about 18.77 acres.

Relative percentage changes of ≥ 20 ºC surface area from the baseline surface area are presented in Table 21, in a similar way as that in Table 19. As the SGD reduction increased from 0% to 30%, the 72-hour average of ≥ 20 ºC surface area could be reduced by more than 15% at all five critical time points. It was most sensitive to the SGD reduction at 11:30 PM, 12/13/2010, or during 11:30 AM, 12/12/2010 – 11:30 AM, 12/15/2010, when a 10.40% SGD reduction could cause a 15% reduction of the 72-hour average of ≥ 20 ºC surface area.

Table 20. Seventy-two-hour averages of warm surface areas (in m^2) for the chronic condition at five critical time points.

	72-Hour Time Window				
	#1	*#2*	*#3*	*#4*	*#5*
	1/9/10 18:00 - 1/12/10 18:00	*1/10/10 13:00 - 1/13/10 13:00*	*12/12/10 11:30 - 12/15/10 11:30*	*12/12/10 12:00 - 12/15/10 12:00*	*1/16/18 19:30 - 1/19/18 19:30*
Baseline	171647	198121	122169	122057	205972
Existing	168429	193779	119892	119780	201630
2.5%	168504	194003	117585	117473	200731
5.0%	165976	190543	113615	113575	194566
7.5%	164181	186701	109544	109504	190647
10.0%	162880	183155	104324	104283	189703
12.5%	161439	179954	101343	101239	187601
15.0%	160143	176875	96990	96936	183928
17.5%	157728	172694	92932	92941	181909
20.0%	155703	169049	89168	89176	179280
22.5%	153483	164833	85269	85278	176946
25.0%	150876	158756	82267	82275	172851
27.5%	147938	155213	79459	79466	168758
30.0%	143744	149150	75981	75978	166045

Table 21. Percentage reductions of the 72-hour average of the ≥ 20 ºC surface area relative to the corresponding baseline surface areas at five critical time points.

	72-Hour Time Window				
	#1	*#2*	*#3*	*#4*	*#5*
	1/9/10 18:00 - 1/12/10 18:00	*1/10/10 13:00 - 1/13/10 13:00*	*12/12/10 11:30 - 12/15/10 11:30*	*12/12/10 12:00 - 12/15/10 12:00*	*1/16/18 19:30 - 1/19/18 19:30*
Existing	1.87%	2.19%	1.86%	1.87%	2.11%
2.5%	1.83%	2.08%	3.75%	3.76%	2.54%
5.0%	3.30%	3.82%	7.00%	6.95%	5.54%
7.5%	4.35%	5.76%	10.33%	10.28%	7.44%
10.0%	5.11%	7.55%	14.61%	14.56%	7.90%
12.5%	5.95%	9.17%	17.05%	17.06%	8.92%
15.0%	6.70%	10.72%	20.61%	20.58%	10.70%
17.5%	8.11%	12.83%	23.93%	23.85%	11.68%
20.0%	9.29%	14.67%	27.01%	26.94%	12.96%
22.5%	10.58%	16.80%	30.20%	30.13%	14.09%

25.0%	12.10%	19.87%	32.66%	32.59%	16.08%
27.5%	13.81%	21.66%	34.96%	34.89%	18.07%
30.0%	16.26%	24.72%	37.81%	37.75%	19.38%
Triger	***28.71%***	***20.44%***	***10.40%***	***10.44%***	***24.00%***

As stated above, when water temperature drops to below 15 ºC, the condition for manatees becomes very severe, as it becomes very harsh for manatees in an environment with water lower than 15 ºC for more than four hours. Naturally, manatees try to avoid < 15 ºC habitats and find warmer habitats to survive in these acute conditions. As such, the existence and extension of ≥ 15 ºC habitats are critical and the analysis of thermal habitats under the acute condition becomes the analysis of thermal habitats ≥ 15 ºC, which are not supposed to be reduced more than 15% in the 4-hour period. This approach is consistent with analyses of salinity and thermal habitats in our previous MFL evaluations, as we focus on reductions of favorable habitats, not on the increases of unfavorable habitats.

The ≥ 15 ºC thermal habitats are simply the summations of ≥ 20 ºC habitats and those between 15 and 20 ºC. Similar to the analysis for the chronic condition, several critical time points were examined, including those when the air temperature were lowest in 2010 and 2018, water temperature in the river was coldest, the 4-hour average of ≥ 15 ºC thermal habitats were lowest, and noncold habitats were most sensitive to the SGD reduction among the lowest 0.02% of thermal habitats.

Table 22 shows 4-hour averages of water volume for the acute condition for manatees at six critical time points in the Homosassa River. At 10:00 AM, 12/14/2010, the river had the smallest amount of 4-hour average of ≥ 15 ºC volume for the BSL condition; however, as the flow reduction increases to greater than 12.5%, the time of lowest 4-hour average of ≥ 15 ºC water volume shifts to 12:000 PM, 1/2/2018. As such, both the time points at 10:00 AM, 12/14/2010 and 12:000 PM, 1/2/2018 were considered as the time points of lowest 4-hour average of ≥ 15 ºC volume. At 7:00 AM, 12/14/2010, the 4-hour average of ≥ 15 ºC volume had the most sensitive reaction to the SGD reduction among the lowest 0.02% noncold water volumes in the river. With a 30% SGD reduction, the lowest 4-hour average of ≥ 15 ºC volume during the 125 months was 128,233 cubic meters, or 4,528,509 cubic feet (33,875,568 gallons).

Table 22. Four-hour averages of ≥ 15 ºC water volumes (in m^3) for the acute condition at six critical time points.

	4-Hour Time Window					
	#1	*#2*	*#3*	*#4*	*#5*	*#6*
	1/11/10 4:00 - 1/11/10 8:00	*1/11/10 23:00 - 1/12/10 3:00*	*12/14/10 5:00 - 12/14/10 9:00*	*12/14/10 8:00 - 12/14/10 12:00*	*1/2/18 10:00 - 1/2/18 14:00*	*1/18/18 5:30 - 1/18/18 9:30*
Baseline	661659	864040	168499	159732	223030	951766
Existing	645215	836524	165875	158231	221214	943332

2.5%	635586	847111	165748	156240	216106	940353
5.0%	619405	824831	165722	154156	203219	914841
7.5%	594811	809955	165635	154079	194195	897032
10.0%	575847	789701	162656	152518	173244	867375
12.5%	562625	764207	164233	151444	151577	845553
15.0%	537304	741771	159510	151370	140124	805638
17.5%	528564	722779	148780	149110	136983	763959
20.0%	507607	699881	138194	143432	133945	724764
22.5%	481961	672478	139672	139099	132618	664596
25.0%	451456	646728	142586	133383	127500	618357
27.5%	407369	619410	144099	130114	125948	579337
30.0%	364620	591578	146964	128233	124637	544231

Relative changes of the 4-hour average of the ≥ 15 ºC water volume from the baseline volumes at the six critical time points are shown in Table 23, in the form percentage reduction. As shown in the table, at 12:00 PM, 1/2/2018, or during 10:00 – 14:00 on 1/2/2018, an 8.05% SGD reduction would trigger a 15% reduction of the 4-hour average of ≥ 15 ºC water volume.

Table 23. Percentage reductions of the 4-hour average of the ≥ 15 ºC water volume relative to the corresponding baseline volumes at six critical time points.

	4-Hour Time Window					
	#1	*#2*	*#3*	*#4*	*#5*	*#6*
	1/11/10 4:00 - 1/11/10 8:00	*1/11/10 23:00 - 1/12/10 3:00*	*12/14/10 5:00 - 12/14/10 9:00*	*12/14/10 8:00 - 12/14/10 12:00*	*1/2/18 10:00 - 1/2/18 14:00*	*1/18/18 5:30 - 1/18/18 9:30*
Existing	2.49%	3.18%	1.56%	0.94%	0.81%	0.89%
2.5%	3.94%	1.96%	1.63%	2.19%	3.10%	1.20%
5.0%	6.39%	4.54%	1.65%	3.49%	8.88%	3.88%
7.5%	10.10%	6.26%	1.70%	3.54%	12.93%	5.75%
10.0%	12.97%	8.60%	3.47%	4.52%	22.32%	8.87%
12.5%	14.97%	11.55%	2.53%	5.19%	32.04%	11.16%
15.0%	18.79%	14.15%	5.33%	5.24%	37.17%	15.35%
17.5%	20.12%	16.35%	11.70%	6.65%	38.58%	19.73%
20.0%	23.28%	19.00%	17.99%	10.20%	39.94%	23.85%
22.5%	27.16%	22.17%	17.11%	12.92%	40.54%	30.17%
25.0%	31.77%	25.15%	15.38%	16.50%	42.83%	35.03%
27.5%	38.43%	28.31%	14.48%	18.54%	43.53%	39.13%
30.0%	44.89%	31.53%	12.78%	19.72%	44.12%	42.82%
Triger	***12.52%***	***15.97%***	***18.81%***	***23.96%***	***8.05%***	***14.79%***

Similar to Tables 22 & 23, 4-hour averages of ≥ 15 ºC surface areas for the acute condition at six critical time points and their percentage changes relative to the corresponding baseline noncold surface areas are listed in Tables 24 and 25. The lowest ≥ 15 ºC surface area occurs at 9:30 AM, 12/14/2010 when the flow reduction is low. However, when the flow reduction increases, the lowest ≥ 15 ºC surface area shifts to 10:00 AM, 1/2/2018. The lowest noncold surface area with a 30% SGD reduction was 104,258 m^2, or 1,122,224 square feet (25.77 acres). Among the six critical time points, the smallest percentage reduction of SDG that would cause a 15% reduction of the 4-hour average of ≥ 15 ºC surface areas was 6.44% and occurred at 10:00 AM, 1/2/2018.

Table 24. Four-hour averages of ≥ 15 ºC surface areas (in m^2) for the acute condition at six critical time points.

	4-Hour Time Window					
	#1	*#2*	*#3*	*#4*	*#5*	*#6*
	1/11/10 4:00 - 1/11/10 8:00	*1/11/10 23:00 - 1/12/10 3:00*	*12/14/10 7:30 - 12/14/10 11:30*	*12/14/10 9:30 - 12/14/10 13:30*	*1/2/18 8:00 - 1/2/18 12:00*	*1/18/18 5:30 - 1/18/18 9:30*
Baseline	616414	813223	123877	146234	230755	847061
Existing	599561	784337	123726	140582	228163	842053
2.5%	593650	798205	121240	138104	220935	839535
5.0%	576240	780683	121144	135583	201631	811984
7.5%	555912	767272	121025	131427	192068	796912
10.0%	535447	750727	118177	128598	170359	772283
12.5%	525322	730915	118926	123606	143442	756511
15.0%	497395	712470	118204	119448	136322	720734
17.5%	494066	694350	118148	119389	130013	688452
20.0%	471888	674958	118077	119335	122219	666636
22.5%	443903	651712	118593	119291	114989	611045
25.0%	413310	631037	118503	119235	114048	556298
27.5%	377055	609825	118441	117377	108416	511600
30.0%	336940	588701	117392	116695	104258	481962

Table 25. Percentage reductions of the 4-hour average of the ≥ 15 ºC surface area relative to the corresponding baseline volumes at six critical time points.

	4-Hour Time Window					
	#1	*#2*	*#3*	*#4*	*#5*	*#6*
	1/11/10 4:00 - 1/11/10 8:00	*1/11/10 23:00 - 1/12/10 3:00*	*12/14/10 7:30 - 12/14/10 11:30*	*12/14/10 9:30 - 12/14/10 13:30*	*1/2/18 8:00 - 1/2/18 12:00*	*1/18/18 5:30 - 1/18/18 9:30*
Existing	2.73%	3.55%	0.12%	3.87%	1.12%	0.59%
2.5%	3.69%	1.85%	2.13%	5.56%	4.26%	0.89%
5.0%	6.52%	4.00%	2.21%	7.28%	12.62%	4.14%
7.5%	9.82%	5.65%	2.30%	10.13%	16.77%	5.92%
10.0%	13.14%	7.68%	4.60%	12.06%	26.17%	8.83%

12.5%	14.78%	10.12%	4.00%	15.47%	37.84%	10.69%
15.0%	19.31%	12.39%	4.58%	18.32%	40.92%	14.91%
17.5%	19.85%	14.62%	4.62%	18.36%	43.66%	18.72%
20.0%	23.45%	17.00%	4.68%	18.39%	47.04%	21.30%
22.5%	27.99%	19.86%	4.27%	18.42%	50.17%	27.86%
25.0%	32.95%	22.40%	4.34%	18.46%	50.58%	34.33%
27.5%	38.83%	25.01%	4.39%	19.73%	53.02%	39.60%
30.0%	45.34%	27.61%	5.24%	20.20%	54.82%	43.10%
Triger	***12.62%***	***17.90%***	***>30%***	***12.15%***	***6.44%***	***15.06%***

4.5. Results of Common Snook Thermal Habitats

Another purpose for considering thermal habitats is to protect Common Snook during the coldest days in winter by ensuring that the favorite thermal habitats for Common Snook in the estuary won't be significantly reduced due to an SGD reduction. Stevens et al (2016) advised the importance of the warm water sources to Common Snook during the coldest days of the winter in coastal estuaries. According to studies conducted by Schafland and Foote (1983) and Blewett and Stevens (2014), Common Snook need 15 ºC or warmer to survive during winter. There were documented evidence of Common Snook die off during severe cold fronts in the region. As such, this study calculated water volumes and surface areas of ≥ 15 ºC in the Homosassa River for all the scenario runs. Unlike the thermal habitat calculation for manatees, no warm water layer thickness (1.158 m) restriction was used in the calculation.

Because water warmer than 15 ºC appears to be a threshold for Common Snook, measured water temperature data during the simulation period for the scenario runs were analyzed to find out the starting and ending times when water temperature was below 15 ºC for each winter. These starting and ending time points are listed in Table 26. If we call the time span from the time point when the first < 15 ºC water temperature was recorded to the time point when the last < 15 ºC water temperature was recorded a Common Snook season for the winter, then the duration of the Common Snook season can vary quite significantly, from only 43.25 days to 149.09 days for the estuary, during the 125-month simulation period. We name this kind of variable duration from one winter to the next winter the varying Common Snook season.

Table 26. Starting and ending time points when water temperature in Homosassa dropped to below 15 ºC during each winter of the scenario simulation period.

Season	Starting Time	Ending Time	Duration (Days)
1	11/17/07 9:30	3/9/08 11:00	113.06
2	10/30/08 1:15	3/5/09 14:00	126.53
3	11/29/09 6:45	3/9/10 12:30	100.24
4	12/2/10 23:45	2/15/11 12:00	74.51

5	1/3/12 4:45	2/15/12 10:45	43.25
6	10/30/12 7:45	3/28/13 10:00	149.09
7	11/14/13 0:00	3/8/14 11:15	114.47
8	11/19/14 4:00	2/22/15 20:15	95.68
9	12/20/15 7:30	2/12/16 13:15	54.24
10	12/10/16 7:00	3/17/17 9:45	97.11
11	12/10/17 2:00	2/4/18 8:45	56.28

Table 27 shows results of the percentage reduction of ≥ 15 ºC thermal habitats for all scenario runs during the 11 varying Common Snook seasons of the 125-month simulation period. The most sensitive Common Snook season to SGD reduction was during 12/2/10 23:45 – 2/15/11 12:00 and the percentage reduction results of ≥ 15 ºC water volume and surface area during this period are also included in the table. It can be seen that as the SGD reduction increases, both ≥ 15 ºC volume and ≥ 15 ºC surface area decrease linearly with the SGD. Although a 30% SGD reduction could cause a 14.56% reduction of the seasonally averaged ≥ 15 ºC water volume during the most sensitive varying Common Snook season, a 15% reduction of the thermal habitats never reached.

Table 27. Percentage reductions of ≥ 15 ºC water volume and surface area for all the 11 varying Common Snook seasons and for most sensitive season during 12/2/10 23:45 – 2/15/11 12:00.

Scenario	Volume Reduction	Surface Area Reduction	Volume Reduction	Surface Area Reduction
	All 11 Varying Seasons		*12/2/10 23:45 – 2/15/11 12:00*	
Existing	0.22%	0.22%	0.88%	0.89%
2.5%	0.29%	0.29%	1.18%	1.17%
5.0%	0.59%	0.59%	2.31%	2.29%
7.5%	0.90%	0.89%	3.51%	3.44%
10.0%	1.21%	1.21%	4.67%	4.60%
12.5%	1.52%	1.52%	5.88%	5.79%
15.0%	1.86%	1.85%	6.97%	6.88%
17.5%	2.19%	2.18%	8.15%	8.04%
20.0%	2.54%	2.53%	9.43%	9.33%
22.5%	2.89%	2.89%	10.71%	10.56%
25.0%	3.26%	3.25%	11.99%	11.85%
27.5%	3.63%	3.63%	13.27%	13.10%
30.0%	4.01%	4.01%	14.56%	14.36%

Alternatively, one may define a Common Snook season as a fixed duration for all the years, simply using the period from the earliest calendar day when < 15 ºC occurred to the latest calendar day when < 15 ºC occurred for all the winters. From Table 26, the earliest such day was October 30 in both 2008 and 2012, while the latest such day was March 28 in 2013. Therefore, the fixed Common Snook season would be a 150-day (or 151-day if a leap year is involved) period from October 30 current year to March 28 of the next year. Table 28 shows results of the percentage reduction of ≥ 15 ºC thermal habitats for all scenario runs during the 11 fixed Common Snook seasons. The most sensitive Common Snook season to SGD reduction was during 10/30/2009 – 3/28/2010, which was is the same winter for the varying Common Snook season (Table 27). Results of the percentage reduction of ≥ 15 ºC water volume and surface area during this period are also included in the table. As expected, a 15% reduction of the seasonally averaged thermal habitats also did not occur, even when the SGD was reduced by 30% during the most sensitive Common Snook season.

Table 28. Percentage reductions of ≥ 15 ºC water volume and surface area for all the 11 fixed Common Snook seasons and for most sensitive fixed season during 10/30/2009 – 3/28/2010.

Scenario	Volume Reduction	Surface Area Reduction	Volume Reduction	Surface Area Reduction
	All Seasons		*10/30/2009 – 3/28/2010*	
Existing	0.13%	0.13%	0.30%	0.31%
2.5%	0.17%	0.17%	0.39%	0.40%
5.0%	0.35%	0.35%	0.80%	0.81%
7.5%	0.54%	0.53%	1.25%	1.28%
10.0%	0.73%	0.72%	1.64%	1.68%
12.5%	0.92%	0.91%	2.06%	2.13%
15.0%	1.12%	1.11%	2.51%	2.59%
17.5%	1.32%	1.31%	2.98%	3.07%
20.0%	1.53%	1.52%	3.41%	3.52%
22.5%	1.74%	1.73%	3.87%	3.98%
25.0%	1.96%	1.95%	4.32%	4.43%
27.5%	2.19%	2.18%	4.78%	4.92%
30.0%	2.42%	2.41%	5.25%	5.41%

The main differences between Tables 27 and 28 came from the fact that a fixed Common Snook season has more days than a varying Common Snook season. As a result, more noncold days with water temperature ≥ 15 ºC were included in the former than in the later. Excluding these noncold day from the calculation makes calculated average thermal habitats more sensitive to the SGD reduction. It was found that there were 401 cold days with water temperature below 15 ºC at one measurement station or more in the Homosassa River. Many cold days occurred consecutively, making 82 cold-day blocks out of the 401 cold days.

Table 29 shows results of percentage reduction of ≥ 15 ºC water volume and surface area during all 82 cold day blocks, (same as those for all 401 cold days), the most sensitive cold-day block, and the most sensitive single cold day during the 125-month scenario simulation period. It can be seen from the table that average ≥ 15 ºC water volume and surface during all 401 cold days would not be reduced by 15%, even with a 30% SGD reduction; however, during the cold-day block on 1/19/2017, a 10.24% SGD reduction would trigger a 15% reduction of ≥ 15 ºC water volume in the Homosassa River, while a 10.51% reduction of SGD would cause a 15% reduction of ≥ 15 ºC surface area. If we look at the most sensitive single cold day to the SGD reduction, it was found that on 12/14/2010, a 5.64% SGD reduction would cause a 15% reduction of ≥ 15 ºC water volume and a 5.03% SGD reduction would reduce ≥ 15 ºC surface area by 15%.

Table 29. Percentage reductions of ≥ 15 ºC water volume and surface area for all 82 cold day blocks (or 401 cold days), the most sensitive cold-day block, and the most sensitive single cold day during the 125-month scenario simulation period.

Scenario	Volume Reduction	Surface Area Reduction	Volume Reduction	Surface Area Reduction	Volume Reductio	Surface Area Reduction
	All <15 ºC Days		Cold-Day block 1/19/2017 – 1/19/2017		Single Cold Day: 12/14/2010	
Existing	0.75%	0.74%	2.49%	3.06%	5.49%	6.36%
2.5%	1.00%	0.98%	3.79%	4.40%	6.74%	7.52%
5.0%	1.99%	1.94%	6.87%	7.36%	12.98%	14.92%
7.5%	3.02%	2.95%	9.94%	10.30%	20.84%	22.37%
10.0%	4.06%	3.97%	14.69%	14.33%	28.93%	30.26%
12.5%	5.09%	4.96%	17.95%	17.60%	39.47%	41.10%
15.0%	6.18%	6.02%	21.33%	21.20%	45.39%	46.77%
17.5%	7.27%	7.09%	26.42%	26.24%	46.66%	48.51%
20.0%	8.38%	8.16%	29.69%	29.23%	47.51%	49.89%
22.5%	9.52%	9.27%	31.97%	31.76%	48.21%	50.04%
25.0%	10.71%	10.42%	34.43%	34.12%	48.72%	50.33%
27.5%	11.89%	11.58%	36.64%	36.38%	49.26%	50.61%
30.0%	13.11%	12.78%	39.37%	39.16%	49.45%	50.76%
Trigger			***10.24%***	***10.51%***	***5.64%***	***5.03%***

4.6 Summary of Model Results of Scenario Runs

As described above, the percentages of flow reduction that would trigger a 15% reduction of salinity and thermal habitats in the Homosassa River have been obtained through a series of model simulations for various flow reduction scenarios. Table 30 is a summary of the triggering percentages of the flow reduction that would cause significant harms to the Homosassa River system.

From Table 30, it can be seen that although ≤ 1 psu salinity habitats are not sensitive to the SGD reduction, ≤ 2 psu salinity habitats are sensitive. As the upper bound of the salinity range increase, the sensitivity of salinity habitats to the SGD reduction becomes weaker. The most sensitive salinity habitat to the SGD reduction is the ≤ 2 psu bottom area, which can be reduced 15% with a 11.09% SGD reduction.

The acute condition for manatee is more sensitive than the chronic condition for manatees to the SGD reduction in the Homosassa River. The most sensitive thermal habitat is the 4-hour average of ≥ 15 ºC surface area, which can be reduced by 15% with a 6.44% reduction of SGD when this thermal habitat is low.

For Common Snook thermal habitats, the single cold day averages of ≥ 15 ºC water volume and surface area are most sensitive to the SGD reduction. A 5.64% SGD reduction could cause a 15% reduction of ≥ 15 ºC water volume, while a 5.03% SGD reduction could trigger a 15% reduction of ≥ 15 ºC surface area.

Table 30. A summary of percentages of flow reduction which would trigger a 15% reduction of salinity and thermal habitats in the Homosassa River.

	Salinity Habitats					
Salinity (psu) ≤	*1*	*2*	*3*	*5*	*10*	*15*
Volume	>30%	11.24%	12.92%	15.41%	>30%	>30%
Bottom Area	>30%	11.10%	12.74%	15.32%	>30%	>30%
Shoreline Length	>30%	16.28%	15.71%	16.51%	>30%	>30%
	Manatee Thermal Habitats					
Thermal Conditions	*Chronic*			*Acute*		
Volume	9.95%			8.05%		
Surface Area	10.40%			6.44%		
	Common Snook Thermal Habitats					
Thermal Conditions	*Cold-Day Block*			*Single Cold Day*		
Volume	10.24%			5.64%		
Surface Area	10.51%			5.03%		

5. Effects of Sea Level Rises

Because the analysis of effects of the SGD reduction on salinity and thermal habitats in the previous section used measured data collected during the previous 10.5 years, it is possible that the proposed MFL may not be valid if the hydrological, meteorological, and other physical conditions which affect salinity and thermal habitats in the river differ significantly from those during the 10.5-year simulation period. One of the physical conditions that are expected to be change and could alter the salinity and thermal characteristics in the estuary is the sea level rise caused by global warming. It is meaningful to see if the proposed MFL still holds a number of years later, when a SLR relative to the average sea level during the 10.5-year simulation period occurs.

This section describes how sea level rises are considered in the hydrodynamic modeling of the Homosassa River and how SLRs would affect salinity and thermal habitats in the Homosassa River estuary. As the objective is to verify the proposed MFL with a SLR in the future, the LAMFE model for the Homosassa River was run for both the BSL condition with a SLR and the proposed MFL condition with the same SLR. Simulated salinity and thermal habitats between the two model runs were compared to check if the 15% habitat reduction criterion would be violated by the proposed MFL with the SLR.

5.1 Sea Level Rise Estimates

As the sea level continue to rise, we need to select a target year in the future to consider SLR effects on salinity and thermal habitats in the Homosassa River. To be consistent with the SWFWMD's regional water supply planning horizon, sea level conditions in 2035 are evaluated. The United States Army Corps of Engineers (USACE) provides SLR estimates at their web site, http://www.corpsclimate.us/ccaceslcurves.cfm, where three types of the SLR can be obtained at several NOAA stations along the Florida Gulf coast: a low estimate, an intermediate estimate, and a high estimate. The closest NOAA stations to the mouth of the Homosassa River are Stations #8726724 (Clearwater Beach FL) and #8727520 (Cedar Key FL). The Clearwater Beach station is about 89,316 m south - southwest of mouth of the Homosassa River and the Cedar Key station is about 51,774 m northwest of the Homosassa mouth. The St. Petersburg station is further south from the mouth of the Homosassa River with a distance of about 114,790 m but has a longer period of record of water level data than the Clearwater Beach station does. As such, the St. Petersburg station is considered as a better station for the SLR estimation than the Clearwater Beach station. Based on this consideration, the low, intermediate, and high sea level rise estimates at the mouth of the Homosassa River in 2035 were calculated from those at the St. Petersburg and Cedar Key stations using an inverse distance weighting interpolation.

Table 31 lists the low, intermediate, and high SLRs from 2012 to 2035 at the St. Petersburg, Cedar Key stations, and at the mouth of the Homosassa River. Over the 23-year period, estimated low, intermediate, and high SLRs at the mouth of the Homosassa River are 4.741, 8.588, and

20.990 cm, respectively. Because 2012 is the middle year of the scenario simulation period, during which there was also sea level rise, adding the same sea level rise estimates to the water level data at the mouth of the Homosassa River during the 125 months of the simulation period is reasonable.

Table 31. Sea level rise estimates at St. Petersburg, Cedar Key, and the mouth of the Homosassa River. SLRs at the St. Petersburg and Cedar Key stations were obtained from a USACE website, while SLRs at the mouth of the Homosassa River were estimated based on those at the former two stations.

	NOAA Station		***Estimated for Homosassa Mouth***
	St. Petersburg	***Cedar Key***	
Low SLR (cm)	5.791	4.267	4.741
Intermediate SLR (cm)	10.058	7.925	8.588
High SLR (cm)	22.250	20.422	20.990

5.2 Model Results for SLR Scenarios

In the SLR model runs, 4.741, 8.588, and 20.990 cm were added to the water level data measured at the open boundaries for the entire 125-month simulation period for the low, intermediate and high SLR estimates, respectively. The added layer of water is assumed to have the same salinity and temperature values as measured top-layer salinity and temperature during the simulation period. The modified boundary conditions at these open boundaries were used to drive the model to simulate effects of low, intermediate, and high SLR estimates on salinity and temperature distributions in the estuarine system. The added SLRs not only increases the average depth of the estuary and thereby the volume of the estuary, but also causes more Gulf water to be transported to the system.

It should be acknowledged that the above treatment of the SLR in the model is far from perfect when considering its effects on hydrodynamics and salinity and thermal transport processes in the Homosassa River, because a SLR could modify several factors controlling physical processes in the estuary. For example, the rainfall pattern in the region could be altered by the SLR, the salinity and temperature characteristics in the Gulf could be quite different with or without a SLR, and the potentiometric surface in the coastal region could be pushed upward by a SLR. Because of the SLR, SGDs to the Homosassa River system would likely be reduced to a certain degree. Clearly, our treatment only considered the direct effect of the SLR on the estuary and didn't consider other consequences caused by the SLR, which are virtually unknown to us because of the lack of data or research on the topics for the region.

The SLR runs were conducted for the BSL scenario and the MFL (5.0% reduction from the BSL) scenario. Model results for these runs are presented and discussed below. For simplicity, time series plots of daily means of simulated salinity habitats, similar to Figures 26 & 27, are omitted here, and only CDF plots of simulated salinity habitats for various flow reductions are presented in the following discussion. For thermal habitats, time series plots of 72-hour and 4-hour moving average similar to Figures 31 - 33 are also omitted here.

5.2.1 Salinity Habitats

Cumulative distribution functions for water volume, bottom area, and shoreline length are depicted in Figures 36, 37, and 38, respectively for salinity ≤ 1, 2, 3, 5, 10, and 15 psu for the BSL condition and for BSL with SLRs (high, intermediate, and low estimates). It can be seen from these figures that the shape of CDFs has been greatly modified by SLR. For salinity volumes, CDF curves of ≤ 2 psu, 3 psu, and 5 psu shift to the left, while CDF curves of ≤ 10 psu and 15 psu shift to the right. As mentioned before, the area between the *y*-axis and the CDF curve numerically represents the average value of the variable for the given sample used to generate the CDF curve. From Fig. 36, it can be seen that average water volumes for salinity ≤ 2, 3, and 5 psu are all reduced with the increase of the SLR. However, ≤ 10 and 15 psu salinity volumes increase as a result of SLR. It may seem strange that the ≤ 1 psu salinity volume also has a slight increase caused by a SLR. This phenomenon is physically possible and can be explained by a slight migration of the salt wedge in the upstream direction due to the increase of the water depth caused by a SLR. Although this slight upstream movement of the salt wedge reduces the ≤ 1 psu salinity bottom area and shoreline length, as shown in Figures 37 and 38, it slightly increases the density stratification just downstream of the springs. As a result, the vertical mixing is to some extent reduced, making the top freshwater layer a little thicker. The final result is a slightly increased ≤ 1 psu salinity volume in the Homosassa River under the SLR condition.

Fig. 37 shows that bottom areas for salinity ≤ 1, 2, 3, 5 and 10 psu are reduced with the increase of the SLR, while the bottom area for salinity ≤ 15 psu increases with the increase of the SLR. The relative reduction for ≤ 10 psu is smaller than that for ≤ 5 psu, which is smaller than the relative reduction of the bottom area for ≤ 3 psu, suggesting that bottom areas for salinity between 3 psu and 5 psu and for salinity between 5 psu and 10 psu increase as the SLR increases. The bottom area for salinity between 10 psu and 15 psu increases with the increase of the SLR at an even higher rate, causing the ≤ 15 psu bottom area to increase with the increase of the SLR. Comparing Fig. 36 with Fig. 37, it can be seen that SLR's effects on bottom areas for different salinity ranges are greater than its effects on different salinity volumes.

Fig. 38 shows that the SLR causes shoreline lengths for salinity ≤ 1, 2, 3, 5, 10, and 15 psu are all reduced with the increase of the SLR. Comparing Figure 38 with Figures 36 & 37, it is clear that SLR's effects on shoreline lengths for different salinity ranges are greater than its effects on corresponding salinity volumes and bottom areas.

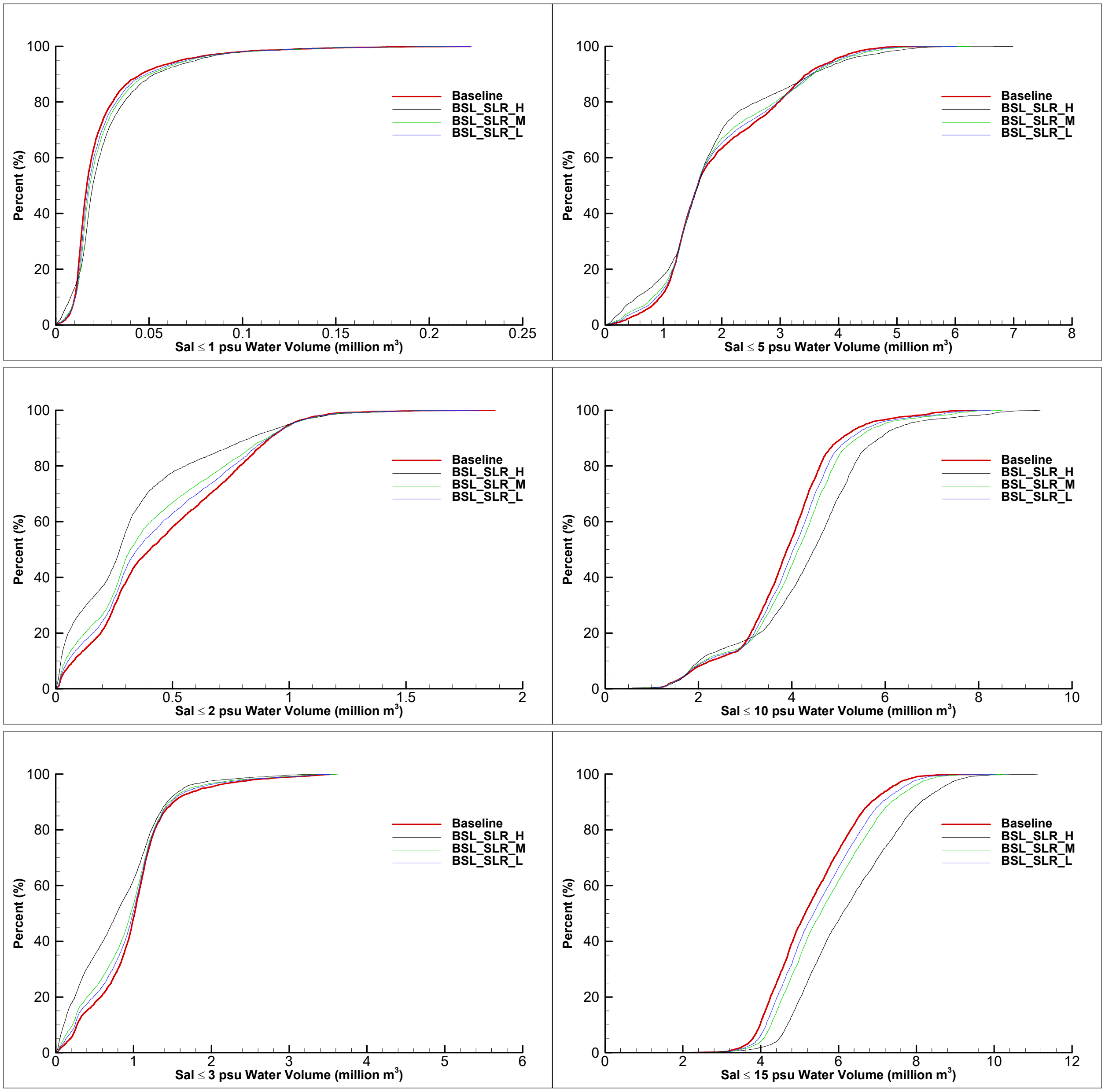

Figure 36 CDFs of water volume for salinity ≤ 1, 2, 3, 5, 10, and 15 psu for the BSL condition (red lines) and for the baseline with the high SLR (black lines), the intermediate SLR (green lines), and low SLR (blue lines) in the Homosassa River.

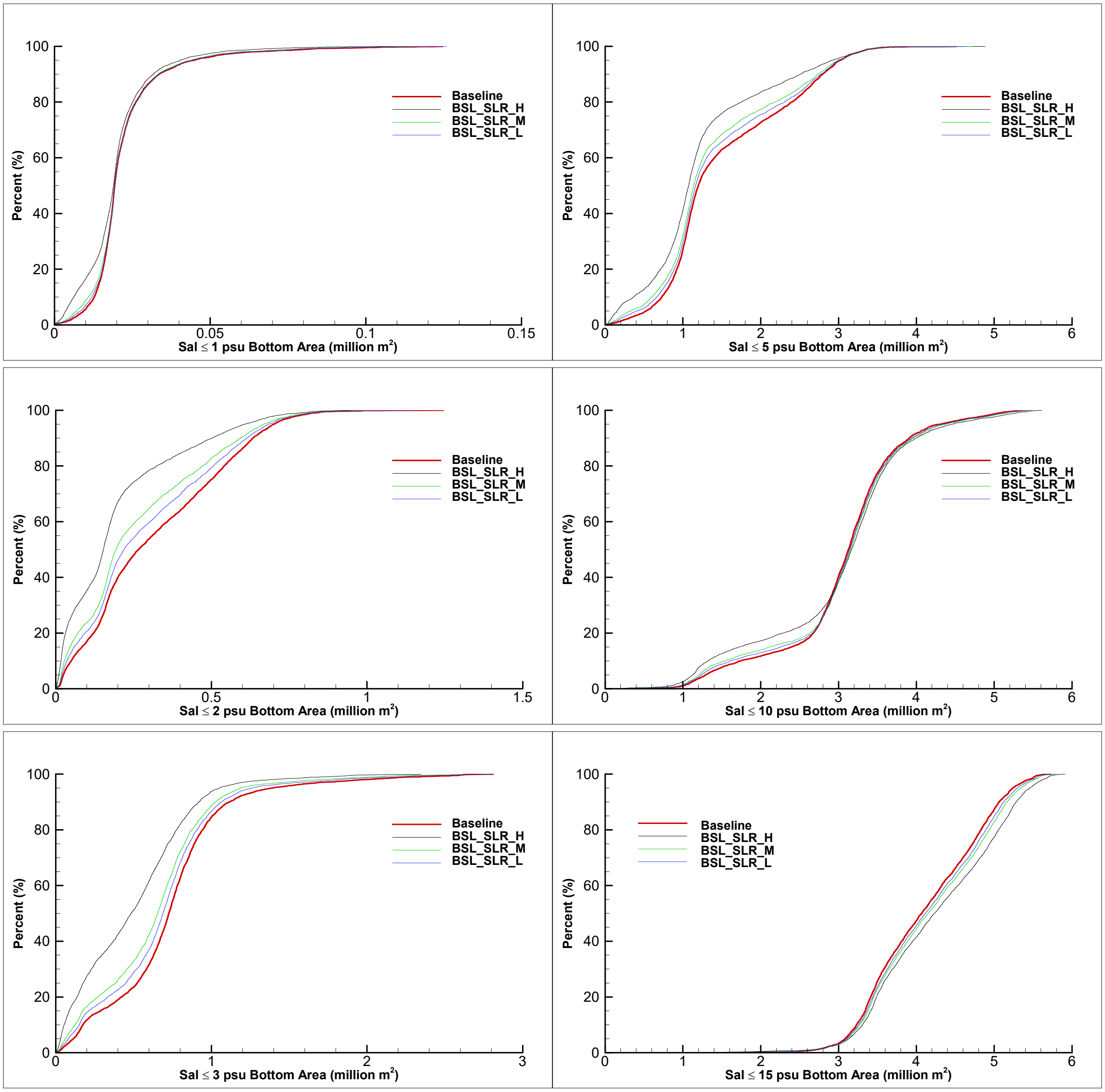

Figure 37 CDFs of bottom area for salinity ≤ 1, 2, 3, 5, 10, and 15 psu for the BSL condition (red lines) and for the baseline with the high SLR (black lines), the intermediate SLR (green lines), and low SLR (blue lines) in the Homosassa River.

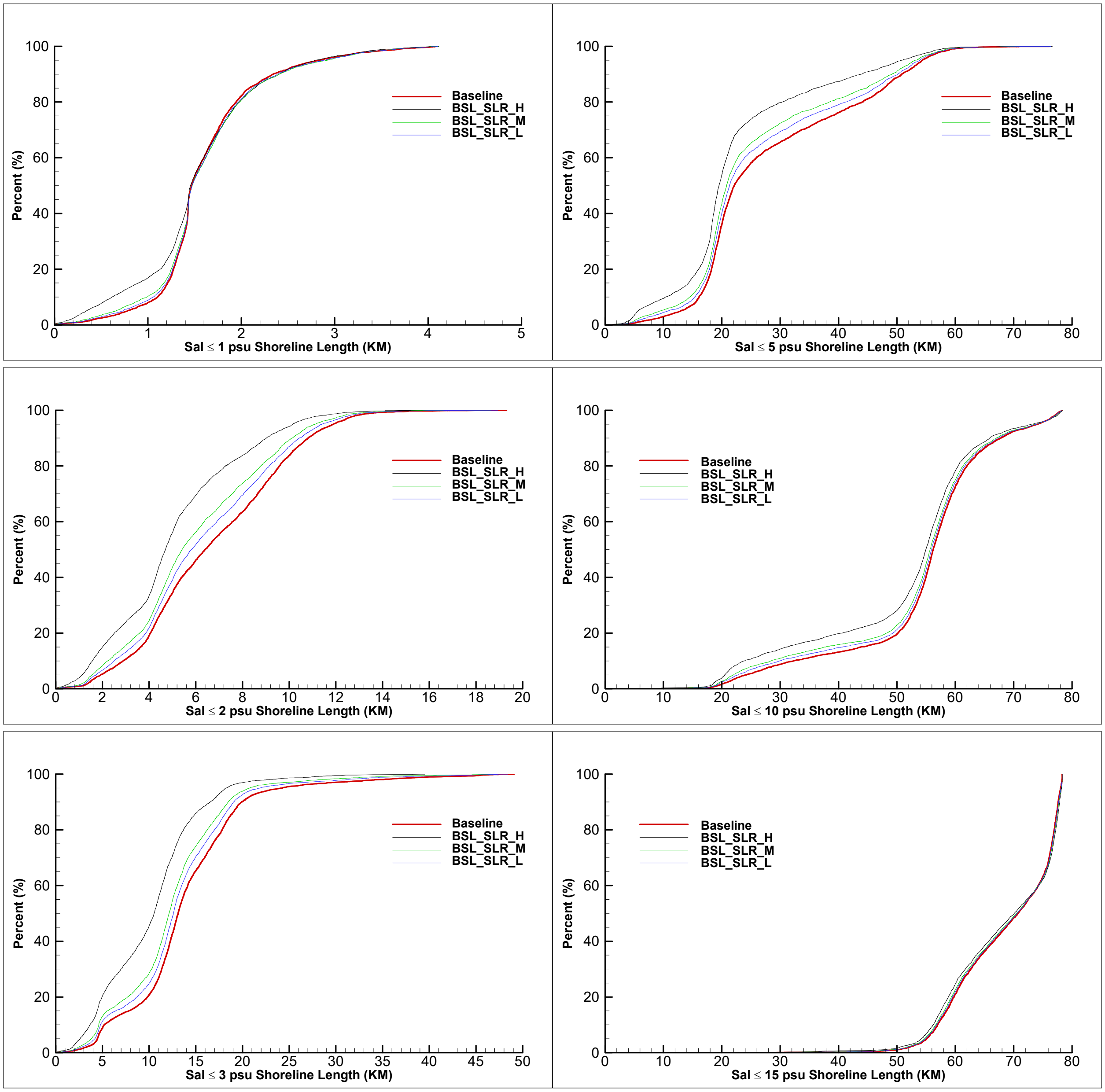

Figure 38 CDFs of shoreline length for salinity ≤ 1, 2, 3, 5, 10, and 15 psu for the BSL condition (red lines) and for the baseline with the high SLR (black lines), the intermediate SLR (green lines), and low SLR (blue lines) in the Homosassa River.

CFDs for water volumes, bottom areas, and shoreline lengths for salinity ≤ 1, 2, 3, 5, 10, and 15 psu for the MFL flow condition and for MFL with SLRs (high, intermediate, and low estimates) are plotted in Figures 39 - 41, which clearly demonstrate effects of high, intermediate, and low SLRs on CDFs of water volumes, bottom areas, and shoreline lengths of different salinity ranges under a 5% flow reduction condition. Comparing Figures 39, 40, and 41 with Figures 36, 37, and 38, respectively, it can be seen that the SLR has the similar effects on CDFs of various salinity habitats under the MFL flow condition as on those under the BSL condition. Generally, salinity habitats of ≤ 2 and 3 psu are reduced more greatly than those for salinity ≤ 10 psu or higher.

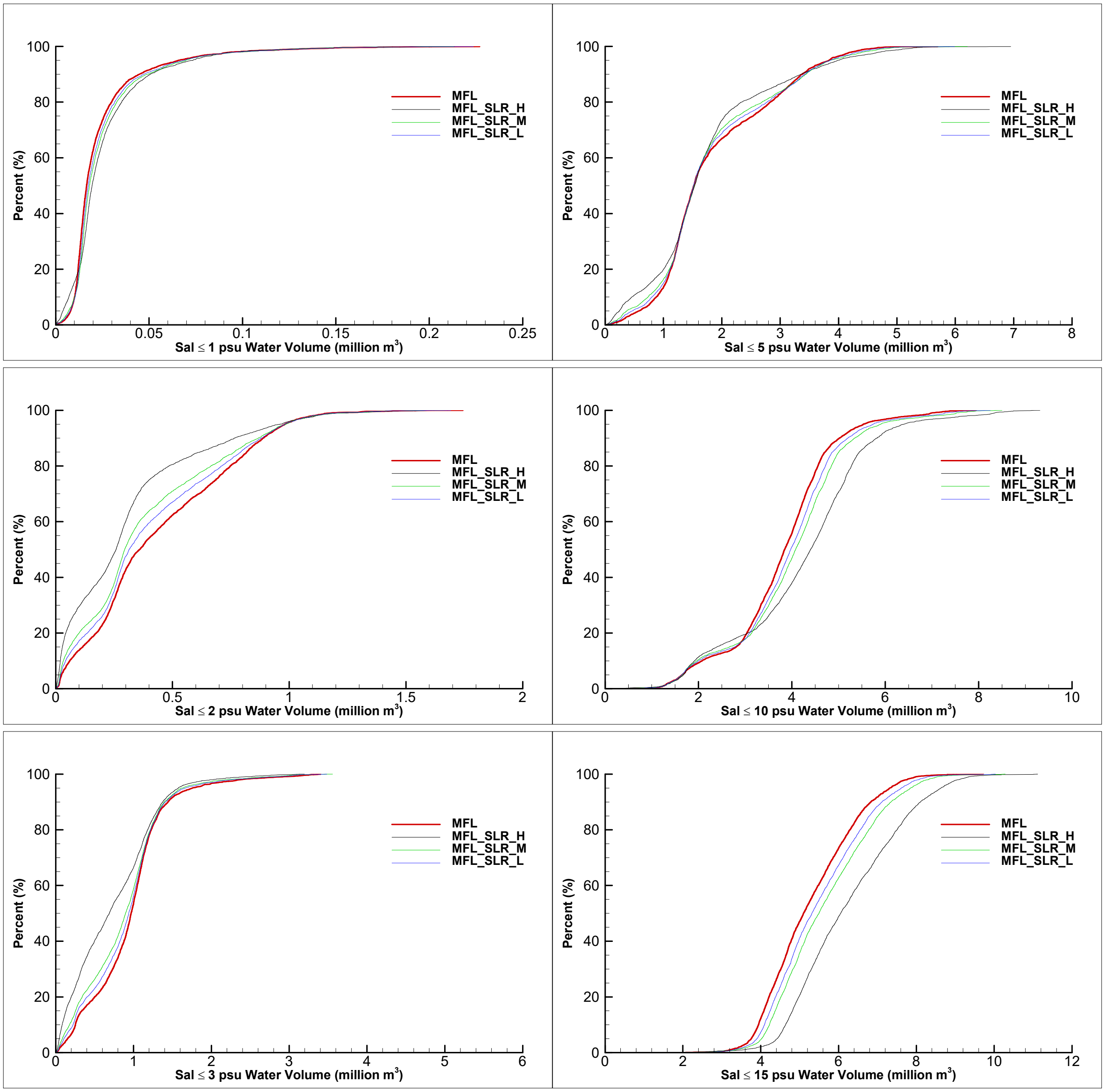

Figure 39 CDFs of water volume for salinity ≤ 1, 2, 3, 5, 10, and 15 psu for the MFL condition (red lines) and for MFL with the high SLR (black lines), the intermediate SLR (green lines), and low SLR (blue lines) in the Homosassa River.

As Figs. 36 – 38 and Figs. 39 – 41 demonstrate SLR effects on salinity habitats for both the BSL and MFL conditions, it is more essential to exam MFL effects on various salinity habitats for the three SLRs. Figures 42 - 44 show comparisons of CDFs of water volume, bottom area, and shoreline length, respectively for salinity ≤ 1, 2, 3, 5, 10, and 15 psu under BSL condition with those under the MFL condition, with the high, intermediate, and low SLRs being added to the downstream open boundary of the Homosassa River. In these figures, the black solid and dashed lines are respectively for BSL and MFL conditions with the high SLR estimate. The red solid and dashed lines are respectively for BSL and MFL conditions with the intermediate SLR, while the blue solid and dashed lines are respectively for BSL and MFL conditions with the low SLR. It can be seen from Figures 42 - 44 that MFL has relatively large effects on low salinity habitats when a SLR is considered.

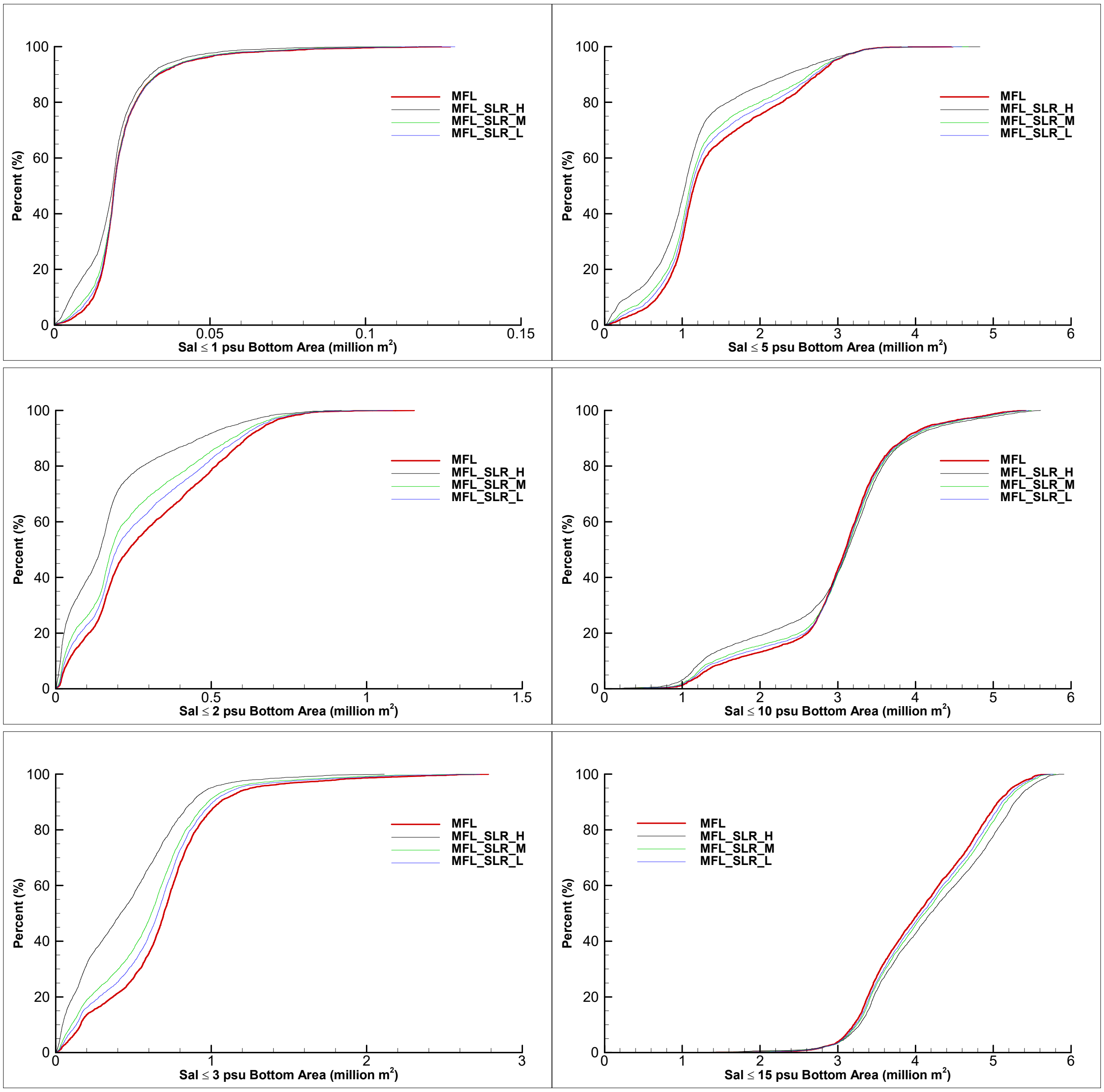

Figure 40 CDFs of bottom area for salinity ≤ 1, 2, 3, 5, 10, and 15 psu for the MFL condition (red lines) and for MFL with the high SLR (black lines), the intermediate SLR (green lines), and low SLR (blue lines) in the Homosassa River.

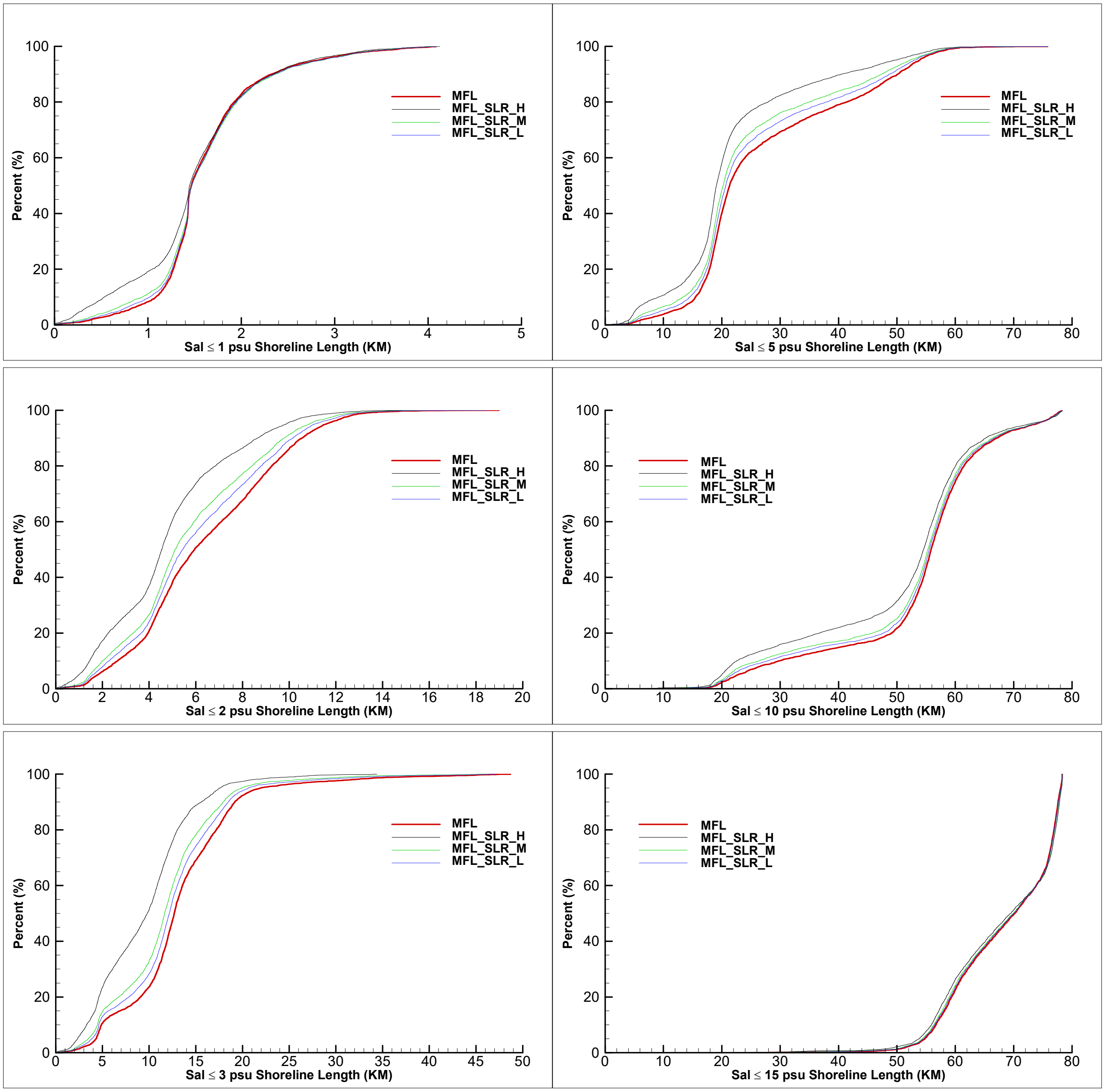

Figure 41 CDFs of shoreline length for salinity ≤ 1, 2, 3, 5, 10, and 15 psu for the MFL condition (red lines) and for MFL with the high SLR (black lines), the intermediate SLR (green lines), and low SLR (blue lines) in the Homosassa River.

Table 32 shows model results of water volume, bottom area, and shoreline length for salinity ≤ 1, 2, 3, 5, 10, and 15 psu under the baseline flow condition, BSL with high SLR, BSL with intermediate SLR, BSL with low SLR, MFL, MFL with high SLR, MFL with intermediate SLR, and MFL with low SLR in the Homosassa River. Units for water volume, bottom area, and shoreline length results in the table are the same as those in Tables 10 - 12 (million cubic meter, million square meters, and kilometers.) The percentage reductions of water volume, bottom area, shoreline length caused by the MFL for the four SLR conditions (no SLR consideration is considered as 0 SLR, or SLR #0) are shown in Table 33.

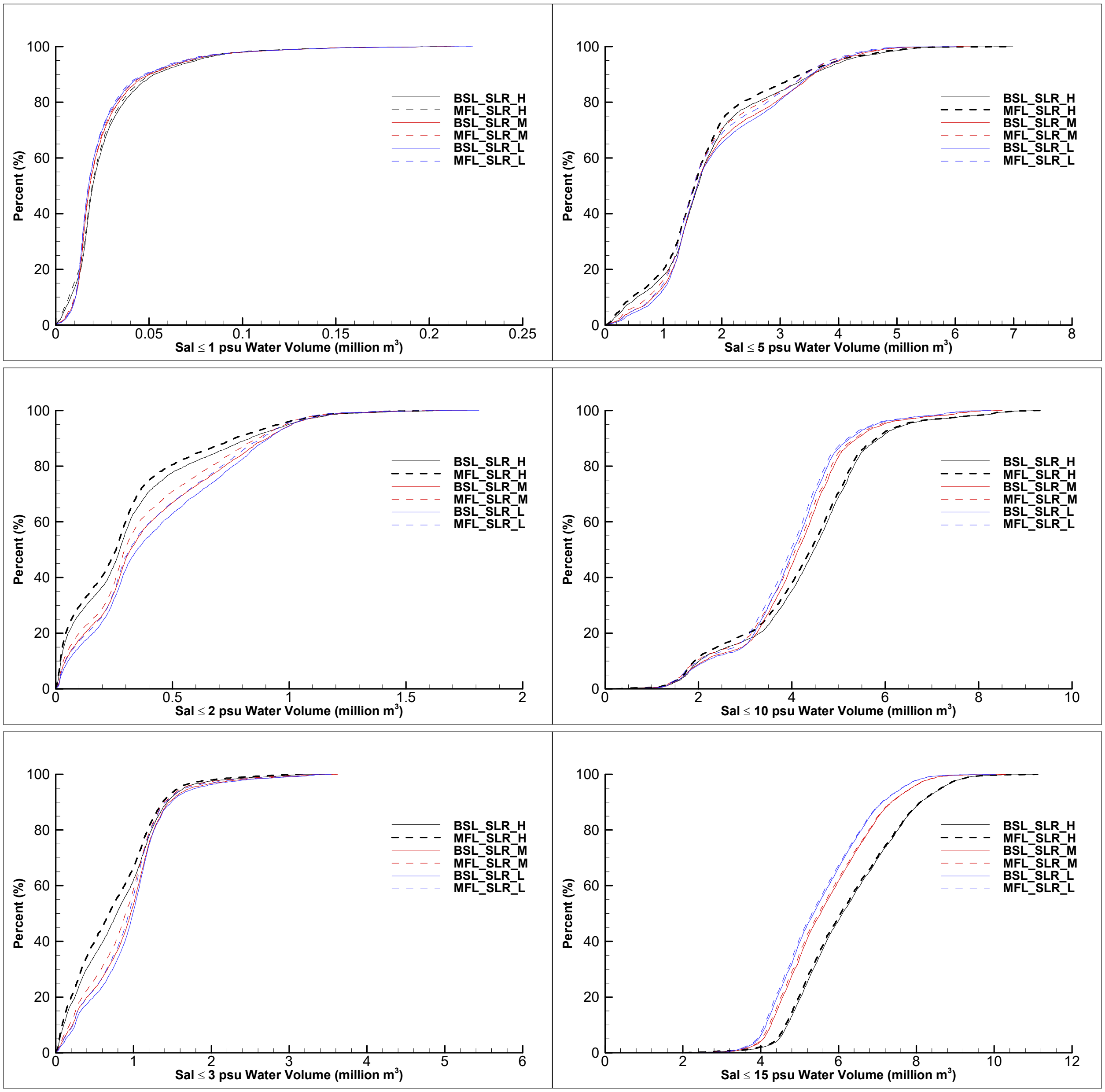

Figure 42 Comparisons of CDFs of water volume for salinity ≤ 1, 2, 3, 5, 10, and 15 psu under baseline flow condition (solid lines) with those under the MFL condition (dashed lines). High (black), intermediate (red), and low (blue) SLRs were added to the downstream open boundary of the Homosassa River.

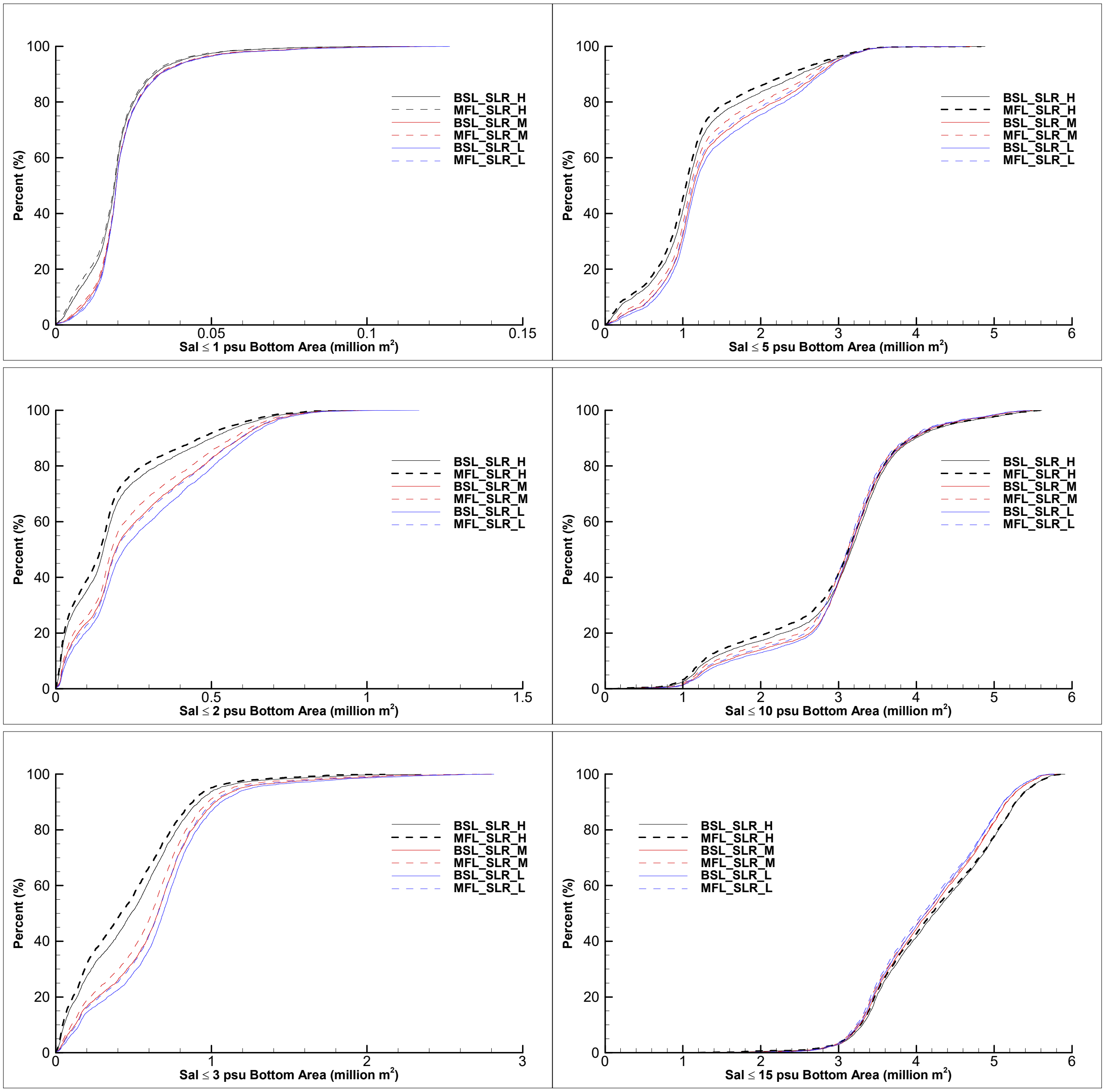

Figure 43 Comparisons of CDFs of bottom area for salinity ≤ 1, 2, 3, 5, 10, and 15 psu under baseline flow condition (solid lines) with those under the MFL condition (dashed lines). High (black), intermediate (red), and low (blue) SLRs were added to the downstream open boundary of the Homosassa River.

Table 33 shows that the biggest relative reduction of water volume caused by the MFL is 8.57%, for salinity ≤ 2 psu and with the high SLR estimate. With the high SLR, the MFL also causes the biggest percentage reduction of bottom area and shoreline length at 8.77% and 6.68%, respectively, both for salinity ≤ 3 psu. Clearly, the 15% criterion of salinity habitat reduction is not violated by MFL, with the consideration of any of the three SLRs.

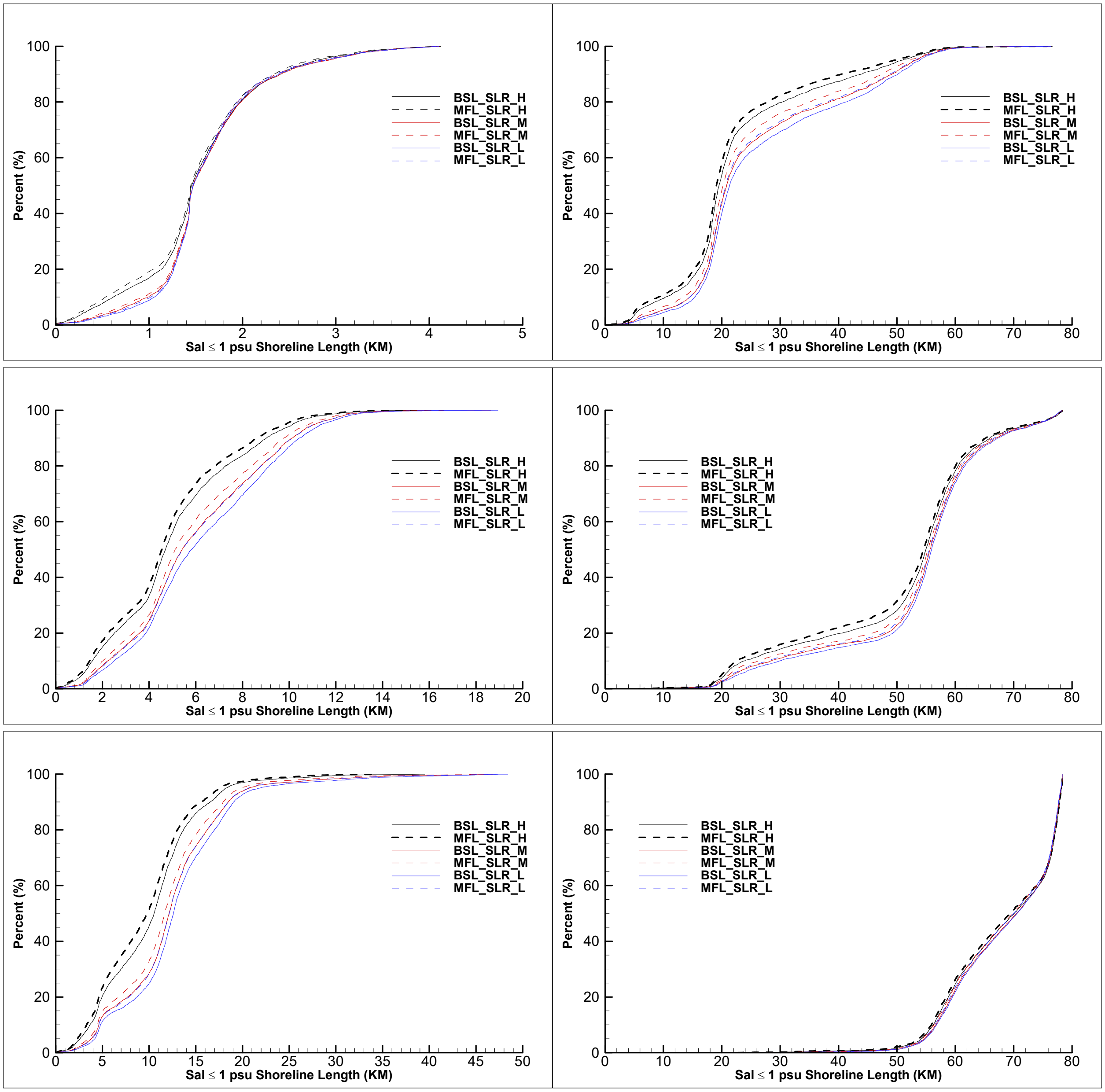

Figure 44 Comparisons of CDFs of shoreline length for salinity ≤ 1, 2, 3, 5, 10, and 15 psu under baseline flow condition (solid lines) with those under the MFL condition (dashed lines). High (black), intermediate (red), and low (blue) SLRs were added to the downstream open boundary of the Homosassa River.

Table 32. Water volumes, bottom areas, and shoreline lengths for salinity ≤ 1, 2, 3, 5, 10, and 15 psu under baseline flow condition, BSL with high SLR, BSL with intermediate SLR, BSL with

low SLR, MFL, MFL with high SLR, MFL with intermediate SLR, and MFL with low SLR in the Homosassa River.

Salinity (psu) ≤	**1**	**2**	**3**	**5**	**10**	**15**
	Water Volume (10^6 m^3)					
Baseline	0.024141	0.471965	0.998198	1.947998	3.853637	5.298407
BSL with high SLR	0.027189	0.340606	0.798230	1.838396	4.325757	6.265940
BSL with interm. SLR	0.026088	0.416467	0.924840	1.911566	4.053661	5.689692
Baseline with low SLR	0.025302	0.441766	0.958730	1.929495	3.964946	5.513842
MFL	0.023850	0.441180	0.941286	1.857378	3.786231	5.265240
MFL with high SLR	0.026194	0.311422	0.732912	1.739569	4.233669	6.224965
MFL with interm. SLR	0.025552	0.385201	0.864665	1.811575	3.976692	5.652883
MFL with low SLR	0.024895	0.410303	0.900065	1.833919	3.892147	5.478444
	Bottom Area (10^6 m^2)					
Baseline	0.022270	0.319397	0.727974	1.522543	3.047483	4.106031
BSL with high SLR	0.019797	0.197945	0.494627	1.243471	2.994997	4.256713
BSL with interm. SLR	0.021781	0.266077	0.635311	1.410697	3.039572	4.180979
Baseline with low SLR	0.022084	0.289837	0.677163	1.461496	3.045787	4.150720
MFL	0.022104	0.298305	0.685807	1.451241	2.996925	4.082263
MFL with high SLR	0.019243	0.180747	0.451266	1.175876	2.932776	4.231264
MFL with interm. SLR	0.021475	0.245825	0.592729	1.336140	2.984409	4.156159
MFL with low SLR	0.021850	0.268907	0.634734	1.388806	2.992767	4.126172
	Shoreline Length (KM)					
Baseline	1.617573	6.732102	13.846741	28.417436	54.317439	68.618924
BSL with high SLR	1.537379	5.050679	10.166741	23.029443	51.279781	68.159389
BSL with interm. SLR	1.613287	5.995899	12.342978	26.079470	53.118313	68.440318
Baseline with low SLR	1.620151	6.321070	13.003641	27.103785	53.653303	68.525583
MFL	1.606833	6.435934	13.197298	27.188131	53.516569	68.296217
MFL with high SLR	1.497454	4.781988	9.4876770	21.977504	50.315034	67.811933
MFL with interm. SLR	1.592354	5.703016	11.693586	24.806251	52.252551	68.101759
MFL with low SLR	1.604012	6.022964	12.361986	25.862354	52.821463	68.190845

Table 33. Percentage reductions of water volume, bottom area, and shoreline length for salinity ≤ 1, 2, 3, 5, 10, and 15 psu caused by the MFL, relative to those under the baseline flow condition for different SLR scenarios.

Salinity (psu) ≤	**1**	**2**	**3**	**5**	**10**	**15**
SLR Scenario	Water Volume					
No SLR (#0)	1.21%	6.52%	5.70%	4.65%	1.75%	0.63%
High SLR (#1)	3.66%	8.57%	8.18%	5.38%	2.13%	0.65%
Interm. SLR (#2)	2.05%	7.51%	6.51%	5.23%	1.90%	0.65%
Low SLR (#3)	1.61%	7.12%	6.12%	4.95%	1.84%	0.64%
	Bottom Area					

No SLR	0.75%	6.60%	5.79%	4.68%	1.66%	0.58%
High SLR	2.80%	8.69%	8.77%	5.44%	2.08%	0.60%
Interm. SLR	1.40%	7.61%	6.70%	5.29%	1.81%	0.59%
Low SLR	1.06%	7.22%	6.27%	4.97%	1.74%	0.59%
	Shoreline Length					
No SLR	0.66%	4.40%	4.69%	4.33%	1.47%	0.47%
High SLR	2.60%	5.32%	6.68%	4.57%	1.88%	0.51%
Interm. SLR	1.30%	4.88%	5.26%	4.88%	1.63%	0.49%
Low SLR	1.00%	4.72%	4.93%	4.58%	1.55%	0.49%

Percentage reductions of altered and natural shorelines for various salinity ranges caused by the MFL, relative to their corresponding shoreline lengths under the baseline flow condition, for no SLR, high SLR, intermediate SLR, and low SLR are shown in Table 34. It can be seen from the table that neither altered nor natural shores for salinity ≤ 1, 2, 3, 5, 10, and 15 psu are reduced by the proposed MFL for more than 10%. In other words, the proposed MFL is valid under various SLR scenarios when altered and natural shoreline lengths are concerned.

Table 34. Relative reductions of altered shoreline length for salinity ≤ 1, 2, 3, 5, 10, and 15 psu caused by the MFL, relative to those under the BSL condition for different SLR scenarios.

Salinity (psu) ≤	**1**	**2**	**3**	**5**	**10**	**15**
SLR Scenario	Altered Shore					
No SLR (#0)	0.57%	3.83%	3.32%	2.27%	0.60%	0.11%
High SLR (#1)	2.32%	4.60%	4.52%	2.90%	0.80%	0.13%
Interm. SLR (#2)	1.14%	4.20%	3.81%	2.60%	0.67%	0.12%
Low SLR (#3)	0.86%	4.05%	3.53%	2.42%	0.62%	0.12%
	Natural Shore					
No SLR	0.83%	5.33%	6.57%	5.86%	1.90%	0.63%
High SLR	3.18%	6.69%	9.45%	6.19%	2.45%	0.68%
Interm. SLR	1.66%	6.05%	7.14%	6.72%	2.11%	0.66%
Low SLR	1.25%	5.75%	6.81%	6.18%	1.99%	0.65%

<u>*5.2.2 Thermal Habitats for Manatees*</u>

Table 35 shows simulated 72-hour moving averages of ≥ 20 ºC water volume, in cubic meters, at the same five critical time points as those shown in Table 18 for the BSL condition, BSL with the high, intermediate, and low SLRs, MFL, and MFL with the high, intermediate, and low SLRs. Percentage reductions of warm water volume caused by the MFL for no SLR and for high, intermediate, and low SLRs are listed in Table 36. From Table 36, it can be seen that with the consideration of the SLR, the proposed MFL will cause warm water volume for manatees to be reduced by 1.09% - 7.89% at the five critical time points.

Table 35. Seventy-two-hour averages of warm water volume (in m^3) under the chronic condition for manatees for various SLR scenarios under the baseline flow and MFL conditions at the five critical time points.

	72-Hour Time Window				
	#1	*#2*	*#3*	*#4*	*#5*
	1/9/10 18:00 *1/12/10 18:00*	*1/10/10 13:00* *1/13/10 13:00*	*12/12/10 12:00* *12/15/10 12:00*	*12/12/10 15:00* *12/15/10 15:00*	*1/16/18 19:30* *1/19/18 19:30*
Baseline	199944	225165	155472	154186	239217
BSL with high SLR	221087	229998	127372	126644	254021
BSL with interm. SLR	210924	233336	143164	142864	242453
Baseline with low SLR	204513	230046	148594	148187	241901
MFL	195321	218720	143510	143029	227046
MFL with high SLR	213246	218920	118012	118480	250557
MFL with interm. SLR	208057	225781	132508	132113	234749
MFL with low SLR	202290	223159	136875	136548	231497

Table 36. Percentage reductions of the 72-hour average of ≥ 20 ºC water volume caused by the MFL at the five critical time points, relative to the corresponding ≥ 20 ºC volumes under the baseline flow condition for different SLR scenarios.

SLR Scenario	72-Hour Time Window				
	#1	*#2*	*#3*	*#4*	*#5*
	1/9/10 18:00 *1/12/10 18:00*	*1/10/10 13:00* *1/13/10 13:00*	*12/12/10 12:00* *12/15/10 12:00*	*12/12/10 15:00* *12/15/10 15:00*	*1/16/18 19:30* *1/19/18 19:30*
No SLR (#0)	2.31%	2.86%	7.69%	7.24%	5.09%
High SLR (#1)	3.55%	4.82%	7.35%	6.45%	1.36%
Interm. SLR (#2)	1.36%	3.24%	7.44%	7.53%	3.18%
Low SLR (#3)	1.09%	2.99%	7.89%	7.85%	4.30%

Table 37 shows simulated 72-hour moving averages of ≥ 20 ºC surface area, in square meters, at the same five critical time points as those shown in Table 20 for the BSL condition, BSL with the high, intermediate, and low SLRs, MFL, and MFL with the three SLRs. Percentage reductions of ≥ 20 ºC surface area caused by the MFL for no SLR and for high, intermediate, and low SLR estimates are listed in Table 38. From Table 38, it can be seen that the MFL causes warm water surface area to be reduced by 1.69% to 7.94% in the Homosassa River at the five critical time points, with the consideration of the three SLRs.

Table 37. Seventy-two-hour averages of ≥ 20 ºC surface area (in m^2) under the chronic condition for manatees for various SLR scenarios under the baseline flow and MFL conditions at the five critical time points.

	72-Hour Time Window				
	#1	*#2*	*#3*	*#4*	*#5*
	1/9/10 18:00 1/12/10 18:00	*1/10/10 13:00 1/13/10 13:00*	*12/12/10 11:30 12/15/10 11:30*	*12/12/10 12:00 12/15/10 12:00*	*1/16/18 19:30 1/19/18 19:30*
Baseline	171647	198121	122169	122057	205972
BSL with high SLR	177746	181761	97283	97456	199050
BSL with interm. SLR	178762	199398	112210	112312	202338
Baseline with low SLR	174109	199618	117226	117227	204940
MFL	165976	190543	113615	113575	194566
MFL with high SLR	168230	168709	91386	91558	195692
MFL with interm. SLR	174889	190401	104488	104500	194220
MFL with low SLR	171122	191122	107923	107993	194883

Table 38. Percentage reductions of the 72-hour average of ≥ 20 ºC surface area caused by the MFL at the five critical time points, relative to the corresponding ≥ 20 ºC surface areas under the baseline flow condition for different SLR scenarios.

SLR Scenario	72-Hour Time Window				
	#1	*#2*	*#3*	*#4*	*#5*
	1/9/10 18:00 1/12/10 18:00	*1/10/10 13:00 1/13/10 13:00*	*12/12/10 11:30 12/15/10 11:30*	*12/12/10 12:00 12/15/10 12:00*	*1/16/18 19:30 1/19/18 19:30*
No SLR (#0)	3.30%	3.82%	7.00%	6.95%	5.54%
High SLR (#1)	5.35%	7.18%	6.06%	6.05%	1.69%
Interm. SLR (#2)	2.17%	4.51%	6.88%	6.96%	4.01%
Low SLR (#3)	1.72%	4.26%	7.94%	7.88%	4.91%

Table 39 shows simulated 4-hour moving averages of ≥ 15 ºC water volume, in cubic meters, at the same six critical time points as those shown in Table 22 for the BSL condition, BSL with the high, intermediate, and low SLRs, MFL, and MFL with the three SLRs. Percentage reductions of noncold water volume caused by the MFL for no SLR and for high, intermediate, and low SLRs are listed in Table 40. From

Table 40 it can be seen that at 12:00 PM, 1/2/2018, the MFL would cause ≥ 15 ºC water volume to be reduced by 8.88%, 6.63%, 19.21% and 15.02% for no SLR, high SLR, intermediate SLR, and low SLR, respectively. At all other 5 time points, the MFL would cause ≥ 15 ºC water volume to be reduced by 0.22% - 9.90%.

Table 39. 4-hour averages of ≥ 15 ºC water volume (in m^3) under the acute condition for manatees for various SLR scenarios under the baseline flow and MFL conditions at the six critical time points.

	4-Hour Time Window					
	#1	*#2*	*#3*	*#4*	*#5*	*#6*
	1/11/10 4:00 1/11/10 8:00	*1/11/10 23:00 1/12/10 3:00*	*12/13/10 22:00 12/14/10 2:00*	*12/14/10 1:00 12/14/10 5:00*	*1/2/18 10:00 1/2/18 14:00*	*1/18/18 5:30 1/18/18 9:30*
Baseline	661659	864040	168499	159732	223030	951766
BSL with high SLR	683985	889095	167125	175631	164109	1012789
BSL with interm. SLR	687314	881913	178133	165557	198443	986809
Baseline with low SLR	674189	873857	172842	159600	220205	971918
MFL	619405	824831	165722	154156	203219	914841
MFL with high SLR	616290	835823	159414	160532	153222	985710
MFL with interm. SLR	645718	839792	176345	165405	160317	937489
MFL with low SLR	625705	834779	172419	159243	187128	922379

Table 40. Percentage reductions of 4-hour average of ≥ 15 ºC water volume caused by the MFL at the six critical time points, relative to the corresponding ≥ 15 ºC water volumes under the baseline flow condition for different SLR scenarios.

SLR Scenario	4-Hour Time Window					
	#1	*#2*	*#3*	*#4*	*#5*	*#6*
	1/11/10 4:00 1/11/10 8:00	*1/11/10 23:00 1/12/10 3:00*	*12/13/10 22:00 12/14/10 2:00*	*12/14/10 1:00 12/14/10 5:00*	*1/2/18 10:00 1/2/18 14:00*	*1/18/18 5:30 1/18/18 9:30*
No SLR (#0)	6.39%	4.54%	1.65%	3.49%	8.88%	3.88%
High SLR (#1)	9.90%	5.99%	4.61%	8.60%	6.63%	2.67%
Interm. SLR (#2)	6.05%	4.78%	1.00%	0.09%	19.21%	5.00%
Low SLR (#3)	7.19%	4.47%	0.24%	0.22%	15.02%	5.10%

Table 41 shows simulated 4-hour moving averages of ≥ 15 ºC surface area, in square meters, at the same six critical time points as those shown in Table 24 for the baseline flow condition, BSL with the high, intermediate, and low SLRs, MFL, and MFL with the three SLRs. Percentage reductions of noncold surface area caused by the MFL for no SLR and for the high, intermediate, and low SLR estimates are listed in Table 42. Only at 10:00 AM, 1/2/2018 and with the intermediate SLR would the ≥ 15 ºC surface area be reduced by more than 15% by the proposed

MFL. Other than this, the ≥ 15 ºC surface area reduction caused by the MFL is ranged between 0.20% and 14.06%.

Table 41. 4-hour averages of ≥ 15 ºC surface area (in m^2) under the acute condition for manatees for various SLR scenarios under the baseline flow and MFL conditions at six critical time points.

	4-Hour Time Window					
	#1	*#2*	*#3*	*#4*	*#5*	*#6*
	1/11/10 4:00 *1/11/10 8:00*	*1/11/10 23:00* *1/12/10 3:00*	*12/13/10 21:30* *12/14/10 1:30*	*12/13/10 22:00* *12/14/10 2:00*	*1/2/18 8:00* *1/2/18 12:00*	*1/18/18 5:30* *1/18/18 9:30*
Baseline	616414	813223	123877	146234	230755	847061
BSL with high SLR	604132	757304	152747	153961	155351	828583
BSL with interm. SLR	634854	799932	134549	144530	184885	854186
Baseline with low SLR	626313	806994	127009	139952	204059	855426
MFL	576240	780683	121144	135583	201631	811984
MFL with high SLR	545710	715118	154770	153257	142843	799062
MFL with interm. SLR	593331	766093	134305	140019	142643	809564
MFL with low SLR	574901	775589	126752	135536	175373	807997

Table 42. Percentage reductions of 4-hour average of ≥ 15 ºC surface area caused by the MFL at the six critical time points, relative to the corresponding ≥ 15 ºC surface areas under the baseline flow condition for different SLR scenarios.

SLR Scenario	4-Hour Time Window					
	#1	*#2*	*#3*	*#4*	*#5*	*#6*
	1/11/10 4:00 *1/11/10 8:00*	*1/11/10 23:00* *1/12/10 3:00*	*12/13/10 21:30* *12/14/10 1:30*	*12/13/10 22:00* *12/14/10 2:00*	*1/2/18 8:00* *1/2/18 12:00*	*1/18/18 5:30* *1/18/18 9:30*
No SLR (#0)	6.52%	4.00%	2.21%	7.28%	12.62%	4.14%
High SLR (#1)	9.67%	5.57%	-1.32%	0.46%	8.05%	3.56%
Interm. SLR (#2)	6.54%	4.23%	0.18%	3.12%	22.85%	5.22%
Low SLR (#3)	8.21%	3.89%	0.20%	3.16%	14.06%	5.54%

Tables 36, 38, 40, and 42 show that the 15% reduction criterion used for manatee thermal habitats could be violated by the proposed MFL when the intermediate and low see level rises are considered. However, the violation would only occur for the acute condition during a 4-hour window centered at 10;00 AM, 1/2/2018, or between 8:00 AM and 12:00 PM on 1/2/2018.

5.2.3 Thermal Habitats for Common Snook

Percentage reductions of ≥ 15 ºC water volume and surface area caused by the MFL, relative to those under the BSL condition for no SLR, high SLR, intermediate SLR, and low SLR during the 11 varying Common Snook seasons are shown in Table 43. The table also lists the largest MFL-induced percentage reductions of ≥ 15 ºC water volume and surface area among the

11 varying Common Snook seasons. They all occurred during 12/2/10 23:45 – 2/15/11 12:00, the same most sensitive Common Snook season to the SGD reduction without considering any SLRs (see Table 27). From Table 43, it can be seen that the proposed MFL does not cause ≥ 15 ºC water volume and surface area to be reduced by 15% for any of the three SLRs, when a time scale of a varying Common Snook season is concerned.

Table 43. MFL-induced percentage reductions of ≥ 15 ºC water volume and surface area, relative to those under the baseline flow condition for different SLR scenarios during all the 11 varying Common Snook seasons and during most sensitive Common Snook season (12/2/10 23:45 – 2/15/11 12:00.)

SLR Scenario	Volume Reduction	Surface Area Reduction	Volume Reduction	Surface Area Reduction
	All 11 Varying Common Snook Seasons		12/2/10 23:45 – 2/15/11 12:00	
No SLR (#0)	0.59%	0.59%	2.31%	2.29%
High SLR (#1)	0.53%	0.55%	2.19%	2.30%
Interm. SLR (#2)	0.56%	0.57%	2.23%	2.31%
Low SLR (#3)	0.58%	0.59%	2.24%	2.27%

Similar to results shown in Table 43 for varying Common Snook seasons, percentage reductions of ≥ 15 ºC water volume and surface area caused by the MFL, relative to those under the BSL condition for various SLRs during the 11 fixed Common Snook seasons and the most sensitive Common Snook season are listed in Table 44. Because a fixed Common Snook season contains more noncold days than a varying Common Snook season, thermal habitats during fixed Common Snook seasons are less sensitive to the MFL for all the SLRs, in comparison with the results during varying Common Snook seasons. Again, the proposed MFL doesn't cause ≥ 15 ºC water volume and surface area to be reduced by 15% for any of the three SLRs, when a time scale of a fixed Common Snook season is used.

Table 44. MFL-induced percentage reductions of ≥ 15 ºC water volume and surface area, relative to those under the baseline flow condition for different SLR scenarios during all the 11 fixed Common Snook seasons and during most sensitive Common Snook season (10/30/2009 – 3/28/2010.)

Scenario	Volume Reduction	Surface Area Reduction	Volume Reduction	Surface Area Reduction
	All 11 Fixed Common Snook Seasons		10/30/2009 – 3/28/2010	
No SLR (#0)	0.35%	0.35%	0.80%	0.81%
High SLR (#1)	0.32%	0.33%	0.72%	0.76%
Interm. SLR (#2)	0.33%	0.34%	0.74%	0.78%

Low SLR (#3)	0.35%	0.35%	0.79%	0.82%

When the time scale is shortened to cold-day blocks or individual cold days, MFL effects on Common Snook thermal habitats become more significant for all the SLR scenarios. Percentage reductions of ≥ 15 ºC water volume and surface area caused by the MFL, relative to those under the BSL condition for various SLRs during the cold days only are shown in Table 45. For all the 401 cold days during the 10.5 years, the average ≥ 15 ºC volume and surface reductions caused by the MFL are all less than 2%, with SLRs slightly hampering the Common Snook thermal habitat reductions, probably because SLRs allow the river to contain more noncold volume and surface area days prior to a cold front arrives. Among the 82 cold-day blocks, the maximum percentage reductions of ≥ 15 ºC volume caused by the MFL for no SLR, low SLR, intermediate SLR, and high SLR are 6.87%, 6.97%, 7.30%, and 7.91%, respectively, while the maximum percentage reductions of ≥ 15 ºC surface area are 7.36%, 7.42%, 7.55%, and 7.85%, respectively.

From Table 45, it can be seen that on the daily time scale, the maximum ≥ 15 ºC volume reductions caused by the MFL can reach 15.26% and 16.56%, respectively for the intermediate and high SLRs, while the maximum ≥ 15 ºC surface area reductions can reach 15.30%, 16.23%, and 18.14%, respectively for the low, intermediate, and high SLRs. Therefore, the proposed MFL can be invalid on individual cold days, when the three SLRs are concerned.

Table 45. Overall percentage reductions during all cold days, maximum percentage reductions among all 82 cold day blocks, and maximum percentage reductions among all 401 days of ≥ 15 ºC water volume and surface area caused by the MFL, relative those under the baseline condition for various SLR scenarios.

SLR Scenario	Volume Reduction	Surface Area Reduction	Max Vol Reduction	Max Surface Area Reduction	Max Vol Reduction	Max Surface Area Reduction
	All < 15 ºC Days		Among 82 <15 ºC Day Blocks		Among 401 < 15 ºC Days	
No SLR (#0)	1.99%	1.94%	6.87%	7.36%	13.32%	14.92%
High SLR (#1)	1.74%	1.73%	7.91%	7.85%	16.58%	18.14%
Interm. SLR (#2)	1.89%	1.88%	7.30%	7.55%	15.26%	16.23%
Low SLR (#3)	1.95%	1.93%	6.97%	7.42%	14.88%	15.30%

In summary, the proposed MFL is checked for the high, intermediate, and low sea level rise estimates. It was found that the proposed MFL holds for salinity habitats with the 15% reduction criterion not being violated. Nevertheless, the proposed MFL could cause the 15% threshold for manatee and Common Snook thermal habitats to be crossed on certain days.

6. Conclusions

The laterally averaged hydrodynamic model LAMFE (Chen et al., 2000; Chen, 2003, Chen, 2004a, Chen, 2004b) was applied to the Homosassa River to simulate circulations and salinity and thermal transport processes in the spring-fed estuary on the Gulf coast of Florida. The river is relatively short and narrow. It has a length of about 13 KM, from its headwaters to the mouth, and a width ranging from about 60 m in the upstream area to over 300 m near the mouth. While the upstream half of the Homosassa River consists of relatively simple channels, the downstream half is complicated because of the existence of many braided channels, which are interconnected and flow through many coastal marsh complexes. The estuarine system is generally well or partially mixed and receives submarine groundwater discharges from the Homosassa Springs, the Homosassa SE Fork, and the Halls River. Salinities in the SGDs vary with the location of the spring vents. Salinity in the SE Fork SGD is mainly fresh, while salinity in the Homosassa Springs SGD varies roughly around 2 psu. For the SGD in the Halls River, salinity is even higher, roughly in the range of 5 – 6 psu. Temperature in the SGD is relatively stable, varying in the range of 22 to 24 degree Celsius depending on tides and the season of the year.

In the model application, 406 longitudinal grids and 15 vertical layers were used to discretize the simulation domain, with grid length varying between 29 m to 281 m and layer thickness varying between 0.3 m to 1.76 m. The model was calibrated and verified against measured real-time data of water level, salinity, and temperature in the Homosassa River, Halls River, and SE Fork during the 34-months period from November 4, 2014 to August 31, 2917.

The application of the LAMFE to the Homosassa River estuary was a success. Skills and R^2 values are generally high for all the parameters simulated at the USGS data collection stations, except for simulated salinities and temperatures at one or two upstream stations due to the lack of temporal variabilities of these parameters. At data stations with low R^2 values or skills for salinity and temperature predictions, however, mean errors and mean absolute errors are generally low. Average R^2 values for water level, salinity, and temperature are 0.86, 0.71, and 0.85 respectively, while average skill assessment parameters for water level, salinity, and temperature are 0.96, 0.91, and 0.92 respectively. Overall mean errors for water level, salinity, and temperature simulations are -0.66 cm, 0.003 psu, and -0.16 ºC, respectively. Overall mean absolute errors for water level, salinity, and temperature simulations are 5.48 cm, 0.46 psu, and 0.66 ºC, respectively.

After the hydrodynamic model was calibrated and verified, it was used to conduct a series of flow reduction scenario runs, including the baseline and existing flow conditions and 2.5% – 30% flow reductions with a 2.5% increment. The scenario simulation period was about 125 months (~10.5 years,) from October 9, 2007 to March 12, 2018. Model results, including salinities and temperatures at all grid cells over the entire 125-month period, were analyzed. Different salinity and thermal habitats were calculated based on simulated salinity and temperature results and bathymetry data using a post-process program. These salinity and thermal habitats include water volumes, bottom areas, and shoreline lengths for salinity ≤ 1, 2, 3, 5, 10, 15, and 20 psu and water volume and surface areas for temperature < 15 ºC, ≥ 15 ºC, and ≥ 20 ºC. For ≥ 15 ºC and ≥ 20 ºC thermal habitats, the volume and surface area calculations were conducted both with and without a depth (or layer thickness) restriction of 3.8 feet (1.158 m.) Water volumes and surface areas for ≥ 15 ºC and ≥ 20 ºC with the 3.8 feet restriction were used in the analysis for manatee protection, while ≥ 15 ºC habitats without the 3.8 ft restriction were used for in the analysis of Common Snook protection.

Calculated salinity and thermal habitats were analyzed to examine how flow reductions affect the availabilities of these habitats and what percentage of flow reduction would cause a significant reduction of a favorite habitat. It was found that the most sensitive salinity habitat to flow reduction is ≤ 2 psu bottom area, which will be reduced by 15% with a 11.09% SGD reduction. The most sensitive manatee thermal habitat to the flow reduction is the 4-hour average of ≥ 15 ºC surface area, which can be reduced by 15% with a 6.44% reduction of SGD when the thermal habitat under the acute condition is low. For Common Snook, the most sensitive thermal habitat is the single cold day average of ≥ 15 ºC surface area, which can be reduced 15% with a 5.03% SGD reduction.

Sea level rises in 2035 relative to 2012, the middle of the 10.5-year scenario simulation period, at the mouth of the Homosassa River were estimated based on those obtained from the USACE web site http://www.corpsclimate.us/ccaceslcurves.cfm for the NOAA St. Petersburg and Cedar Key stations by the inverse distance weighting method. The low, intermediate, and high SLRs were estimated to be 4.741, 8.588, and 20.990 cm, respectively over the 23-year span. These SLRs were added to open boundaries at the mouth of the Homosassa River, Salt River, and Mason Creek to drive the hydrodynamic model in simulating the BSL and the MFL (5% flow reduction) conditions. It should be noted that not all effects of a SLR on circulations and salinity and temperature transport processes in the river were considered in the analysis. Many other factors associated with a SLR were not included in the simulations, including the groundwater level rise that could be caused by a SLR.

The purpose for considering SLRs in the MFL re-evaluation is to see if a proposed MFL is still valid when there is a SLR in the future. In consistence with the District planning horizon, it is desirable to find out if the MFL established using the 125-month period between 2007 and 2018 would be violated 23 years later if a 10.5-year period between 2030 and 2040 were used in the analysis. The assumption here is that the baseline conditions during the two 10.5-year periods were the same except for the sea level rise.

To analyze MFL effects on salinity and thermal habitats with a SLR, the relative changes of the habitats caused by the proposed MFL with a SLR should be compared with those for the baseline flow condition with the same SLR. Model results suggest that a sea level rise could significantly change salinity and thermal characteristics in the Homosassa River. Using the same 15% criterion to define a significant harm, the proposed MFL (5% reduction of SGDs) does not cross the threshold for salinity habitats for all SLRs. However, when the manatee thermal habitats under the acute condition are considered, the proposed MFL becomes invalid if the intermediate and low SLRs are concerned. For Common Snook thermal habitats, the 15% reduction criterion for ≥ 15 ºC volume could be violated occasionally by the proposed MFL if any of the three SLR scenarios occurs.

7. References

Blewett, D.A. and Stevens, P.W., 2014. Temperature variability in a subtropical estuary and implications for common snook *Centropomus undecimalis*, a cold-sensitive fish. Gulf of Mexico Science, 32(1).

Blumberg, A.F., Kim, B.N., 2000. Flow Balance in St. Andrew Bay Revealed Through Hydrodynamic Simulations. *Estuaries*, 23, 21 – 33

Chen, X., 1997. Simulating Salinity Distributions in the Lower Hillsborough River with a Laterally Averaged Two-Dimensional Hydrodynamic Model. Technical Report, Southwest Florida Water Management District, Brooksville, Florida.

Chen, X., 1999. Study of Salt Transport in the Lower Hillsborough River Using a Laterally Averaged Two-Dimensional Hydrodynamic Model. Technical Report, Southwest Florida Water Management District, Tampa, Florida.

Chen, X., M.S. Flannery and D.L. Moore. 2000. Response times of salinity in relation to changes in freshwater inflows in the Lower Hillsborough River. *Estuaries*. 23:735-742.

Chen, X., 2003a. An efficient finite difference scheme for simulating hydrodynamics in narrow rivers and estuaries. *International Journal for Numerical Methods in Fluids*, 42: 233-247.

Chen, X., 2003b. Coupling a 3D model with a 2DV model using a free-surface correction method. In (M. L. Spaulding, ed.) *Proceedings of ASCE Estuarine and Coastal Modeling 8*, 769-783.

Chen, X., 2004a. *Simulating Hydrodynamics and Salinity Transport in the Lower Hillsborough River During February 2001 - December 2002*. Technical Report, Southwest Florida Water Management District, Tampa, Fla.

Chen, X., 2004b. Modeling hydrodynamics and salt transport in the Alafia River estuary, Florida during May 1999–December 2001. *Estuarine, Coastal and Shelf Science*, 61 (3), 477-490.

Chen, X., 2004c. Using a piecewise linear bottom to fit the bed variation in a laterally averaged, z-coordinate hydrodynamic model. *International Journal for Numerical Methods in Fluids*. 44: 1185-1205.

Chen, X., 2005. *Simulating Hydrodynamics in the Lower Alafia River Estuary*. Technical Report, Southwest Florida Water Management District, Tampa, Fla.

Chen, X., 2006. Using a Dynamically Coupled 3D-2DV Model to Simulate Hydrodynamics in the Lower Peace River – Upper Charlotte Harbor System in Southwest Florida. In (M. L. Spaulding, ed.) *Proceedings of ASCE Estuarine and Coastal Modeling 9*, 72 -89.

Chen, X., 2007a. *Simulating Hydrodynamics in the Lower Peace River – Lower Myakka River - Upper Charlotte Harbor System, Florida during May 2003 – July 2004.* Technical Report, Southwest Florida Water Management District, Tampa, Florida.

Chen. 2007b. A laterally averaged two-dimensional trajectory model for estimating transport time scales in the Alafia River estuary, Florida. *Estuarine*, *Coastal and Shelf Science*, 75: 358-370, doi:10.1016/j.ecss.2007.04.020.

Chen. 2007c. Dynamic coupling of a three-dimensional hydrodynamic model with a laterally averaged, two-dimensional hydrodynamic model. *Journal of Geophysical Research*, 112, C07022, doi:10.1029/2006JC003805.

Chen, X., 2008a. *Hydrodynamic Simulations of the Lower Peace River – Lower Myakka River – Upper Charlotte Harbor System in Support of Determining Minimum Flows for the LPR and LMR in Southwest Florida*. Technical Report, Southwest Florida Water Management District, Tampa, Florida.

Chen, X., 2008b. Simulating Hydrodynamics in the Upper Charlotte Harbor and Its Major Tributaries in Florida. *Journal of Coastal Research*, SI 52: 149 – 162.

Chen, X., 2008c. Simulating Hydrodynamics in the Manatee and Braden River Estuaries in Southwest Florida using a Multi-Block Model. *Proceedings of ASCE Estuarine and Coastal Modeling 10*, 358 – 372.

Chen, X., 2010. *Hydrodynamic Simulations of the Lower Peace River – Lower Myakka River – Upper Charlotte Harbor System in Support of Determining Minimum Flows for the LPR and LMR in Southwest Florida*. Technical Report, Southwest Florida Water Management District, Tampa, Florida.

Chen, X., 2011. *User's Manual for a Laterally Averaged Model for Estuaries.* Technical Report, Southwest Florida Water Management District, Tampa, Florida.

Chen, X., 2012a. *Simulating Hydrodynamics and Salinity Transport Processes in the Manatee/Braden River Estuarine System Using a Multi-Block Model.* Technical Report, Southwest Florida Water Management District, Tampa, Florida.

Chen, X., 2012b. A sensitivity analysis of low salinity habitats simulated by a hydrodynamic model in the Manatee River estuary in Southwest Florida, USA. *Estuarine*, *Coastal and Shelf Science*, 104 - 105: 80-90, doi:10.1016/j.ecss.2012.03.023.

Chen, X., 2012c. Responses of simulated low salinity habitats to uncertainties of gauged and ungauged flows in the Myakka River estuary in Florida. *Proceedings of ASCE Estuarine and Coastal Modeling 12,* 435 – 456.

Chen, X., 2012d. Simulating hydrodynamics in a spring-fed estuary using a three-dimensional unstructured Cartesian grid model. *Estuarine, Coastal and Shelf Science 115*, 246 – 259, doi:10.1016/j.ecss.2012.09.007.

Chen, X., 2013. Evaluating the Response of the Residence Time to Flow in the Lower Peace River Estuary in Florida, USA. *Coastal Hazards, Trends in Engineering Mechanics Special Publication No.2, ASCE-EMI*. 149 -162.

Chen, X., 2017. *An Evaluation of Effects of Flow Reduction on Salinity and Thermal Habitats and Transport Time Scales in Crystal River/Kings Bay*. Technical Report, Southwest Florida Water Management District, Tampa, Florida. 130p.

Chen, X., 2018. *A Modeling Study of Effects of Flow Reduction on Salinity and Thermal Habitats in the Homosassa River.* Technical Report, Southwest Florida Water Management District, Tampa, Florida. 100p.

Chen, X., Flannery, M.S., 1997. Use of a Hydrodynamic Model for Establishing a Minimum Freshwater Flow to the Lower Hillsborough River. In (M. L. Spaulding and A. F. Blumberg, eds.) *Proceedings of ASCE Estuarine and Coastal Modeling 5*, 663-678.

Flannery, M.S., Chen, X., Heyl, M., Munson, A., Dachsteiner, M., 2007. *The Determination of Minimum Flows for the Lower Alafia River Estuary*. Southwest Florida Water Management District, Brooksville, Florida.

Ganju, N.K., Hayn, M., Chen, S.-N., Howarth, R.W., Dickhudt, P.J., Aretxabaleta, A.L., Marino, R., 2012. Tidal and Groundwater Fluxes to a Shallow, Microtidal Estuary: Constraining Inputs Through Field Observations and Hydrodynamic Modeling. *Estuaries and Coasts* 35(5), 1285-1298, doi: 10.1007/s12237-012-9515-x.

Hamrick, J.M., 1992. *A three-dimensional environmental fluid dynamic computer code: Theoretical and computational aspects*. Special Report 317. The College of William and Mary, Virginia Institute of Marine Science, VA.

HSW Engineering, Inc., 2011. A Modeling Study of the Relationship of Freshwater Flow with the Salinity and Thermal Characteristic of the Homosassa River. Prepared for Southwest Florida Water Management District, Tampa, Fla 33637.

Jay, D.A., Smith, J.D., 1990. Residual circulation in shallow estuaries, 2, Weakly stratified and partially mixed, narrow estuaries, *Journal of Geophysical Research*, 95, 733-748.

Janicki Environmental, Inc., Applied Technology & Management. 2007. *Impacts of Withdrawals on the Thermal Regime of the Weeki Wachee River*. Prepared for Southwest Florida Water Management District, Tampa, Fla 33637.

Johnson, B.H., Kim, K.W., Heath, R., Hsieh, B., Butler, L., 1991. Validation of a Three-Dimensional Hydrodynamic Model of Chesapeake Bay, *Journal of Hydraulic Engineering*, 117 (1), 2 – 20.

Levesque, V.A., Oberg, K.A., 2012. Computing discharge using the index velocity method: U.S. Geological Survey Techniques and Methods 3–A23, 148 p.

Prandle, D., 1985. On salinity regimes and the vertical structure of residual flows in narrow tidal estuaries. *Estuarine Coastal and Shelf Science*, 20, 615–635.

Rouhani, S., Sucsy, P., Hall, G., Osburn, W., Wild, M. 2007. *Analysis of Blue Spring Discharge Data to Determine a Minimum Flow Regime*. Prepared for St. Johns River Water Management District, Palatka, Fla. 32178.

Shafland, P.L. and Foot, K. J. 1983. A lower lethal temperature for fingerling snook, *Centropomus undecimalis*. *Gulf of Mexico Science.* 6 (2).

Stevens, P.W., Blewett, D.A., Boucek, R.E., Rehage, J.S., Winner, B.L., Young, J.M., Whittington, J.A. and Paperno, R., 2016. Resilience of a tropical sport fish population to a severe cold event varies across five estuaries in southern Florida. *Ecosphere*, 7(8).

Vanasse Hangen Brustlin (VHB), Inc., 2014. *Chassahowitzka Discharge Measurement and Prediction*, Letter Report to the Southwest Florida Water Management District. 14p.

Vanasse Hangen Brustlin (VHB), Inc., 2014. *Supplemental Water Quality Data Collection in Support of Homosassa River MFL Revaluation*, Report to the Southwest Florida Water Management District. 101p.

Vanasse Hangen Brustlin (VHB), Inc., 2018. *January 2018 Progress Report for Flow Monitoring in Springs Coast*. Memorandum to the Southwest Florida Water Management District. 2p.

Wang, P., 2007. *Shoreline Mapping and Bathymetric Survey for the Homosassa River Systems.* Final Report submitted to Southwest Florida Water Management District, by Department of Geology, University of South Florida, Tampa, FL 33620.

Warner, J.C., Geyer, W.R., Lerczak, J.A., 2005. Numerical modeling of an estuary: A comprehensive skill assessment. *Journal of Geophysical Research* 110, C05001, doi:10.1029/2004JC002691.

Warner, J.C., Sherwood, C.R., Signell, R.P., Harris, C.K., Arango, H.G., 2008. Development of a three-dimensional, regional, coupled wave, current, and sediment-transport model. *Computers & Geosciences* 34: 1284–1306.

Willmott, C.J., 1981. On the validation of models. *Physical Geography* 2, 184-194.

Worthy, G.A.J., Miculka, T.A., Wright, S.D., 2000. Manatee Response to Cold: How Cold is Too Cold? *Florida Manatees and Warm Water, Proceedings of the Warm-Water Workshop*, Jupiter, Fla., pp. 1 - 6

Yobbi, D.K., Knochenmus, L.A., 1989. *Effects of river discharge and high-tide stage on salinity intrusion in the Weeki Wachee, Crystal, and Withlacoochee River estuaries, Southwest Florida*. Water-Resources Investigations Report 88-4116, U.S. Geological Survey, Tallahassee, Florida.

Yobbi, D.K., 2016. Chassahowitzka and Southeast Fork of the Homosassa Rivers Discharge Letter Report. Submitted to Southwest Florida Water Management District. 40 p.

Appendix A. Water Level Data

In all the time series plots in Appendixes A - F, straight-line segments represent missing data during their respectively time periods, if measured parameters are not supposed to vary linearly with time during these time periods.

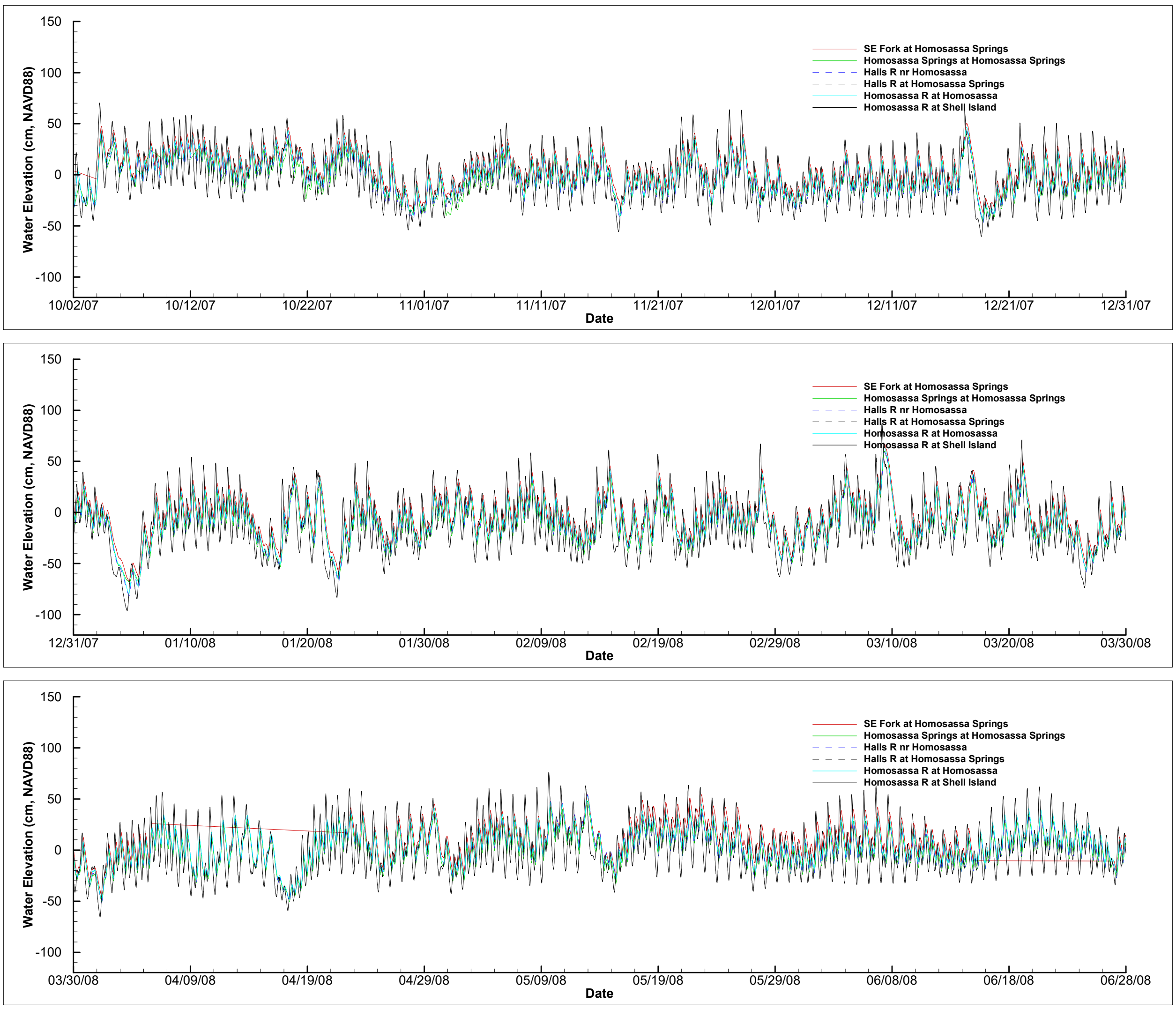

Figure A - 1. Measured real-time water levels at USGS SE Fork Homosassa Spring (read solid lines), Homosassa Springs at Homosassa Springs (green solid lines), Halls River near Homosassa (blue dashed lines), Halls River at Homosassa Springs (black dashed lines), Homosassa River at Homosassa (cyan solid lines), and Homosassa River at Shell Island (black solid lines) stations in the Homosassa River during 10/2/2007 – 6/28/2008.

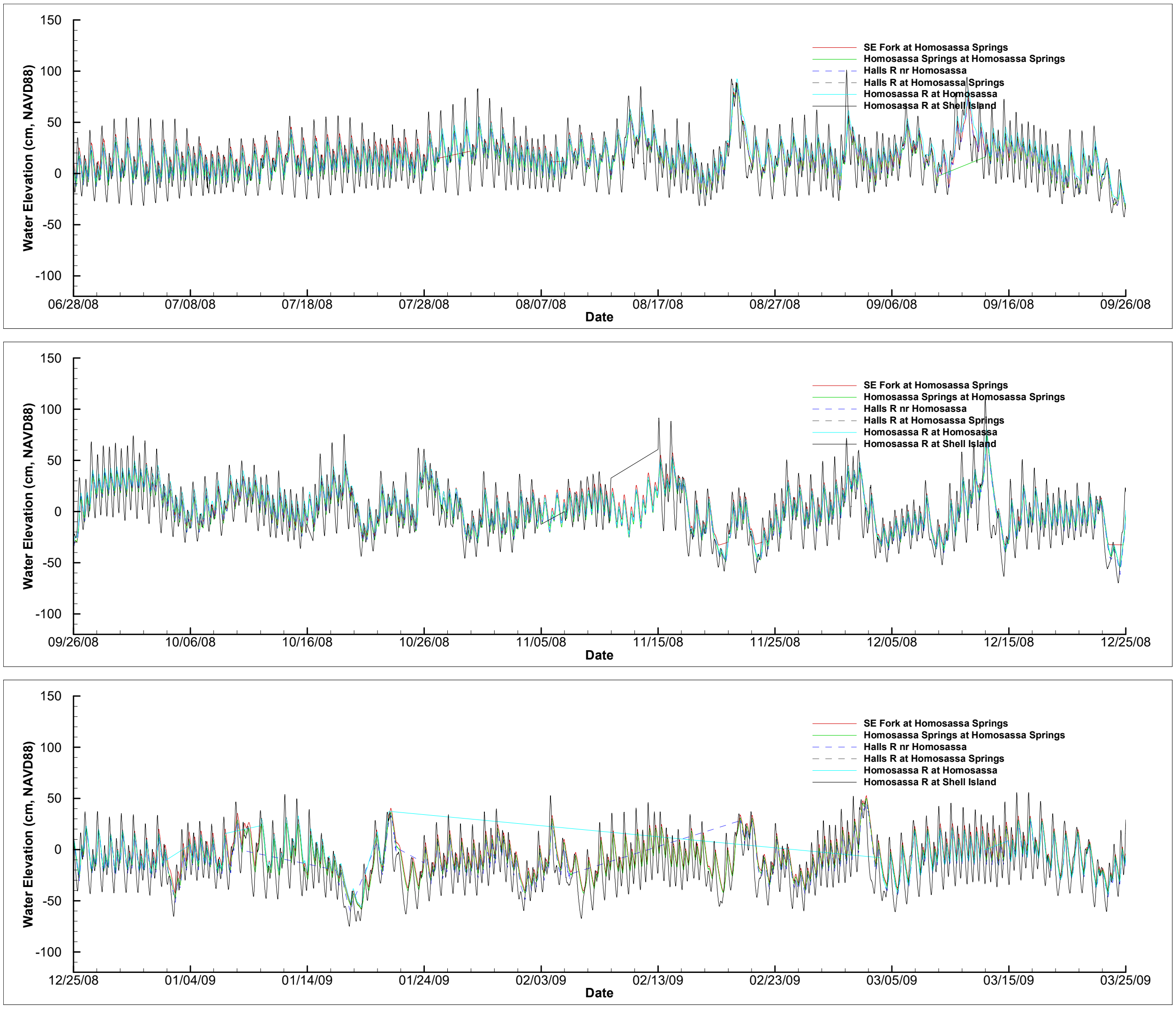

Figure A - 2. Measured real-time water levels at USGS SE Fork Homosassa Spring (read solid lines), Homosassa Springs at Homosassa Springs (green solid lines), Halls River near Homosassa (blue dashed lines), Halls River at Homosassa Springs (black dashed lines), Homosassa River at Homosassa (cyan solid lines), and Homosassa River at Shell Island (black solid lines) stations in the Homosassa River during 6/28/2008 – 3/25/2009.

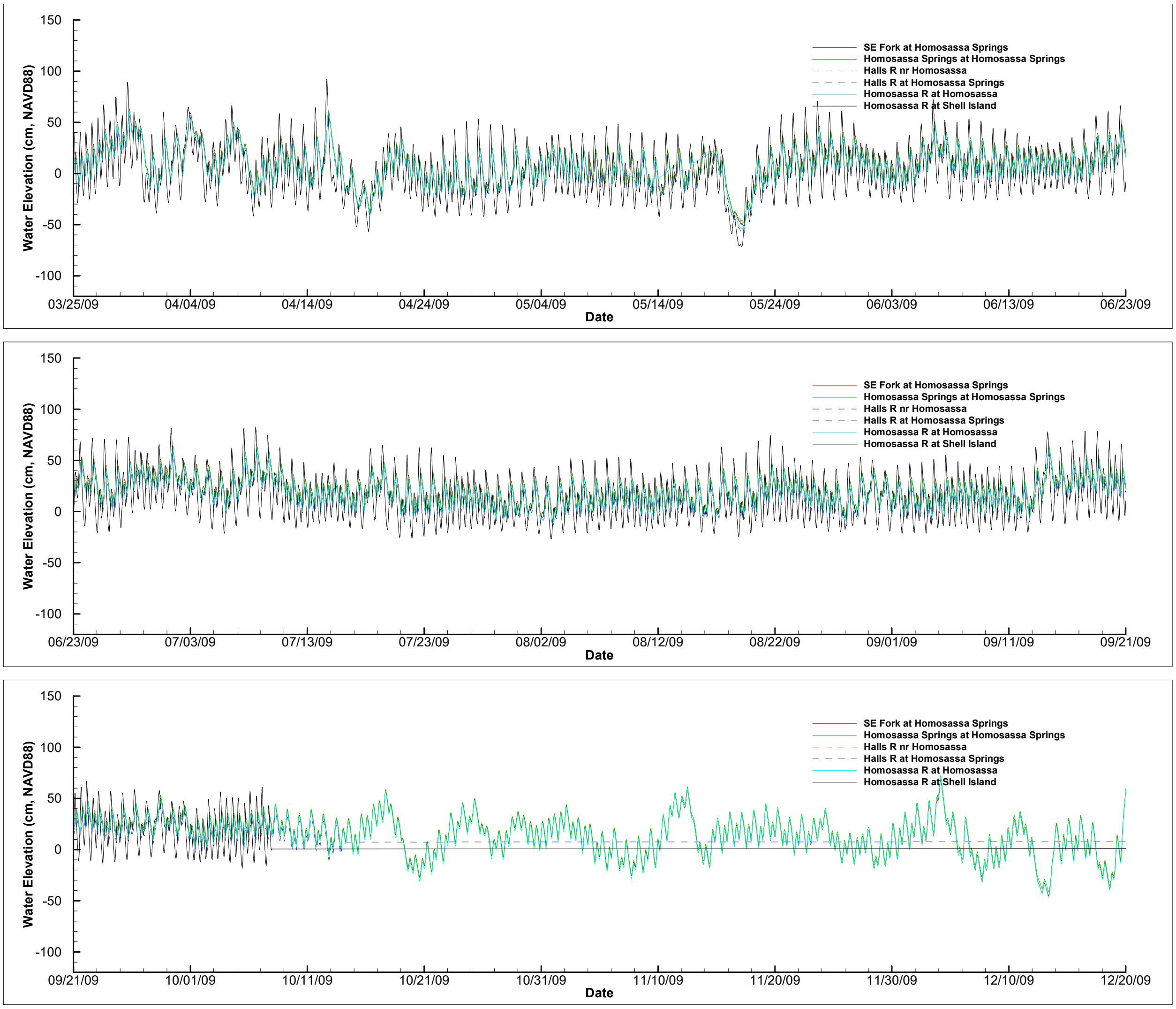

Figure A - 3. Measured real-time water levels at USGS SE Fork Homosassa Spring (read solid lines), Homosassa Springs at Homosassa Springs (green solid lines), Halls River near Homosassa (blue dashed lines), Halls River at Homosassa Springs (black dashed lines), Homosassa River at Homosassa (cyan solid lines), and Homosassa River at Shell Island (black solid lines) stations in the Homosassa River during 3/25/2009 – 12/20/2009.

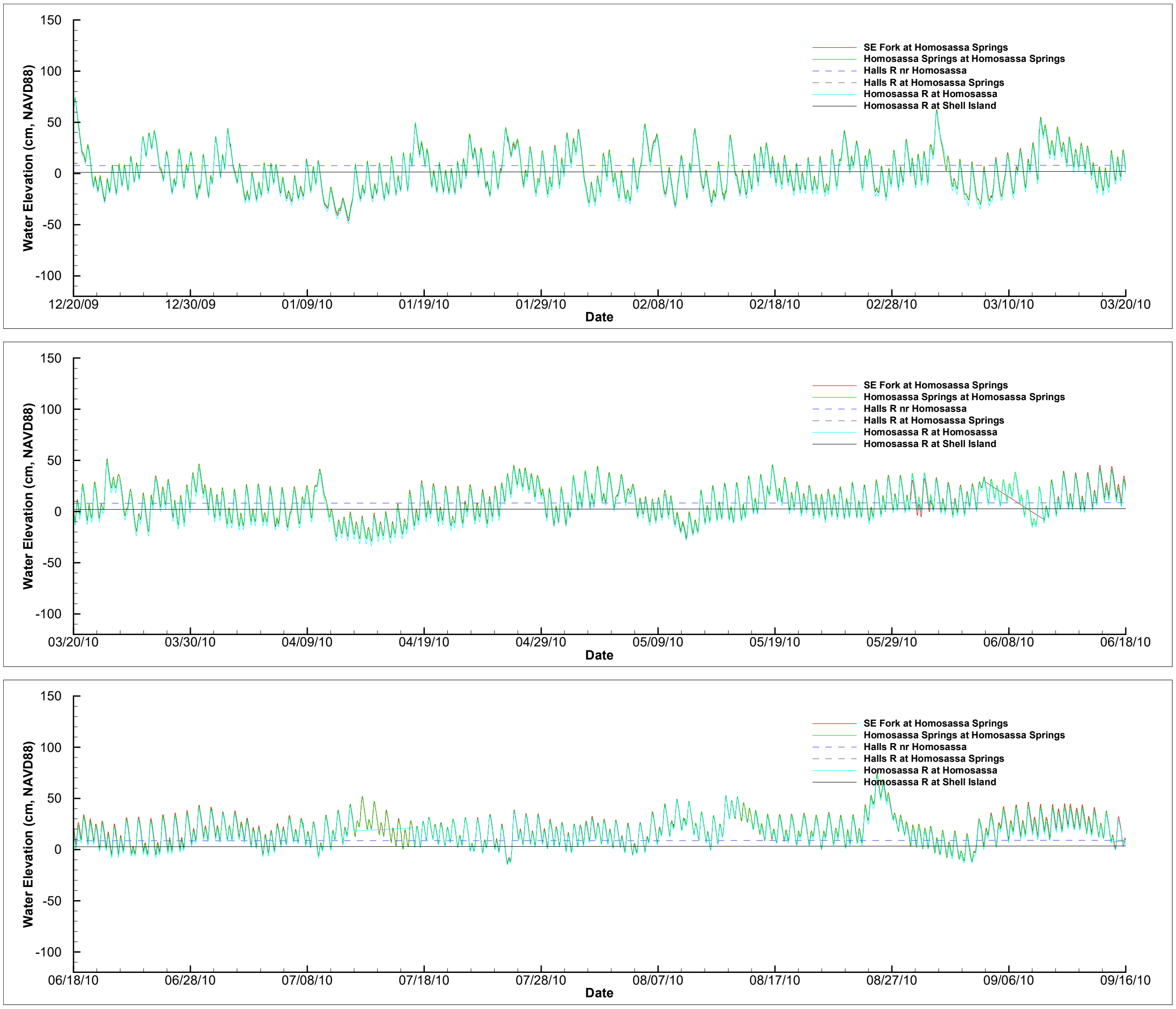

Figure A - 4. Measured real-time water levels at USGS SE Fork Homosassa Spring (read solid lines), Homosassa Springs at Homosassa Springs (green solid lines), Halls River near Homosassa (blue dashed lines), Halls River at Homosassa Springs (black dashed lines), Homosassa River at Homosassa (cyan solid lines), and Homosassa River at Shell Island (black solid lines) stations in the Homosassa River during 12/20/2009 – 9/16/2010.

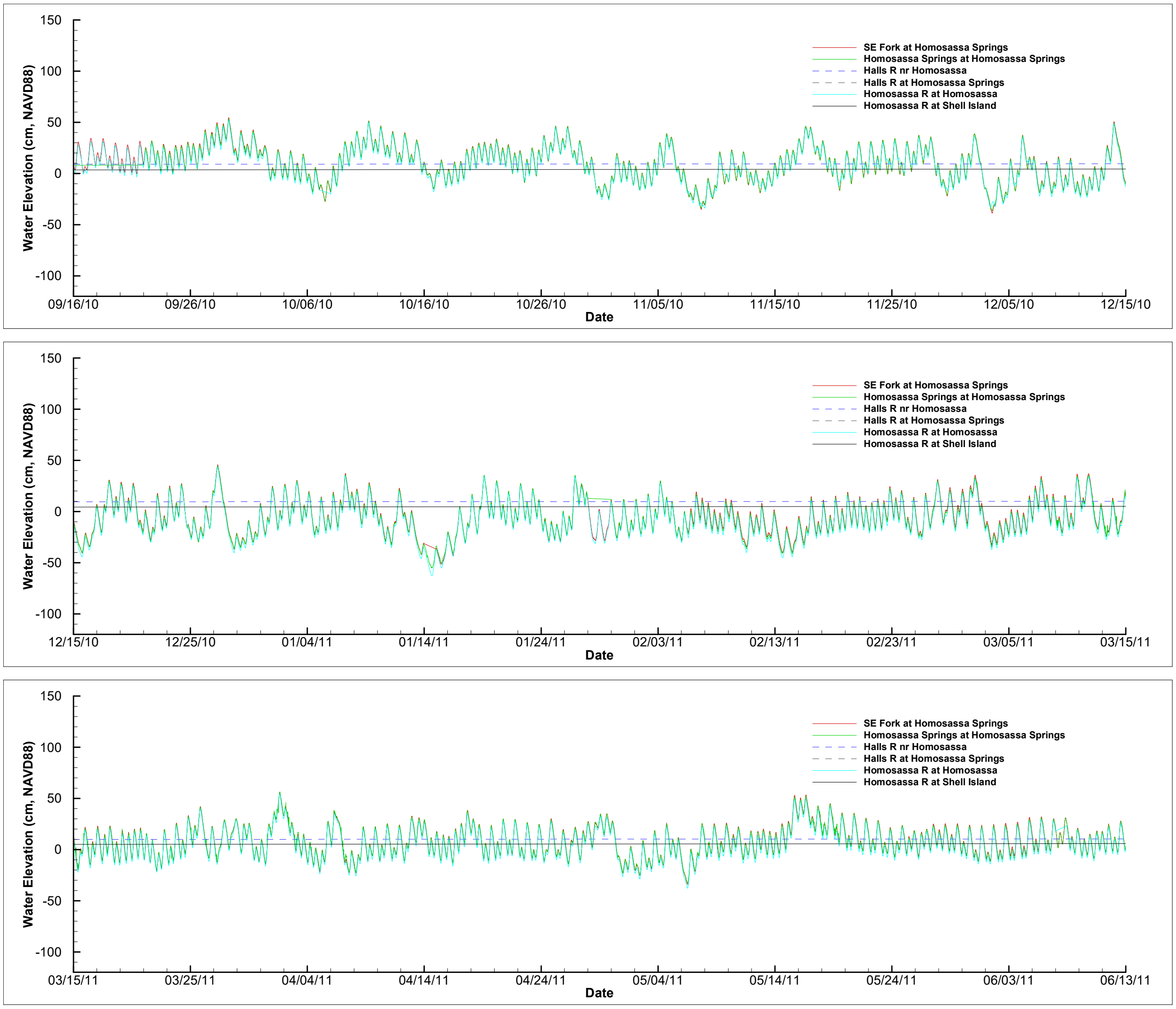

Figure A - 5. Measured real-time water levels at USGS SE Fork Homosassa Spring (read solid lines), Homosassa Springs at Homosassa Springs (green solid lines), Halls River near Homosassa (blue dashed lines), Halls River at Homosassa Springs (black dashed lines), Homosassa River at Homosassa (cyan solid lines), and Homosassa River at Shell Island (black solid lines) stations in the Homosassa River during 9/16/2010 – 6/13/2011.

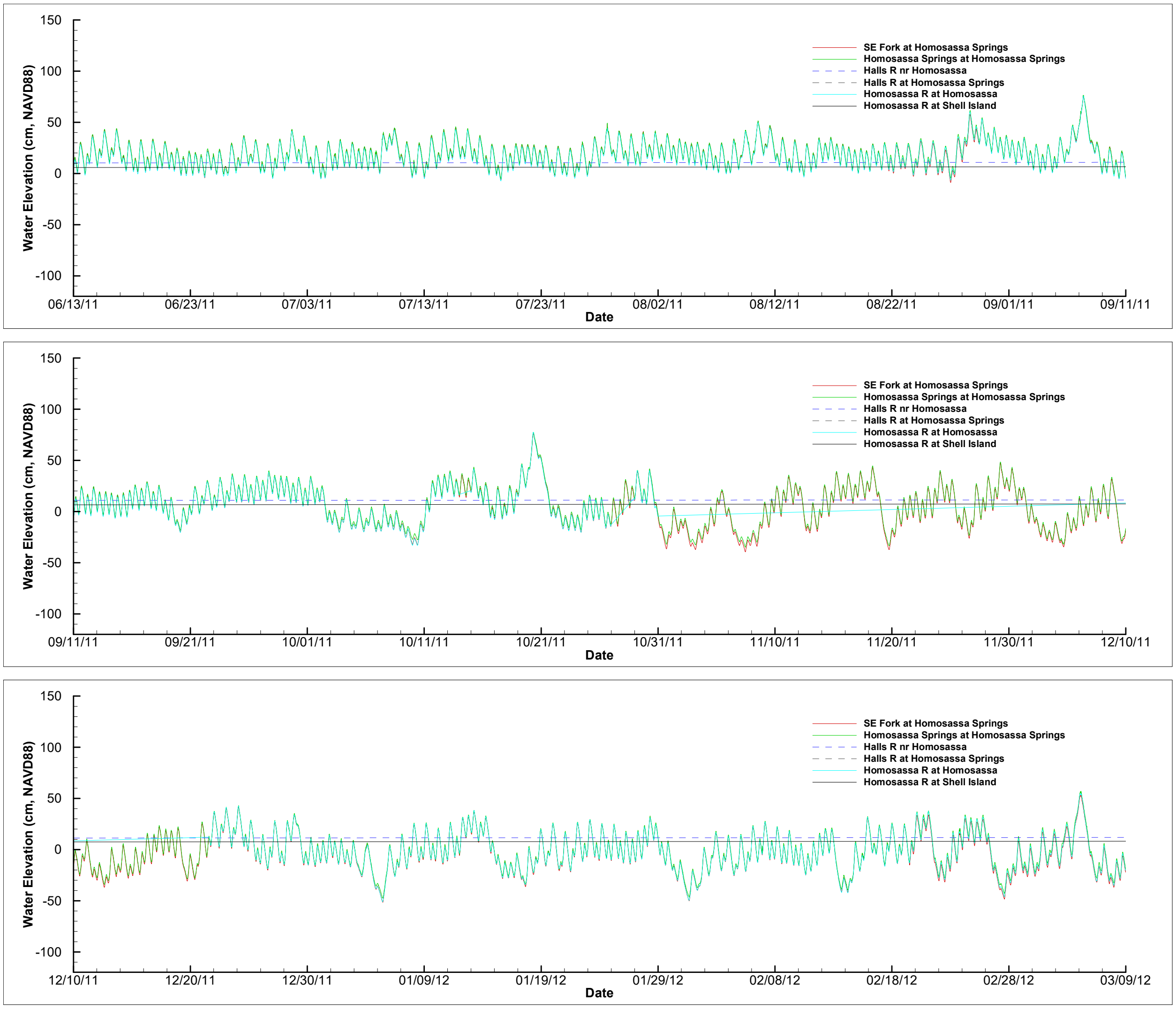

Figure A - 6. Measured real-time water levels at USGS SE Fork Homosassa Spring (read solid lines), Homosassa Springs at Homosassa Springs (green solid lines), Halls River near Homosassa (blue dashed lines), Halls River at Homosassa Springs (black dashed lines), Homosassa River at Homosassa (cyan solid lines), and Homosassa River at Shell Island (black solid lines) stations in the Homosassa River during 6/13/2011 – 3/9/2012.

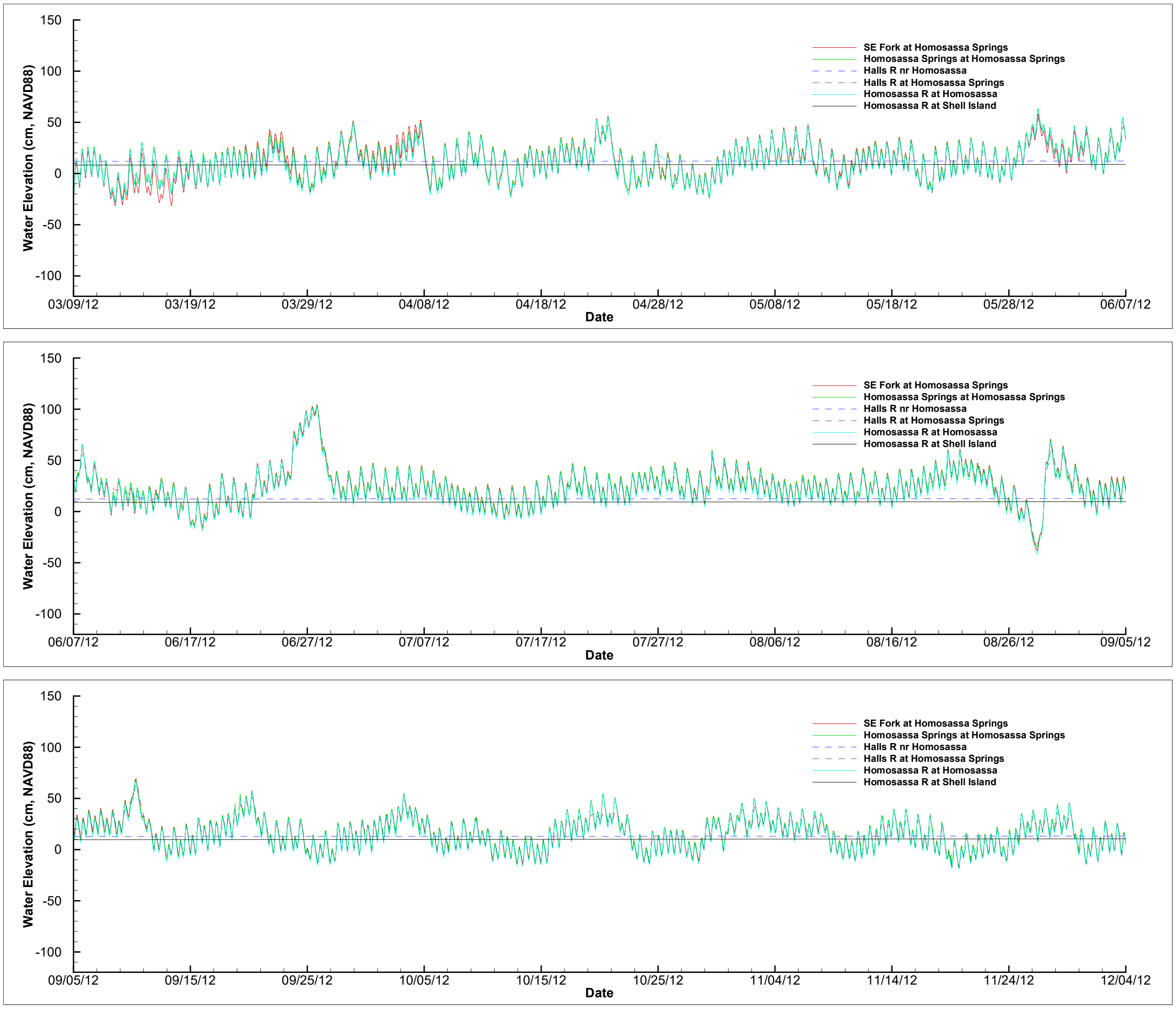

Figure A - 7. Measured real-time water levels at USGS SE Fork Homosassa Spring (read solid lines), Homosassa Springs at Homosassa Springs (green solid lines), Halls River near Homosassa (blue dashed lines), Halls River at Homosassa Springs (black dashed lines), Homosassa River at Homosassa (cyan solid lines), and Homosassa River at Shell Island (black solid lines) stations in the Homosassa River during 3/9/2012 – 12/4/2012.

Figure A - 8. Measured real-time water levels at USGS SE Fork Homosassa Spring (read solid lines), Homosassa Springs at Homosassa Springs (green solid lines), Halls River near Homosassa (blue dashed lines), Halls River at Homosassa Springs (black dashed lines), Homosassa River at Homosassa (cyan solid lines), and Homosassa River at Shell Island (black solid lines) stations in the Homosassa River during 12/4/2012 – 8/31/2013.

Figure A - 9. Measured real-time water levels at USGS SE Fork Homosassa Spring (read solid lines), Homosassa Springs at Homosassa Springs (green solid lines), Halls River near Homosassa (blue dashed lines), Halls River at Homosassa Springs (black dashed lines), Homosassa River at Homosassa (cyan solid lines), and Homosassa River at Shell Island (black solid lines) stations in the Homosassa River during 8/31/2013 – 5/28/2014.

Figure A - 10. Measured real-time water levels at USGS SE Fork Homosassa Spring (read solid lines), Homosassa Springs at Homosassa Springs (green solid lines), Halls River near Homosassa (blue dashed lines), Halls River at Homosassa Springs (black dashed lines), Homosassa River at Homosassa (cyan solid lines), and Homosassa River at Shell Island (black solid lines) stations in the Homosassa River during 5/28/2014 – 2/22/2015.

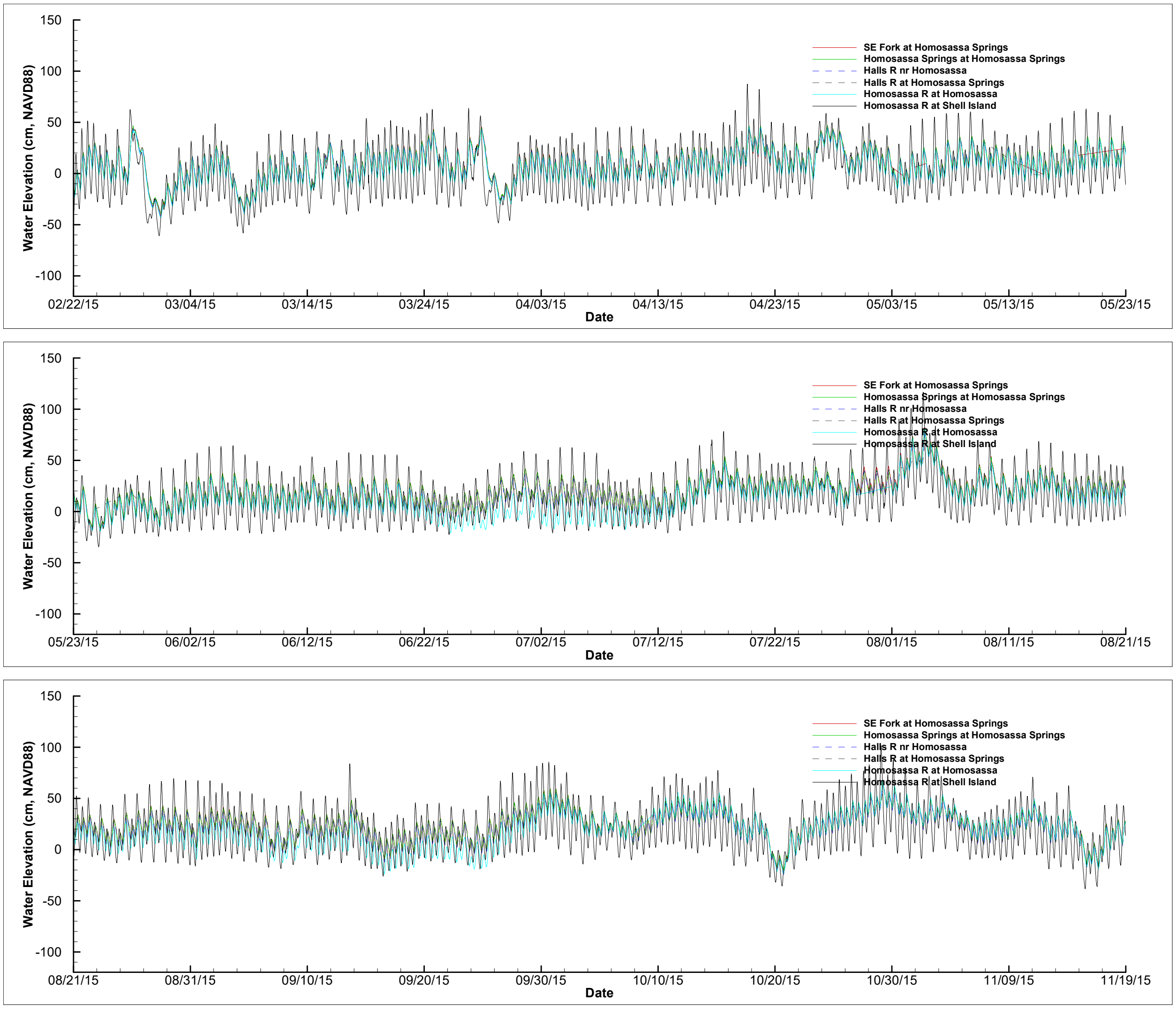

Figure A - 11. Measured real-time water levels at USGS SE Fork Homosassa Spring (read solid lines), Homosassa Springs at Homosassa Springs (green solid lines), Halls River near Homosassa (blue dashed lines), Halls River at Homosassa Springs (black dashed lines), Homosassa River at Homosassa (cyan solid lines), and Homosassa River at Shell Island (black solid lines) stations in the Homosassa River during 2/22/2015 – 11/19/2015.

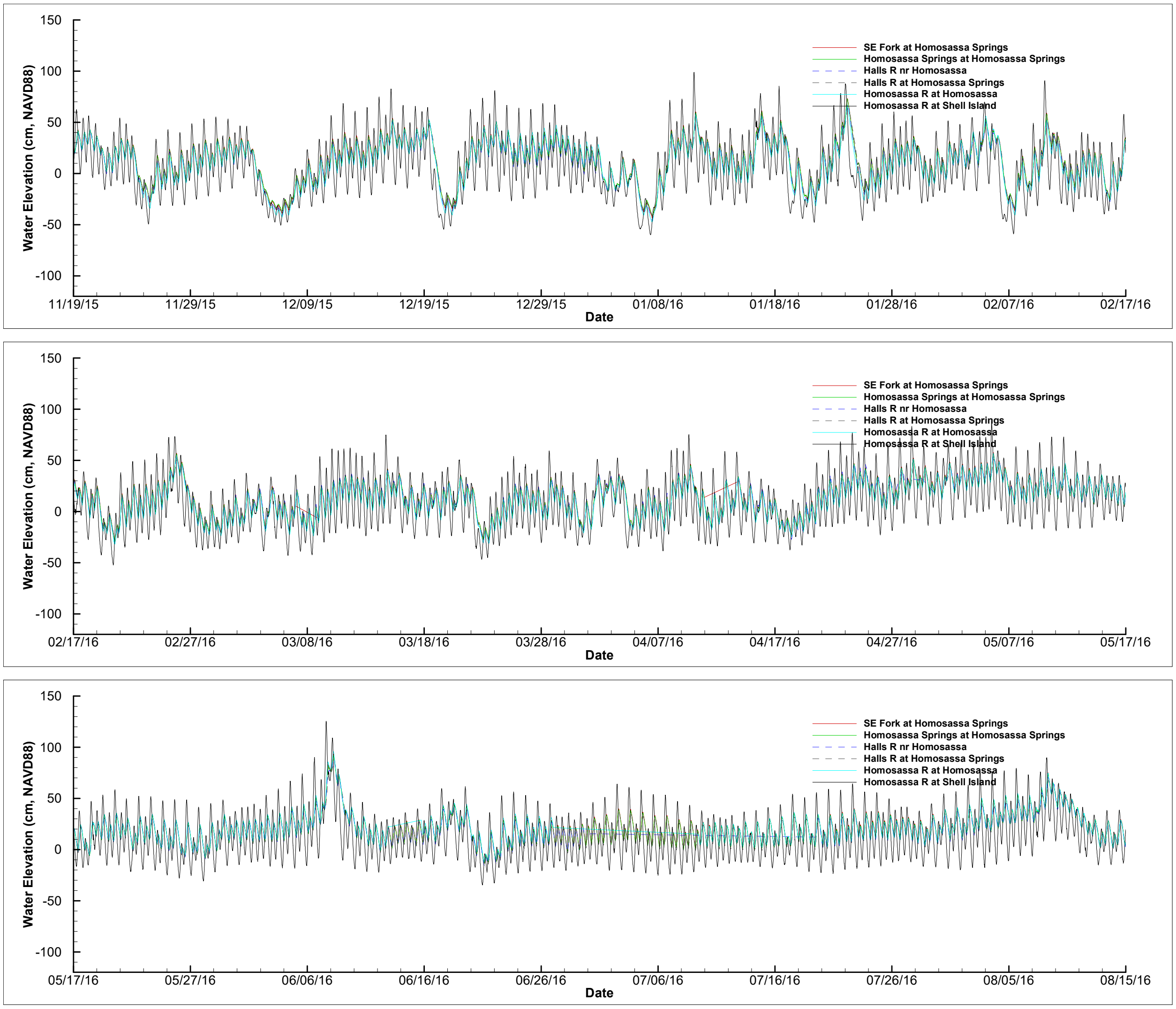

Figure A - 12. Measured real-time water levels at USGS SE Fork Homosassa Spring (read solid lines), Homosassa Springs at Homosassa Springs (green solid lines), Halls River near Homosassa (blue dashed lines), Halls River at Homosassa Springs (black dashed lines), Homosassa River at Homosassa (cyan solid lines), and Homosassa River at Shell Island (black solid lines) stations in the Homosassa River during 11/19/2015 – 8/15/2016.

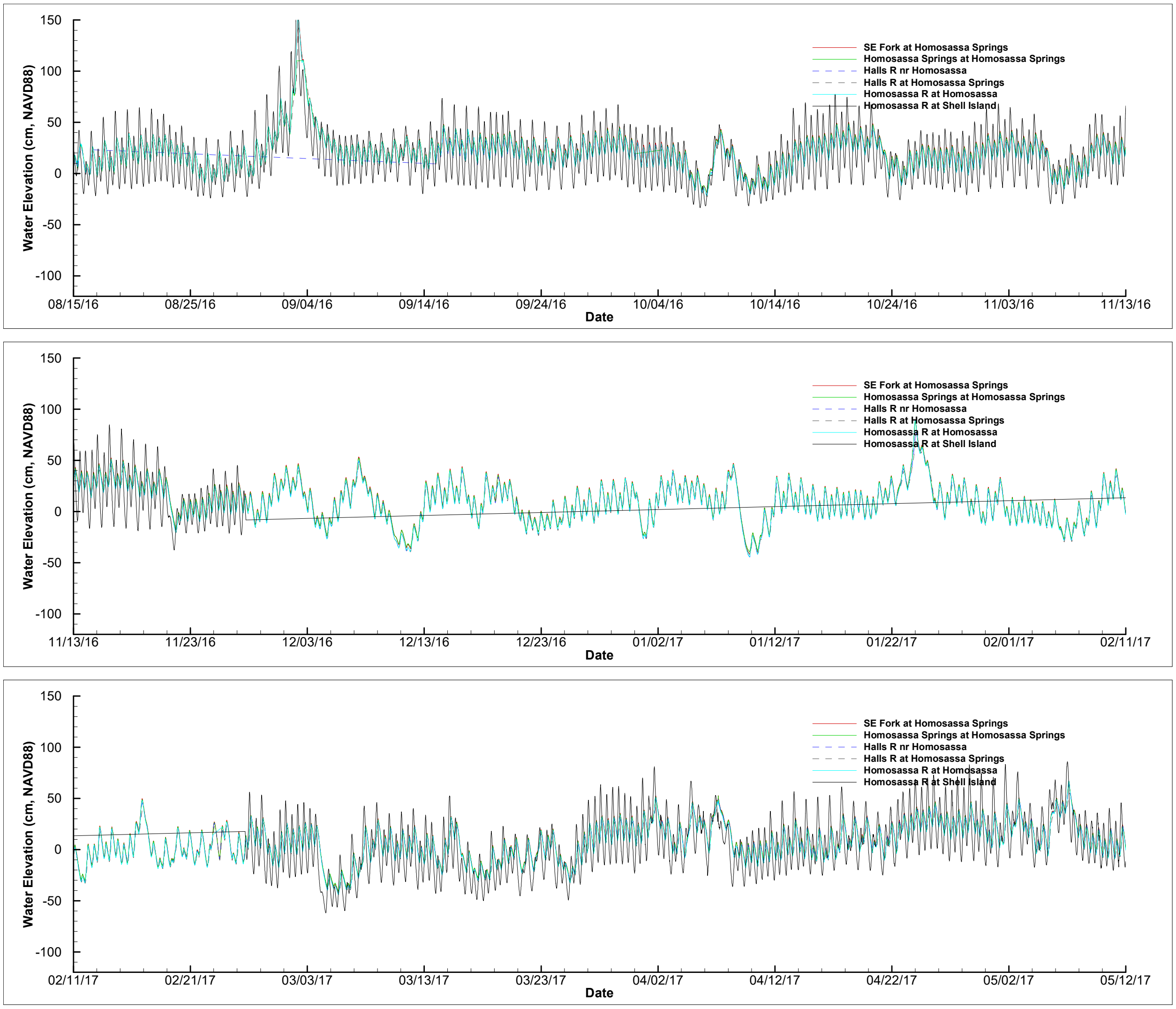

Figure A - 13. Measured real-time water levels at USGS SE Fork Homosassa Spring (read solid lines), Homosassa Springs at Homosassa Springs (green solid lines), Halls River near Homosassa (blue dashed lines), Halls River at Homosassa Springs (black dashed lines), Homosassa River at Homosassa (cyan solid lines), and Homosassa River at Shell Island (black solid lines) stations in the Homosassa River during 8/15/2016 – 5/12/2017.

Appendix B. Salinity Data

Figure B - 1. Measured real-time salinities at USGS SE Fork Homosassa Spring (pink line, top panel), Homosassa Springs at Homosassa Springs (orange line, top panel), Halls River near Homosassa (blue line, top panel), Halls River at Homosassa Springs (green line, top panel), Homosassa River at Homosassa (middle panel), and Homosassa River at Shell Island (bottom panel) stations in the Homosassa River during 10/2/2007 - 12/31/2007.

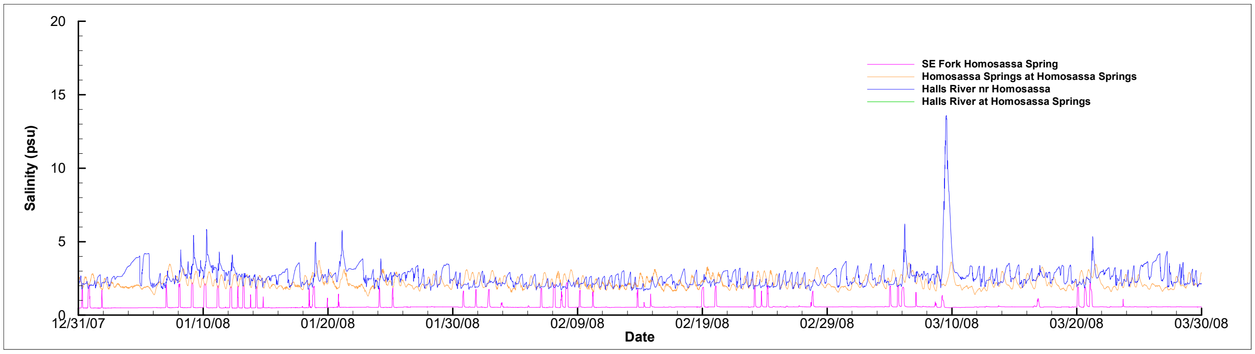

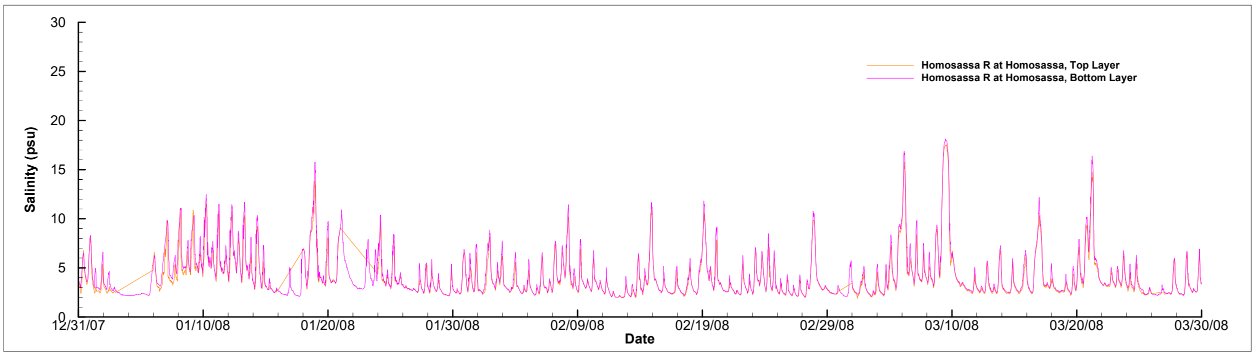

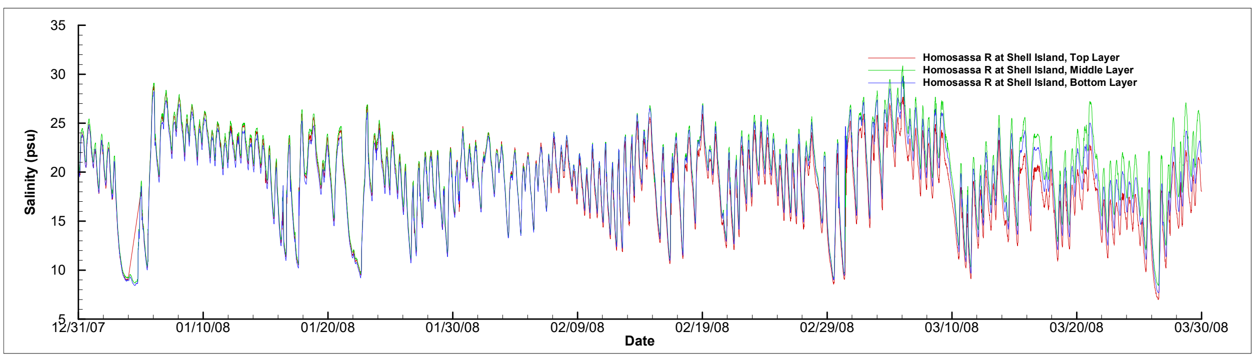

Figure B - 2. Measured real-time salinities at USGS SE Fork Homosassa Spring (pink line, top panel), Homosassa Springs at Homosassa Springs (orange line, top panel), Halls River near Homosassa (blue line, top panel), Halls River at Homosassa Springs (green line, top panel), Homosassa River at Homosassa (middle panel), and Homosassa River at Shell Island (bottom panel) stations in the Homosassa River during 12/31/2007 – 3/30/2008.

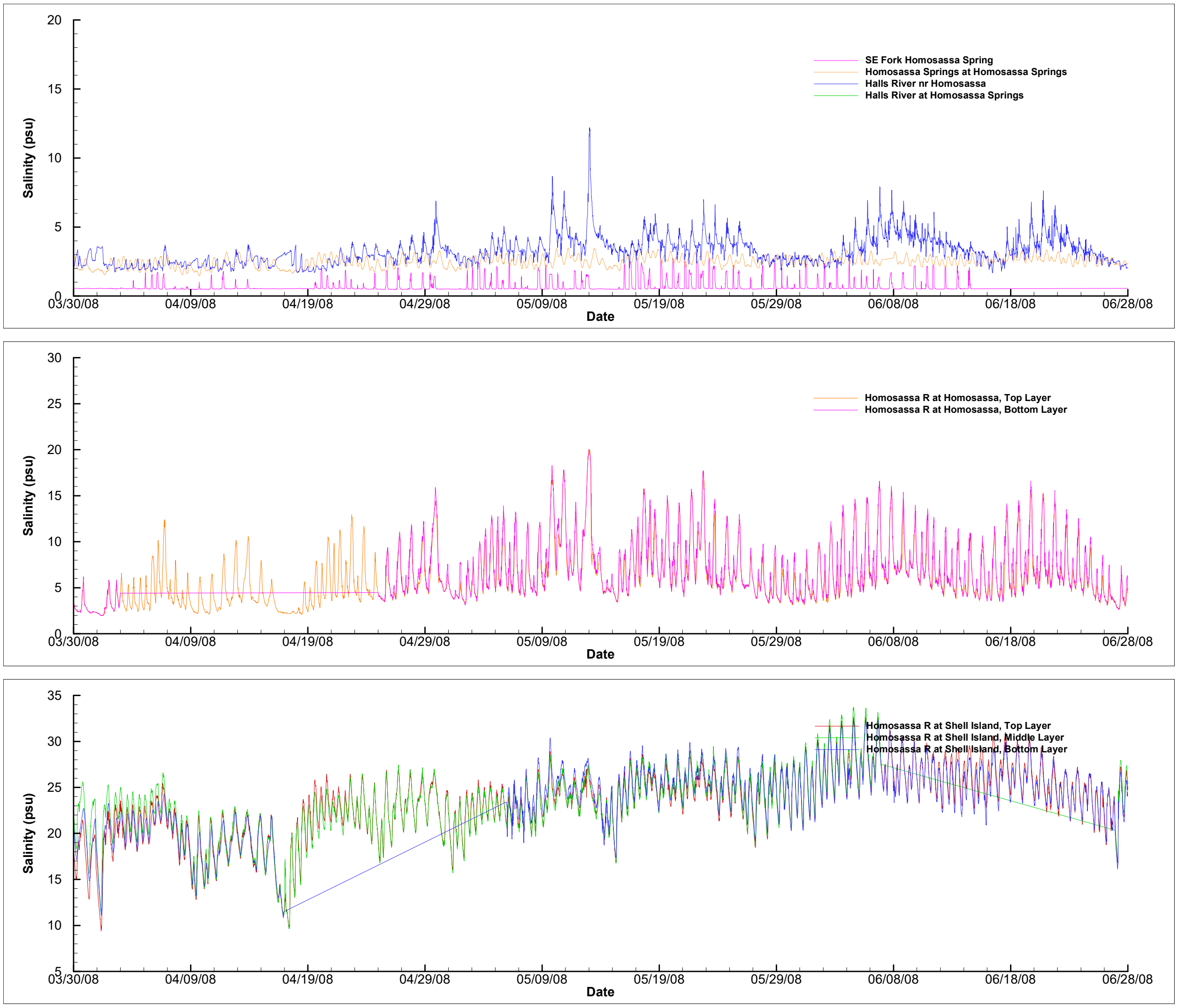

Figure B - 3. Measured real-time salinities at USGS SE Fork Homosassa Spring (pink line, top panel), Homosassa Springs at Homosassa Springs (orange line, top panel), Halls River near Homosassa (blue line, top panel), Halls River at Homosassa Springs (green line, top panel), Homosassa River at Homosassa (middle panel), and Homosassa River at Shell Island (bottom panel) stations in the Homosassa River during 3/30/2008 – 6/28/2008.

Figure B - 4. Measured real-time salinities at USGS SE Fork Homosassa Spring (pink line, top panel), Homosassa Springs at Homosassa Springs (orange line, top panel), Halls River near Homosassa (blue line, top panel), Halls River at Homosassa Springs (green line, top panel), Homosassa River at Homosassa (middle panel), and Homosassa River at Shell Island (bottom panel) stations in the Homosassa River during 6/28/2008 – 9/26/2008.

Figure B - 5. Measured real-time salinities at USGS SE Fork Homosassa Spring (pink line, top panel), Homosassa Springs at Homosassa Springs (orange line, top panel), Halls River near Homosassa (blue line, top panel), Halls River at Homosassa Springs (green line, top panel), Homosassa River at Homosassa (middle panel), and Homosassa River at Shell Island (bottom panel) stations in the Homosassa River during 9/26/2008 – 12/25/2008.

Figure B - 6. Measured real-time salinities at USGS SE Fork Homosassa Spring (pink line, top panel), Homosassa Springs at Homosassa Springs (orange line, top panel), Halls River near Homosassa (blue line, top panel), Halls River at Homosassa Springs (green line, top panel), Homosassa River at Homosassa (middle panel), and Homosassa River at Shell Island (bottom panel) stations in the Homosassa River during 12/25/2008 – 3/25/2009.

Figure B - 7. Measured real-time salinities at USGS SE Fork Homosassa Spring (pink line, top panel), Homosassa Springs at Homosassa Springs (orange line, top panel), Halls River near Homosassa (blue line, top panel), Halls River at Homosassa Springs (green line, top panel), Homosassa River at Homosassa (middle panel), and Homosassa River at Shell Island (bottom panel) stations in the Homosassa River during 3/25/2009 – 6/23/2009.

Figure B - 8. Measured real-time salinities at USGS SE Fork Homosassa Spring (pink line, top panel), Homosassa Springs at Homosassa Springs (orange line, top panel), Halls River near Homosassa (blue line, top panel), Halls River at Homosassa Springs (green line, top panel), Homosassa River at Homosassa (middle panel), and Homosassa River at Shell Island (bottom panel) stations in the Homosassa River during 6/23/2009 – 9/21/2009.

Figure B - 9. Measured real-time salinities at USGS SE Fork Homosassa Spring (pink line, top panel), Homosassa Springs at Homosassa Springs (orange line, top panel), Halls River near Homosassa (blue line, top panel), Halls River at Homosassa Springs (green line, top panel), Homosassa River at Homosassa (middle panel), and Homosassa River at Shell Island (bottom panel) stations in the Homosassa River during 9/21/2009 – 12/20/2009.

Figure B - 10. Measured real-time salinities at USGS SE Fork Homosassa Spring (pink line, top panel), Homosassa Springs at Homosassa Springs (orange line, top panel), Halls River near Homosassa (blue line, top panel), Halls River at Homosassa Springs (green line, top panel), Homosassa River at Homosassa (middle panel), and Homosassa River at Shell Island (bottom panel) stations in the Homosassa River during 12/20/2009 – 3/20/2010.

Figure B - 11. Measured real-time salinities at USGS SE Fork Homosassa Spring (pink line, top panel), Homosassa Springs at Homosassa Springs (orange line, top panel), Halls River near Homosassa (blue line, top panel), Halls River at Homosassa Springs (green line, top panel), Homosassa River at Homosassa (middle panel), and Homosassa River at Shell Island (bottom panel) stations in the Homosassa River during 3/20/2010 – 6/18/2010.

Figure B - 12. Measured real-time salinities at USGS SE Fork Homosassa Spring (pink line, top panel), Homosassa Springs at Homosassa Springs (orange line, top panel), Halls River near Homosassa (blue line, top panel), Halls River at Homosassa Springs (green line, top panel), Homosassa River at Homosassa (middle panel), and Homosassa River at Shell Island (bottom panel) stations in the Homosassa River during 6/18/2010 – 9/16/2010.

Figure B - 13. Measured real-time salinities at USGS SE Fork Homosassa Spring (pink line, top panel), Homosassa Springs at Homosassa Springs (orange line, top panel), Halls River near Homosassa (blue line, top panel), Halls River at Homosassa Springs (green line, top panel), Homosassa River at Homosassa (middle panel), and Homosassa River at Shell Island (bottom panel) stations in the Homosassa River during 9/16/2010 – 12/15/2010.

Figure B - 14. Measured real-time salinities at USGS SE Fork Homosassa Spring (pink line, top panel), Homosassa Springs at Homosassa Springs (orange line, top panel), Halls River near Homosassa (blue line, top panel), Halls River at Homosassa Springs (green line, top panel), Homosassa River at Homosassa (middle panel), and Homosassa River at Shell Island (bottom panel) stations in the Homosassa River during 12/15/2010 – 3/15/2011.

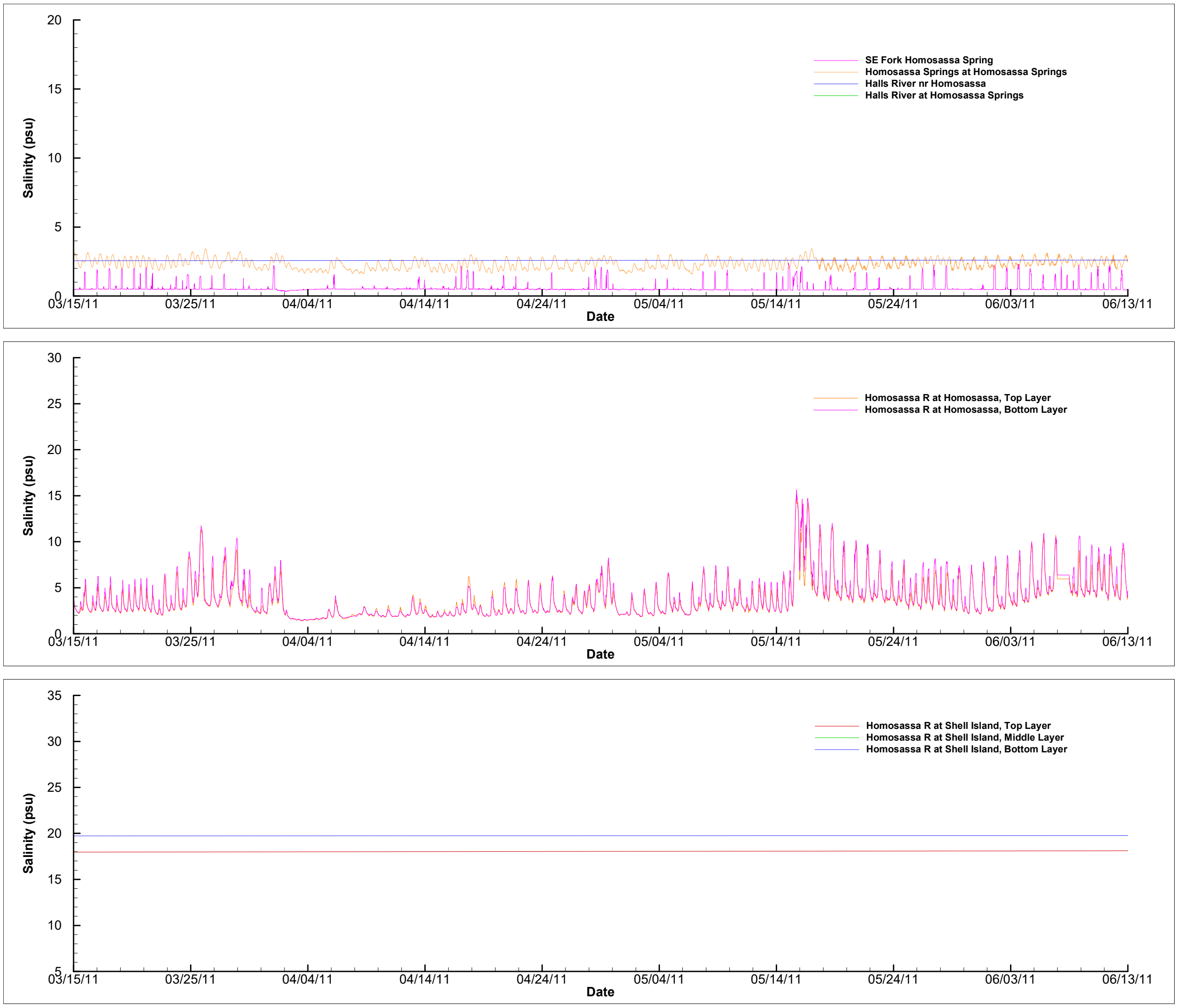

Figure B - 15. Measured real-time salinities at USGS SE Fork Homosassa Spring (pink line, top panel), Homosassa Springs at Homosassa Springs (orange line, top panel), Halls River near Homosassa (blue line, top panel), Halls River at Homosassa Springs (green line, top panel), Homosassa River at Homosassa (middle panel), and Homosassa River at Shell Island (bottom panel) stations in the Homosassa River during 3/15/2011 – 6/13/2011.

Figure B - 16. Measured real-time salinities at USGS SE Fork Homosassa Spring (pink line, top panel), Homosassa Springs at Homosassa Springs (orange line, top panel), Halls River near Homosassa (blue line, top panel), Halls River at Homosassa Springs (green line, top panel), Homosassa River at Homosassa (middle panel), and Homosassa River at Shell Island (bottom panel) stations in the Homosassa River during 6/13/2011 – 9/11/2011.

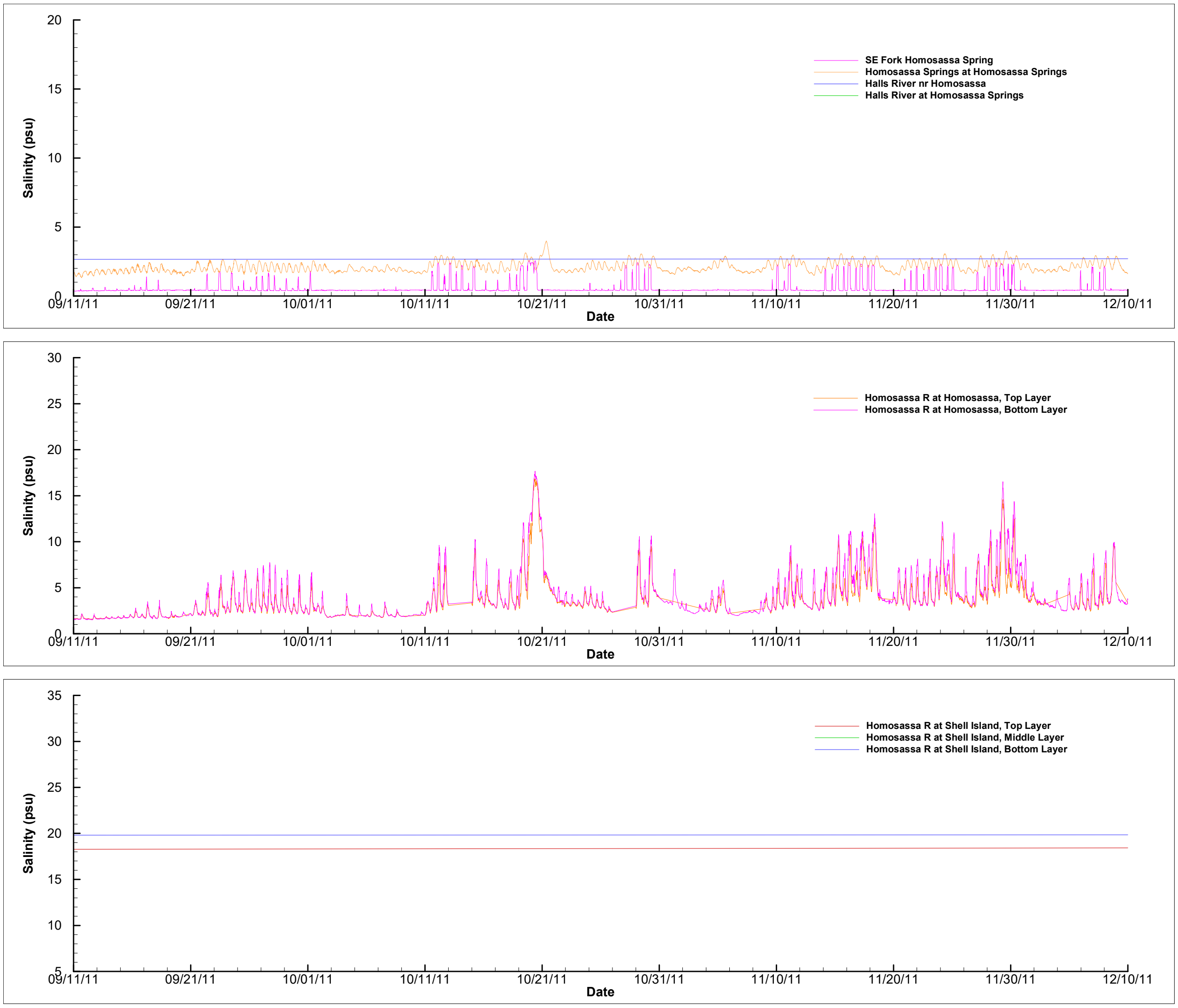

Figure B - 17. Measured real-time salinities at USGS SE Fork Homosassa Spring (pink line, top panel), Homosassa Springs at Homosassa Springs (orange line, top panel), Halls River near Homosassa (blue line, top panel), Halls River at Homosassa Springs (green line, top panel), Homosassa River at Homosassa (middle panel), and Homosassa River at Shell Island (bottom panel) stations in the Homosassa River during 9/11/2011 – 12/10/2011.

Figure B - 18. Measured real-time salinities at USGS SE Fork Homosassa Spring (pink line, top panel), Homosassa Springs at Homosassa Springs (orange line, top panel), Halls River near Homosassa (blue line, top panel), Halls River at Homosassa Springs (green line, top panel), Homosassa River at Homosassa (middle panel), and Homosassa River at Shell Island (bottom panel) stations in the Homosassa River during 12/10/2011 – 3/9/2012.

Figure B - 19. Measured real-time salinities at USGS SE Fork Homosassa Spring (pink line, top panel), Homosassa Springs at Homosassa Springs (orange line, top panel), Halls River near Homosassa (blue line, top panel), Halls River at Homosassa Springs (green line, top panel), Homosassa River at Homosassa (middle panel), and Homosassa River at Shell Island (bottom panel) stations in the Homosassa River during 3/9/2012 – 6/7/2012.

Figure B - 20. Measured real-time salinities at USGS SE Fork Homosassa Spring (pink line, top panel), Homosassa Springs at Homosassa Springs (orange line, top panel), Halls River near Homosassa (blue line, top panel), Halls River at Homosassa Springs (green line, top panel), Homosassa River at Homosassa (middle panel), and Homosassa River at Shell Island (bottom panel) stations in the Homosassa River during 6/7/2012 – 9/5/2012.

Figure B - 21. Measured real-time salinities at USGS SE Fork Homosassa Spring (pink line, top panel), Homosassa Springs at Homosassa Springs (orange line, top panel), Halls River near Homosassa (blue line, top panel), Halls River at Homosassa Springs (green line, top panel), Homosassa River at Homosassa (middle panel), and Homosassa River at Shell Island (bottom panel) stations in the Homosassa River during 9/5/2012 – 12/4/2012.

Figure B - 22. Measured real-time salinities at USGS SE Fork Homosassa Spring (pink line, top panel), Homosassa Springs at Homosassa Springs (orange line, top panel), Halls River near Homosassa (blue line, top panel), Halls River at Homosassa Springs (green line, top panel), Homosassa River at Homosassa (middle panel), and Homosassa River at Shell Island (bottom panel) stations in the Homosassa River during 12/4/2012 – 3/4/2013.

Figure B - 23. Measured real-time salinities at USGS SE Fork Homosassa Spring (pink line, top panel), Homosassa Springs at Homosassa Springs (orange line, top panel), Halls River near Homosassa (blue line, top panel), Halls River at Homosassa Springs (green line, top panel), Homosassa River at Homosassa (middle panel), and Homosassa River at Shell Island (bottom panel) stations in the Homosassa River during 3/4/2013 – 6/2/2013.

Figure B - 24. Measured real-time salinities at USGS SE Fork Homosassa Spring (pink line, top panel), Homosassa Springs at Homosassa Springs (orange line, top panel), Halls River near Homosassa (blue line, top panel), Halls River at Homosassa Springs (green line, top panel), Homosassa River at Homosassa (middle panel), and Homosassa River at Shell Island (bottom panel) stations in the Homosassa River during 6/2/2013 - 8/31/2013.

Figure B - 25. Measured real-time salinities at USGS SE Fork Homosassa Spring (pink line, top panel), Homosassa Springs at Homosassa Springs (orange line, top panel), Halls River near Homosassa (blue line, top panel), Halls River at Homosassa Springs (green line, top panel), Homosassa River at Homosassa (middle panel), and Homosassa River at Shell Island (bottom panel) stations in the Homosassa River during 8/31/2013 – 11/29/2013

Figure B - 26. Measured real-time salinities at USGS SE Fork Homosassa Spring (pink line, top panel), Homosassa Springs at Homosassa Springs (orange line, top panel), Halls River near Homosassa (blue line, top panel), Halls River at Homosassa Springs (green line, top panel), Homosassa River at Homosassa (middle panel), and Homosassa River at Shell Island (bottom panel) stations in the Homosassa River during 11/29/2013 – 2/27/2014.

Figure B - 27. Measured real-time salinities at USGS SE Fork Homosassa Spring (pink line, top panel), Homosassa Springs at Homosassa Springs (orange line, top panel), Halls River near Homosassa (blue line, top panel), Halls River at Homosassa Springs (green line, top panel), Homosassa River at Homosassa (middle panel), and Homosassa River at Shell Island (bottom panel) stations in the Homosassa River during 2/27/2014 – 5/28/2014.

Figure B - 28. Measured real-time salinities at USGS SE Fork Homosassa Spring (pink line, top panel), Homosassa Springs at Homosassa Springs (orange line, top panel), Halls River near Homosassa (blue line, top panel), Halls River at Homosassa Springs (green line, top panel), Homosassa River at Homosassa (middle panel), and Homosassa River at Shell Island (bottom panel) stations in the Homosassa River during 5/28/2014 – 8/26/2014.

Figure B - 29. Measured real-time salinities at USGS SE Fork Homosassa Spring (pink line, top panel), Homosassa Springs at Homosassa Springs (orange line, top panel), Halls River near Homosassa (blue line, top panel), Halls River at Homosassa Springs (green line, top panel), Homosassa River at Homosassa (middle panel), and Homosassa River at Shell Island (bottom panel) stations in the Homosassa River during 8/26/2014 – 11/24/2014.

Figure B - 30. Measured real-time salinities at USGS SE Fork Homosassa Spring (pink line, top panel), Homosassa Springs at Homosassa Springs (orange line, top panel), Halls River near Homosassa (blue line, top panel), Halls River at Homosassa Springs (green line, top panel), Homosassa River at Homosassa (middle panel), and Homosassa River at Shell Island (bottom panel) stations in the Homosassa River during 11/24/2014 – 2/22/2015.

Figure B - 31. Measured real-time salinities at USGS SE Fork Homosassa Spring (pink line, top panel), Homosassa Springs at Homosassa Springs (orange line, top panel), Halls River near Homosassa (blue line, top panel), Halls River at Homosassa Springs (green line, top panel), Homosassa River at Homosassa (middle panel), and Homosassa River at Shell Island (bottom panel) stations in the Homosassa River during 2/22/2015 – 5/23/2015.

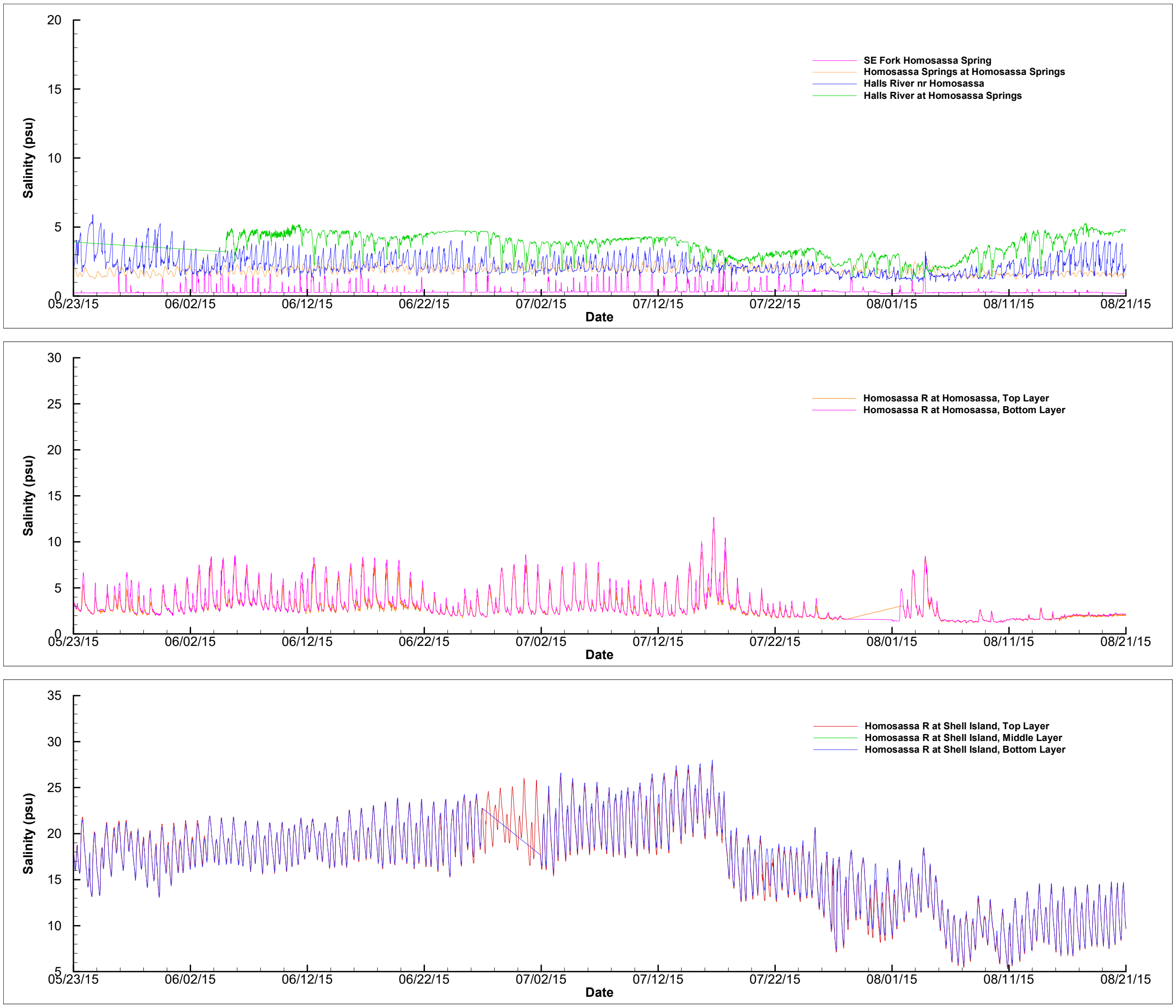

Figure B - 32. Measured real-time salinities at USGS SE Fork Homosassa Spring (pink line, top panel), Homosassa Springs at Homosassa Springs (orange line, top panel), Halls River near Homosassa (blue line, top panel), Halls River at Homosassa Springs (green line, top panel), Homosassa River at Homosassa (middle panel), and Homosassa River at Shell Island (bottom panel) stations in the Homosassa River during 5/23/2015 – 8/21/2015.

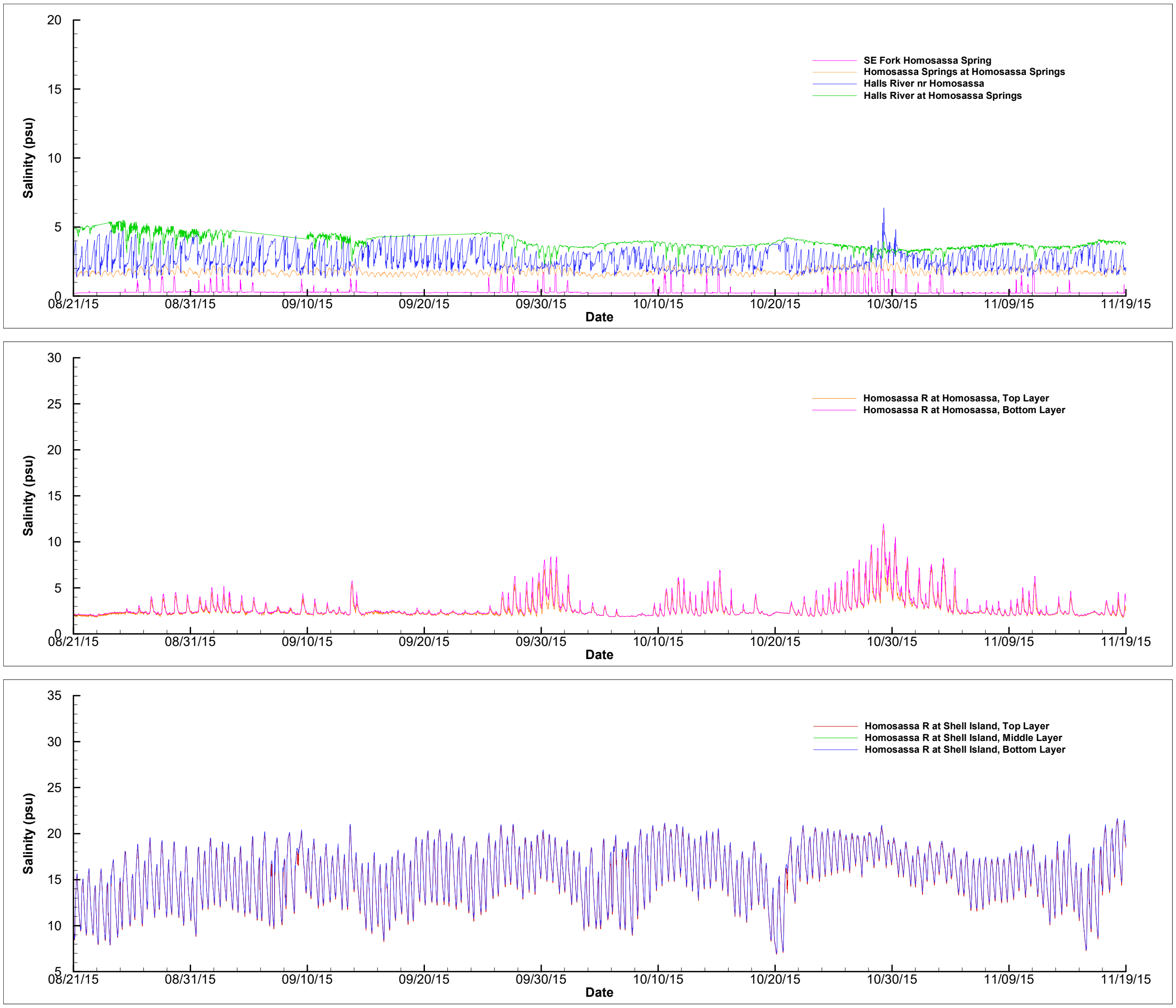

Figure B - 33. Measured real-time salinities at USGS SE Fork Homosassa Spring (pink line, top panel), Homosassa Springs at Homosassa Springs (orange line, top panel), Halls River near Homosassa (blue line, top panel), Halls River at Homosassa Springs (green line, top panel), Homosassa River at Homosassa (middle panel), and Homosassa River at Shell Island (bottom panel) stations in the Homosassa River during 8/21/2015 – 11/19/2015.

Figure B - 34. Measured real-time salinities at USGS SE Fork Homosassa Spring (pink line, top panel), Homosassa Springs at Homosassa Springs (orange line, top panel), Halls River near Homosassa (blue line, top panel), Halls River at Homosassa Springs (green line, top panel), Homosassa River at Homosassa (middle panel), and Homosassa River at Shell Island (bottom panel) stations in the Homosassa River during 11/19/2015 – 2/17/2016.

Figure B - 35. Measured real-time salinities at USGS SE Fork Homosassa Spring (pink line, top panel), Homosassa Springs at Homosassa Springs (orange line, top panel), Halls River near Homosassa (blue line, top panel), Halls River at Homosassa Springs (green line, top panel), Homosassa River at Homosassa (middle panel), and Homosassa River at Shell Island (bottom panel) stations in the Homosassa River during 2/17/2016 – 5/17/2016.

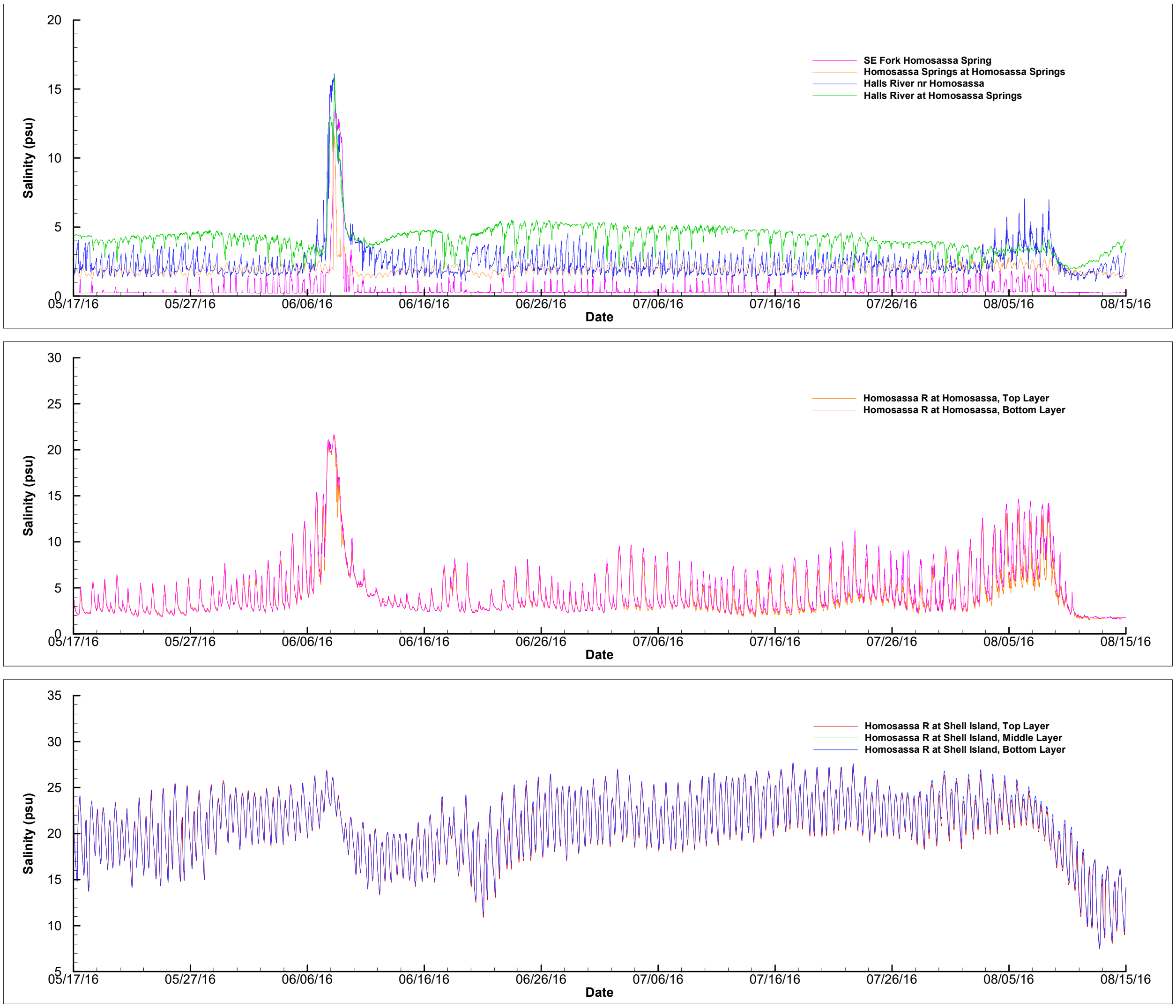

Figure B - 36. Measured real-time salinities at USGS SE Fork Homosassa Spring (pink line, top panel), Homosassa Springs at Homosassa Springs (orange line, top panel), Halls River near Homosassa (blue line, top panel), Halls River at Homosassa Springs (green line, top panel), Homosassa River at Homosassa (middle panel), and Homosassa River at Shell Island (bottom panel) stations in the Homosassa River during 5/17/2016 – 8/15/2016.

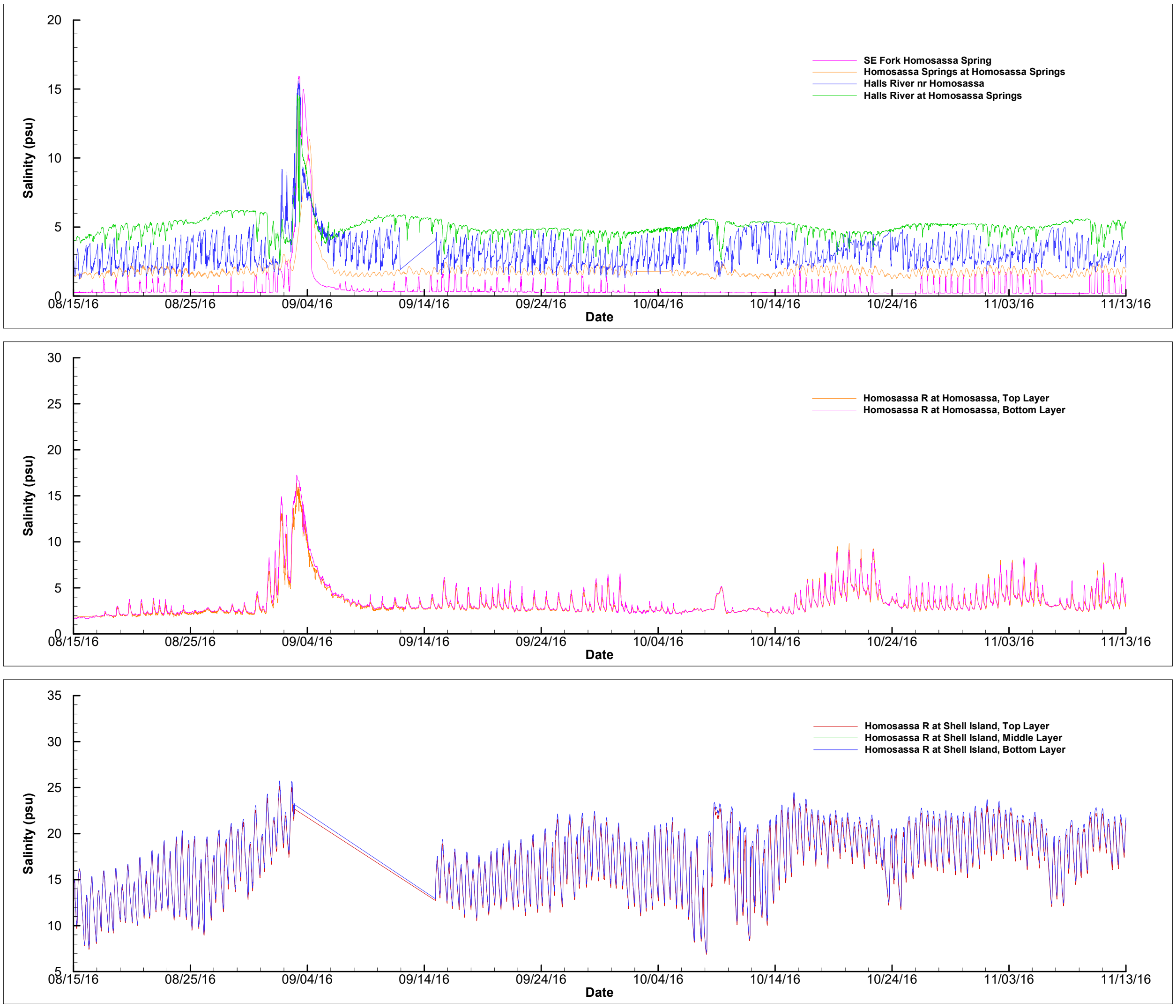

Figure B - 37. Measured real-time salinities at USGS SE Fork Homosassa Spring (pink line, top panel), Homosassa Springs at Homosassa Springs (orange line, top panel), Halls River near Homosassa (blue line, top panel), Halls River at Homosassa Springs (green line, top panel), Homosassa River at Homosassa (middle panel), and Homosassa River at Shell Island (bottom panel) stations in the Homosassa River during 8/15/2016 – 11/13/2016.

Figure B - 38. Measured real-time salinities at USGS SE Fork Homosassa Spring (pink line, top panel), Homosassa Springs at Homosassa Springs (orange line, top panel), Halls River near Homosassa (blue line, top panel), Halls River at Homosassa Springs (green line, top panel), Homosassa River at Homosassa (middle panel), and Homosassa River at Shell Island (bottom panel) stations in the Homosassa River during 11/13/2016 – 2/11/2017.

Figure B - 39. Measured real-time salinities at USGS SE Fork Homosassa Spring (pink line, top panel), Homosassa Springs at Homosassa Springs (orange line, top panel), Halls River near Homosassa (blue line, top panel), Halls River at Homosassa Springs (green line, top panel), Homosassa River at Homosassa (middle panel), and Homosassa River at Shell Island (bottom panel) stations in the Homosassa River during 2/11/2017 – 5/12/2017.

Appendix C. Temperature Data

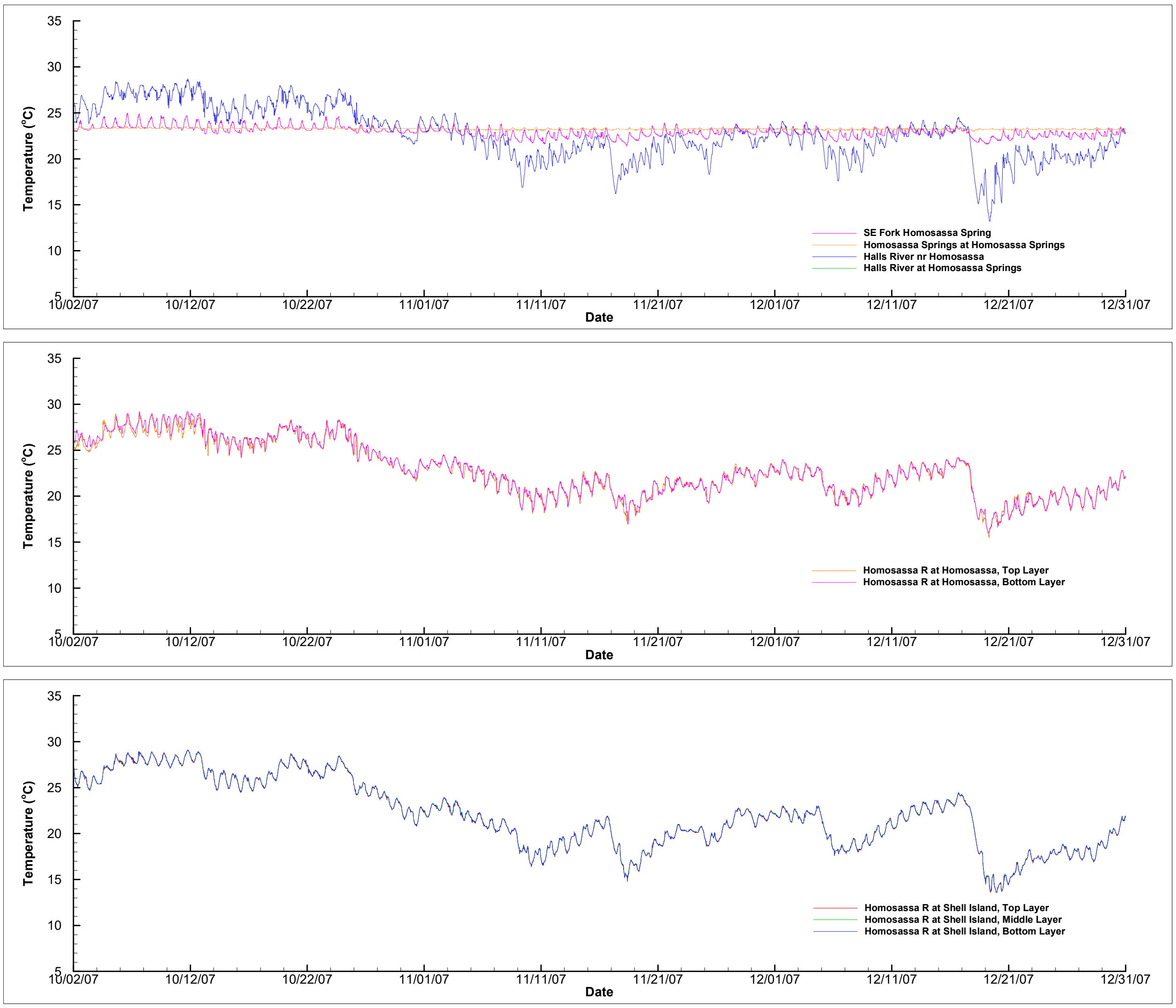

Figure C - 1. Measured real-time temperatures at USGS SE Fork Homosassa Spring (pink line, top panel), Homosassa Springs at Homosassa Springs (orange line, top panel), Halls River near Homosassa (blue line, top panel), Halls River at Homosassa Springs (green line, top panel), Homosassa River at Homosassa (middle panel), and Homosassa River at Shell Island (bottom panel) stations in the Homosassa River during 10/2/2007 - 12/31/2007.

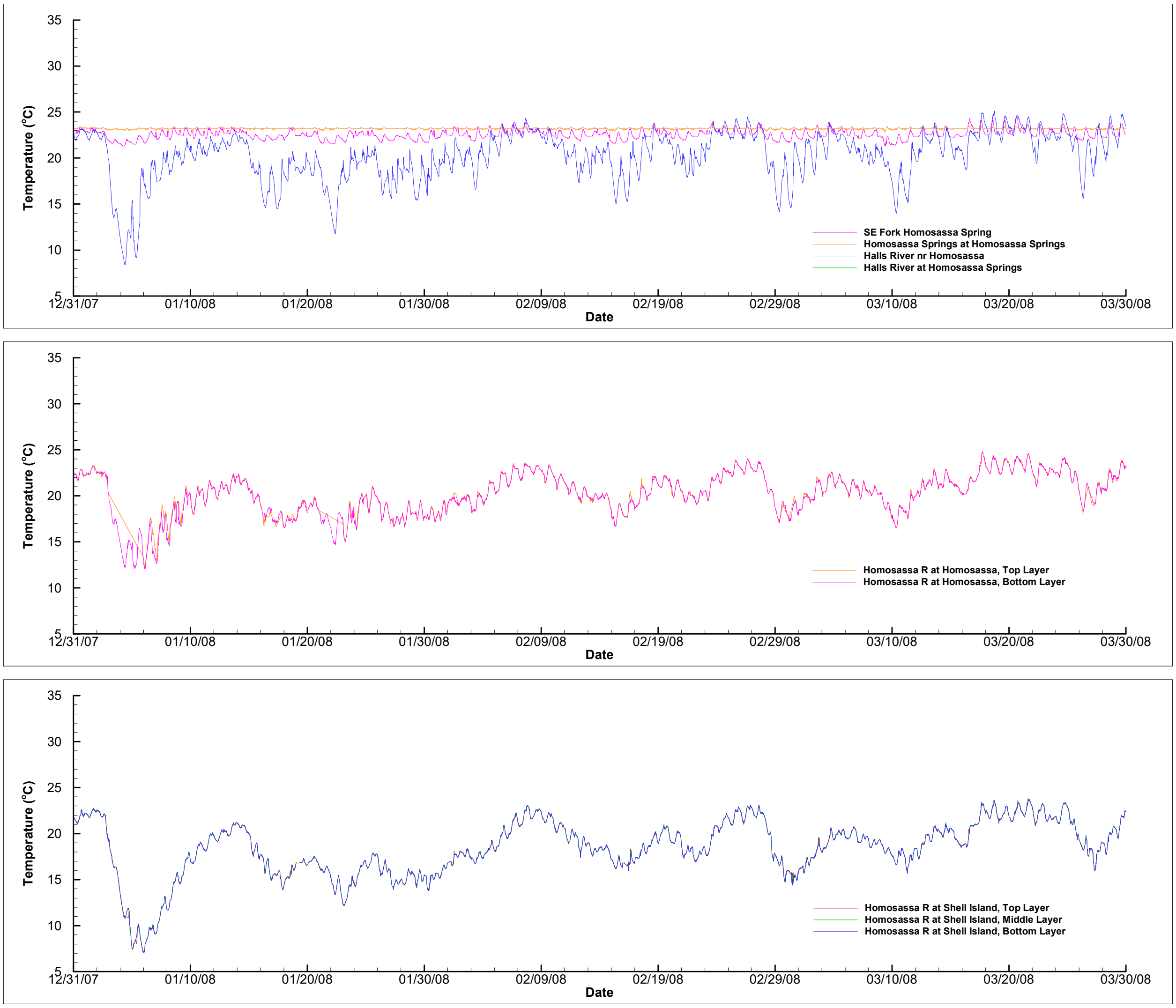

Figure C - 2. Measured real-time temperatures at USGS SE Fork Homosassa Spring (pink line, top panel), Homosassa Springs at Homosassa Springs (orange line, top panel), Halls River near Homosassa (blue line, top panel), Halls River at Homosassa Springs (green line, top panel), Homosassa River at Homosassa (middle panel), and Homosassa River at Shell Island (bottom panel) stations in the Homosassa River during 12/31/2007 – 3/30/2008.

Figure C - 3. Measured real-time temperatures at USGS SE Fork Homosassa Spring (pink line, top panel), Homosassa Springs at Homosassa Springs (orange line, top panel), Halls River near Homosassa (blue line, top panel), Halls River at Homosassa Springs (green line, top panel), Homosassa River at Homosassa (middle panel), and Homosassa River at Shell Island (bottom panel) stations in the Homosassa River during 3/30/2008 – 6/28/2008.

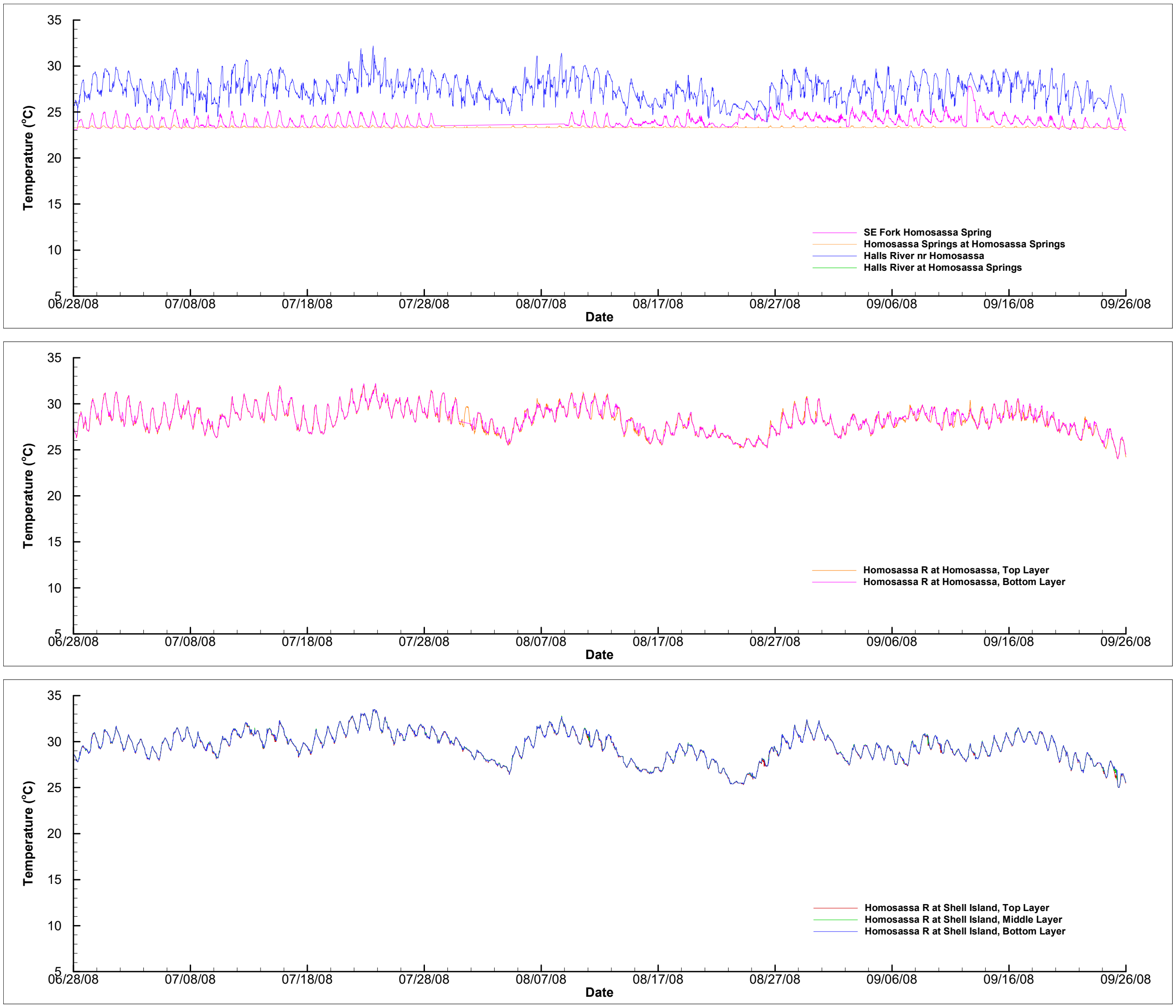

Figure C - 4. Measured real-time temperatures at USGS SE Fork Homosassa Spring (pink line, top panel), Homosassa Springs at Homosassa Springs (orange line, top panel), Halls River near Homosassa (blue line, top panel), Halls River at Homosassa Springs (green line, top panel), Homosassa River at Homosassa (middle panel), and Homosassa River at Shell Island (bottom panel) stations in the Homosassa River during 6/28/2008 – 9/26/2008.

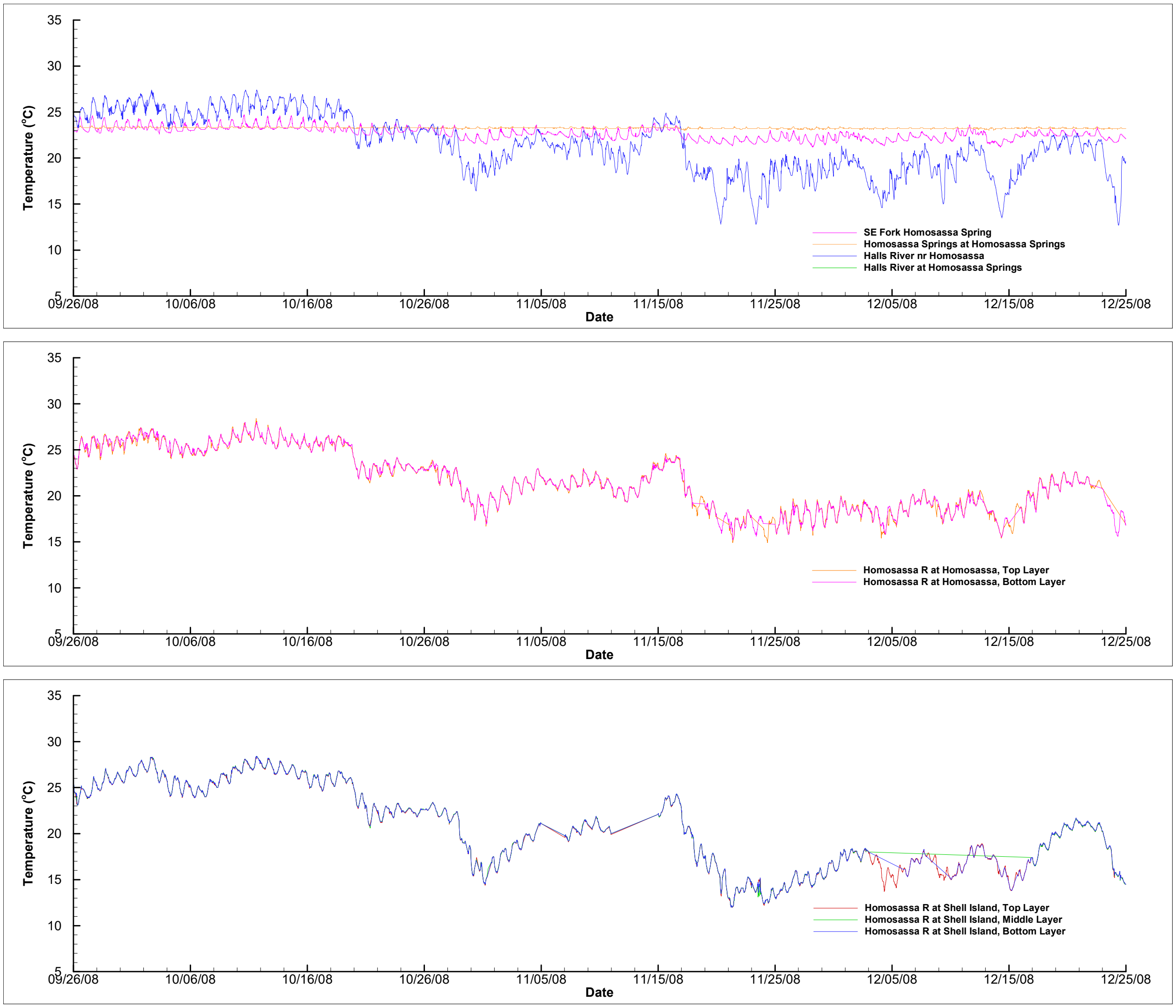

Figure C - 5. Measured real-time temperatures at USGS SE Fork Homosassa Spring (pink line, top panel), Homosassa Springs at Homosassa Springs (orange line, top panel), Halls River near Homosassa (blue line, top panel), Halls River at Homosassa Springs (green line, top panel), Homosassa River at Homosassa (middle panel), and Homosassa River at Shell Island (bottom panel) stations in the Homosassa River during 9/26/2008 – 12/25/2008.

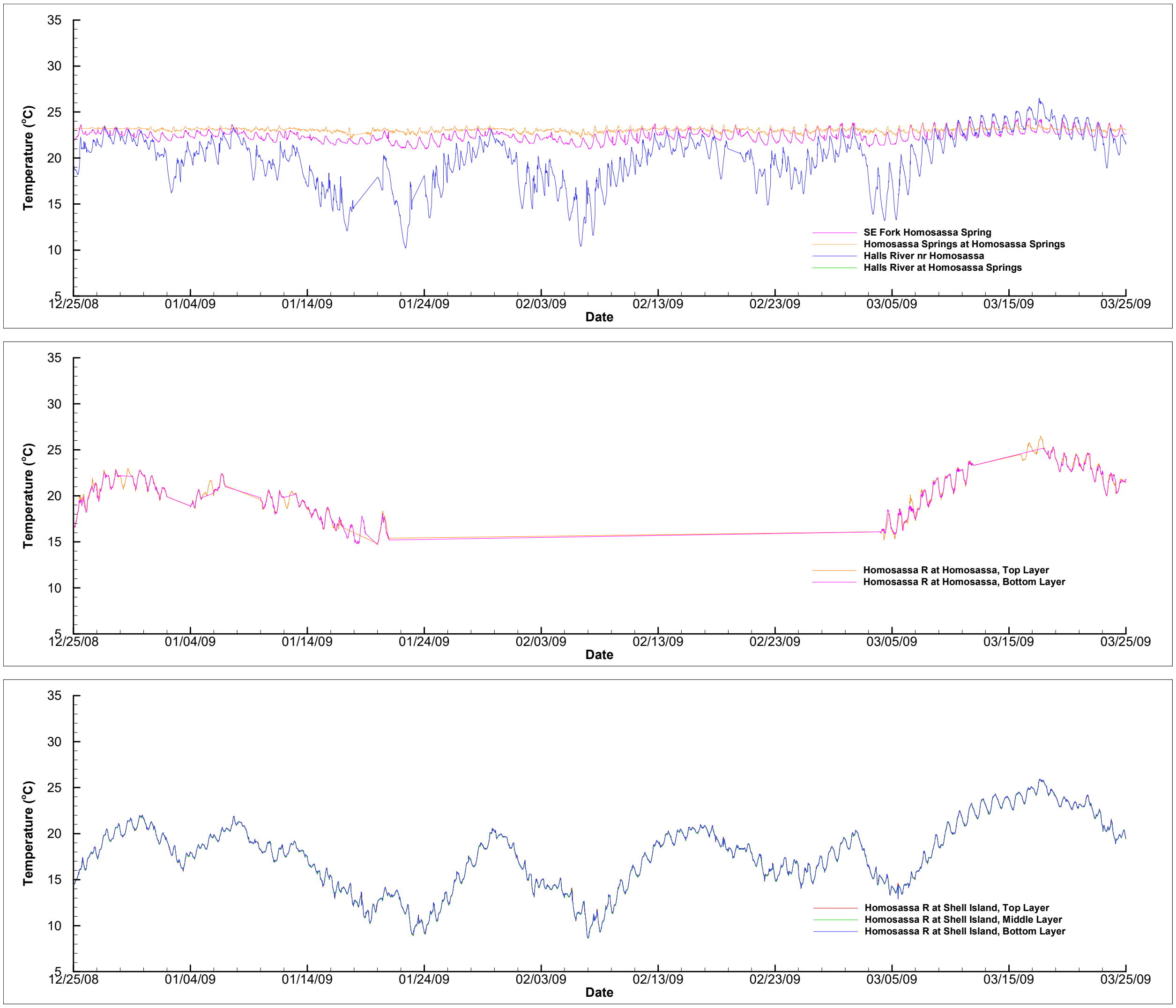

Figure C - 6..Measured real-time temperatures at USGS SE Fork Homosassa Spring (pink line, top panel), Homosassa Springs at Homosassa Springs (orange line, top panel), Halls River near Homosassa (blue line, top panel), Halls River at Homosassa Springs (green line, top panel), Homosassa River at Homosassa (middle panel), and Homosassa River at Shell Island (bottom panel) stations in the Homosassa River during 12/25/2008 – 3/25/2009.

Figure C - 7. Measured real-time temperatures at USGS SE Fork Homosassa Spring (pink line, top panel), Homosassa Springs at Homosassa Springs (orange line, top panel), Halls River near Homosassa (blue line, top panel), Halls River at Homosassa Springs (green line, top panel), Homosassa River at Homosassa (middle panel), and Homosassa River at Shell Island (bottom panel) stations in the Homosassa River during 3/25/2009 – 6/23/2009.

Figure C - 8. Measured real-time temperatures at USGS SE Fork Homosassa Spring (pink line, top panel), Homosassa Springs at Homosassa Springs (orange line, top panel), Halls River near Homosassa (blue line, top panel), Halls River at Homosassa Springs (green line, top panel), Homosassa River at Homosassa (middle panel), and Homosassa River at Shell Island (bottom panel) stations in the Homosassa River during 6/23/2009 – 9/21/2009.

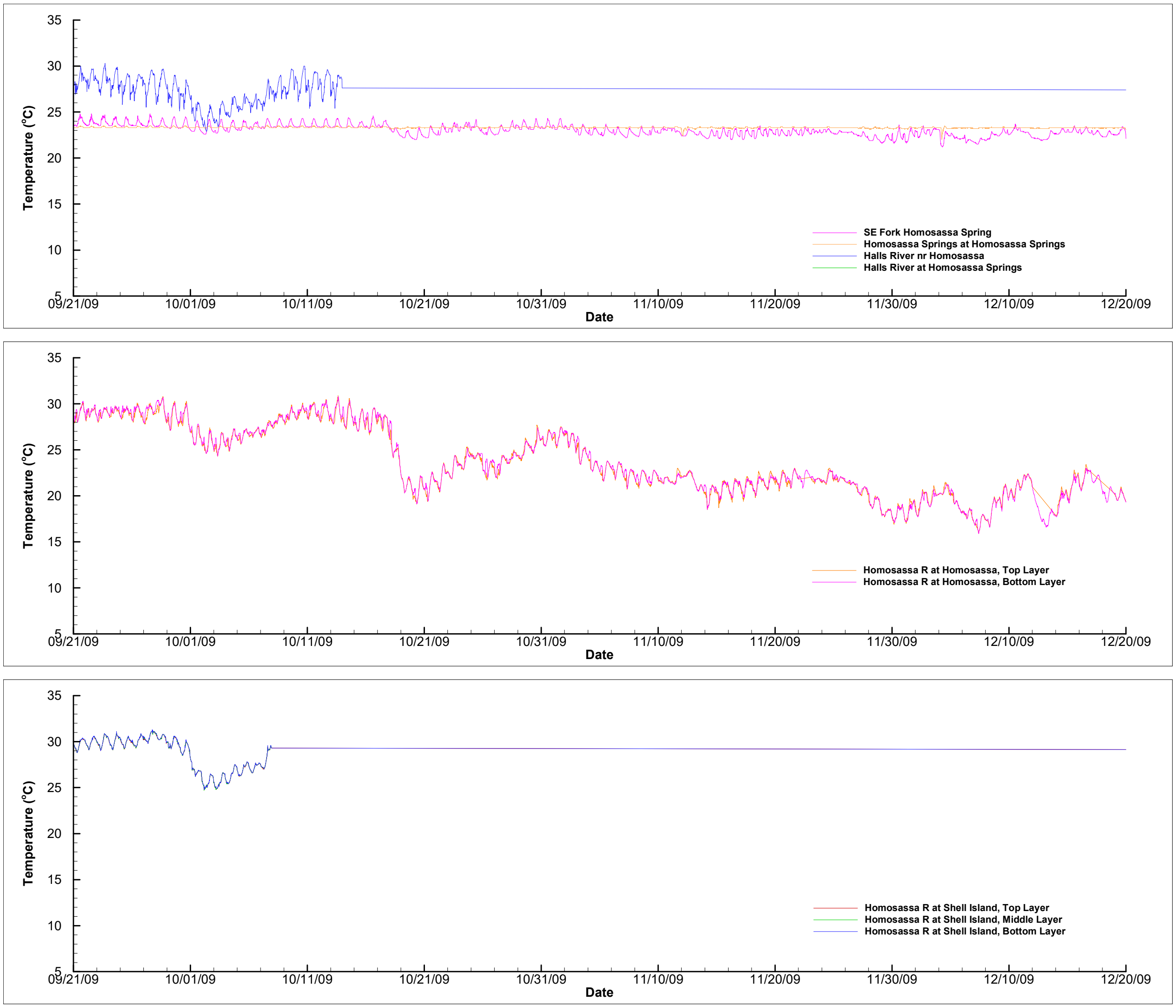

Figure C - 9. Measured real-time temperatures at USGS SE Fork Homosassa Spring (pink line, top panel), Homosassa Springs at Homosassa Springs (orange line, top panel), Halls River near Homosassa (blue line, top panel), Halls River at Homosassa Springs (green line, top panel), Homosassa River at Homosassa (middle panel), and Homosassa River at Shell Island (bottom panel) stations in the Homosassa River during 9/21/2009 – 12/20/2009.

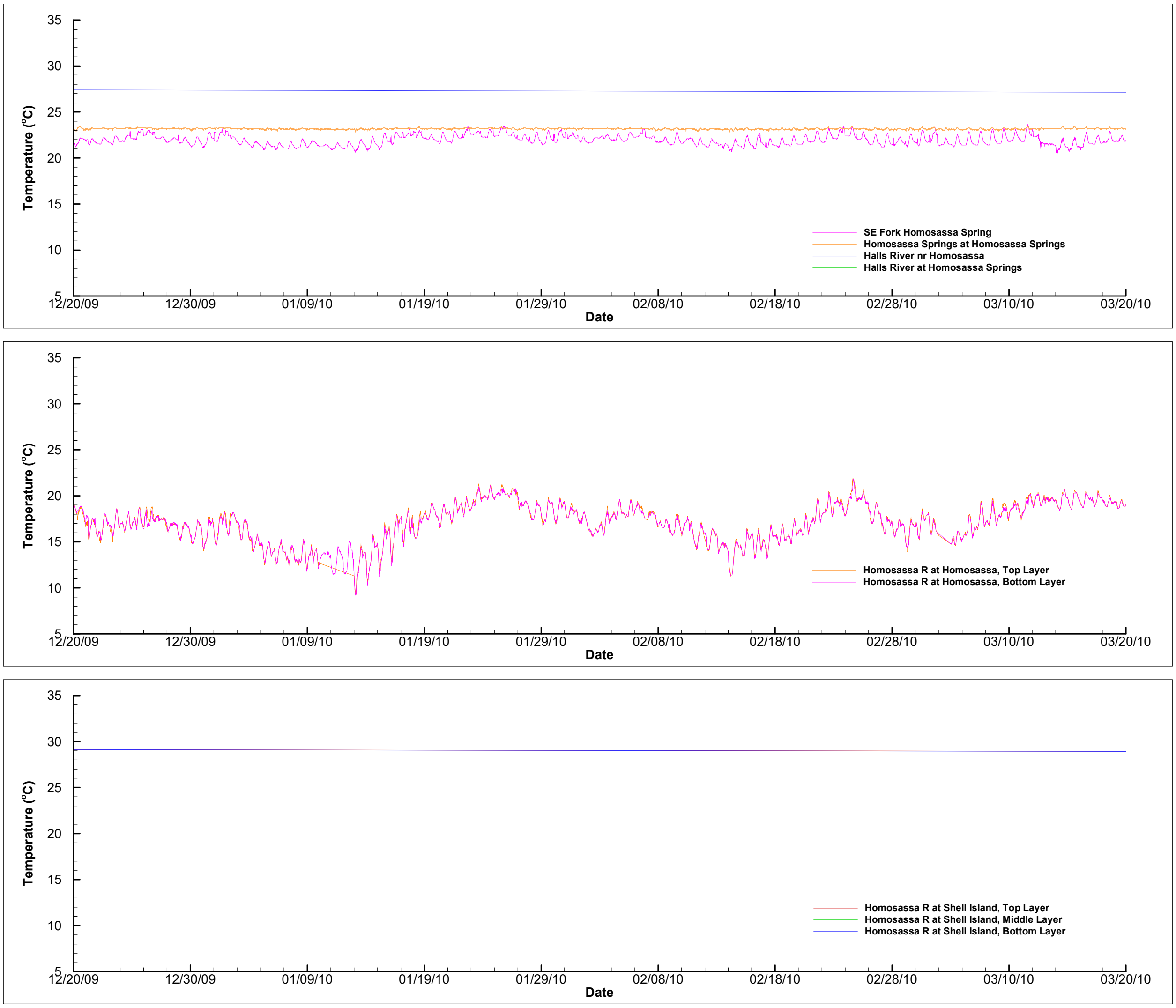

Figure C - 10. Measured real-time temperatures at USGS SE Fork Homosassa Spring (pink line, top panel), Homosassa Springs at Homosassa Springs (orange line, top panel), Halls River near Homosassa (blue line, top panel), Halls River at Homosassa Springs (green line, top panel), Homosassa River at Homosassa (middle panel), and Homosassa River at Shell Island (bottom panel) stations in the Homosassa River during 12/20/2009 – 3/20/2010.

Figure C - 11. Measured real-time temperatures at USGS SE Fork Homosassa Spring (pink line, top panel), Homosassa Springs at Homosassa Springs (orange line, top panel), Halls River near Homosassa (blue line, top panel), Halls River at Homosassa Springs (green line, top panel), Homosassa River at Homosassa (middle panel), and Homosassa River at Shell Island (bottom panel) stations in the Homosassa River during 3/20/2010 – 6/18/2010.

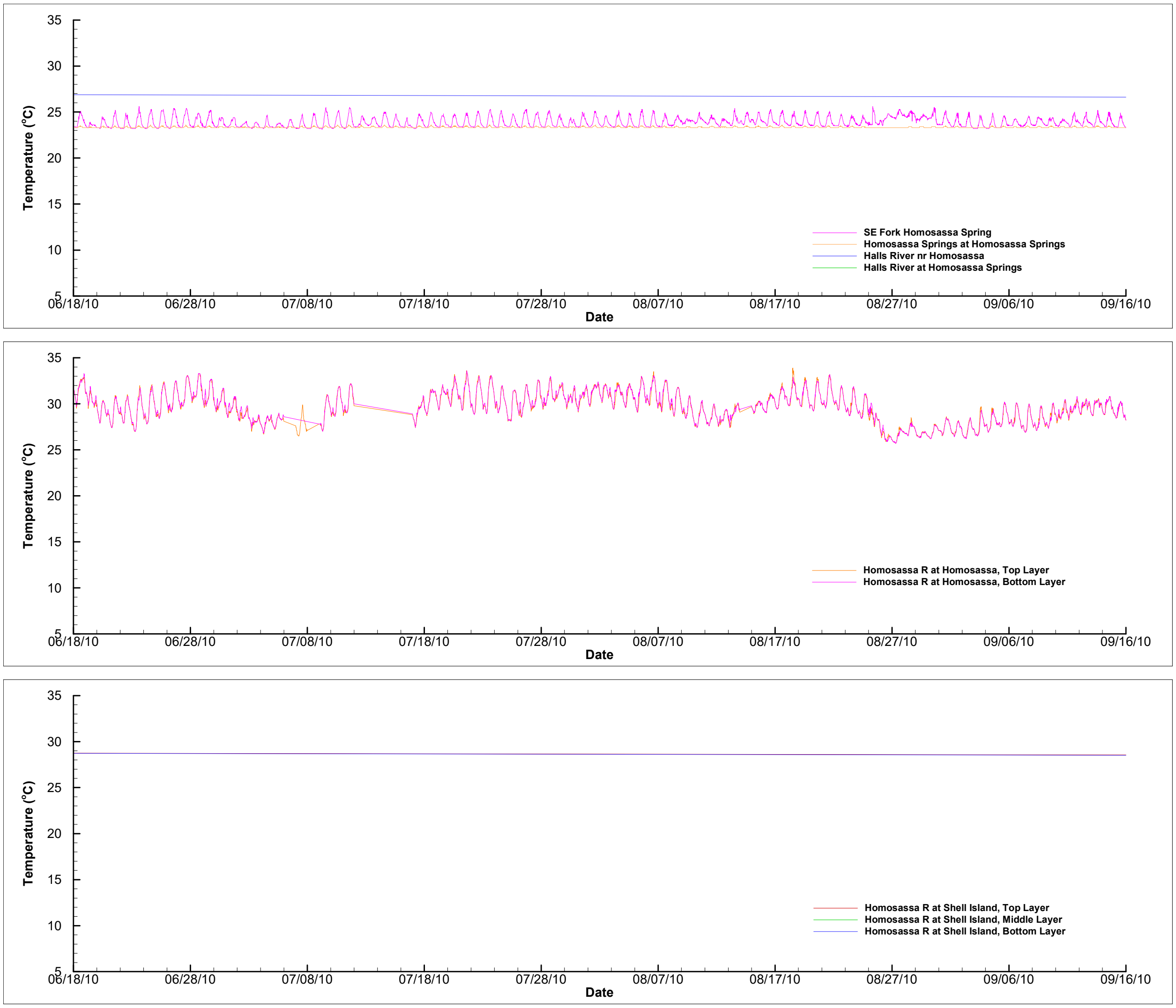

Figure C - 12. Measured real-time temperatures at USGS SE Fork Homosassa Spring (pink line, top panel), Homosassa Springs at Homosassa Springs (orange line, top panel), Halls River near Homosassa (blue line, top panel), Halls River at Homosassa Springs (green line, top panel), Homosassa River at Homosassa (middle panel), and Homosassa River at Shell Island (bottom panel) stations in the Homosassa River during 6/18/2010 – 9/16/2010.

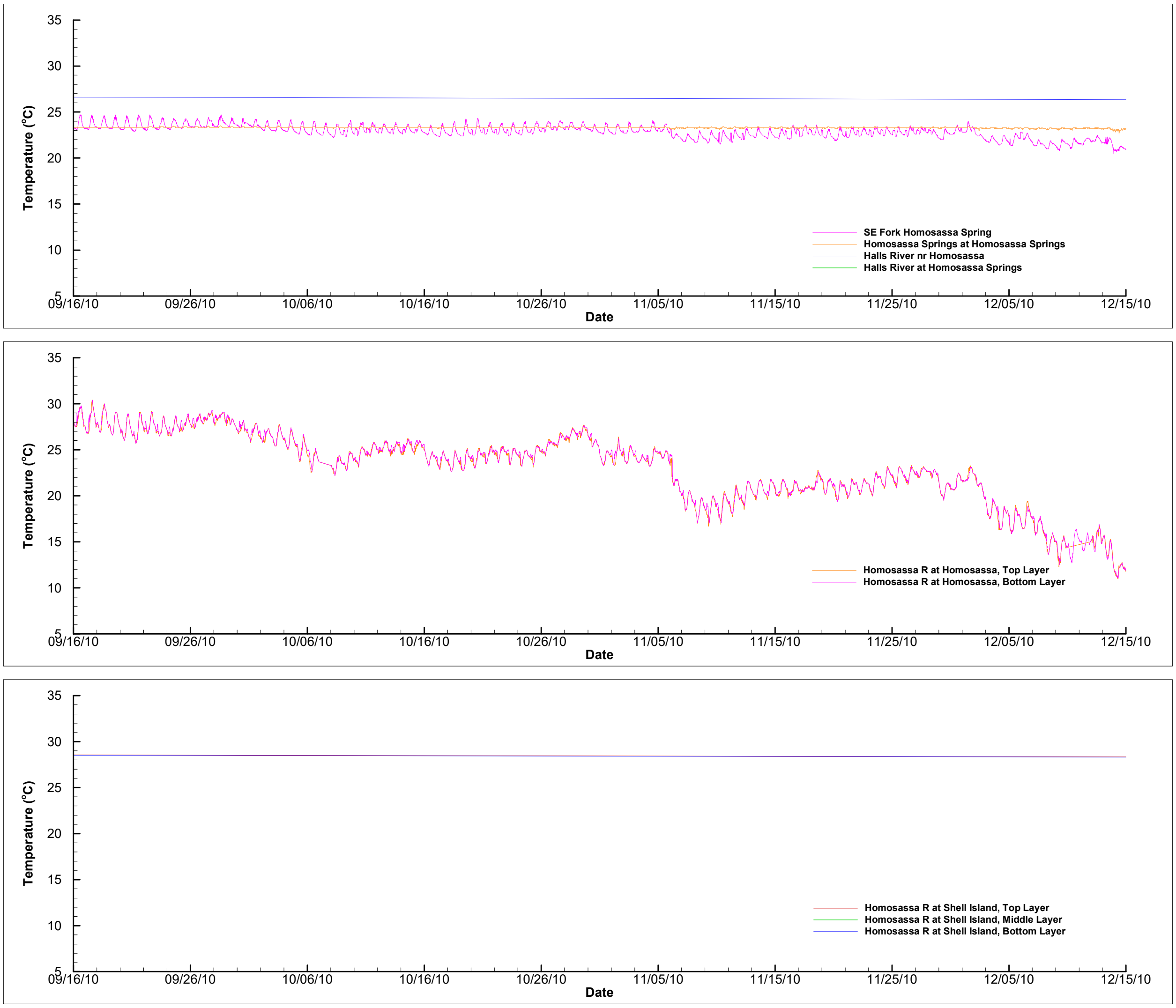

Figure C - 13. Measured real-time temperatures at USGS SE Fork Homosassa Spring (pink line, top panel), Homosassa Springs at Homosassa Springs (orange line, top panel), Halls River near Homosassa (blue line, top panel), Halls River at Homosassa Springs (green line, top panel), Homosassa River at Homosassa (middle panel), and Homosassa River at Shell Island (bottom panel) stations in the Homosassa River during 9/16/2010 – 12/15/2010.

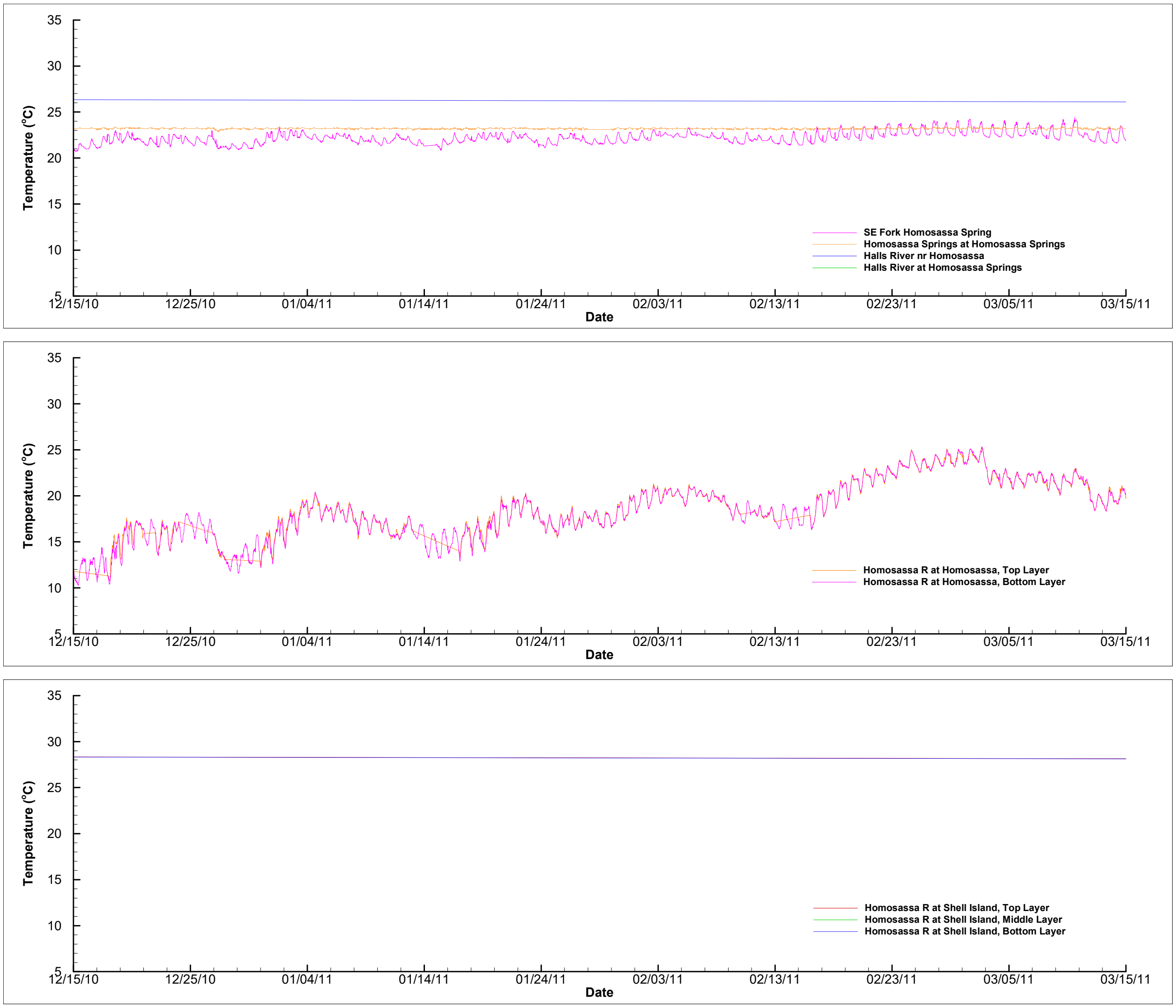

Figure C - 14. Measured real-time temperatures at USGS SE Fork Homosassa Spring (pink line, top panel), Homosassa Springs at Homosassa Springs (orange line, top panel), Halls River near Homosassa (blue line, top panel), Halls River at Homosassa Springs (green line, top panel), Homosassa River at Homosassa (middle panel), and Homosassa River at Shell Island (bottom panel) stations in the Homosassa River during 12/15/2010 – 3/15/2011.

Figure C - 15. Measured real-time temperatures at USGS SE Fork Homosassa Spring (pink line, top panel), Homosassa Springs at Homosassa Springs (orange line, top panel), Halls River near Homosassa (blue line, top panel), Halls River at Homosassa Springs (green line, top panel), Homosassa River at Homosassa (middle panel), and Homosassa River at Shell Island (bottom panel) stations in the Homosassa River during 3/15/2011 – 6/13/2011.

Figure C - 16. Measured real-time temperatures at USGS SE Fork Homosassa Spring (pink line, top panel), Homosassa Springs at Homosassa Springs (orange line, top panel), Halls River near Homosassa (blue line, top panel), Halls River at Homosassa Springs (green line, top panel), Homosassa River at Homosassa (middle panel), and Homosassa River at Shell Island (bottom panel) stations in the Homosassa River during 6/13/2011 – 9/11/2011.

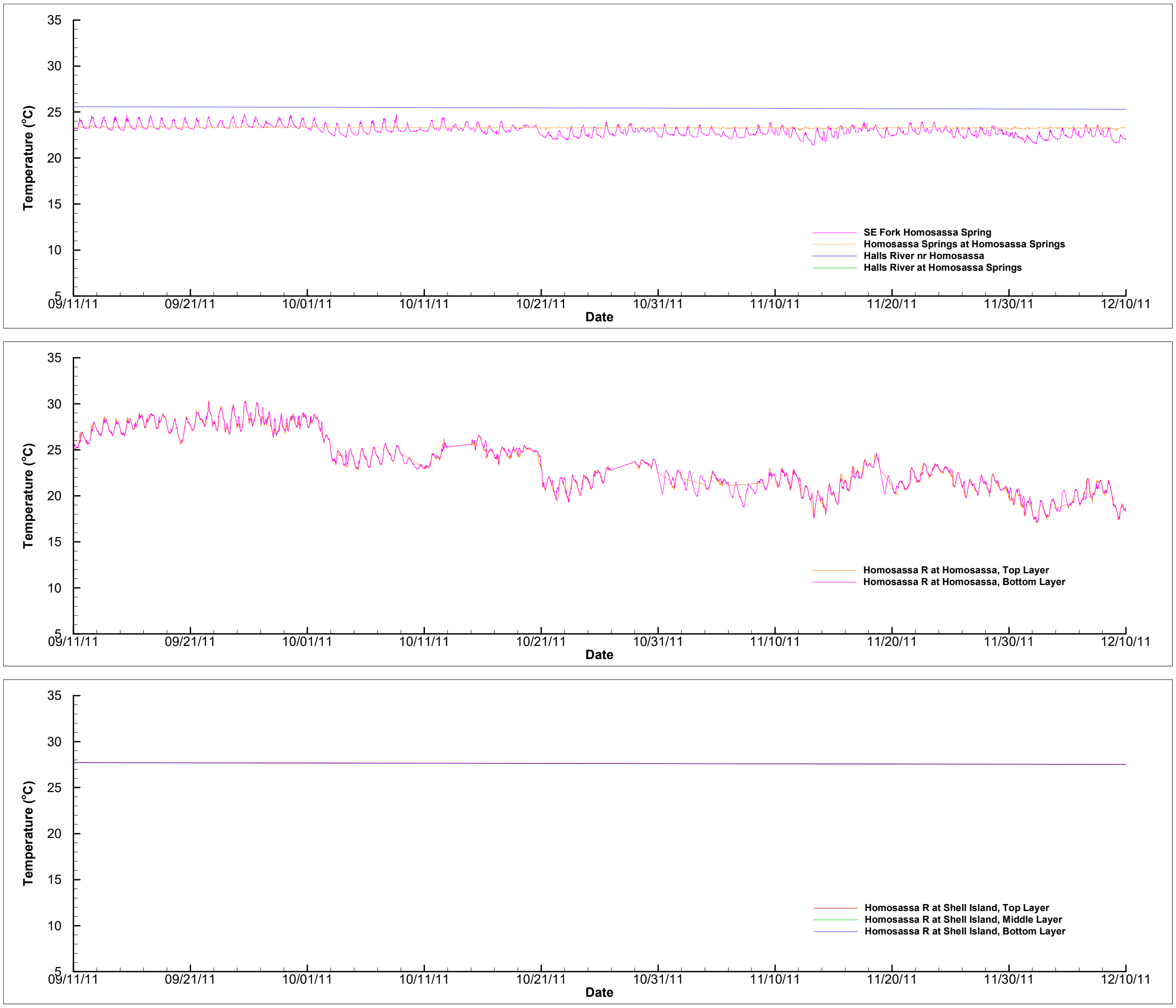

Figure C - 17. Measured real-time temperatures at USGS SE Fork Homosassa Spring (pink line, top panel), Homosassa Springs at Homosassa Springs (orange line, top panel), Halls River near Homosassa (blue line, top panel), Halls River at Homosassa Springs (green line, top panel), Homosassa River at Homosassa (middle panel), and Homosassa River at Shell Island (bottom panel) stations in the Homosassa River during 9/11/2011 – 12/10/2011.

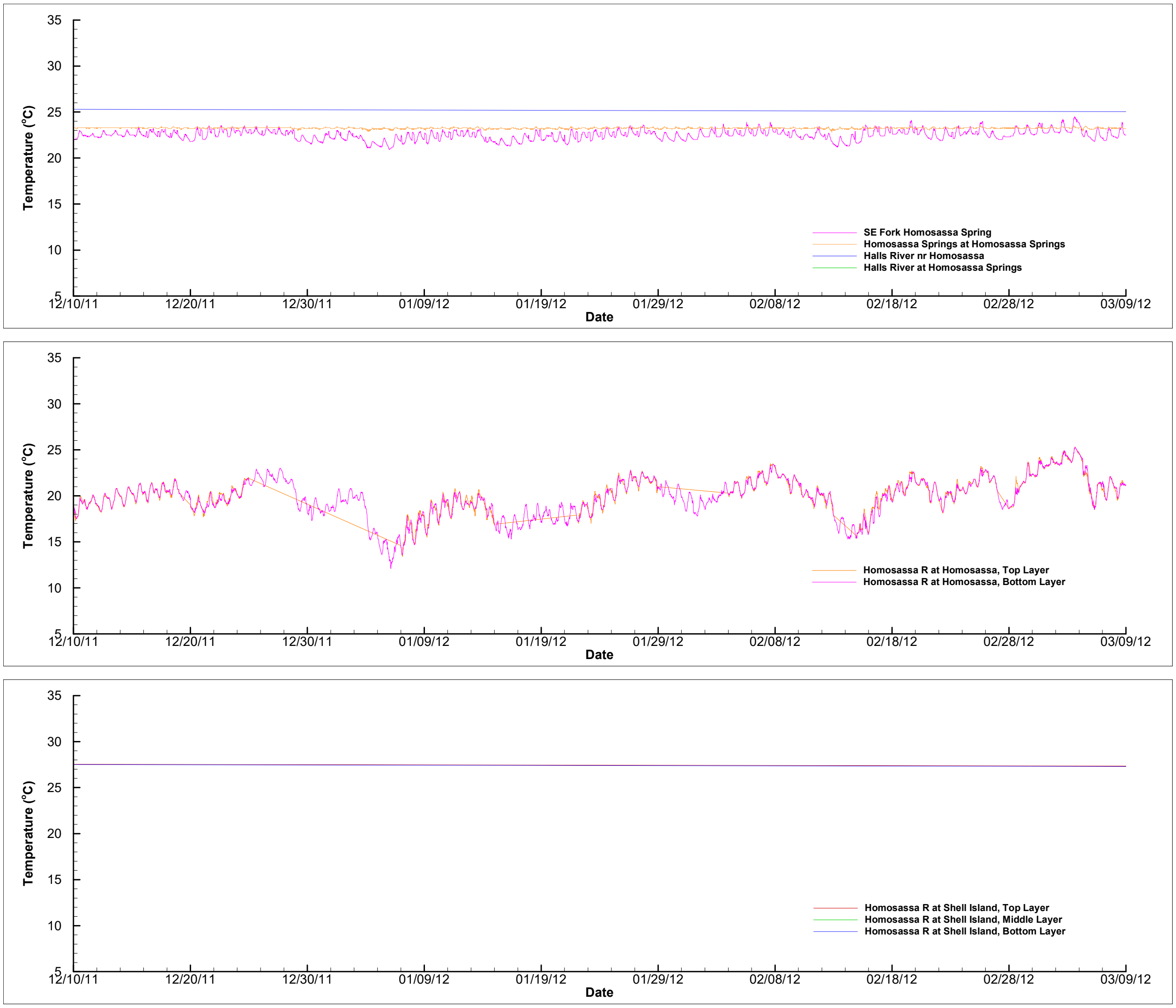

Figure C - 18. Measured real-time temperatures at USGS SE Fork Homosassa Spring (pink line, top panel), Homosassa Springs at Homosassa Springs (orange line, top panel), Halls River near Homosassa (blue line, top panel), Halls River at Homosassa Springs (green line, top panel), Homosassa River at Homosassa (middle panel), and Homosassa River at Shell Island (bottom panel) stations in the Homosassa River during 12/10/2011 – 3/9/2012.

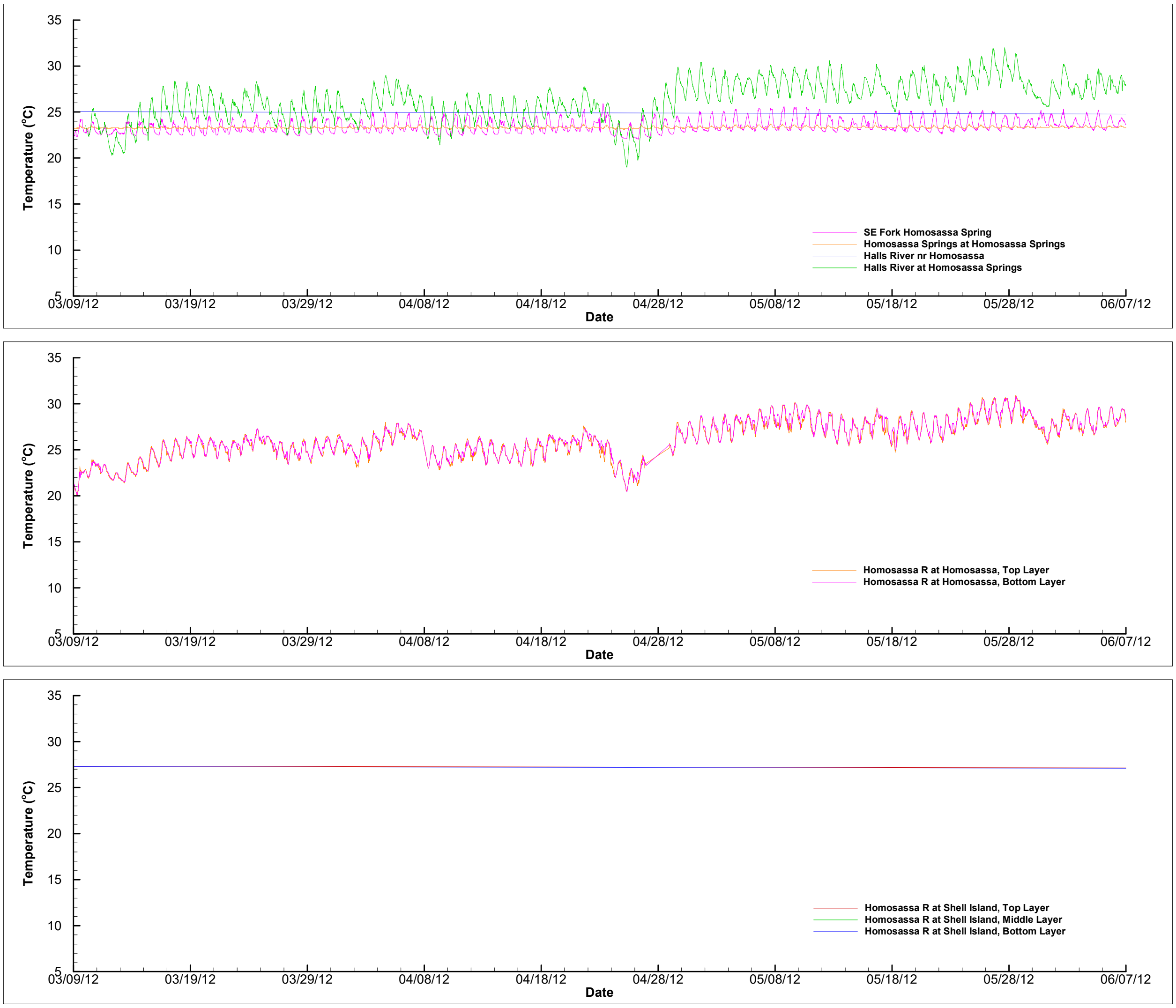

Figure C - 19. Measured real-time temperatures at USGS SE Fork Homosassa Spring (pink line, top panel), Homosassa Springs at Homosassa Springs (orange line, top panel), Halls River near Homosassa (blue line, top panel), Halls River at Homosassa Springs (green line, top panel), Homosassa River at Homosassa (middle panel), and Homosassa River at Shell Island (bottom panel) stations in the Homosassa River during 3/9/2012 – 6/7/2012.

Figure C - 20. Measured real-time temperatures at USGS SE Fork Homosassa Spring (pink line, top panel), Homosassa Springs at Homosassa Springs (orange line, top panel), Halls River near Homosassa (blue line, top panel), Halls River at Homosassa Springs (green line, top panel), Homosassa River at Homosassa (middle panel), and Homosassa River at Shell Island (bottom panel) stations in the Homosassa River during 6/7/2012 – 9/5/2012.

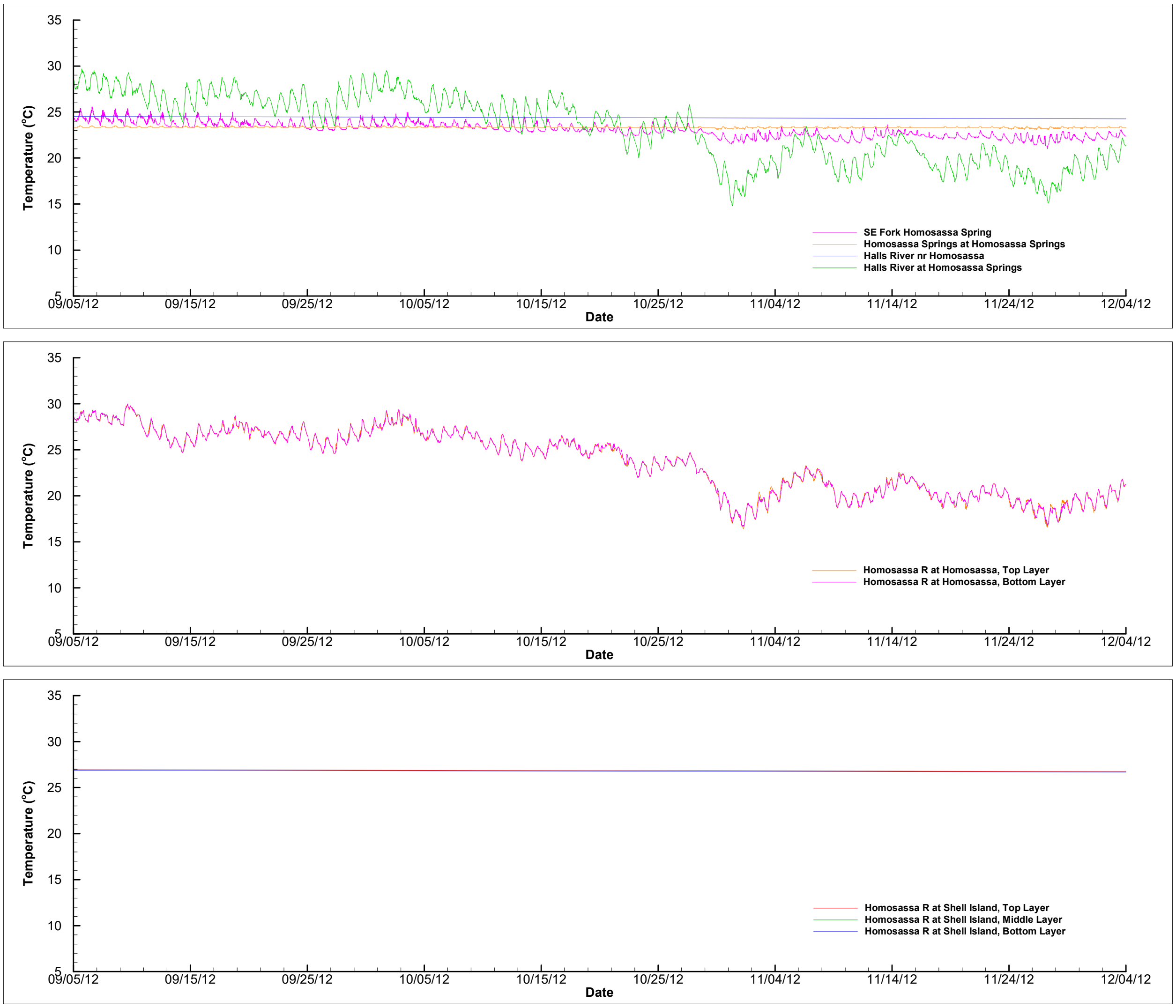

Figure C - 21. Measured real-time temperatures at USGS SE Fork Homosassa Spring (pink line, top panel), Homosassa Springs at Homosassa Springs (orange line, top panel), Halls River near Homosassa (blue line, top panel), Halls River at Homosassa Springs (green line, top panel), Homosassa River at Homosassa (middle panel), and Homosassa River at Shell Island (bottom panel) stations in the Homosassa River during 9/5/2012 – 12/4/2012.

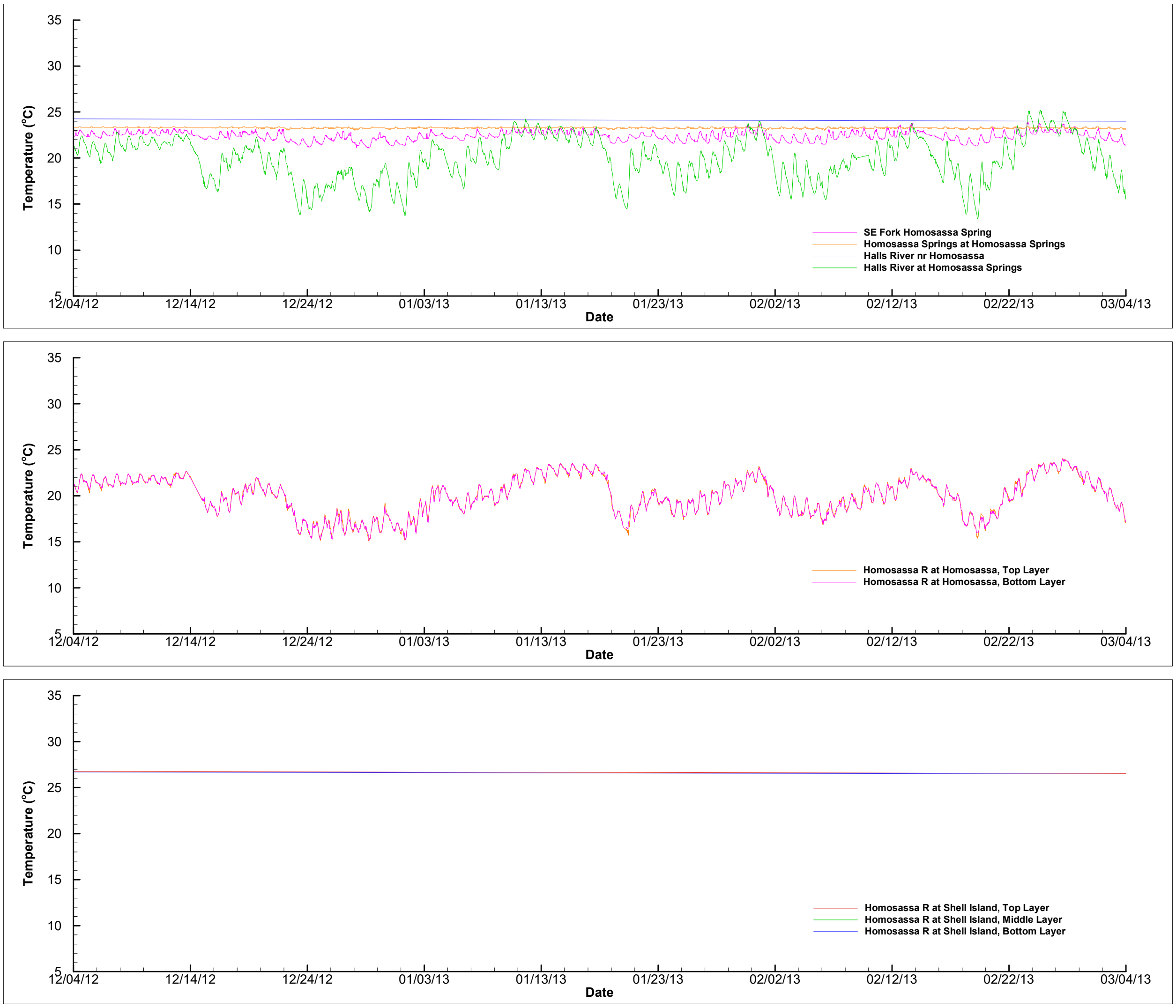

Figure C - 22. Measured real-time temperatures at USGS SE Fork Homosassa Spring (pink line, top panel), Homosassa Springs at Homosassa Springs (orange line, top panel), Halls River near Homosassa (blue line, top panel), Halls River at Homosassa Springs (green line, top panel), Homosassa River at Homosassa (middle panel), and Homosassa River at Shell Island (bottom panel) stations in the Homosassa River during 12/4/2012 – 3/4/2013.

Figure C - 23. Measured real-time temperatures at USGS SE Fork Homosassa Spring (pink line, top panel), Homosassa Springs at Homosassa Springs (orange line, top panel), Halls River near Homosassa (blue line, top panel), Halls River at Homosassa Springs (green line, top panel), Homosassa River at Homosassa (middle panel), and Homosassa River at Shell Island (bottom panel) stations in the Homosassa River during 3/4/2013 – 6/2/2013.

Figure C - 24. Measured real-time temperatures at USGS SE Fork Homosassa Spring (pink line, top panel), Homosassa Springs at Homosassa Springs (orange line, top panel), Halls River near Homosassa (blue line, top panel), Halls River at Homosassa Springs (green line, top panel), Homosassa River at Homosassa (middle panel), and Homosassa River at Shell Island (bottom panel) stations in the Homosassa River during 6/2/2013 – 8/31/2013.

Figure C - 25. Measured real-time temperatures at USGS SE Fork Homosassa Spring (pink line, top panel), Homosassa Springs at Homosassa Springs (orange line, top panel), Halls River near Homosassa (blue line, top panel), Halls River at Homosassa Springs (green line, top panel), Homosassa River at Homosassa (middle panel), and Homosassa River at Shell Island (bottom panel) stations in the Homosassa River during 8/31/2013 – 11/29/2013.

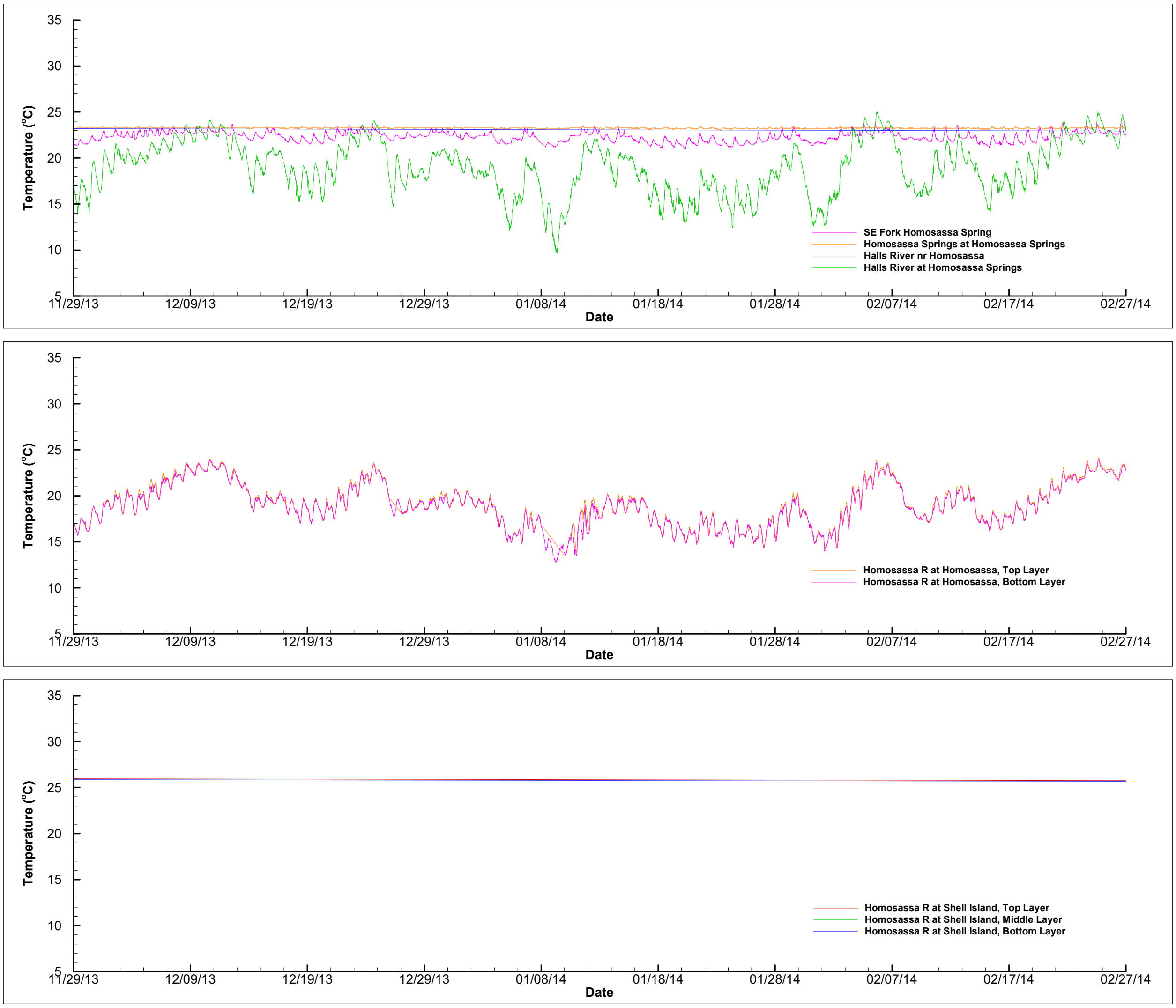

Figure C - 26. Measured real-time temperatures at USGS SE Fork Homosassa Spring (pink line, top panel), Homosassa Springs at Homosassa Springs (orange line, top panel), Halls River near Homosassa (blue line, top panel), Halls River at Homosassa Springs (green line, top panel), Homosassa River at Homosassa (middle panel), and Homosassa River at Shell Island (bottom panel) stations in the Homosassa River during 11/29/2013 - 2/27/2014.

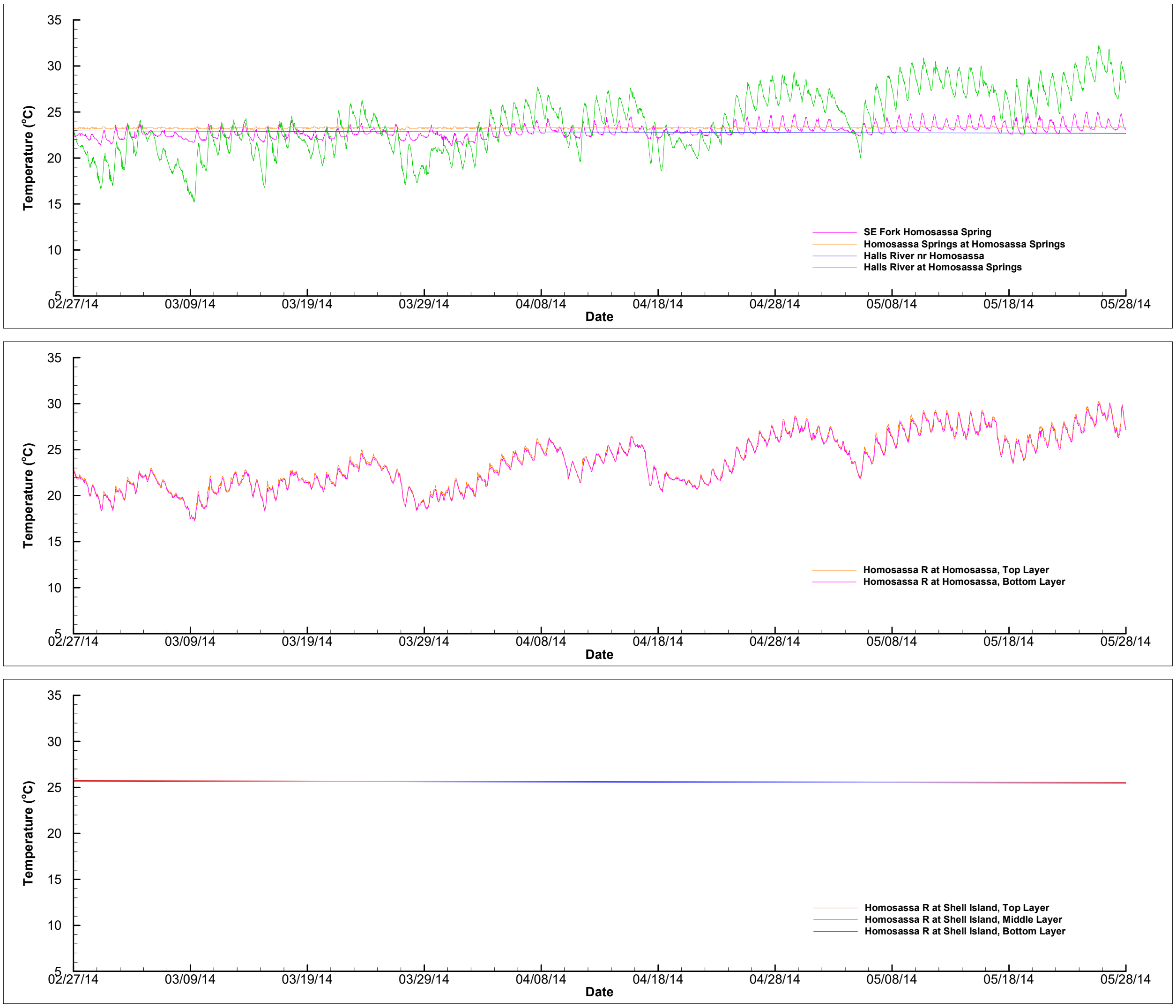

Figure C - 27. Measured real-time temperatures at USGS SE Fork Homosassa Spring (pink line, top panel), Homosassa Springs at Homosassa Springs (orange line, top panel), Halls River near Homosassa (blue line, top panel), Halls River at Homosassa Springs (green line, top panel), Homosassa River at Homosassa (middle panel), and Homosassa River at Shell Island (bottom panel) stations in the Homosassa River during 2/27/2014 – 5/28/2014.

Figure C - 28. Measured real-time temperatures at USGS SE Fork Homosassa Spring (pink line, top panel), Homosassa Springs at Homosassa Springs (orange line, top panel), Halls River near Homosassa (blue line, top panel), Halls River at Homosassa Springs (green line, top panel), Homosassa River at Homosassa (middle panel), and Homosassa River at Shell Island (bottom panel) stations in the Homosassa River during 5/28/2014 – 8/26/2014.

Figure C - 29. Measured real-time temperatures at USGS SE Fork Homosassa Spring (pink line, top panel), Homosassa Springs at Homosassa Springs (orange line, top panel), Halls River near Homosassa (blue line, top panel), Halls River at Homosassa Springs (green line, top panel), Homosassa River at Homosassa (middle panel), and Homosassa River at Shell Island (bottom panel) stations in the Homosassa River during 8/26/2014 – 11/24/2014.

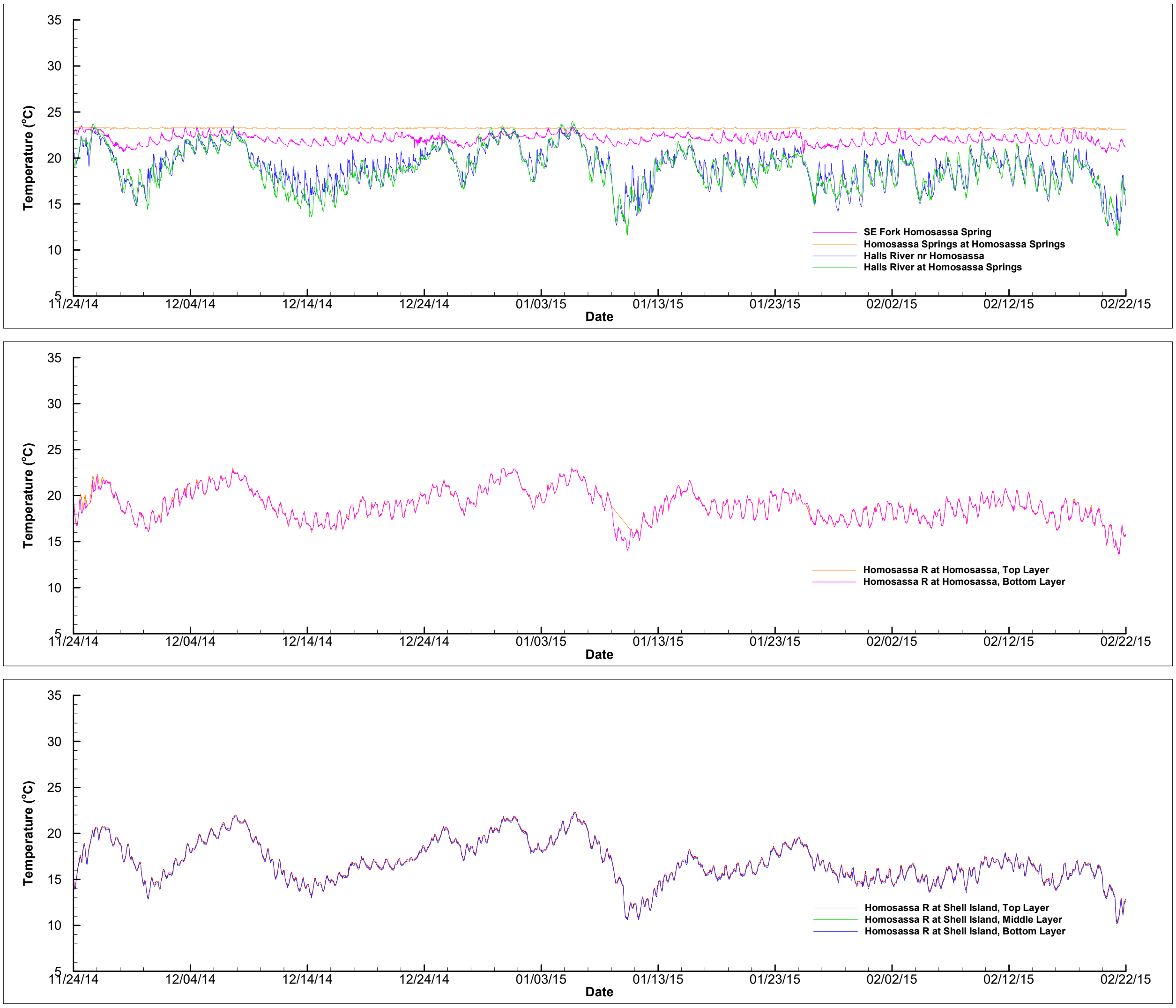

Figure C - 30. Measured real-time temperatures at USGS SE Fork Homosassa Spring (pink line, top panel), Homosassa Springs at Homosassa Springs (orange line, top panel), Halls River near Homosassa (blue line, top panel), Halls River at Homosassa Springs (green line, top panel), Homosassa River at Homosassa (middle panel), and Homosassa River at Shell Island (bottom panel) stations in the Homosassa River during 11/24/2014 – 2/22/2015.

Figure C - 31. Measured real-time temperatures at USGS SE Fork Homosassa Spring (pink line, top panel), Homosassa Springs at Homosassa Springs (orange line, top panel), Halls River near Homosassa (blue line, top panel), Halls River at Homosassa Springs (green line, top panel), Homosassa River at Homosassa (middle panel), and Homosassa River at Shell Island (bottom panel) stations in the Homosassa River during 2/22/2015 – 5/23/2015.

Figure C - 32. Measured real-time temperatures at USGS SE Fork Homosassa Spring (pink line, top panel), Homosassa Springs at Homosassa Springs (orange line, top panel), Halls River near Homosassa (blue line, top panel), Halls River at Homosassa Springs (green line, top panel), Homosassa River at Homosassa (middle panel), and Homosassa River at Shell Island (bottom panel) stations in the Homosassa River during 5/23/2015 – 8/21/2015.

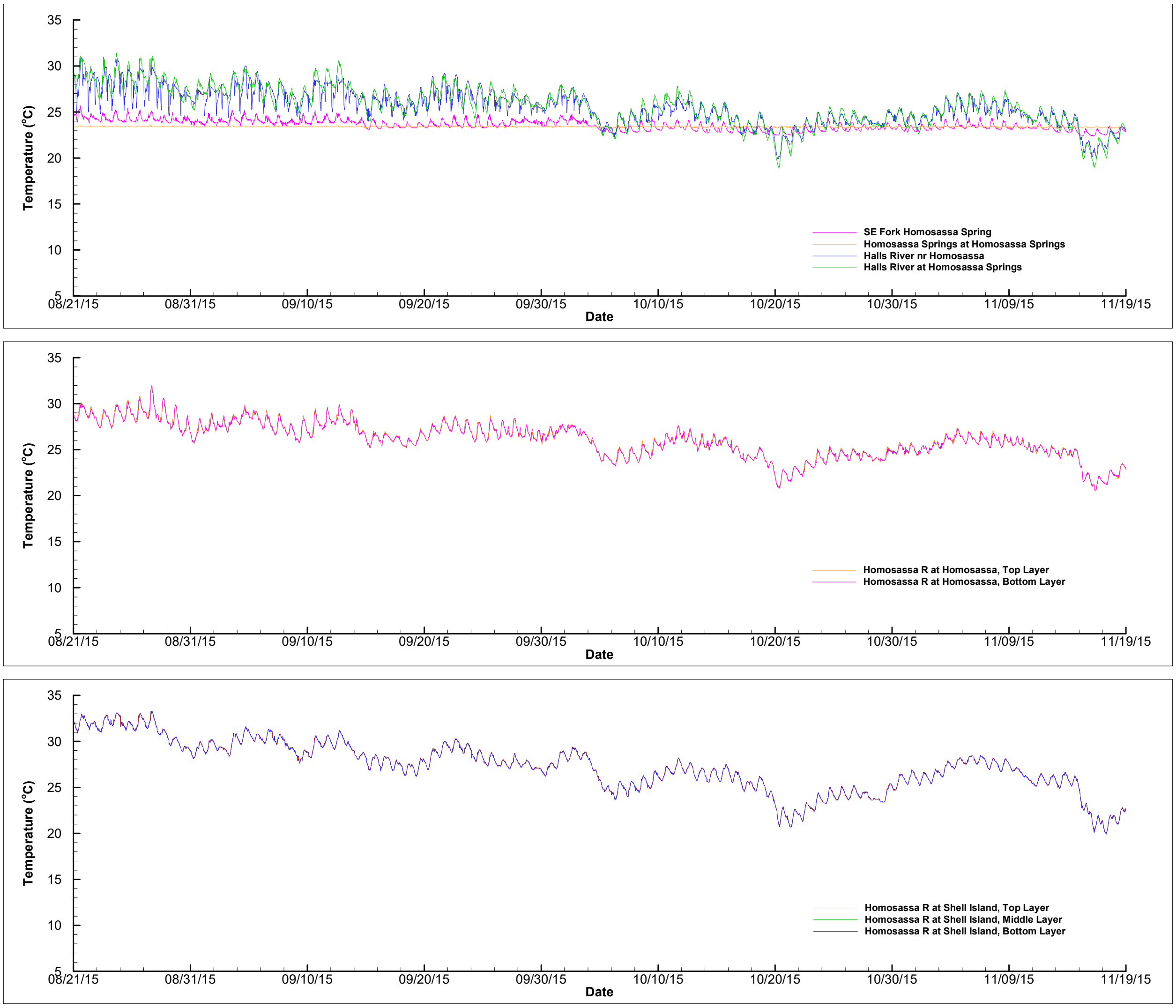

Figure C - 33. Measured real-time temperatures at USGS SE Fork Homosassa Spring (pink line, top panel), Homosassa Springs at Homosassa Springs (orange line, top panel), Halls River near Homosassa (blue line, top panel), Halls River at Homosassa Springs (green line, top panel), Homosassa River at Homosassa (middle panel), and Homosassa River at Shell Island (bottom panel) stations in the Homosassa River during 8/21/2015 – 11/19/2015.

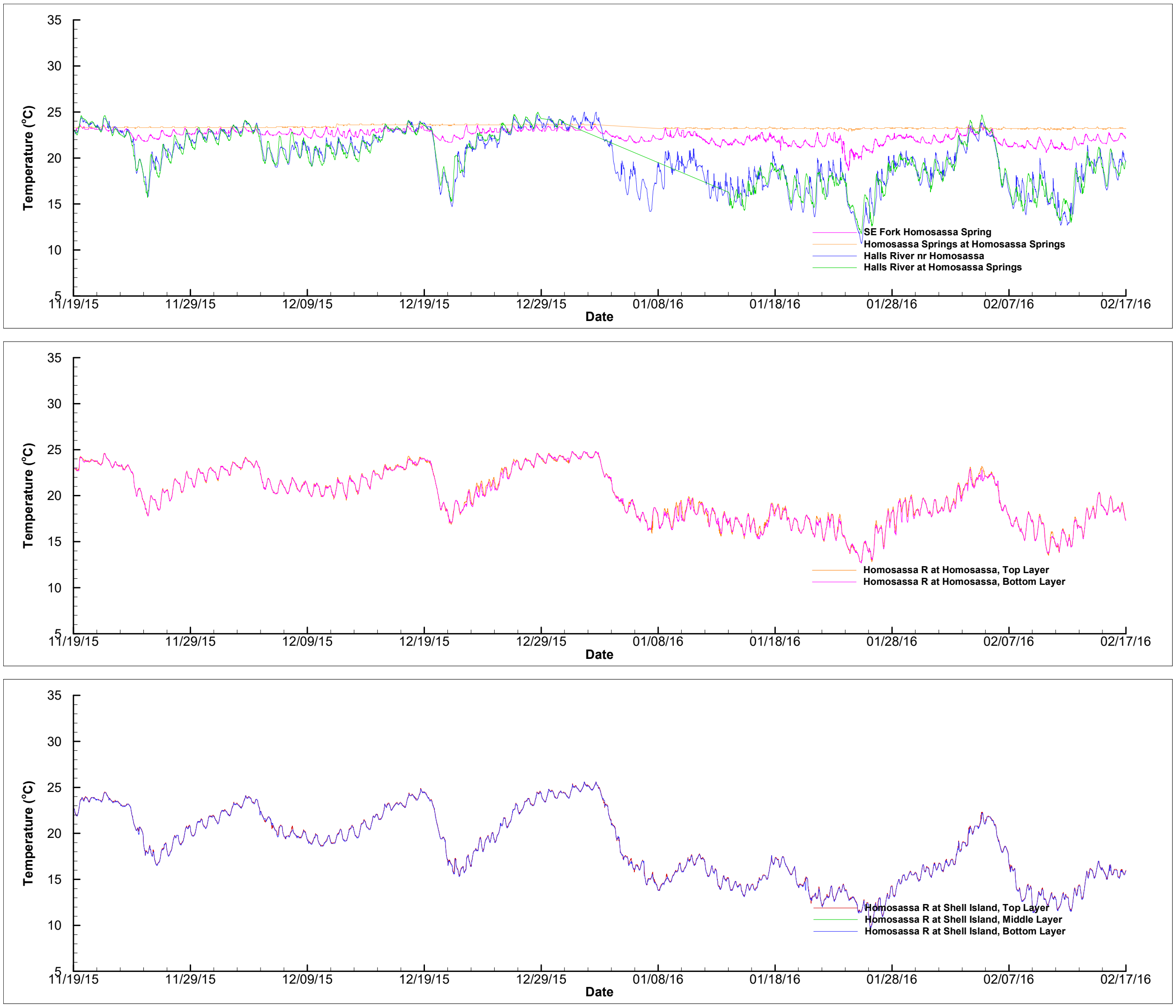

Figure C - 34. Measured real-time temperatures at USGS SE Fork Homosassa Spring (pink line, top panel), Homosassa Springs at Homosassa Springs (orange line, top panel), Halls River near Homosassa (blue line, top panel), Halls River at Homosassa Springs (green line, top panel), Homosassa River at Homosassa (middle panel), and Homosassa River at Shell Island (bottom panel) stations in the Homosassa River during 11/19/2015 – 2/17/2016.

Figure C - 35. Measured real-time temperatures at USGS SE Fork Homosassa Spring (pink line, top panel), Homosassa Springs at Homosassa Springs (orange line, top panel), Halls River near Homosassa (blue line, top panel), Halls River at Homosassa Springs (green line, top panel), Homosassa River at Homosassa (middle panel), and Homosassa River at Shell Island (bottom panel) stations in the Homosassa River during 2/17/2016 – 5/17/2016.

Figure C - 36. Measured real-time temperatures at USGS SE Fork Homosassa Spring (pink line, top panel), Homosassa Springs at Homosassa Springs (orange line, top panel), Halls River near Homosassa (blue line, top panel), Halls River at Homosassa Springs (green line, top panel), Homosassa River at Homosassa (middle panel), and Homosassa River at Shell Island (bottom panel) stations in the Homosassa River during 5/17/2016 – 8/15/2016.

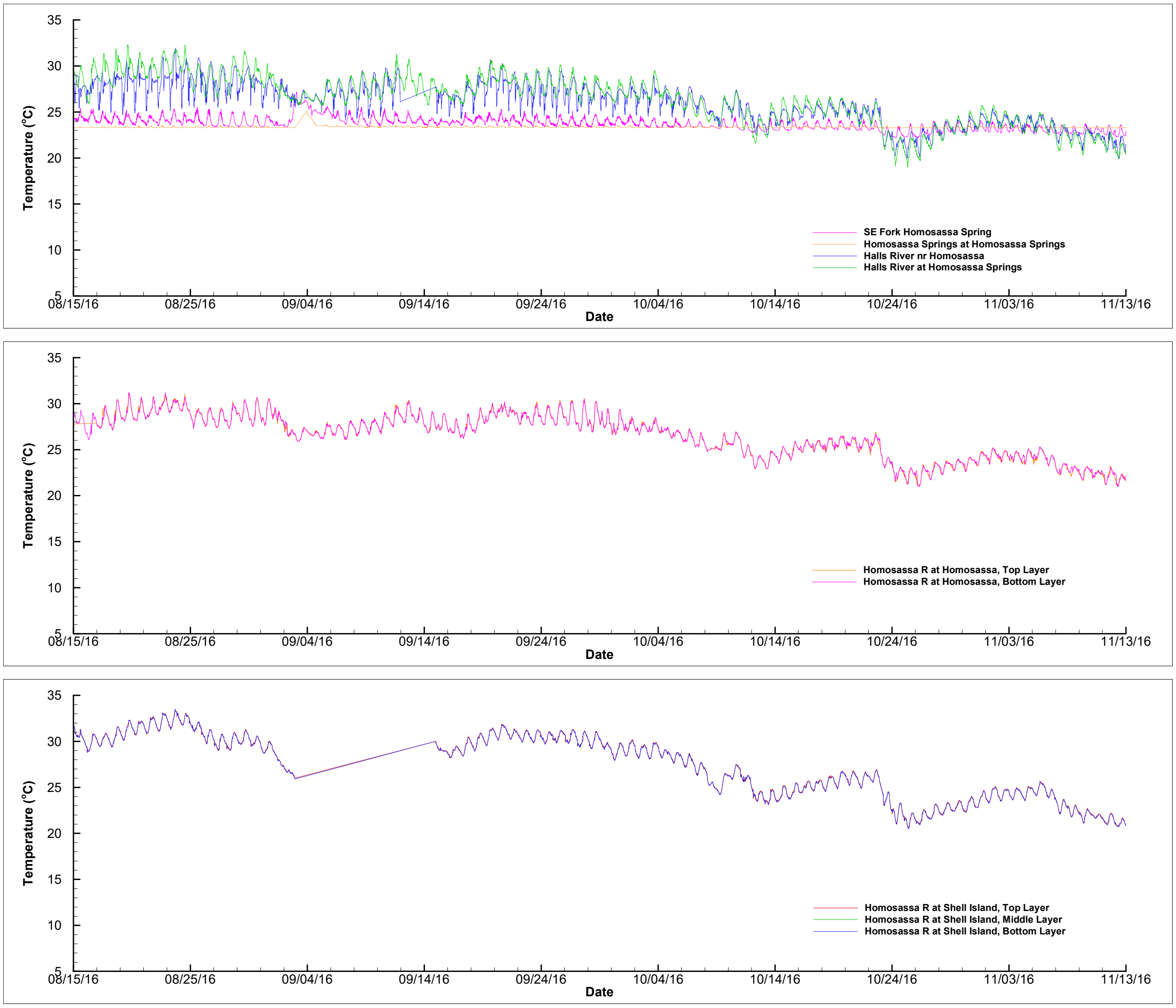

Figure C - 37. Measured real-time temperatures at USGS SE Fork Homosassa Spring (pink line, top panel), Homosassa Springs at Homosassa Springs (orange line, top panel), Halls River near Homosassa (blue line, top panel), Halls River at Homosassa Springs (green line, top panel), Homosassa River at Homosassa (middle panel), and Homosassa River at Shell Island (bottom panel) stations in the Homosassa River during 8/15/2016 – 11/13/2016.

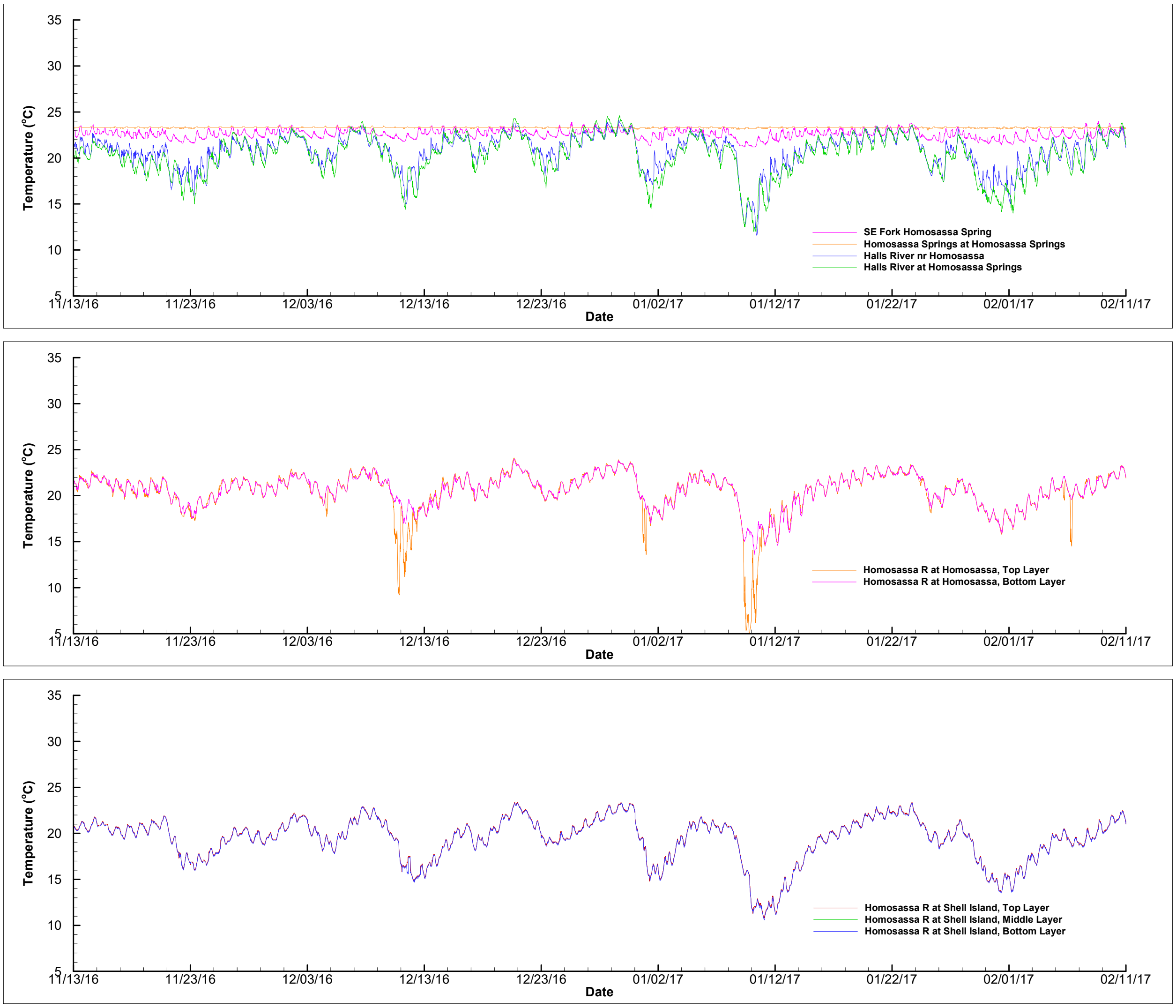

Figure C - 38. Measured real-time temperatures at USGS SE Fork Homosassa Spring (pink line, top panel), Homosassa Springs at Homosassa Springs (orange line, top panel), Halls River near Homosassa (blue line, top panel), Halls River at Homosassa Springs (green line, top panel), Homosassa River at Homosassa (middle panel), and Homosassa River at Shell Island (bottom panel) stations in the Homosassa River during 11/13/2016 – 2/11/2017.

Figure C - 39. Measured real-time temperatures at USGS SE Fork Homosassa Spring (pink line, top panel), Homosassa Springs at Homosassa Springs (orange line, top panel), Halls River near Homosassa (blue line, top panel), Halls River at Homosassa Springs (green line, top panel), Homosassa River at Homosassa (middle panel), and Homosassa River at Shell Island (bottom panel) stations in the Homosassa River during 2/11/2017 – 5/12/2017.

Appendix D. Simulated and Measured Water Levels

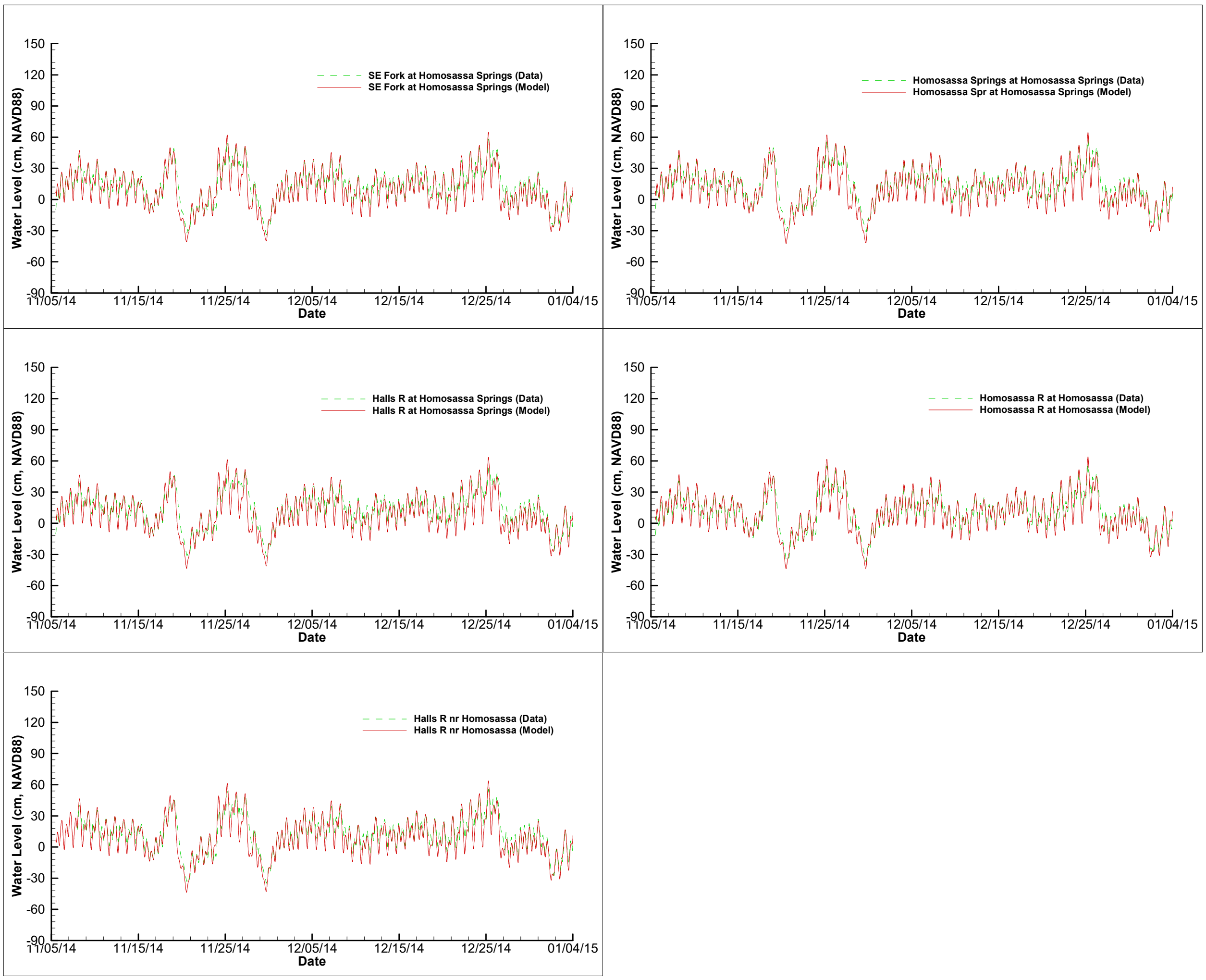

Figure D - 1. Comparisons of simulated (red lines) and measured (dashed green lines) water levels at SE Fork at Homosassa Spring (top left), Homosassa Springs at Homosassa Springs (top right), Halls River at Homosassa Springs (middle left), Halls River near Homosassa (bottom left), and Homosassa River at Homosassa (middle right) stations during 11/5/2014 – 1/4/2015.

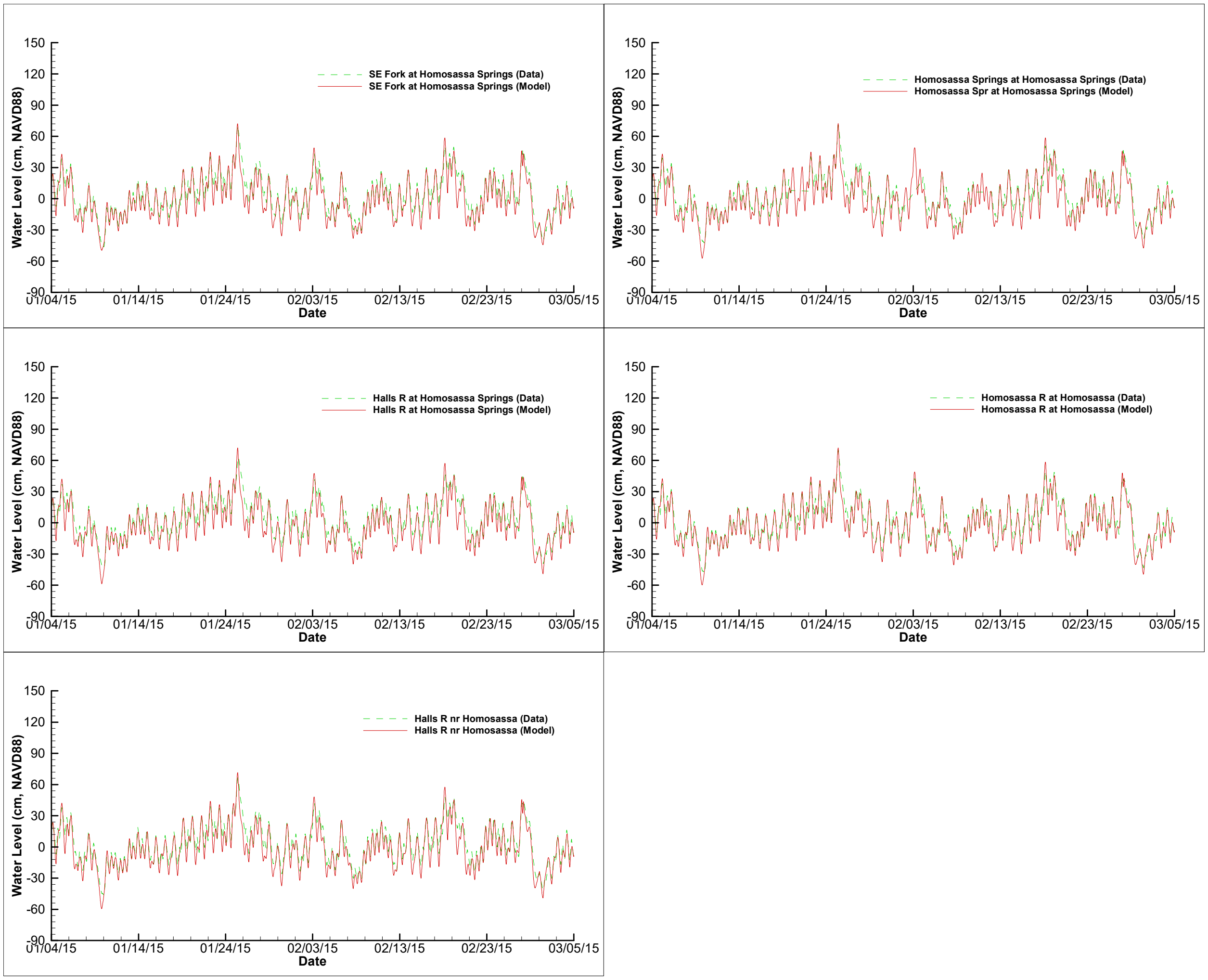

Figure D - 2. Comparisons of simulated (red lines) and measured (dashed green lines) water levels at SE Fork at Homosassa Spring (top left), Homosassa Springs at Homosassa Springs (top right), Halls River at Homosassa Springs (middle left), Halls River near Homosassa (bottom left), and Homosassa River at Homosassa (middle right) stations during 1/4/2015 - 3/5/2015.

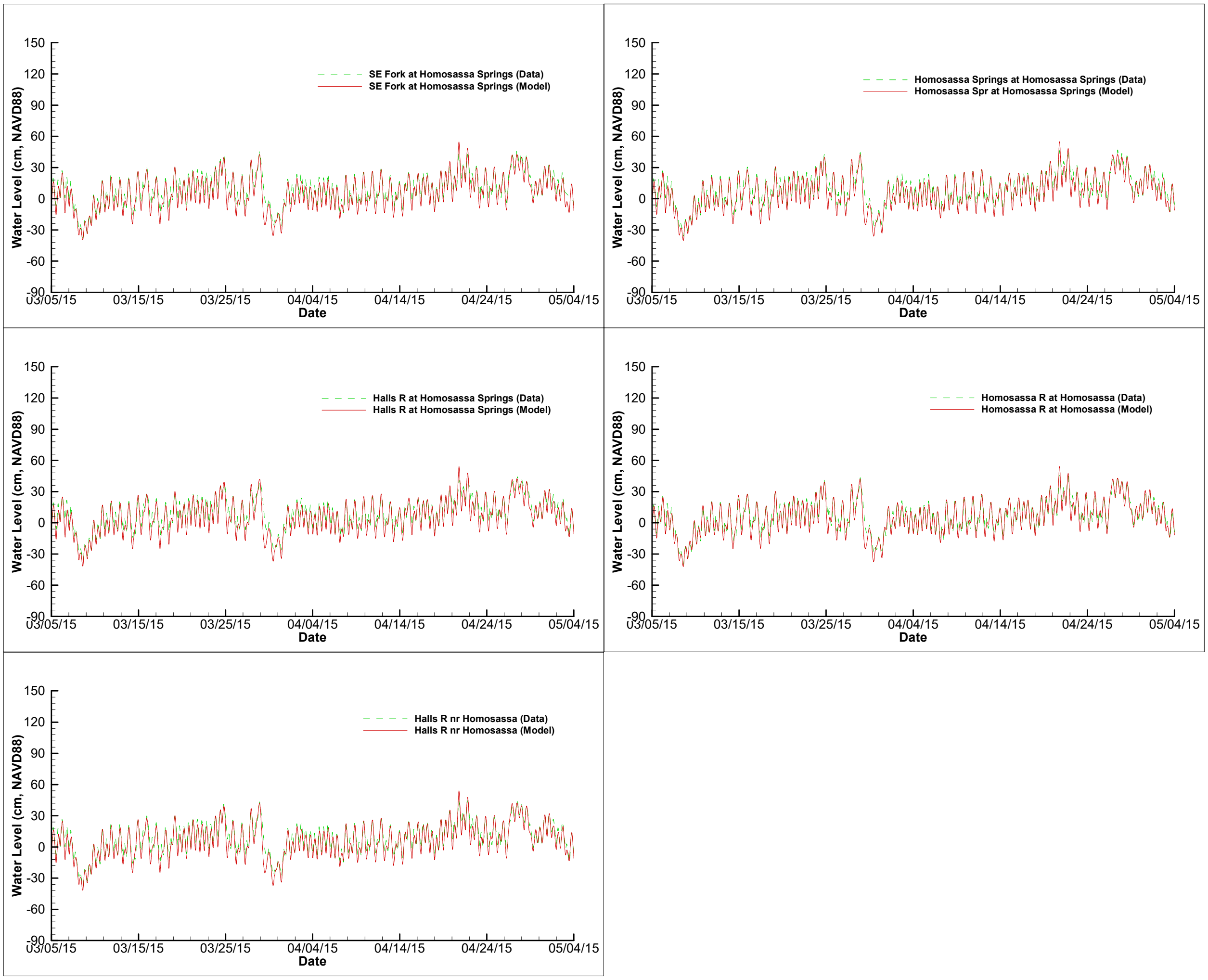

Figure D - 3. Comparisons of simulated (red lines) and measured (dashed green lines) water levels at SE Fork at Homosassa Spring (top left), Homosassa Springs at Homosassa Springs (top right), Halls River at Homosassa Springs (middle left), Halls River near Homosassa (bottom left), and Homosassa River at Homosassa (middle right) stations during 3/5/2015 – 5/4/2015.

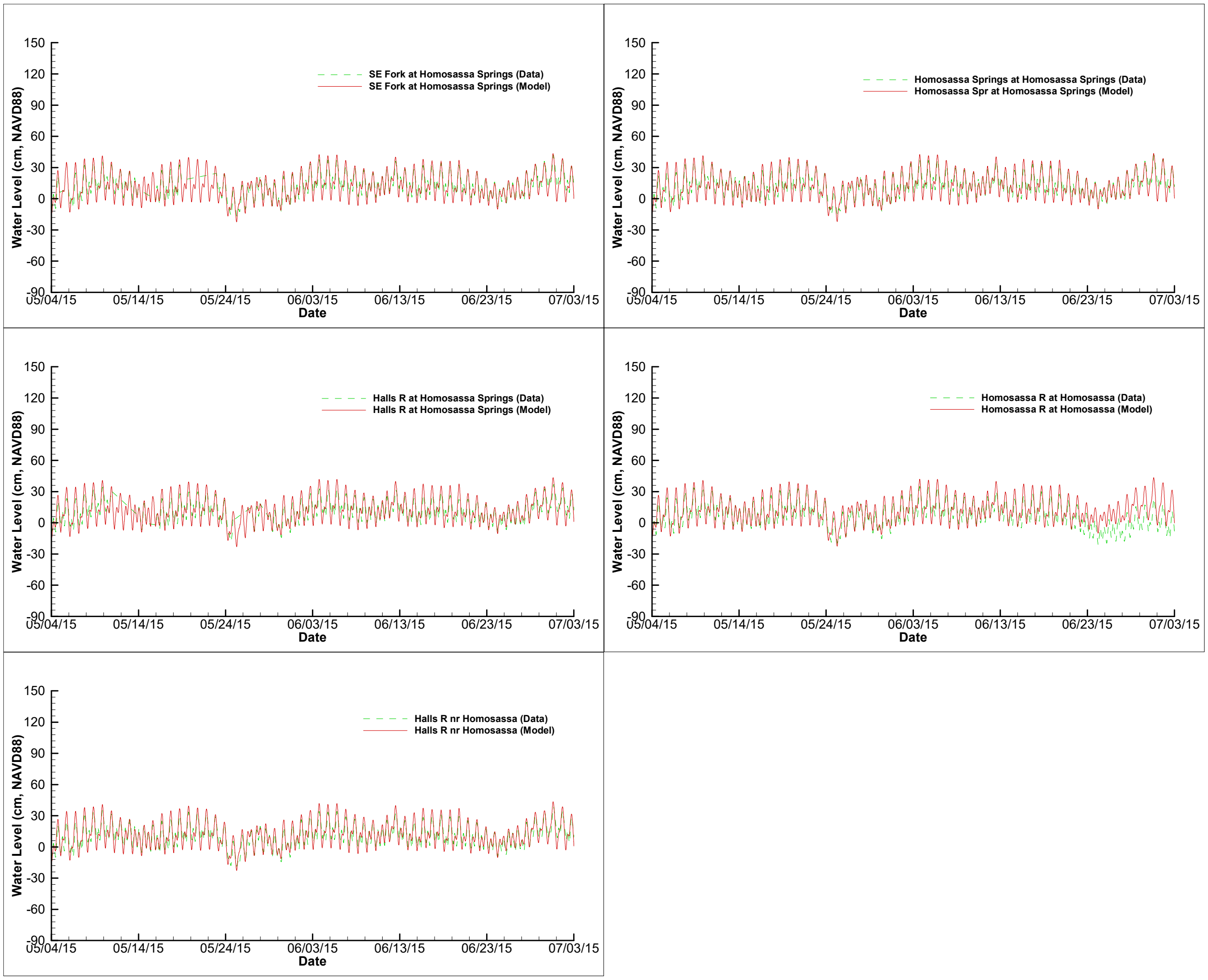

Figure D - 4. Comparisons of simulated (red lines) and measured (dashed green lines) water levels at SE Fork at Homosassa Spring (top left), Homosassa Springs at Homosassa Springs (top right), Halls River at Homosassa Springs (middle left), Halls River near Homosassa (bottom left), and Homosassa River at Homosassa (middle right) stations during 5/4/2015 – 7/3/2015.

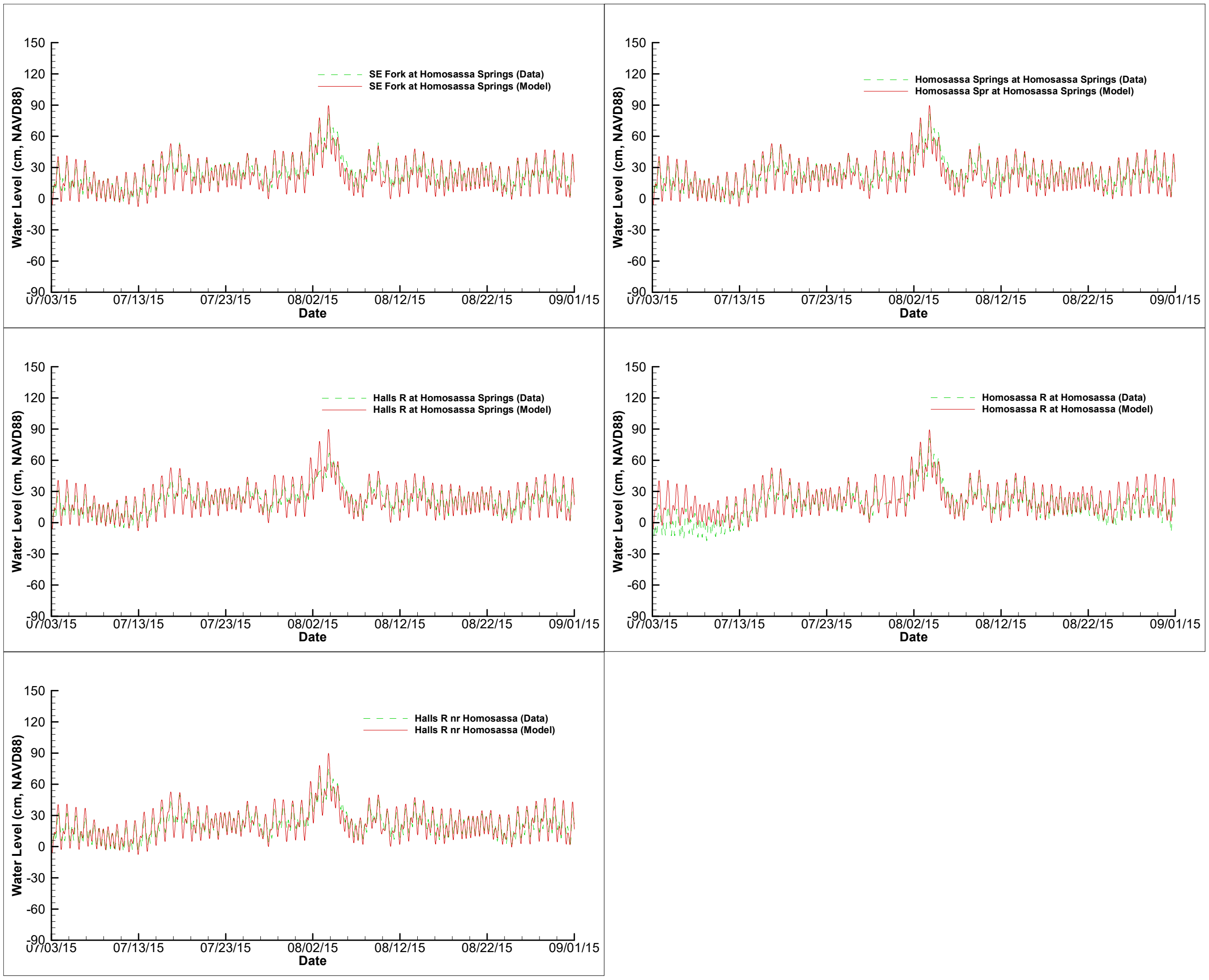

Figure D - 5. Comparisons of simulated (red lines) and measured (dashed green lines) water levels at SE Fork at Homosassa Spring (top left), Homosassa Springs at Homosassa Springs (top right), Halls River at Homosassa Springs (middle left), Halls River near Homosassa (bottom left), and Homosassa River at Homosassa (middle right) stations during 7/3/2015 – 9/1/2015.

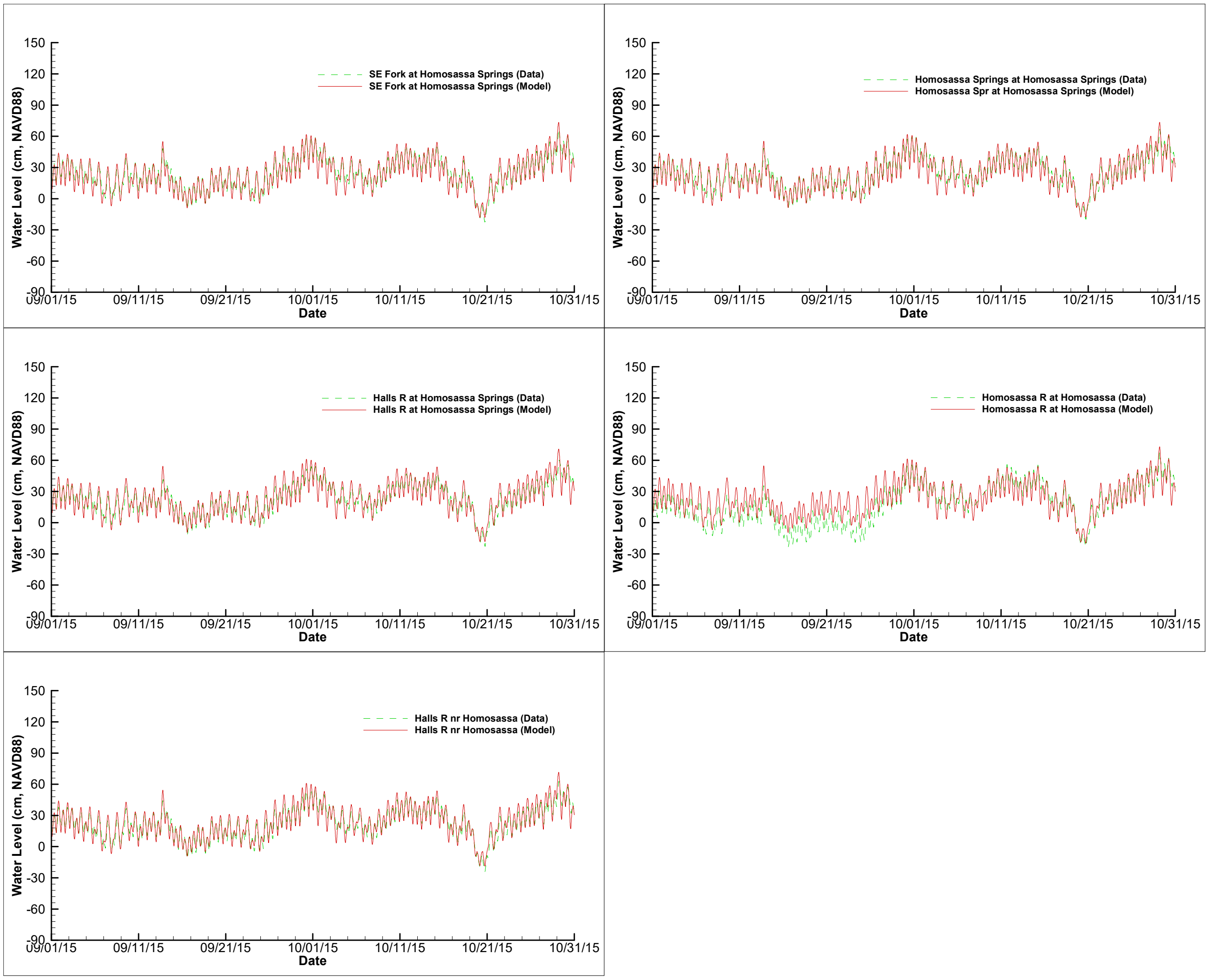

Figure D - 6. Comparisons of simulated (red lines) and measured (dashed green lines) water levels at SE Fork at Homosassa Spring (top left), Homosassa Springs at Homosassa Springs (top right), Halls River at Homosassa Springs (middle left), Halls River near Homosassa (bottom left), and Homosassa River at Homosassa (middle right) stations during 9/1/2015 - 10/31/2015.

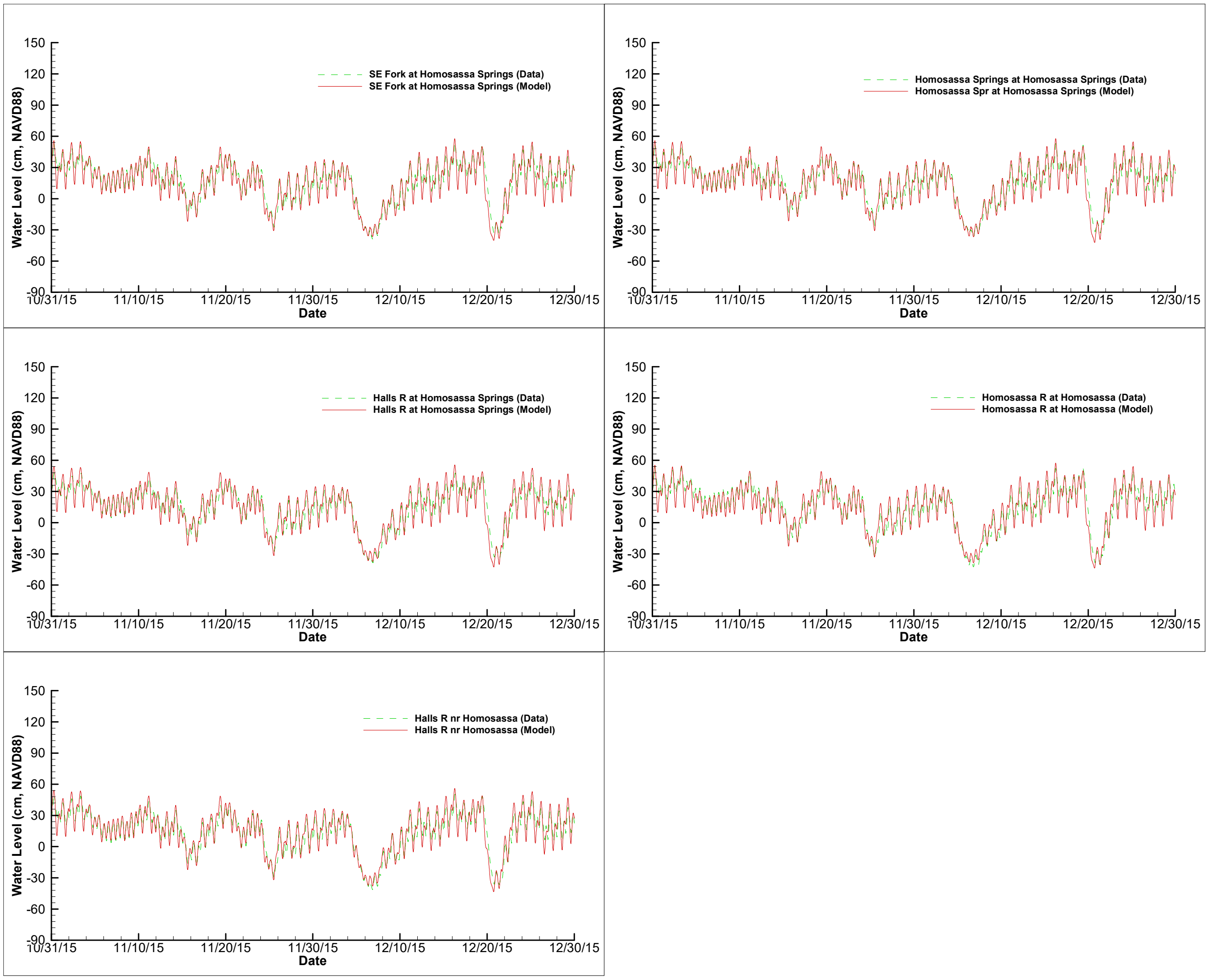

Figure D - 7. Comparisons of simulated (red lines) and measured (dashed green lines) water levels at SE Fork at Homosassa Spring (top left), Homosassa Springs at Homosassa Springs (top right), Halls River at Homosassa Springs (middle left), Halls River near Homosassa (bottom left), and Homosassa River at Homosassa (middle right) stations during 10/31/2015 – 12/30/2015.

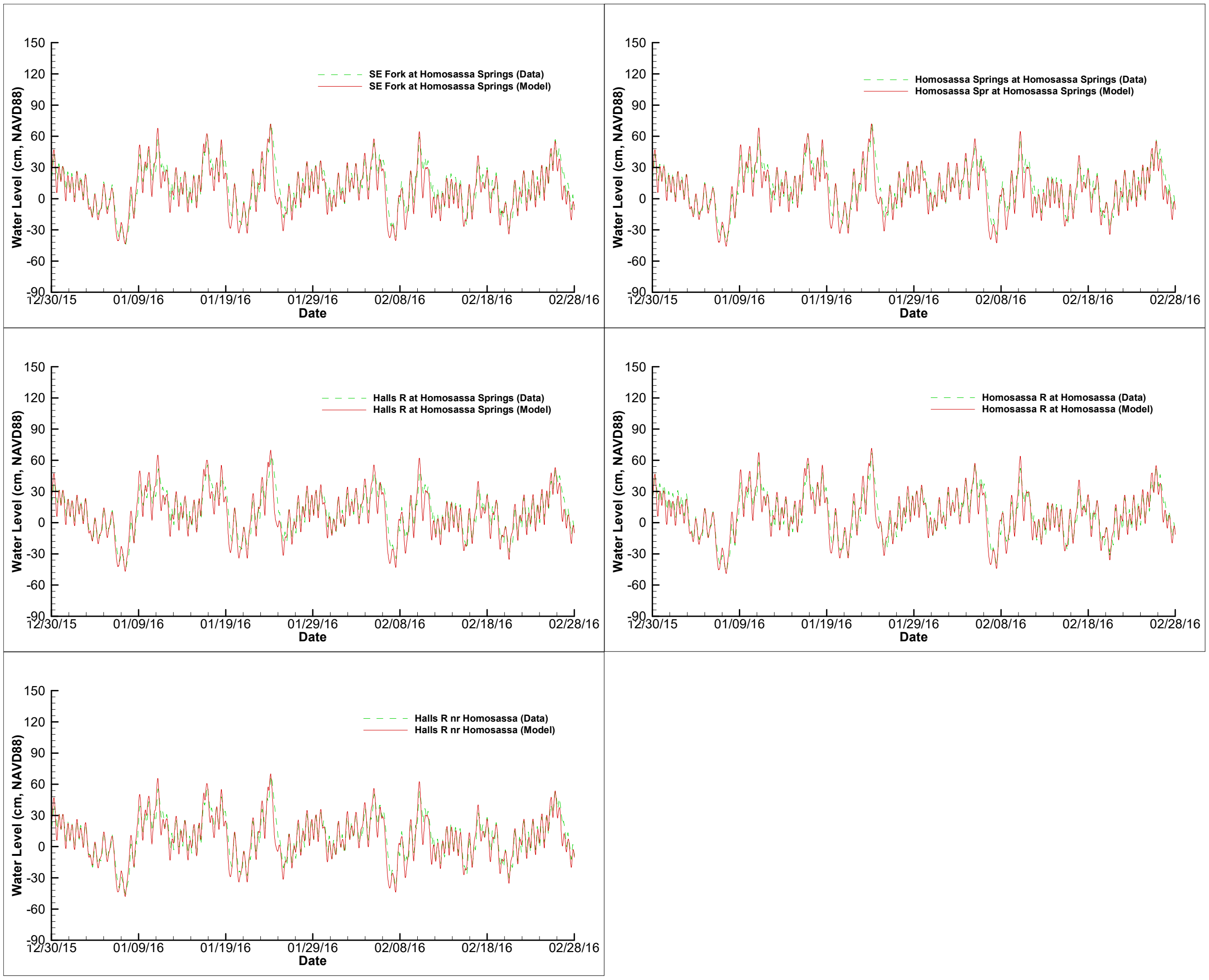

Figure D - 8. Comparisons of simulated (red lines) and measured (dashed green lines) water levels at SE Fork at Homosassa Spring (top left), Homosassa Springs at Homosassa Springs (top right), Halls River at Homosassa Springs (middle left), Halls River near Homosassa (bottom left), and Homosassa River at Homosassa (middle right) stations during 12/30/2015 – 2/28/2016.

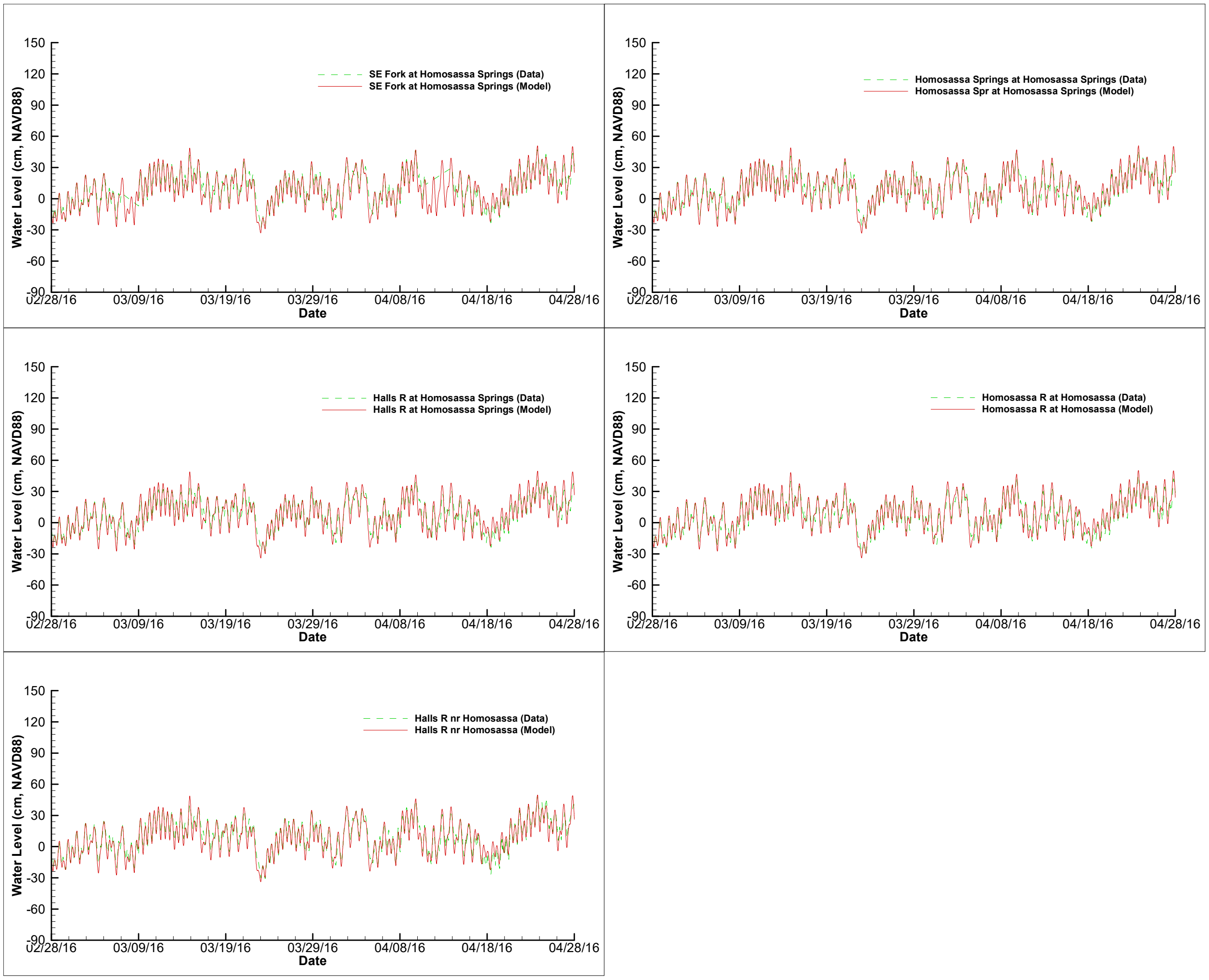

Figure D - 9. Comparisons of simulated (red lines) and measured (dashed green lines) water levels at SE Fork at Homosassa Spring (top left), Homosassa Springs at Homosassa Springs (top right), Halls River at Homosassa Springs (middle left), Halls River near Homosassa (bottom left), and Homosassa River at Homosassa (middle right) stations during 2/28/2016 – 4/28/2016.

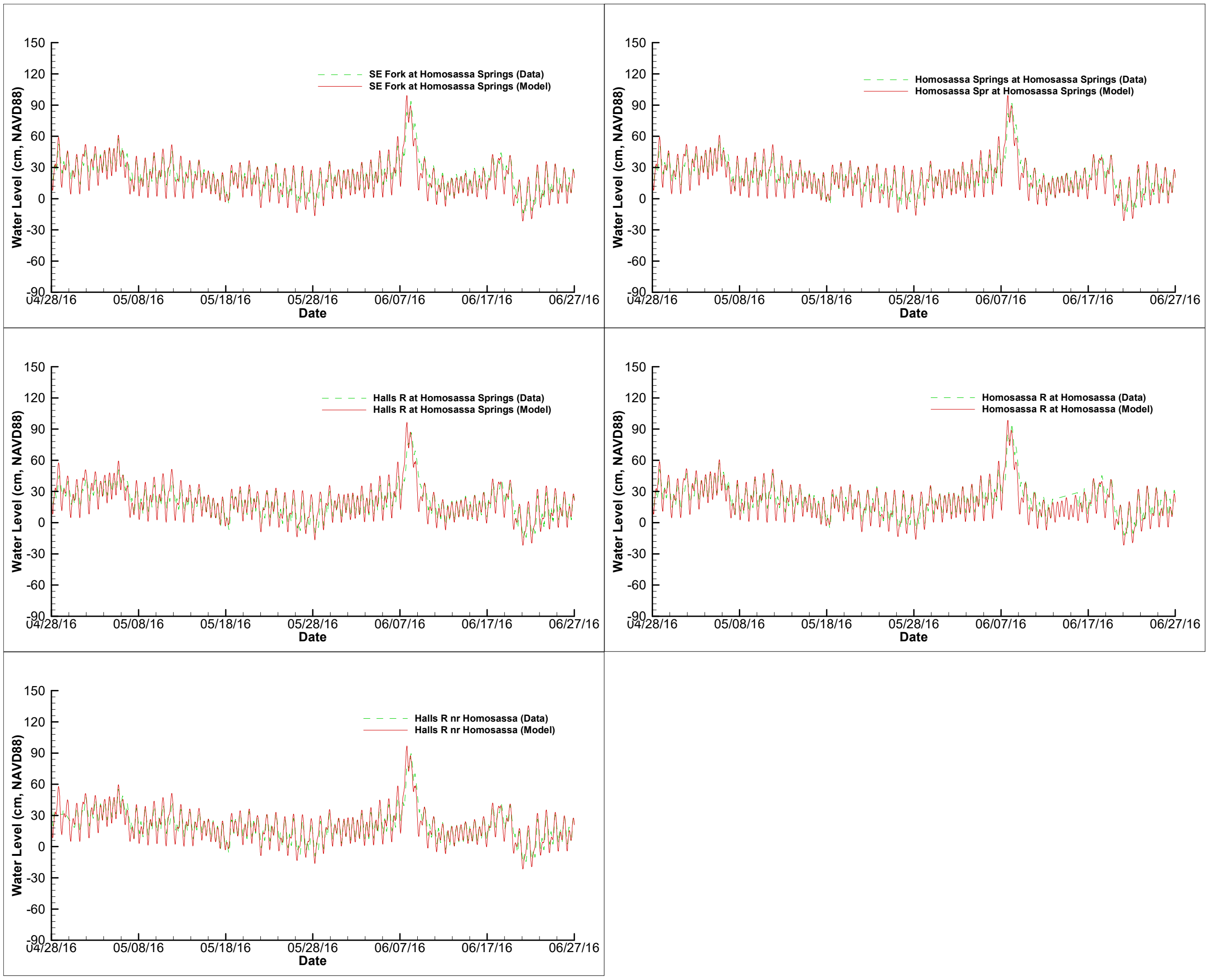

Figure D - 10. Comparisons of simulated (red lines) and measured (dashed green lines) water levels at SE Fork at Homosassa Spring (top left), Homosassa Springs at Homosassa Springs (top right), Halls River at Homosassa Springs (middle left), Halls River near Homosassa (bottom left), and Homosassa River at Homosassa (middle right) stations during 4/28/2016 – 6/27/2016.

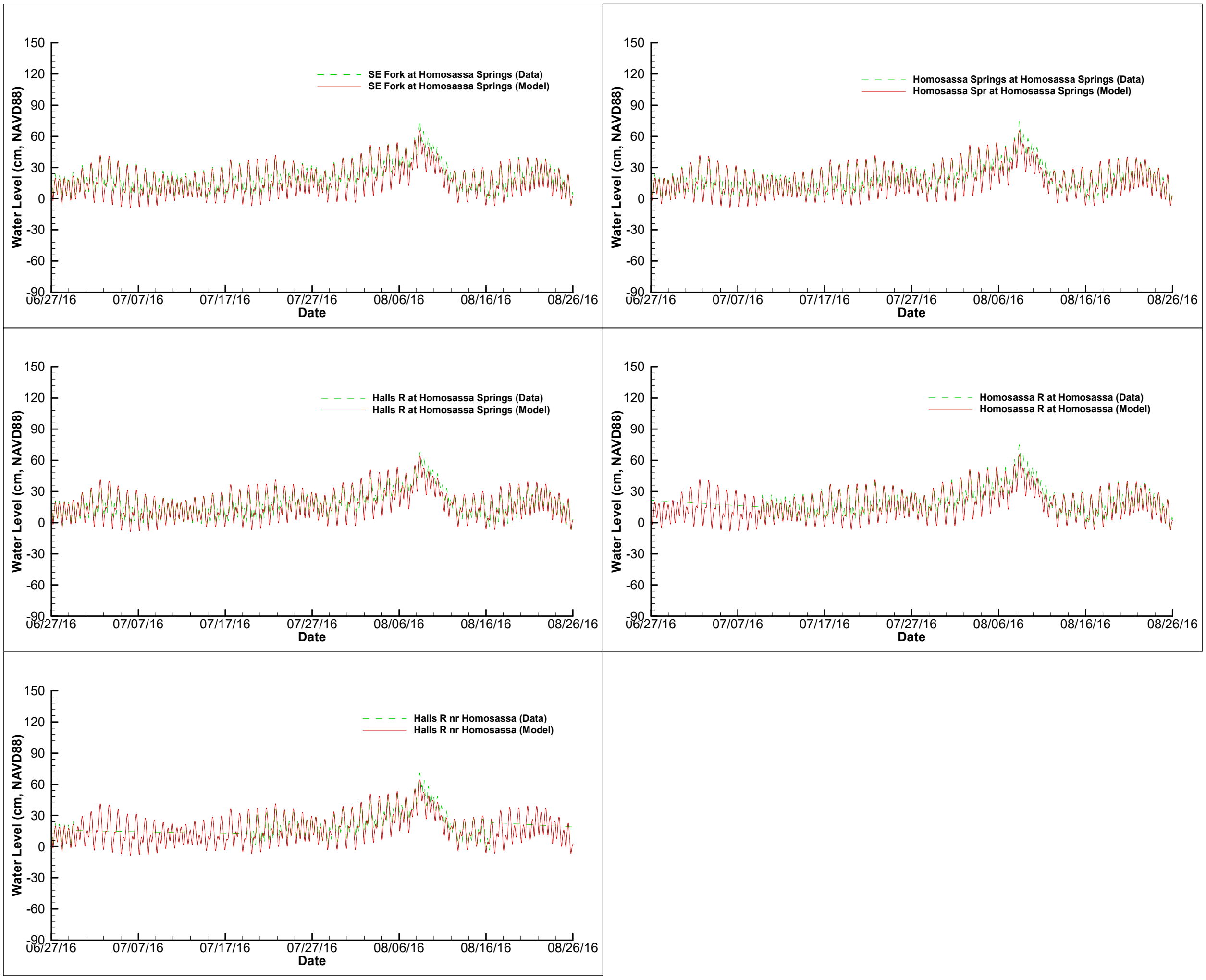

Figure D - 11. Comparisons of simulated (red lines) and measured (dashed green lines) water levels at SE Fork at Homosassa Spring (top left), Homosassa Springs at Homosassa Springs (top right), Halls River at Homosassa Springs (middle left), Halls River near Homosassa (bottom left), and Homosassa River at Homosassa (middle right) stations during 6/27/2016 – 8/26/2016.

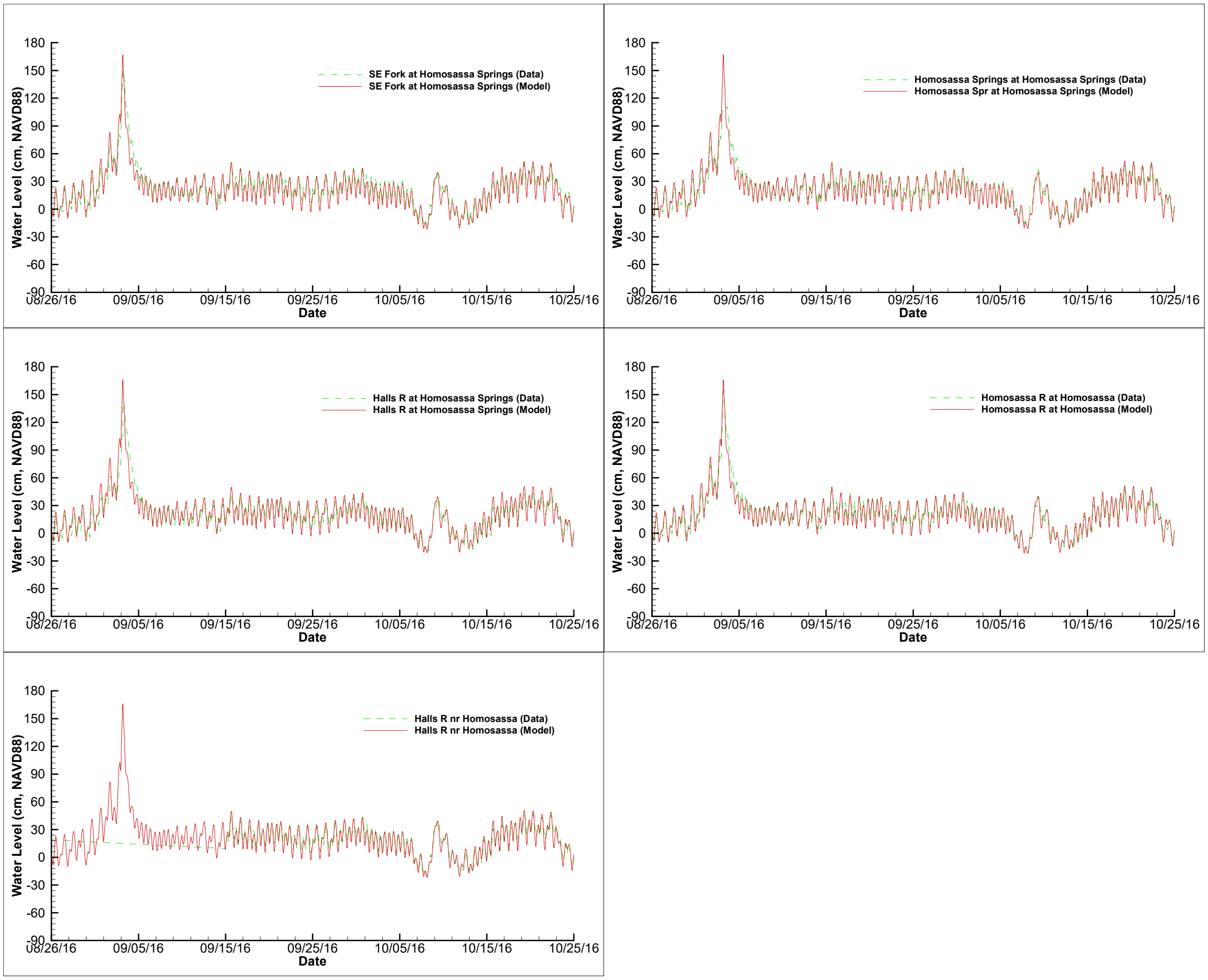

Figure D - 12. Comparisons of simulated (red lines) and measured (dashed green lines) water levels at SE Fork at Homosassa Spring (top left), Homosassa Springs at Homosassa Springs (top right), Halls River at Homosassa Springs (middle left), Halls River near Homosassa (bottom left), and Homosassa River at Homosassa (middle right) stations during 8/26/2016 – 10/25/2016.

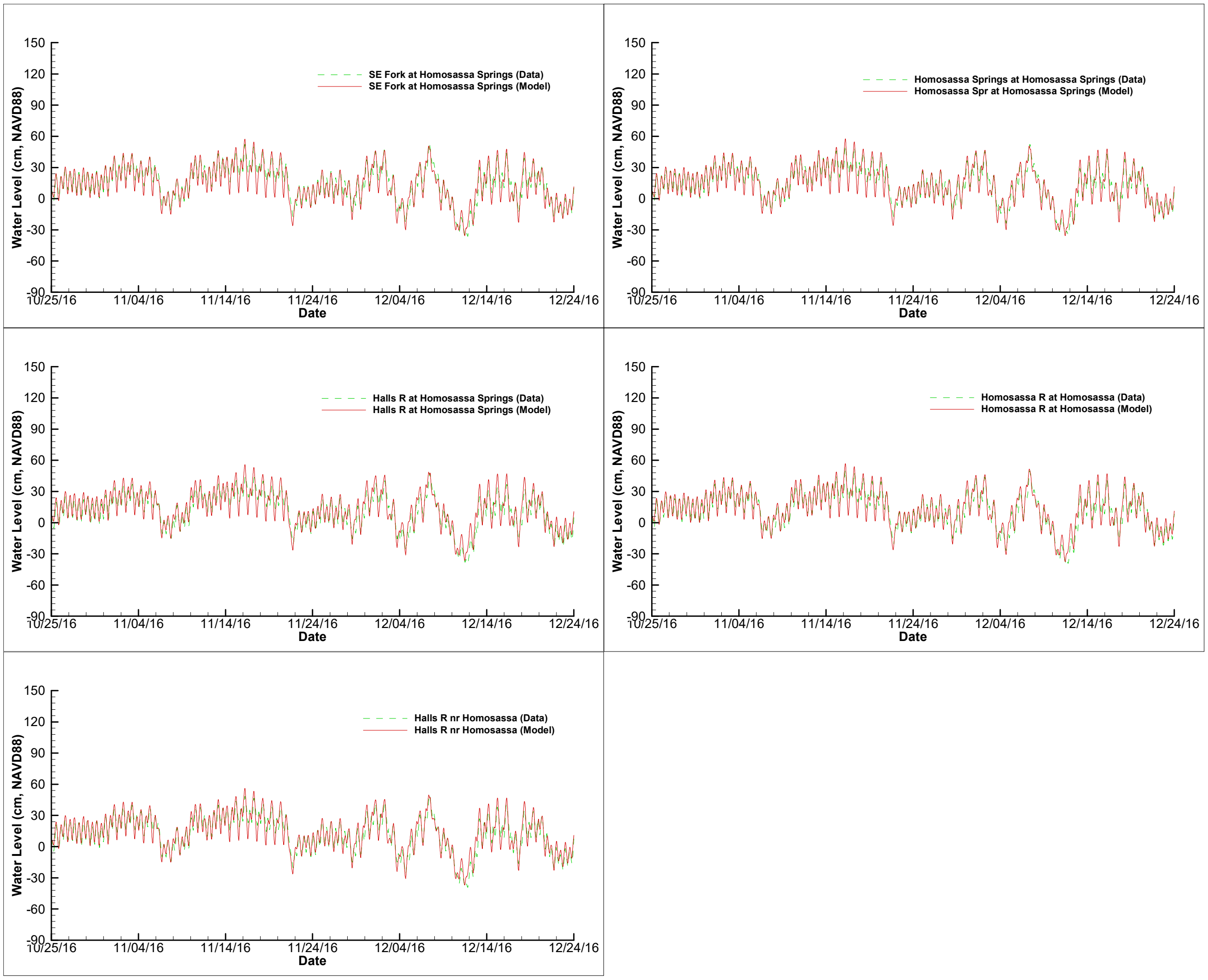

Figure D - 13. Comparisons of simulated (red lines) and measured (dashed green lines) water levels at SE Fork at Homosassa Spring (top left), Homosassa Springs at Homosassa Springs (top right), Halls River at Homosassa Springs (middle left), Halls River near Homosassa (bottom left), and Homosassa River at Homosassa (middle right) stations during 10/25/2016 – 12/24/2016.

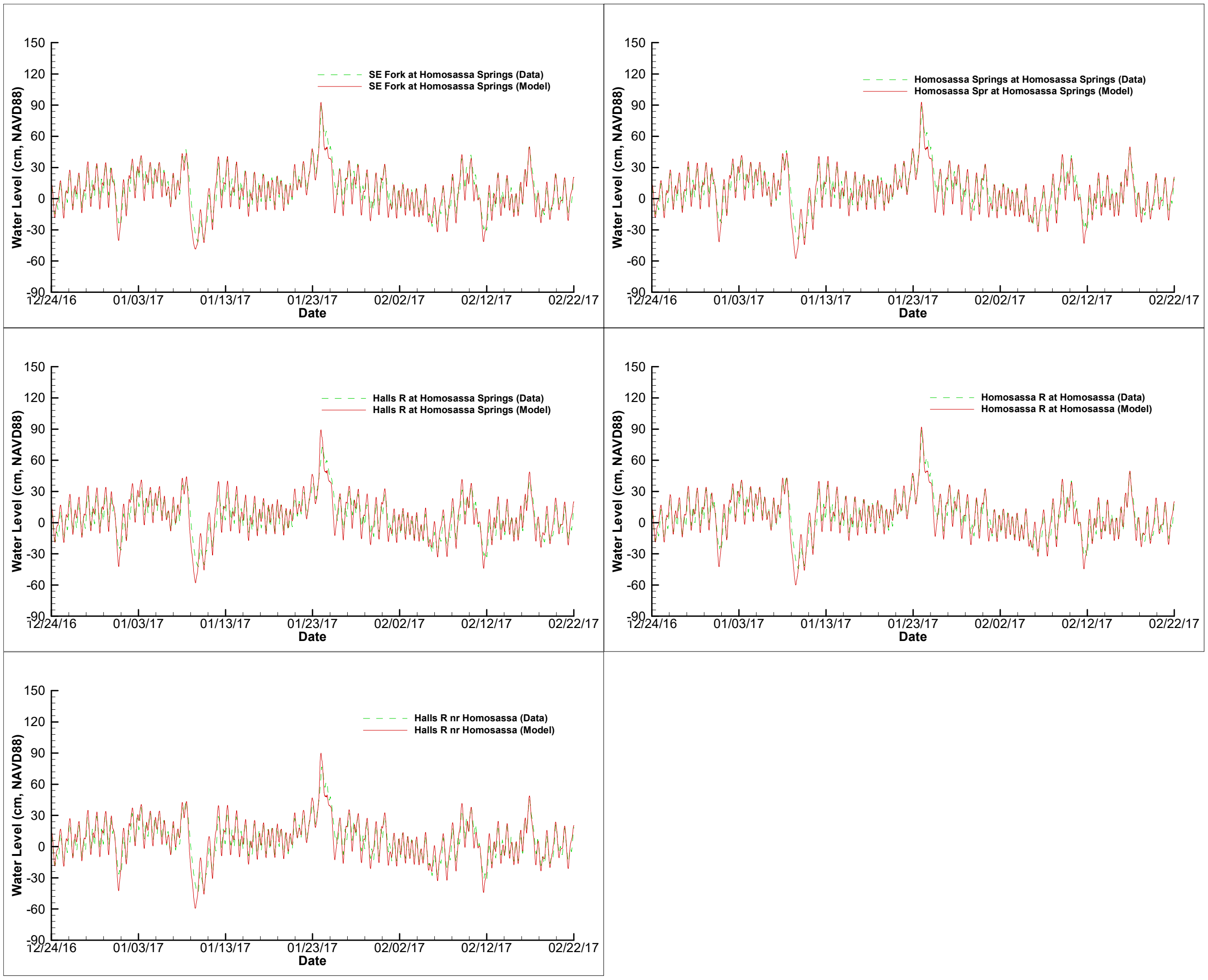

Figure D - 14. Comparisons of simulated (red lines) and measured (dashed green lines) water levels at SE Fork at Homosassa Spring (top left), Homosassa Springs at Homosassa Springs (top right), Halls River at Homosassa Springs (middle left), Halls River near Homosassa (bottom left), and Homosassa River at Homosassa (middle right) stations during 12/24/2016 – 2/22/2017.

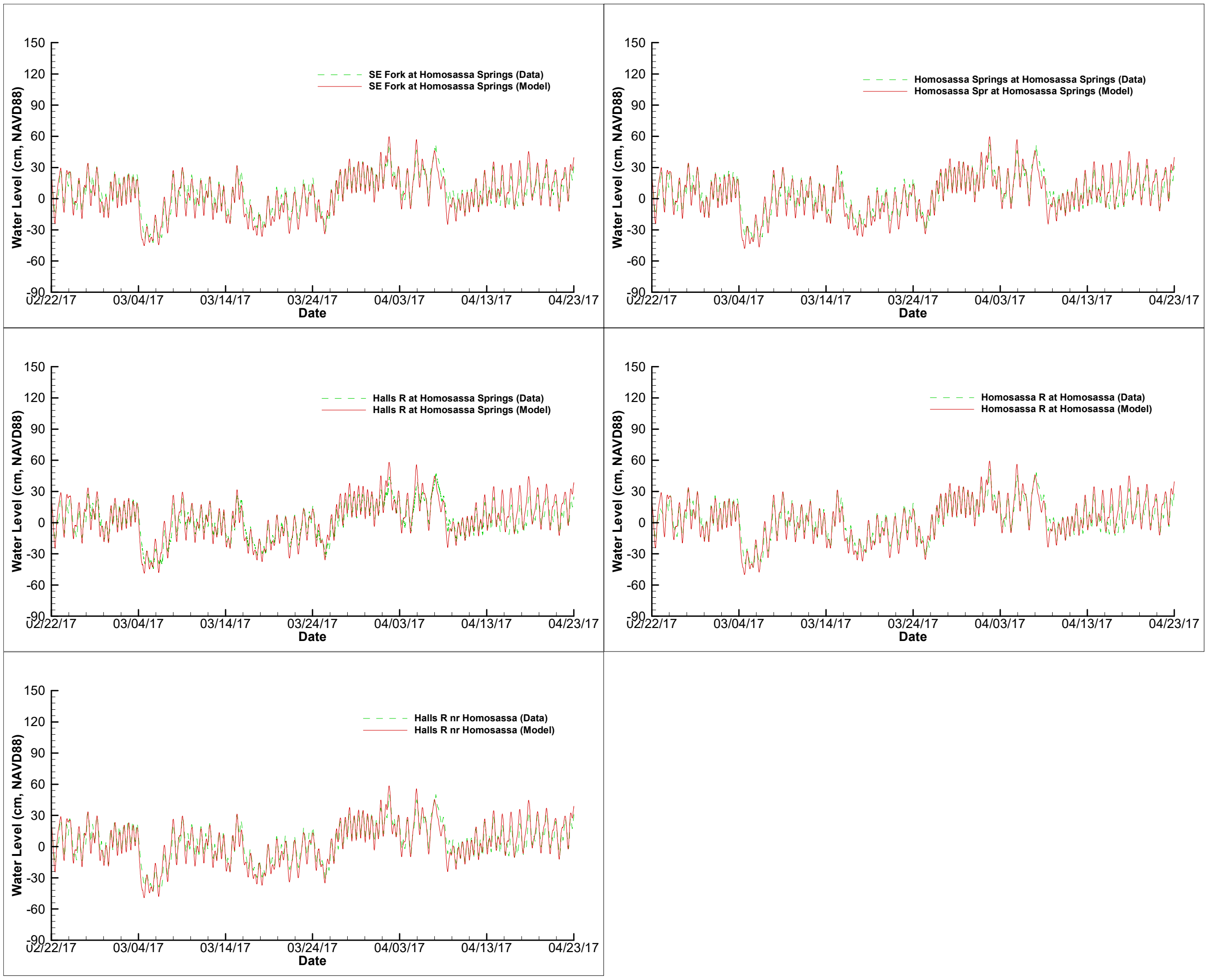

Figure D - 15. Comparisons of simulated (red lines) and measured (dashed green lines) water levels at SE Fork at Homosassa Spring (top left), Homosassa Springs at Homosassa Springs (top right), Halls River at Homosassa Springs (middle left), Halls River near Homosassa (bottom left), and Homosassa River at Homosassa (middle right) stations during 2/22/2017 - 4/23/2017.

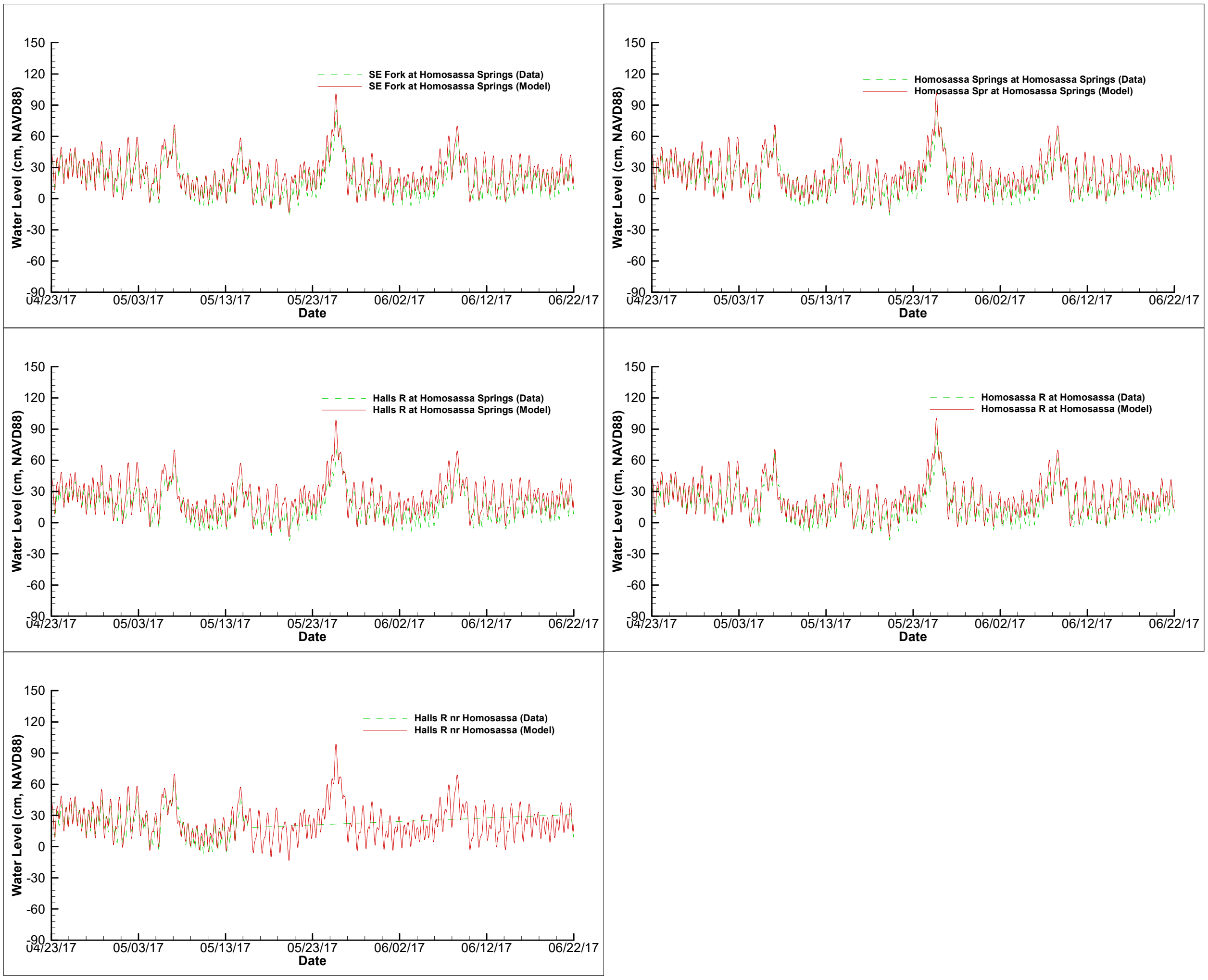

Figure D - 16. Comparisons of simulated (red lines) and measured (dashed green lines) water levels at SE Fork at Homosassa Spring (top left), Homosassa Springs at Homosassa Springs (top right), Halls River at Homosassa Springs (middle left), Halls River near Homosassa (bottom left), and Homosassa River at Homosassa (middle right) stations during 4/23/2017 – 6/22/2017.

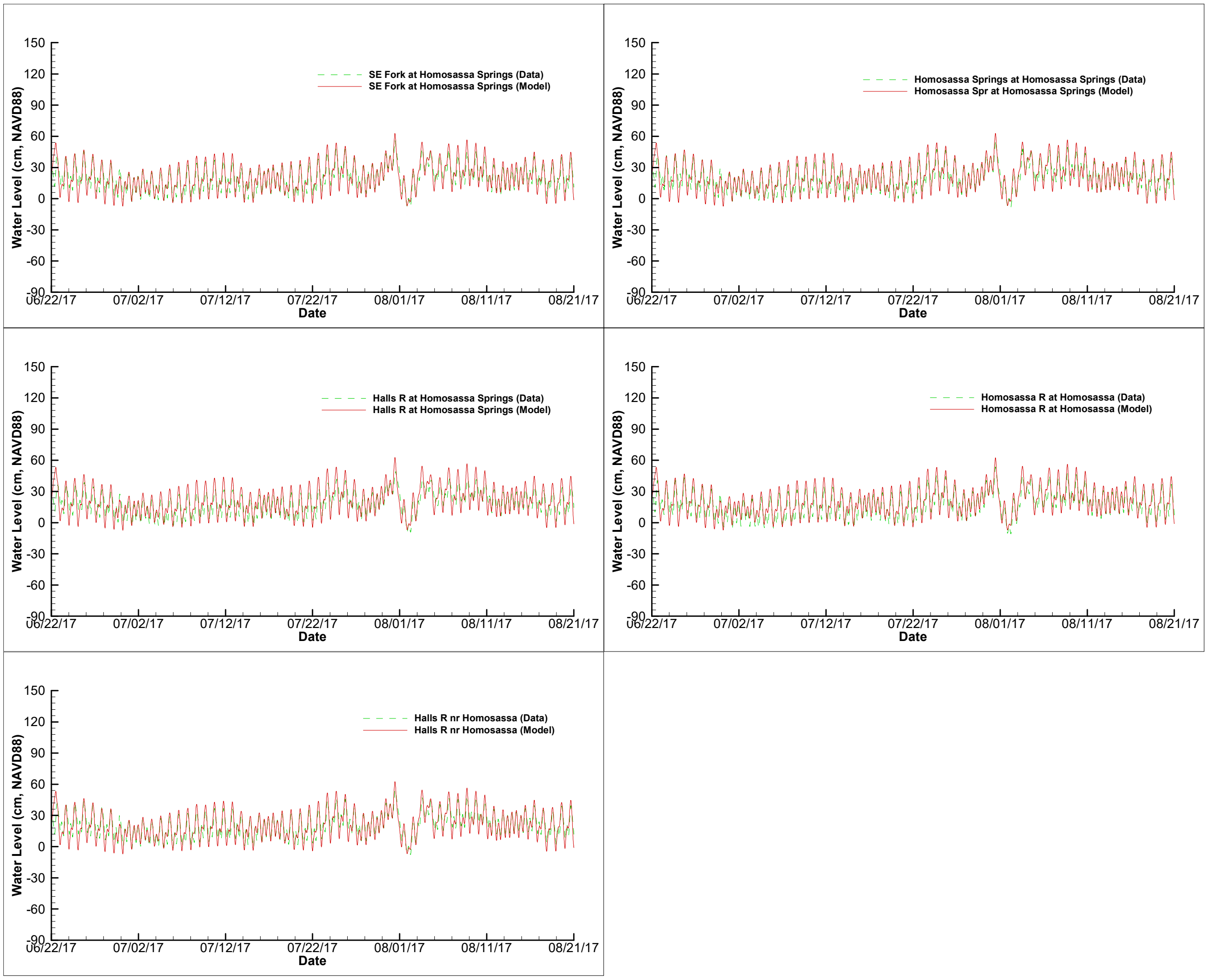

Figure D - 17. Comparisons of simulated (red lines) and measured (dashed green lines) water levels at SE Fork at Homosassa Spring (top left), Homosassa Springs at Homosassa Springs (top right), Halls River at Homosassa Springs (middle left), Halls River near Homosassa (bottom left), and Homosassa River at Homosassa (middle right) stations during 6/22/2017 – 8/21/2017.

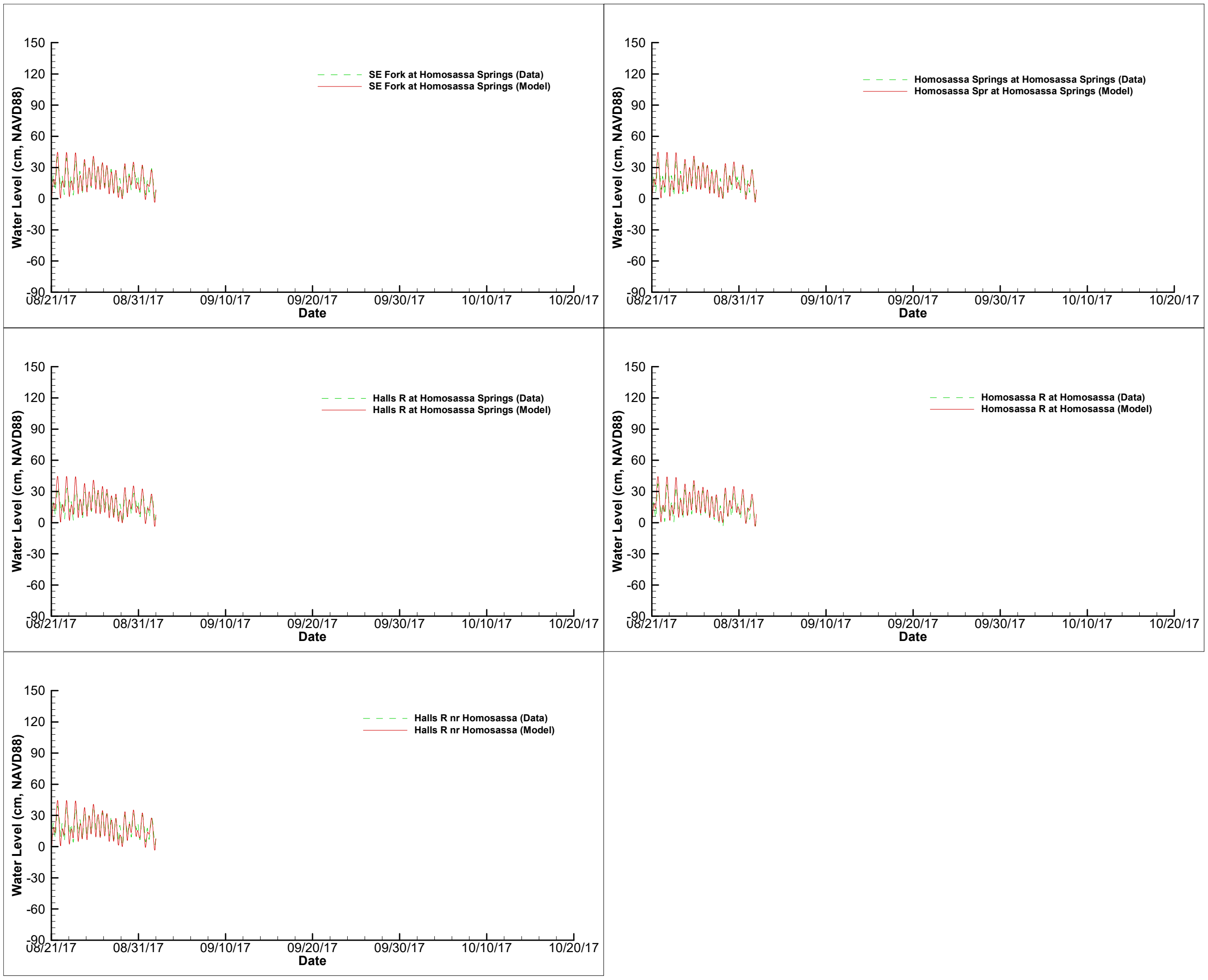

Figure D - 18. Comparisons of simulated (red lines) and measured (dashed green lines) water levels at SE Fork at Homosassa Spring (top left), Homosassa Springs at Homosassa Springs (top right), Halls River at Homosassa Springs (middle left), Halls River near Homosassa (bottom left), and Homosassa River at Homosassa (middle right) stations during 8/21/2017 – 10/20/2017.

Appendix E. Simulated and Measured Salinities

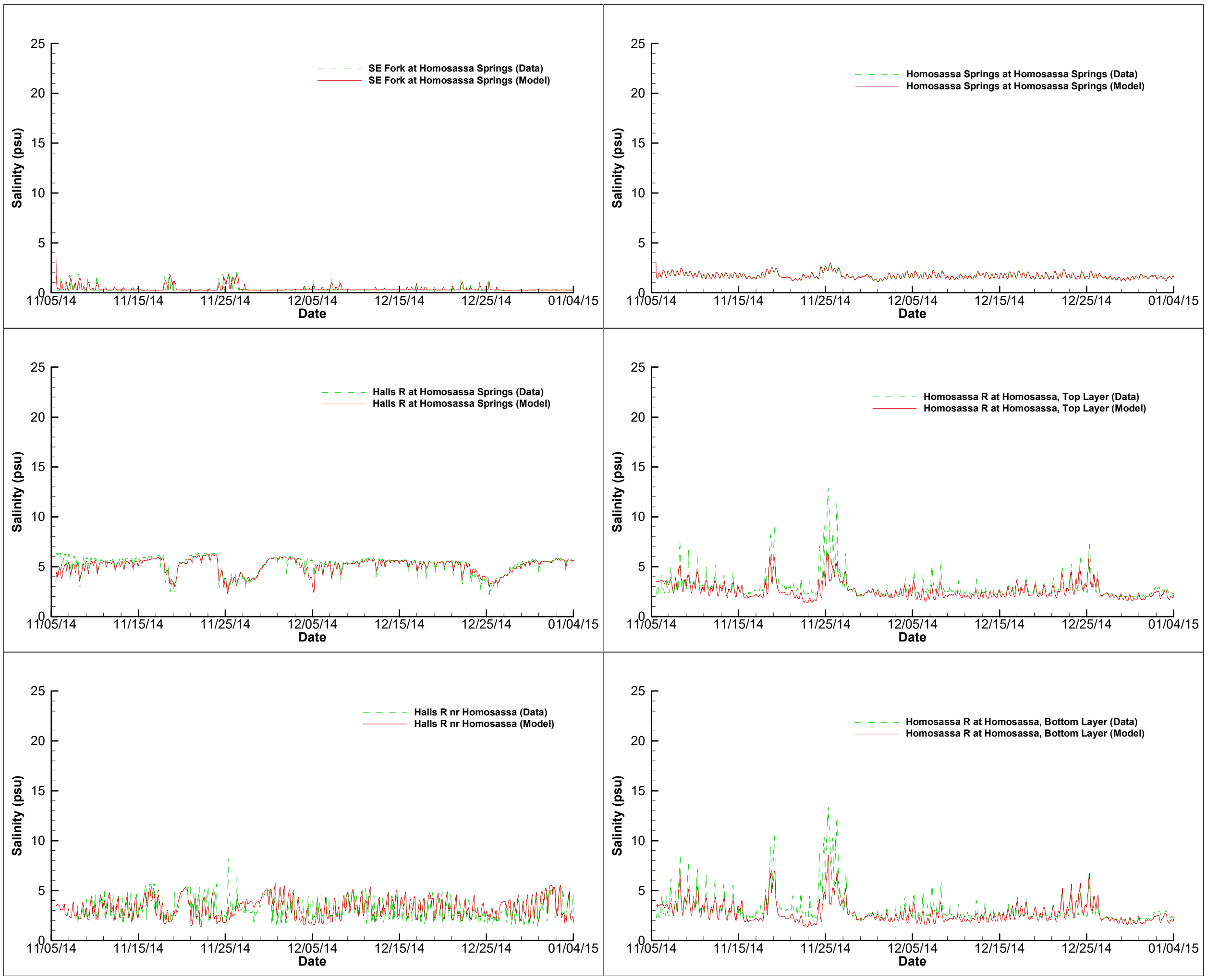

Figure E - 1. Comparisons of simulated (red lines) and measured (dashed green lines) salinities at SE Fork at Homosassa Spring (top left), Homosassa Springs at Homosassa Springs (top right), Halls River at Homosassa Springs (middle left), Halls River near Homosassa (bottom left), and Homosassa River at Homosassa (middle right for the top layer and bottom right for the bottom layer) stations during 11/5/2014 – 1/4/2015.

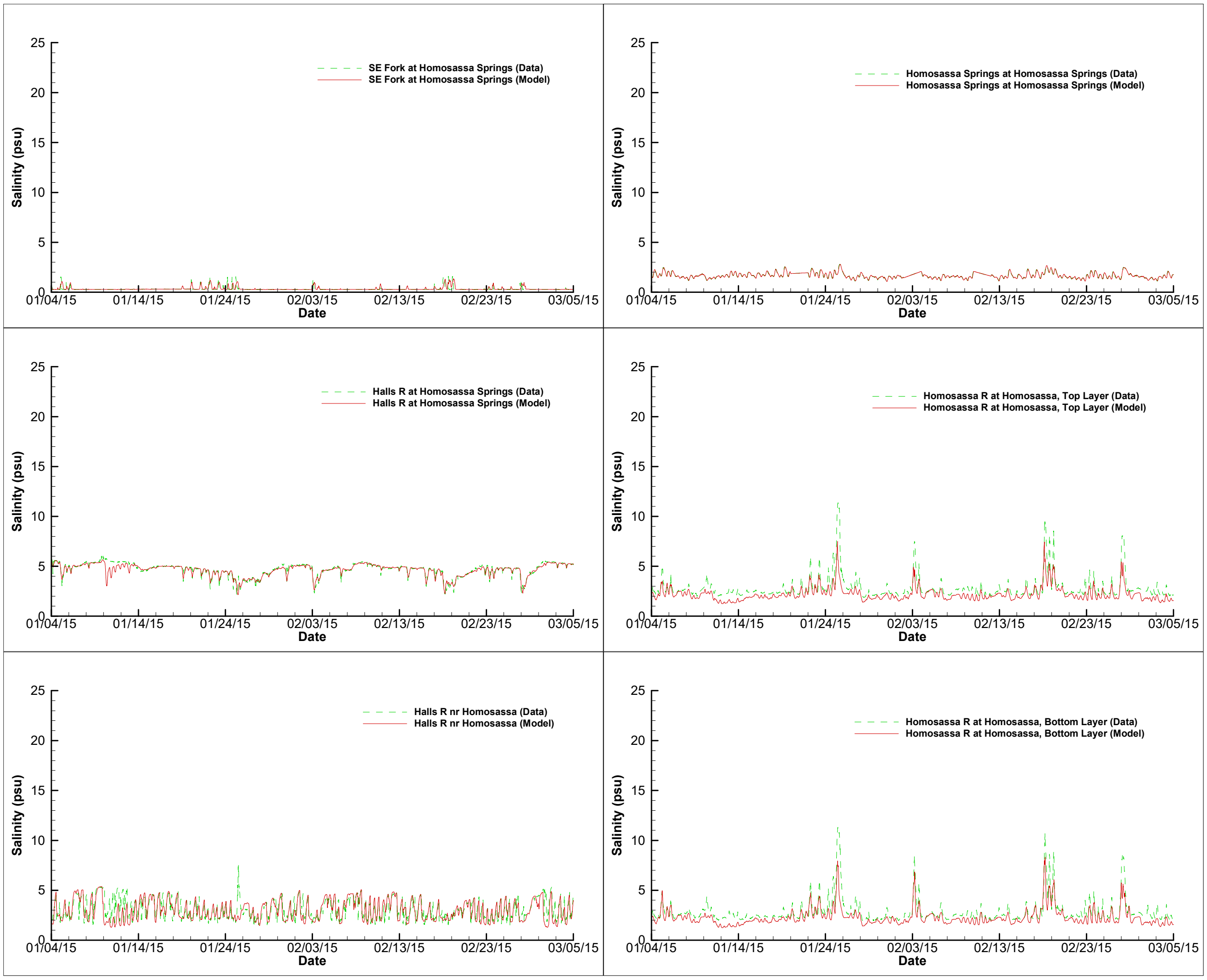

Figure E - 2. Comparisons of simulated (red lines) and measured (dashed green lines) salinities at SE Fork at Homosassa Spring (top left), Homosassa Springs at Homosassa Springs (top right), Halls River at Homosassa Springs (middle left), Halls River near Homosassa (bottom left), and Homosassa River at Homosassa (middle right for the top layer and bottom right for the bottom layer) stations during 1/4/2015 – 3/5/2015.

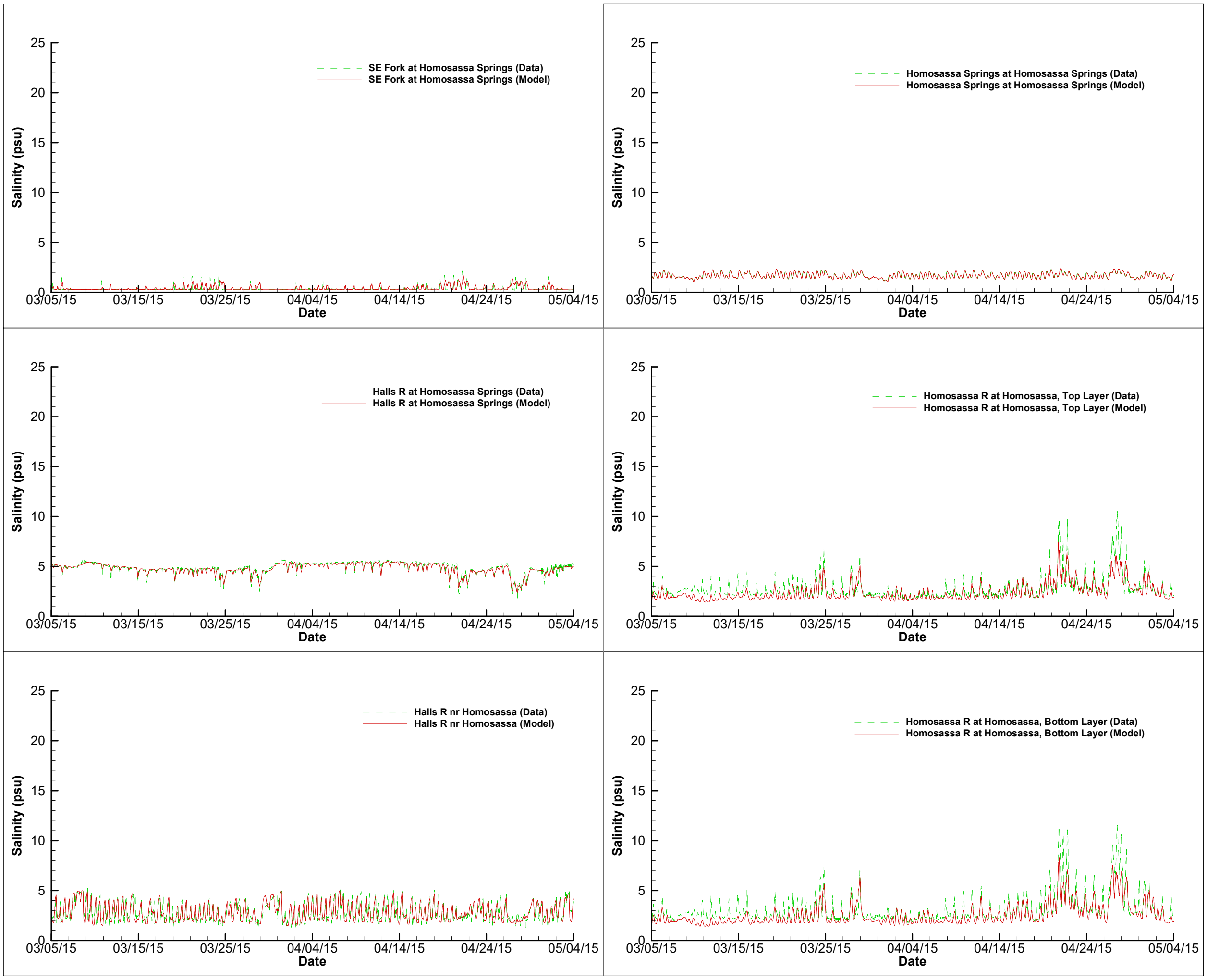

Figure E - 3. Comparisons of simulated (red lines) and measured (dashed green lines) salinities at SE Fork at Homosassa Spring (top left), Homosassa Springs at Homosassa Springs (top right), Halls River at Homosassa Springs (middle left), Halls River near Homosassa (bottom left), and Homosassa River at Homosassa (middle right for the top layer and bottom right for the bottom layer) stations during 3/5/2015 – 5/4/2015.

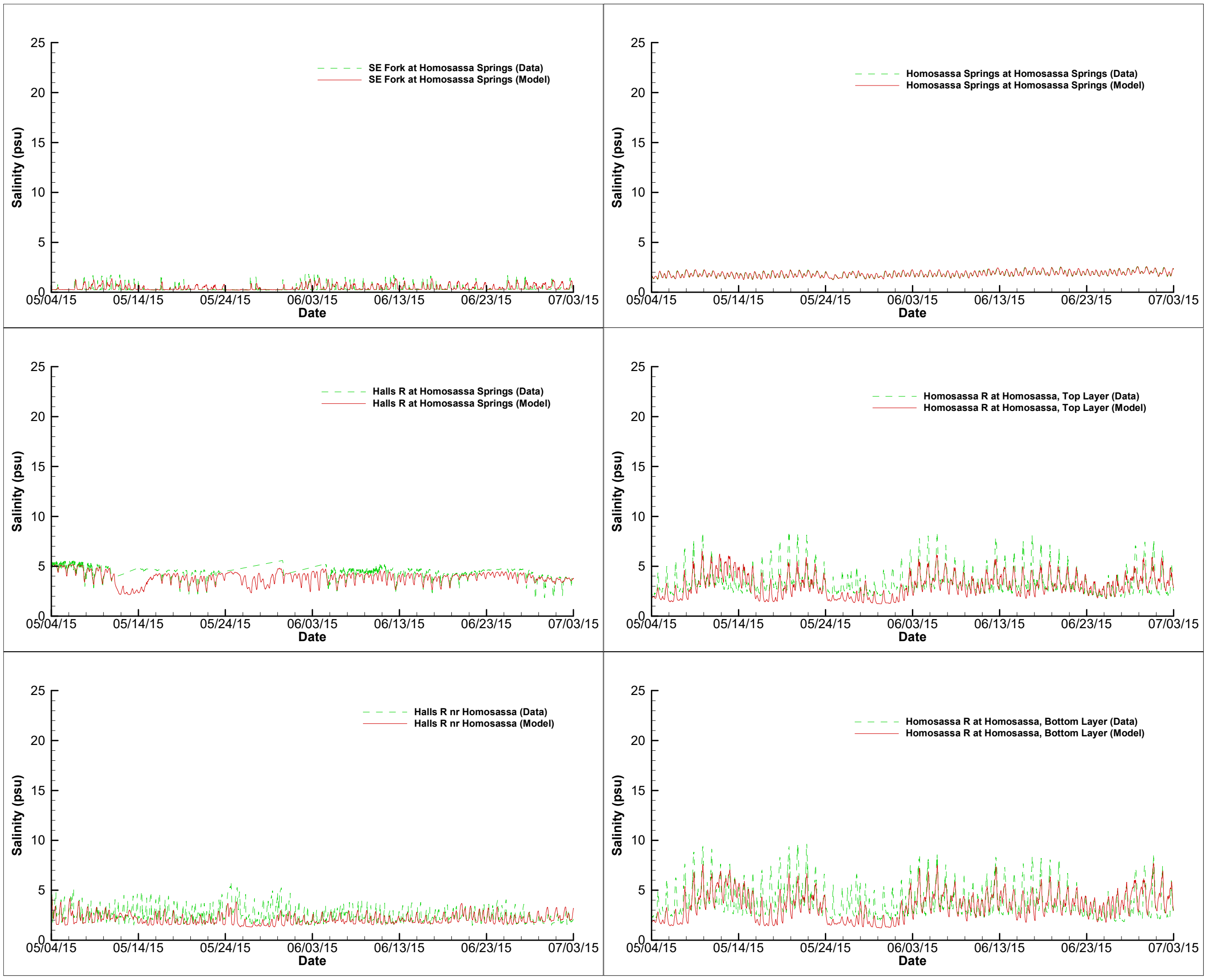

Figure E - 4. Comparisons of simulated (red lines) and measured (dashed green lines) salinities at SE Fork at Homosassa Spring (top left), Homosassa Springs at Homosassa Springs (top right), Halls River at Homosassa Springs (middle left), Halls River near Homosassa (bottom left), and Homosassa River at Homosassa (middle right for the top layer and bottom right for the bottom layer) stations during 5/4/2015 – 7/3/2015.

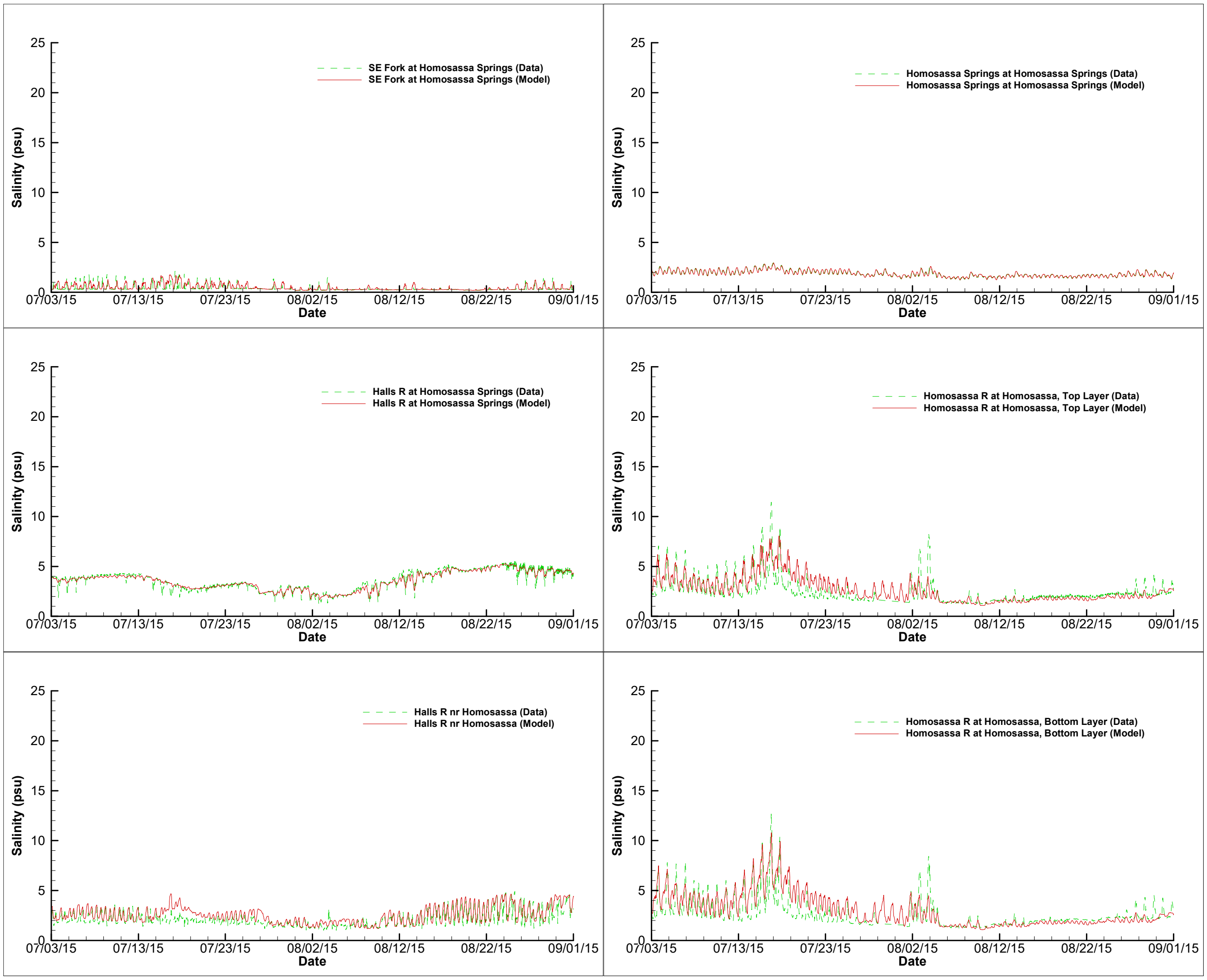

Figure E - 5. Comparisons of simulated (red lines) and measured (dashed green lines) salinities at SE Fork at Homosassa Spring (top left), Homosassa Springs at Homosassa Springs (top right), Halls River at Homosassa Springs (middle left), Halls River near Homosassa (bottom left), and Homosassa River at Homosassa (middle right for the top layer and bottom right for the bottom layer) stations during 7/3/2015 – 9/1/2015.

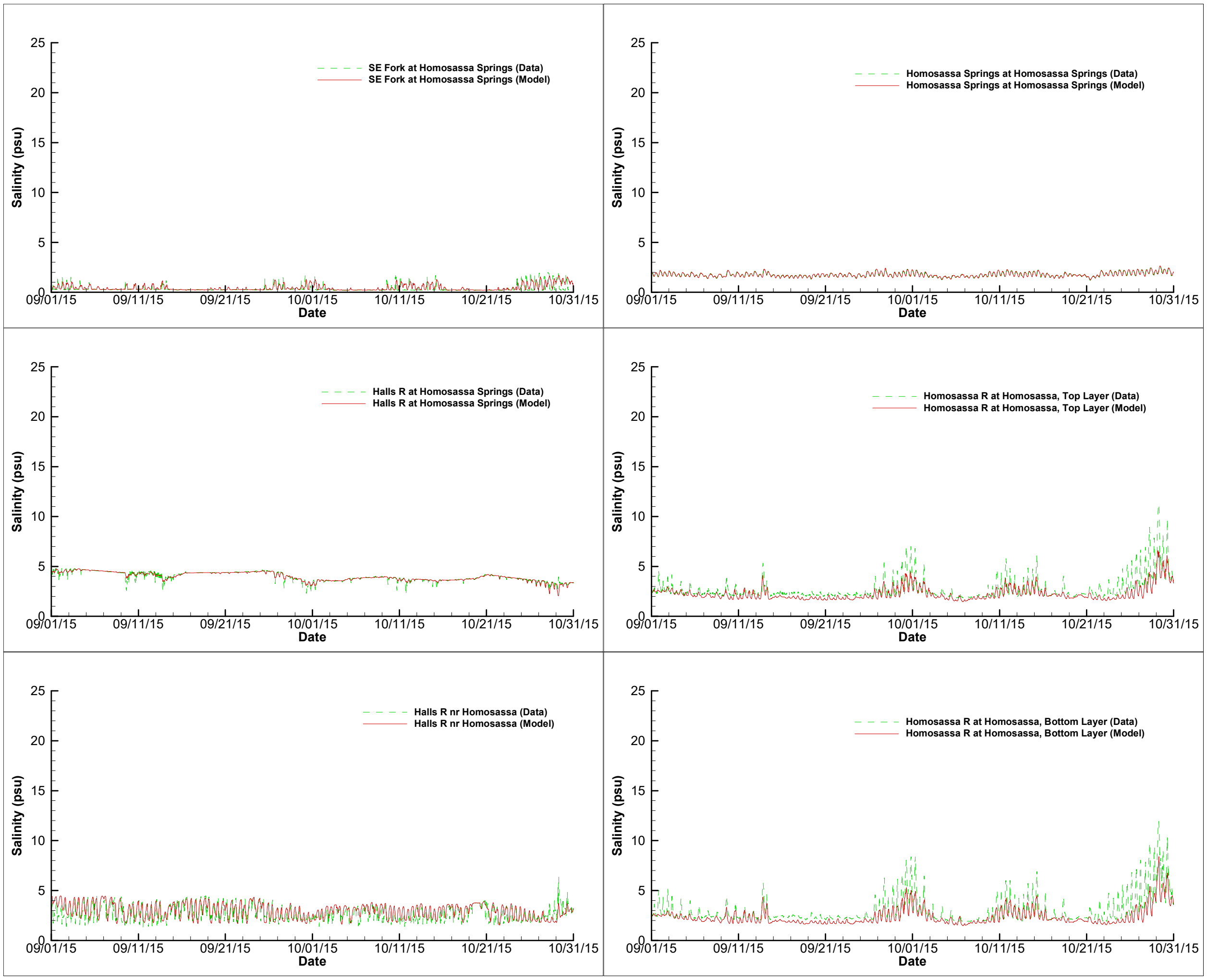

Figure E - 6. Comparisons of simulated (red lines) and measured (dashed green lines) salinities at SE Fork at Homosassa Spring (top left), Homosassa Springs at Homosassa Springs (top right), Halls River at Homosassa Springs (middle left), Halls River near Homosassa (bottom left), and Homosassa River at Homosassa (middle right for the top layer and bottom right for the bottom layer) stations during 9/1/2015 – 10/31/2015.

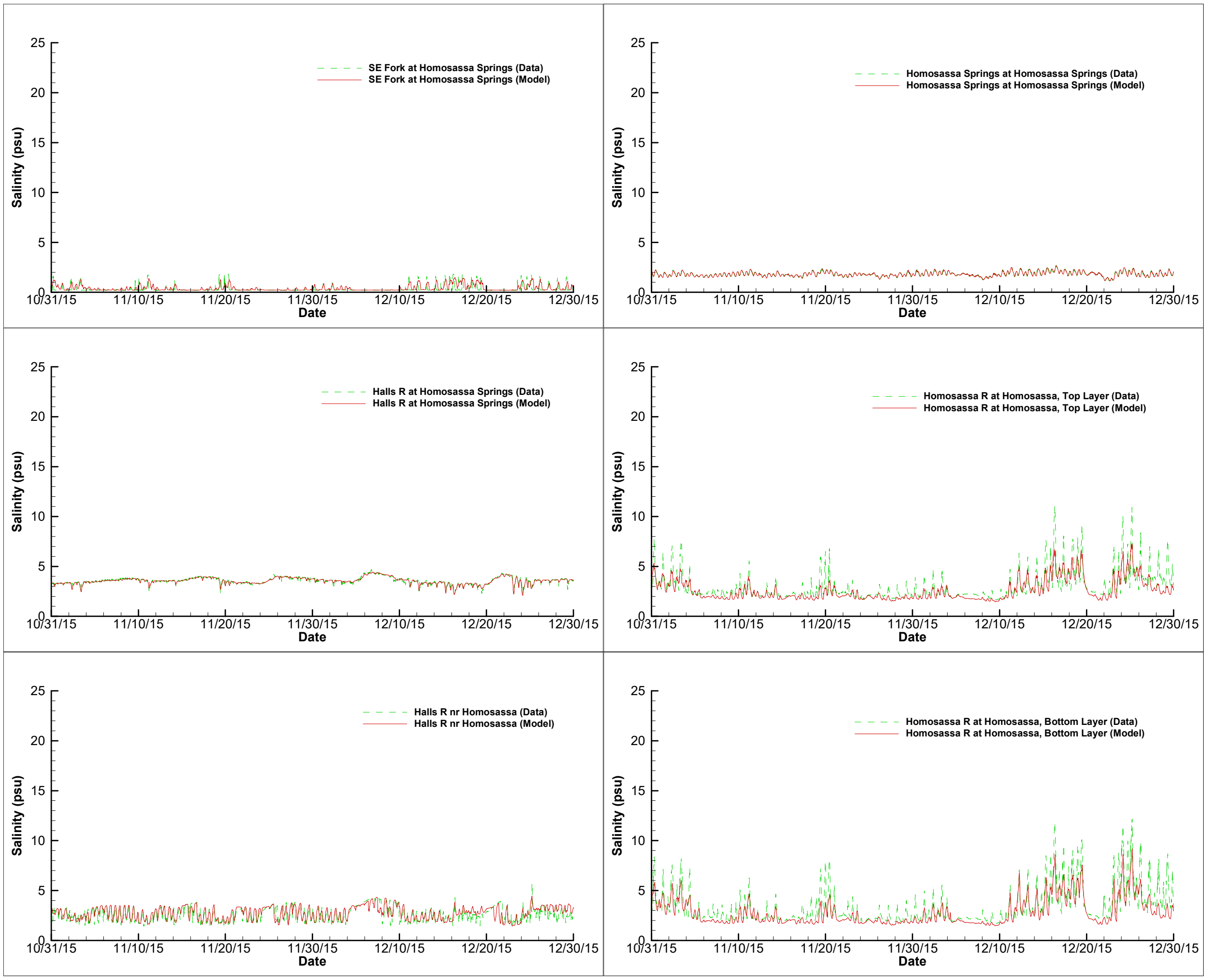

Figure E - 7. Comparisons of simulated (red lines) and measured (dashed green lines) salinities at SE Fork at Homosassa Spring (top left), Homosassa Springs at Homosassa Springs (top right), Halls River at Homosassa Springs (middle left), Halls River near Homosassa (bottom left), and Homosassa River at Homosassa (middle right for the top layer and bottom right for the bottom layer) stations during 10/31/2015 – 12/30/2015.

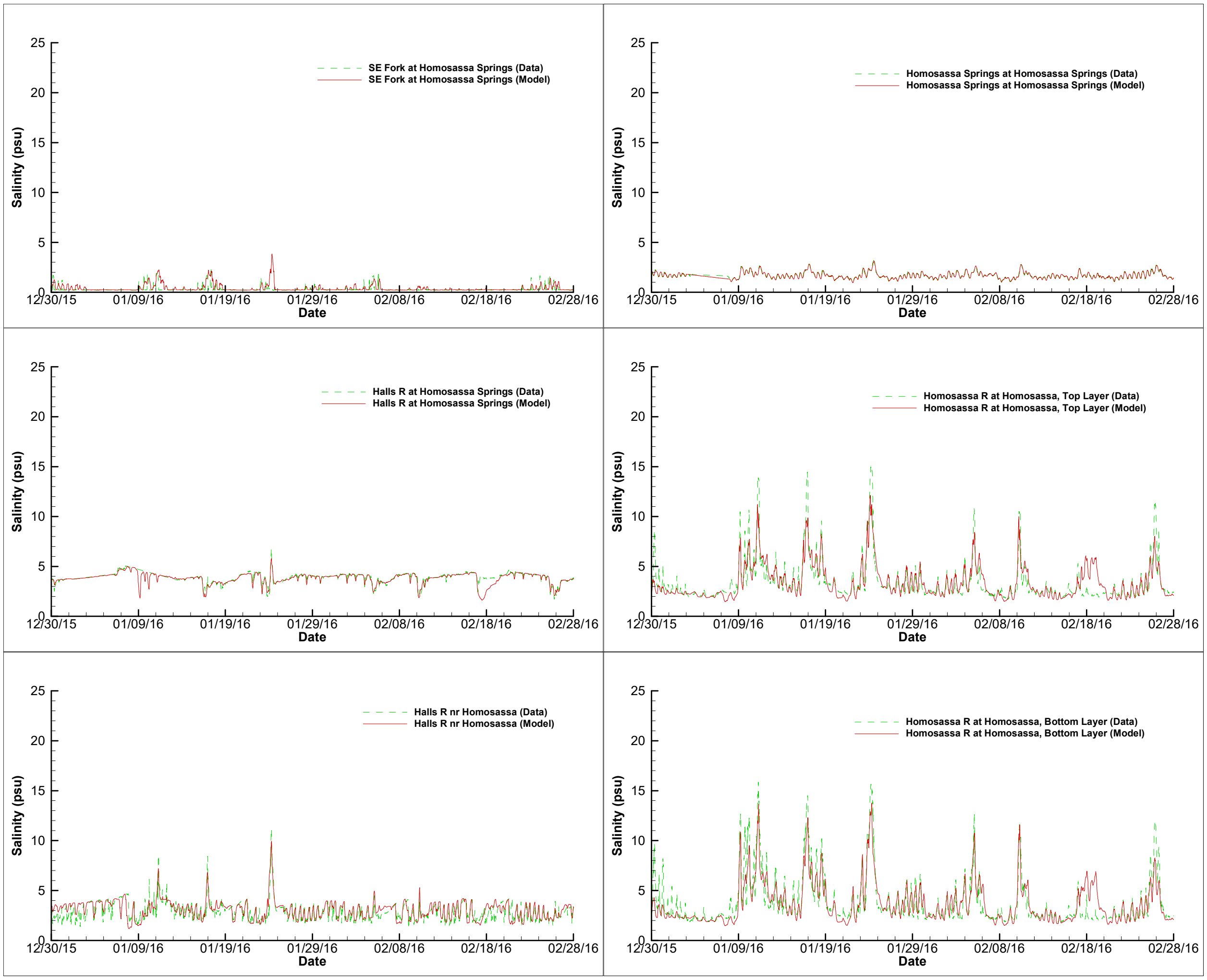

Figure E - 8. Comparisons of simulated (red lines) and measured (dashed green lines) salinities at SE Fork at Homosassa Spring (top left), Homosassa Springs at Homosassa Springs (top right), Halls River at Homosassa Springs (middle left), Halls River near Homosassa (bottom left), and Homosassa River at Homosassa (middle right for the top layer and bottom right for the bottom layer) stations during 12/30/2015 – 2/28/2016.

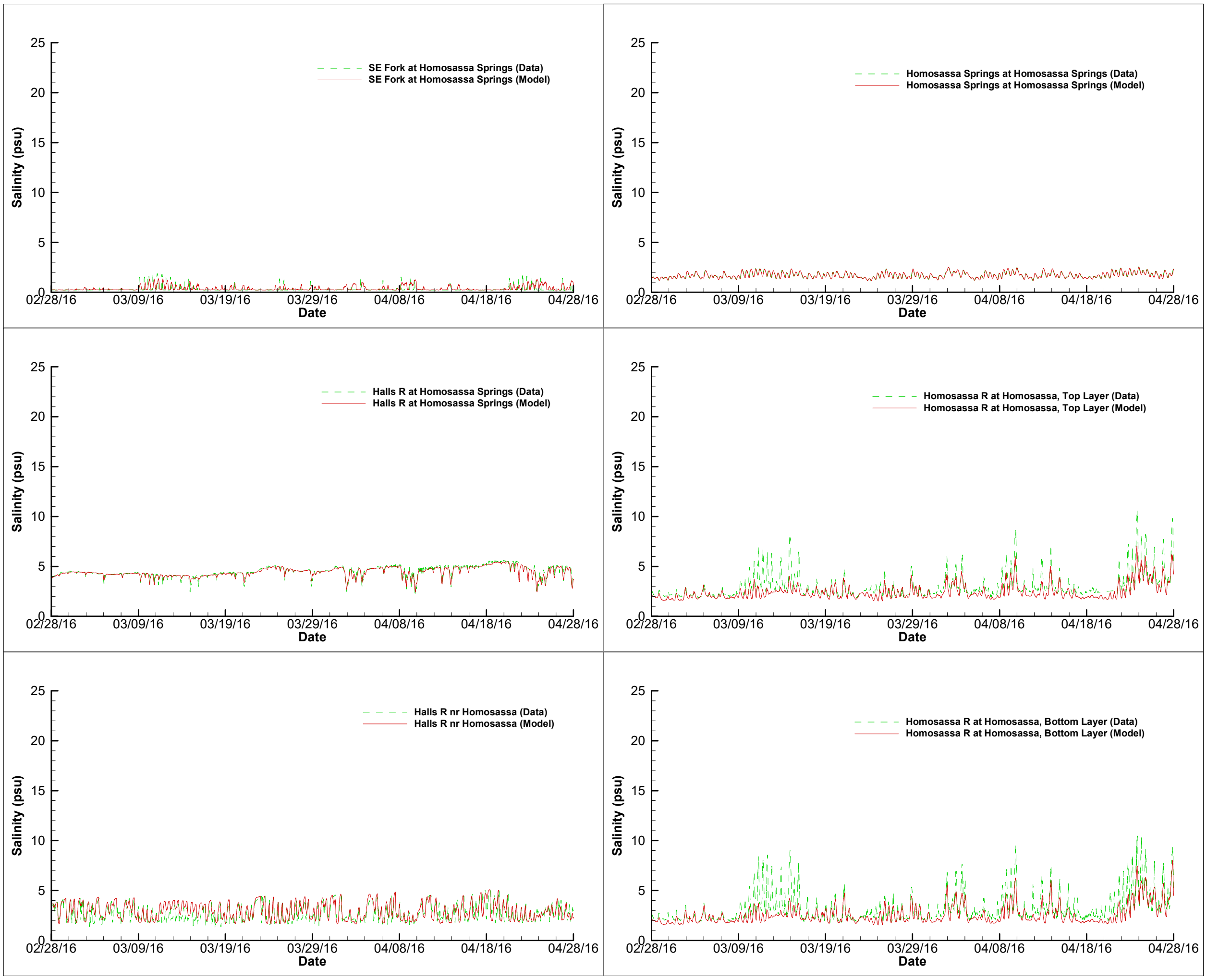

Figure E - 9. Comparisons of simulated (red lines) and measured (dashed green lines) salinities at SE Fork at Homosassa Spring (top left), Homosassa Springs at Homosassa Springs (top right), Halls River at Homosassa Springs (middle left), Halls River near Homosassa (bottom left), and Homosassa River at Homosassa (middle right for the top layer and bottom right for the bottom layer) stations during 2/28/2016 – 4/28/2016.

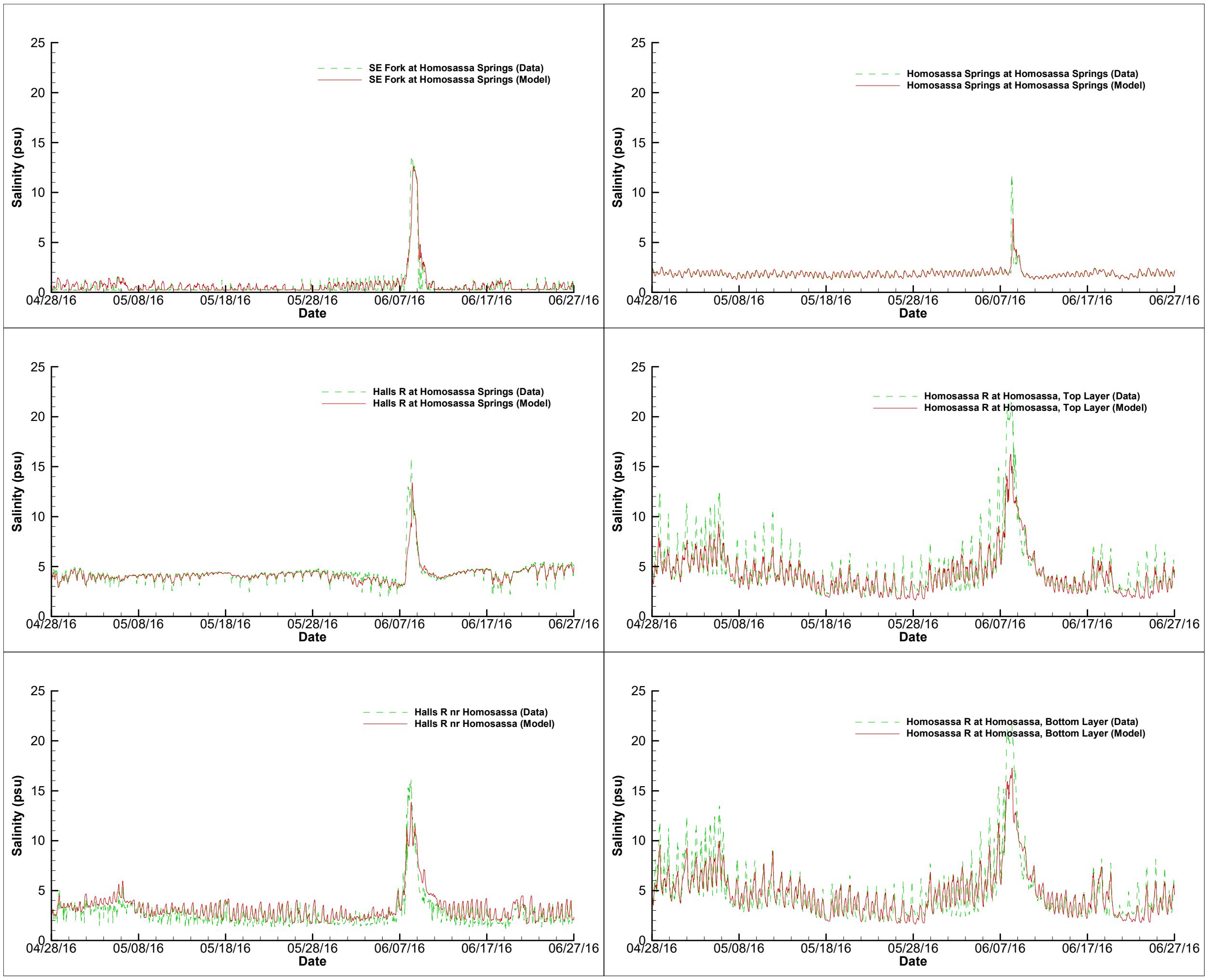

Figure E - 10. Comparisons of simulated (red lines) and measured (dashed green lines) salinities at SE Fork at Homosassa Spring (top left), Homosassa Springs at Homosassa Springs (top right), Halls River at Homosassa Springs (middle left), Halls River near Homosassa (bottom left), and Homosassa River at Homosassa (middle right for the top layer and bottom right for the bottom layer) stations during 4/28/2016 – 6/27/2016.

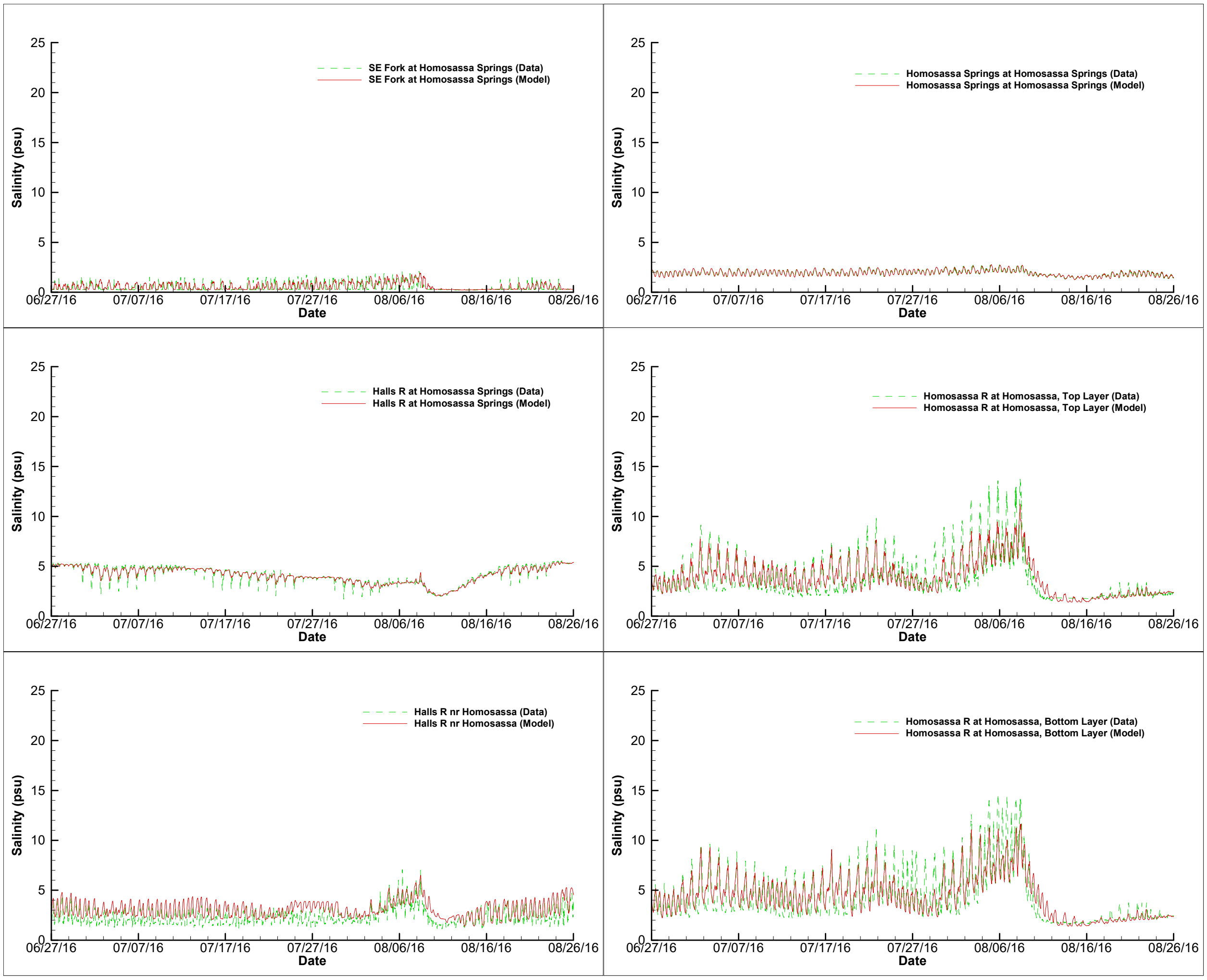

Figure E - 11. Comparisons of simulated (red lines) and measured (dashed green lines) salinities at SE Fork at Homosassa Spring (top left), Homosassa Springs at Homosassa Springs (top right), Halls River at Homosassa Springs (middle left), Halls River near Homosassa (bottom left), and Homosassa River at Homosassa (middle right for the top layer and bottom right for the bottom layer) stations during 6/27/2016 – 8/26/2016.

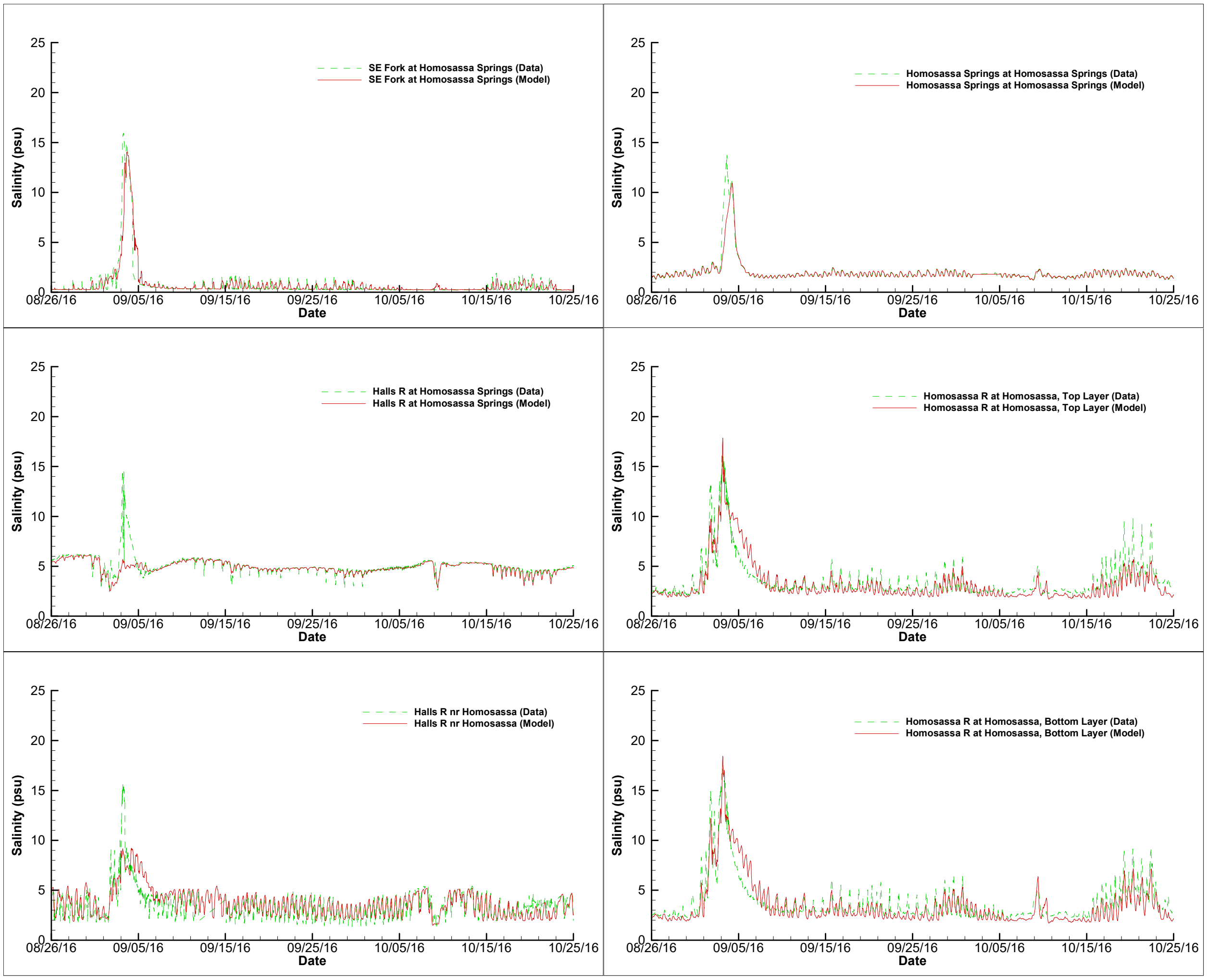

Figure E - 12. Comparisons of simulated (red lines) and measured (dashed green lines) salinities at SE Fork at Homosassa Spring (top left), Homosassa Springs at Homosassa Springs (top right), Halls River at Homosassa Springs (middle left), Halls River near Homosassa (bottom left), and Homosassa River at Homosassa (middle right for the top layer and bottom right for the bottom layer) stations during 8/26/2016 – 10/25/2016.

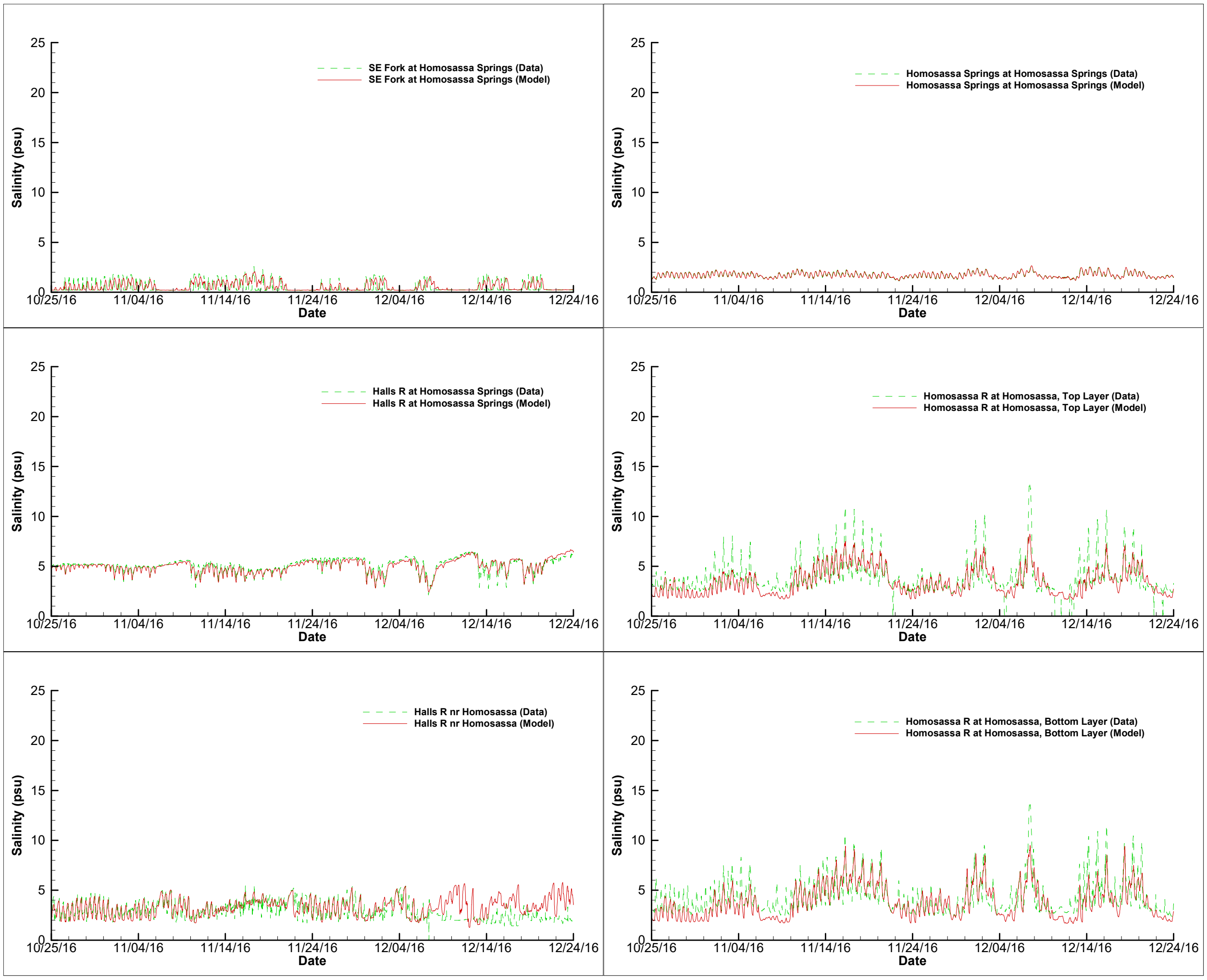

Figure E - 13. Comparisons of simulated (red lines) and measured (dashed green lines) salinities at SE Fork at Homosassa Spring (top left), Homosassa Springs at Homosassa Springs (top right), Halls River at Homosassa Springs (middle left), Halls River near Homosassa (bottom left), and Homosassa River at Homosassa (middle right for the top layer and bottom right for the bottom layer) stations during 10/25/2016 – 12/24/2016.

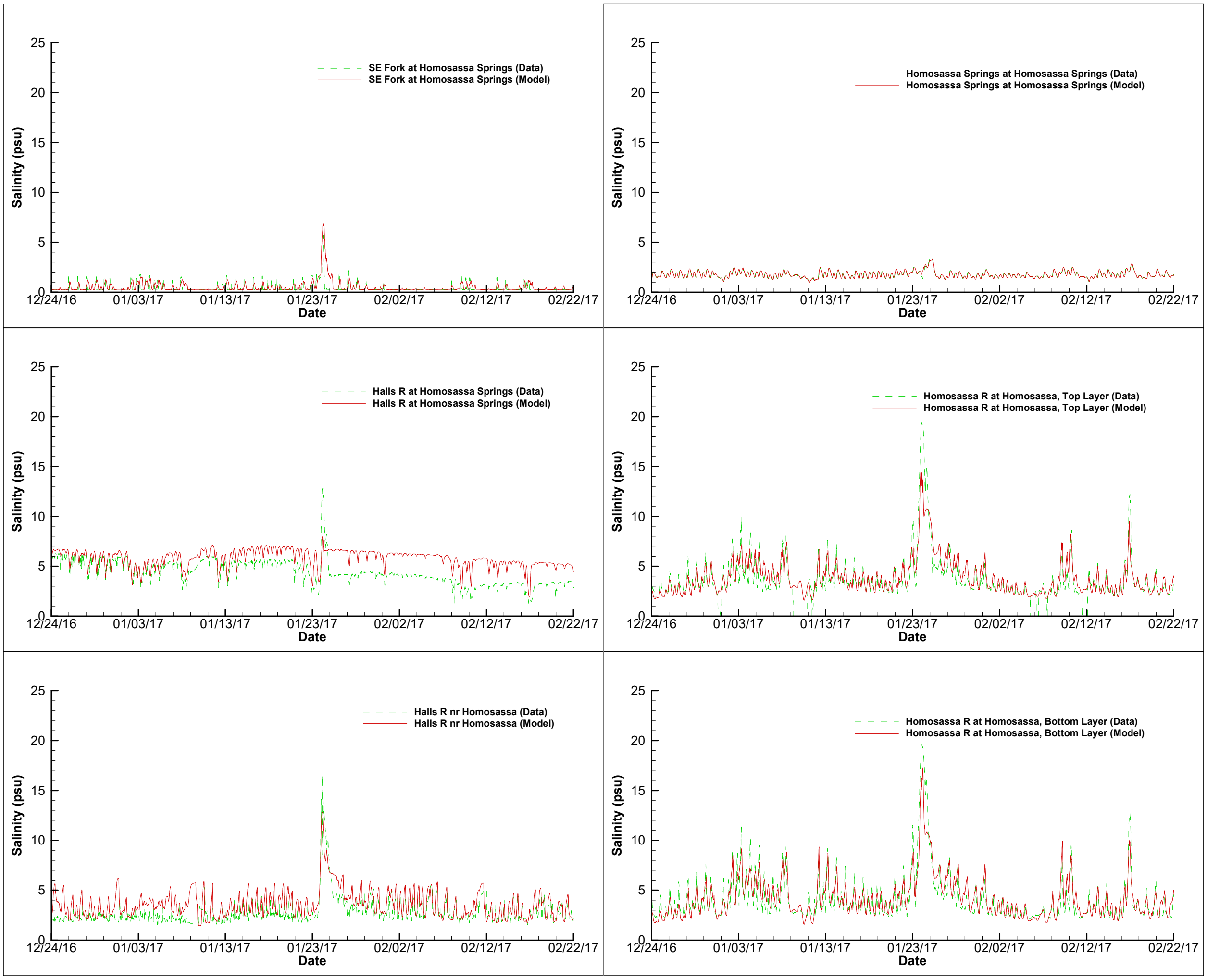

Figure E - 14. Comparisons of simulated (red lines) and measured (dashed green lines) salinities at SE Fork at Homosassa Spring (top left), Homosassa Springs at Homosassa Springs (top right), Halls River at Homosassa Springs (middle left), Halls River near Homosassa (bottom left), and Homosassa River at Homosassa (middle right for the top layer and bottom right for the bottom layer) stations during 12/24/2016 – 2/22/2017.

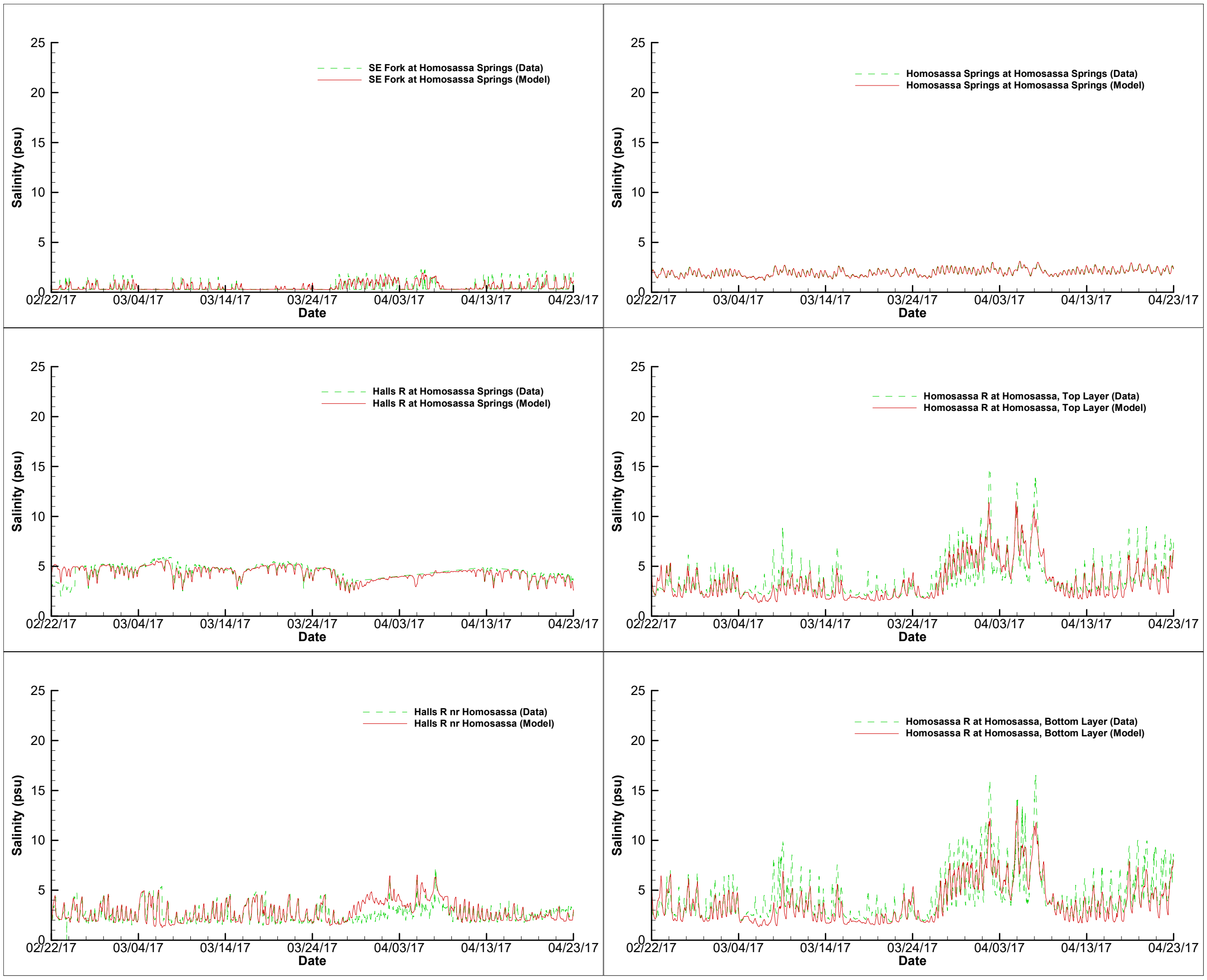

Figure E - 15. Comparisons of simulated (red lines) and measured (dashed green lines) salinities at SE Fork at Homosassa Spring (top left), Homosassa Springs at Homosassa Springs (top right), Halls River at Homosassa Springs (middle left), Halls River near Homosassa (bottom left), and Homosassa River at Homosassa (middle right for the top layer and bottom right for the bottom layer) stations during 2/22/2017 – 4/23/2017.

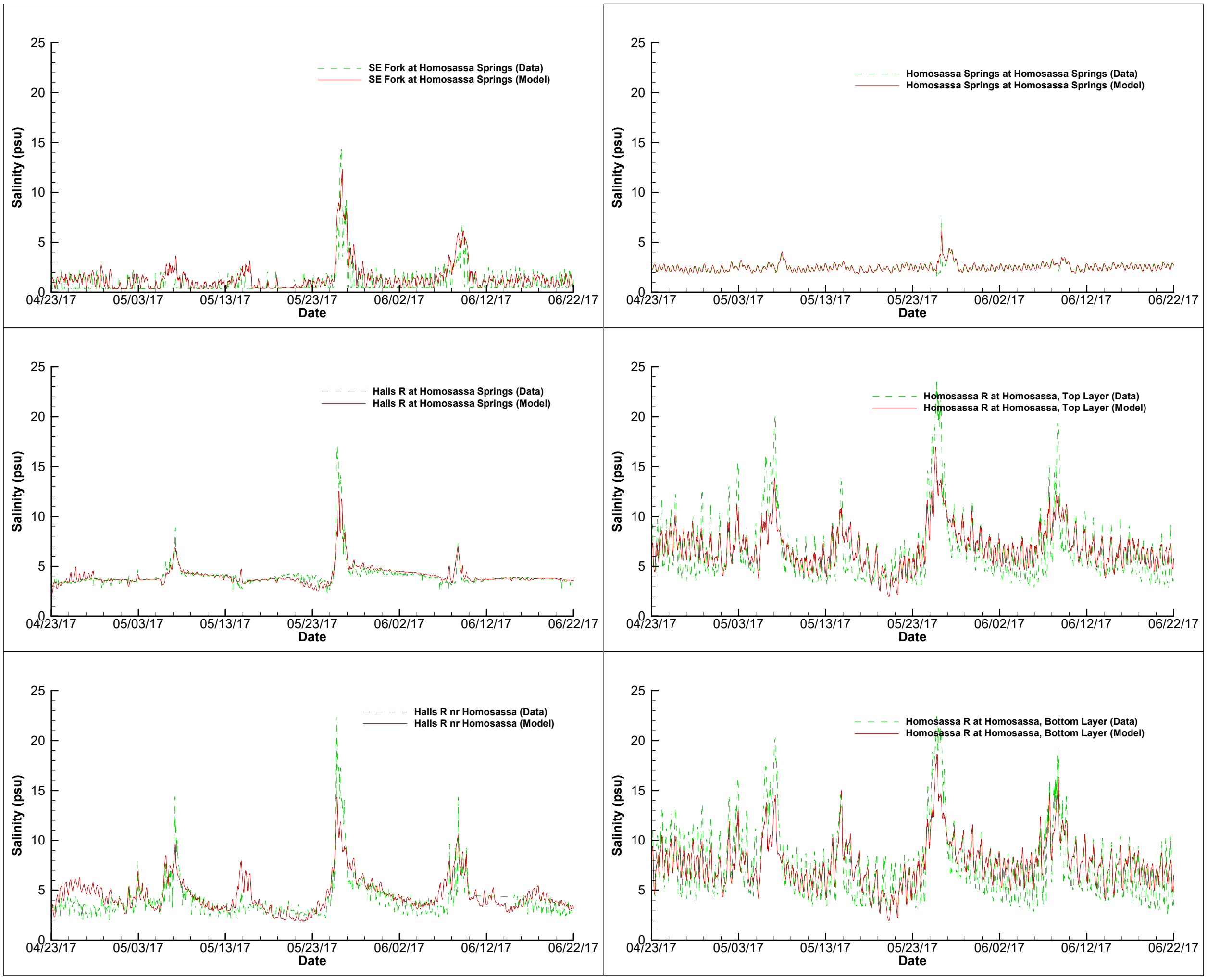

Figure E - 16. Comparisons of simulated (red lines) and measured (dashed green lines) salinities at SE Fork at Homosassa Spring (top left), Homosassa Springs at Homosassa Springs (top right), Halls River at Homosassa Springs (middle left), Halls River near Homosassa (bottom left), and Homosassa River at Homosassa (middle right for the top layer and bottom right for the bottom layer) stations during 4/23/2017 – 6/22/2017.

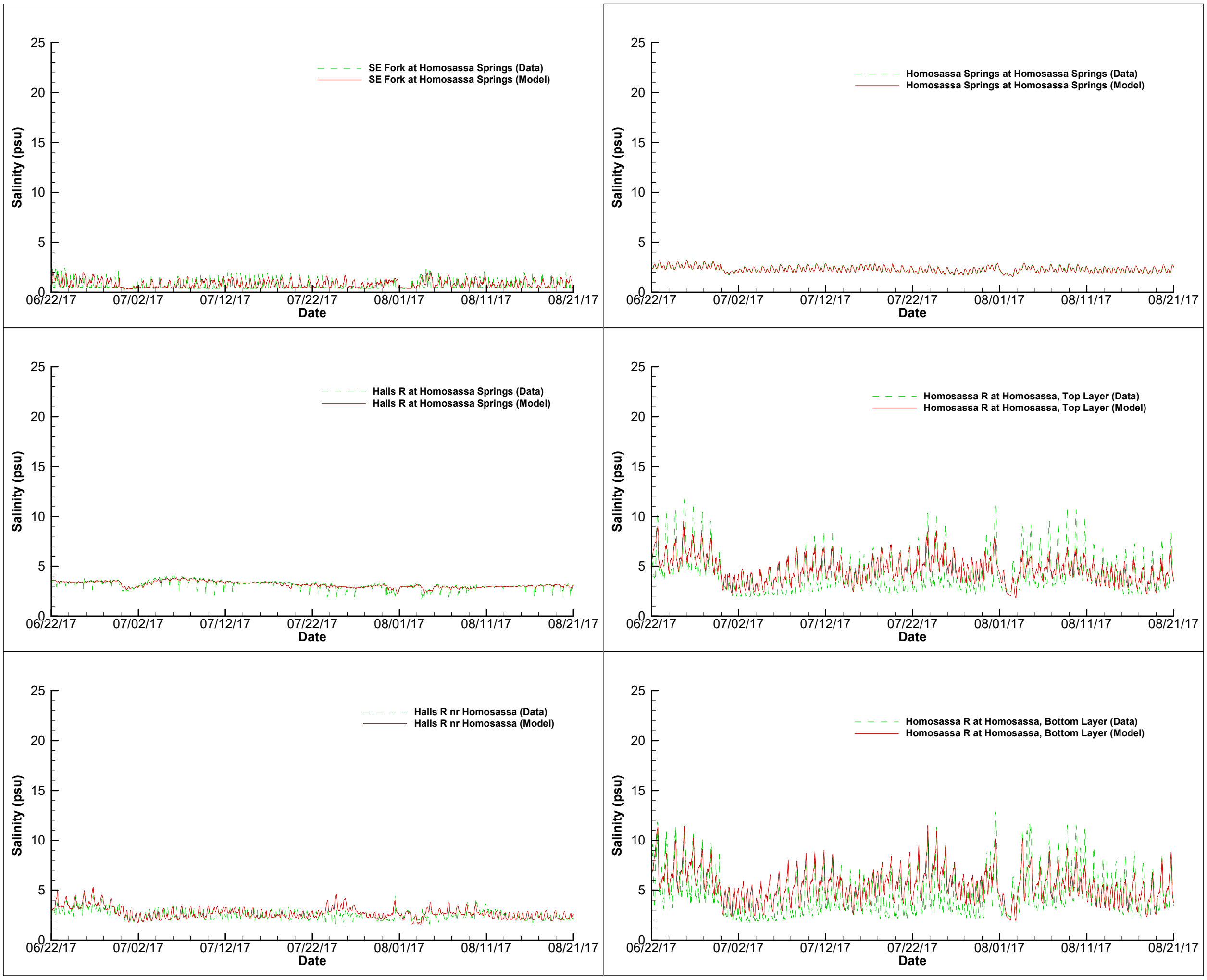

Figure E - 17. Comparisons of simulated (red lines) and measured (dashed green lines) salinities at SE Fork at Homosassa Spring (top left), Homosassa Springs at Homosassa Springs (top right), Halls River at Homosassa Springs (middle left), Halls River near Homosassa (bottom left), and Homosassa River at Homosassa (middle right for the top layer and bottom right for the bottom layer) stations during 6/22/2017 – 8/21/2017.

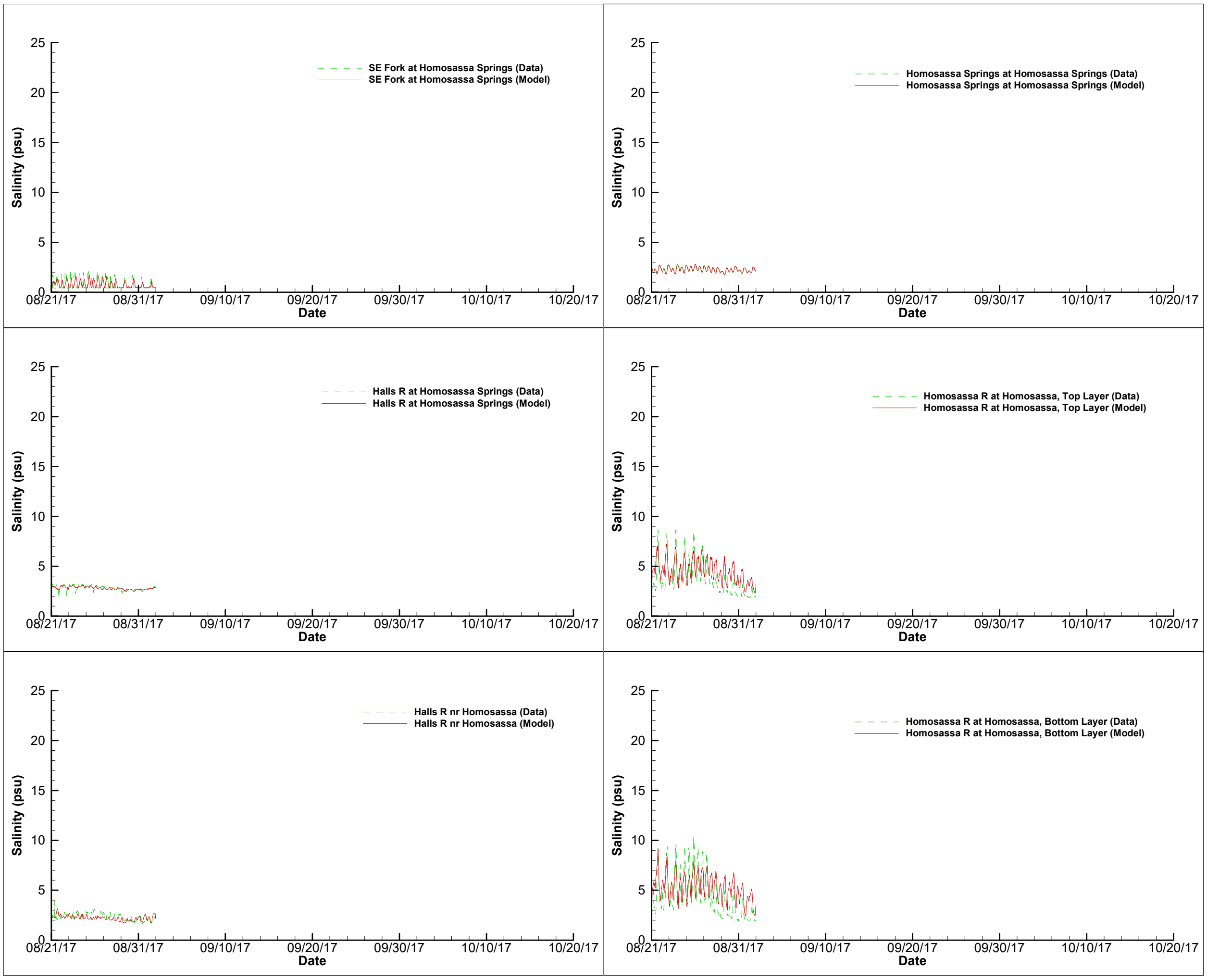

Figure E - 18. Comparisons of simulated (red lines) and measured (dashed green lines) salinities at SE Fork at Homosassa Spring (top left), Homosassa Springs at Homosassa Springs (top right), Halls River at Homosassa Springs (middle left), Halls River near Homosassa (bottom left), and Homosassa River at Homosassa (middle right for the top layer and bottom right for the bottom layer) stations during 8/21/2017 – 10/20/2017.

Appendix F. Simulated and Measured Temperatures

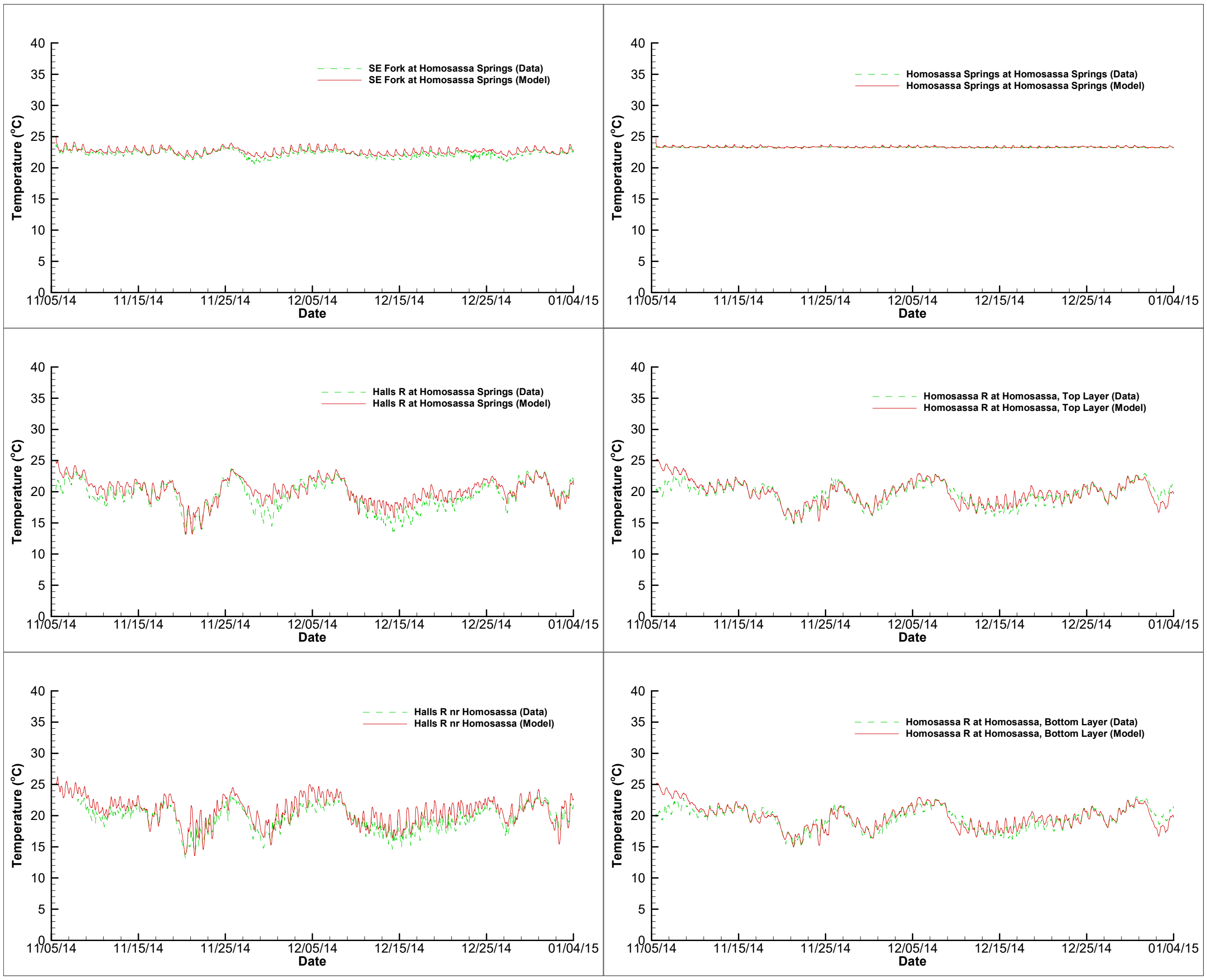

Figure F - 1. Comparisons of simulated (red lines) and measured (dashed green lines) temperatures at SE Fork at Homosassa Spring (top left), Homosassa Springs at Homosassa Springs (top right), Halls River at Homosassa Springs (middle left), Halls River near Homosassa (bottom left), and Homosassa River at Homosassa (middle right for the top layer and bottom right for the bottom layer) stations during 11/5/2014 – 1/4/2015.

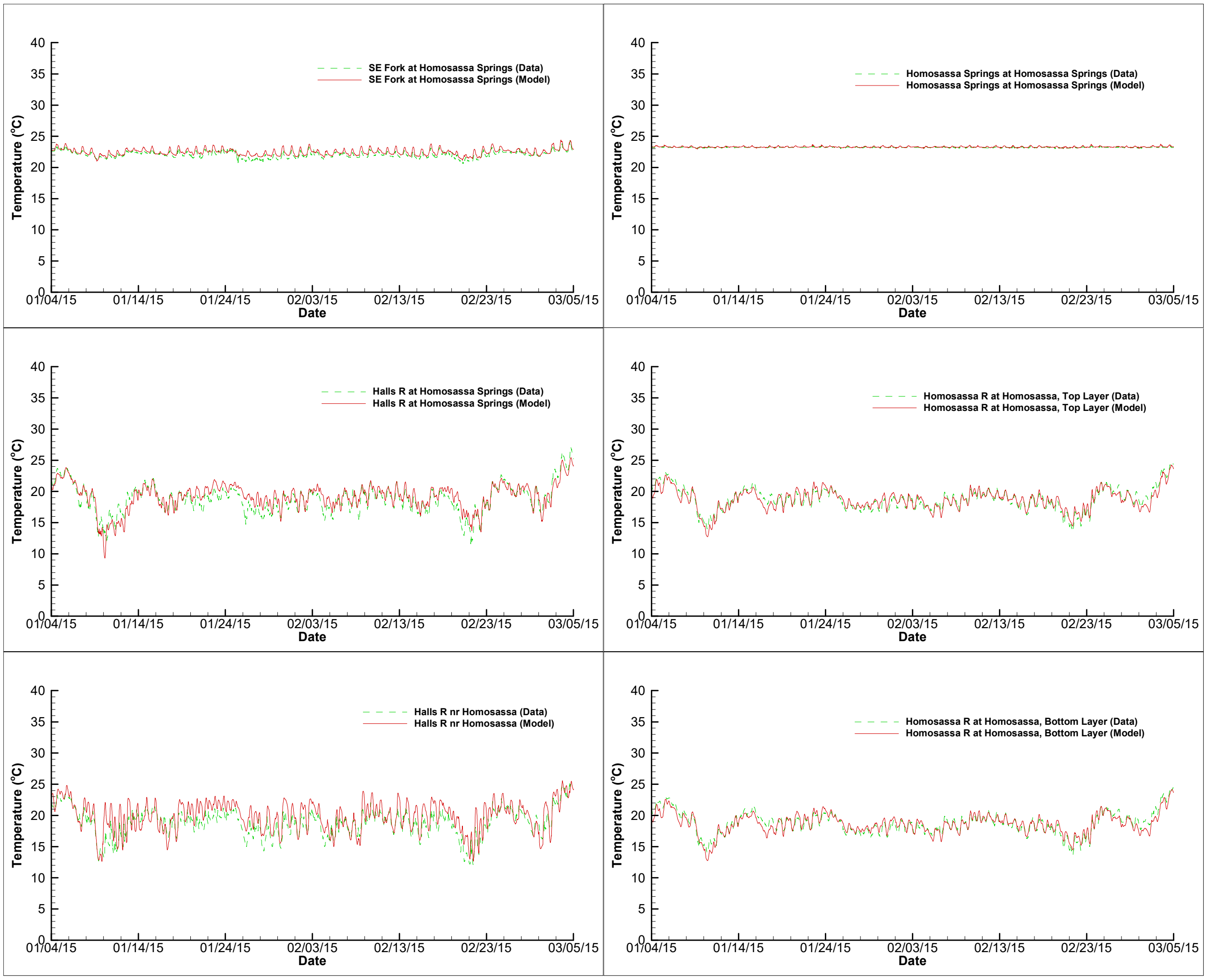

Figure F - 2. Comparisons of simulated (red lines) and measured (dashed green lines) temperatures at SE Fork at Homosassa Spring (top left), Homosassa Springs at Homosassa Springs (top right), Halls River at Homosassa Springs (middle left), Halls River near Homosassa (bottom left), and Homosassa River at Homosassa (middle right for the top layer and bottom right for the bottom layer) stations during 1/4/2015 – 3/5/2015.

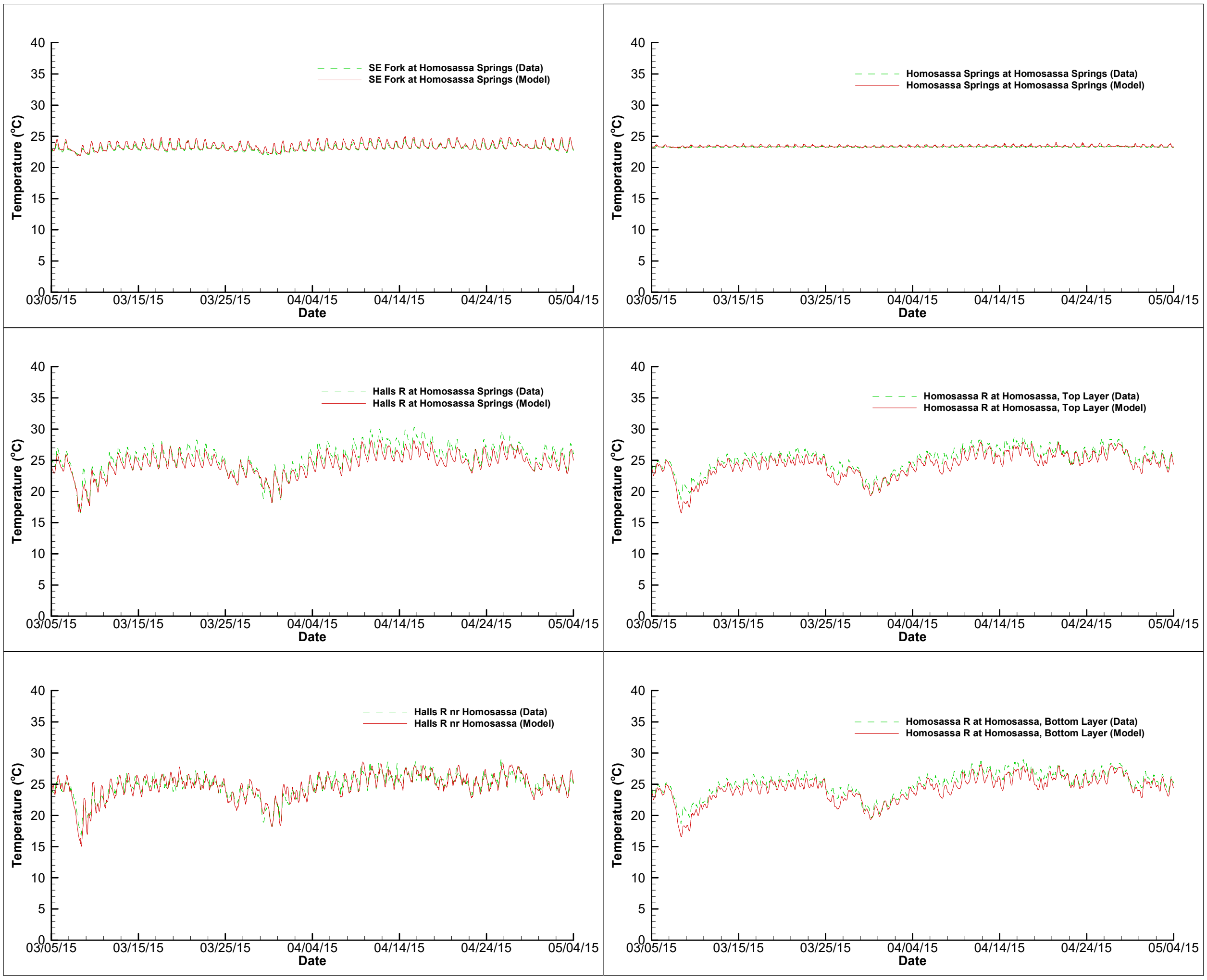

Figure F - 3. Comparisons of simulated (red lines) and measured (dashed green lines) temperatures at SE Fork at Homosassa Spring (top left), Homosassa Springs at Homosassa Springs (top right), Halls River at Homosassa Springs (middle left), Halls River near Homosassa (bottom left), and Homosassa River at Homosassa (middle right for the top layer and bottom right for the bottom layer) stations during 3/5/2015 – 5/4/2015.

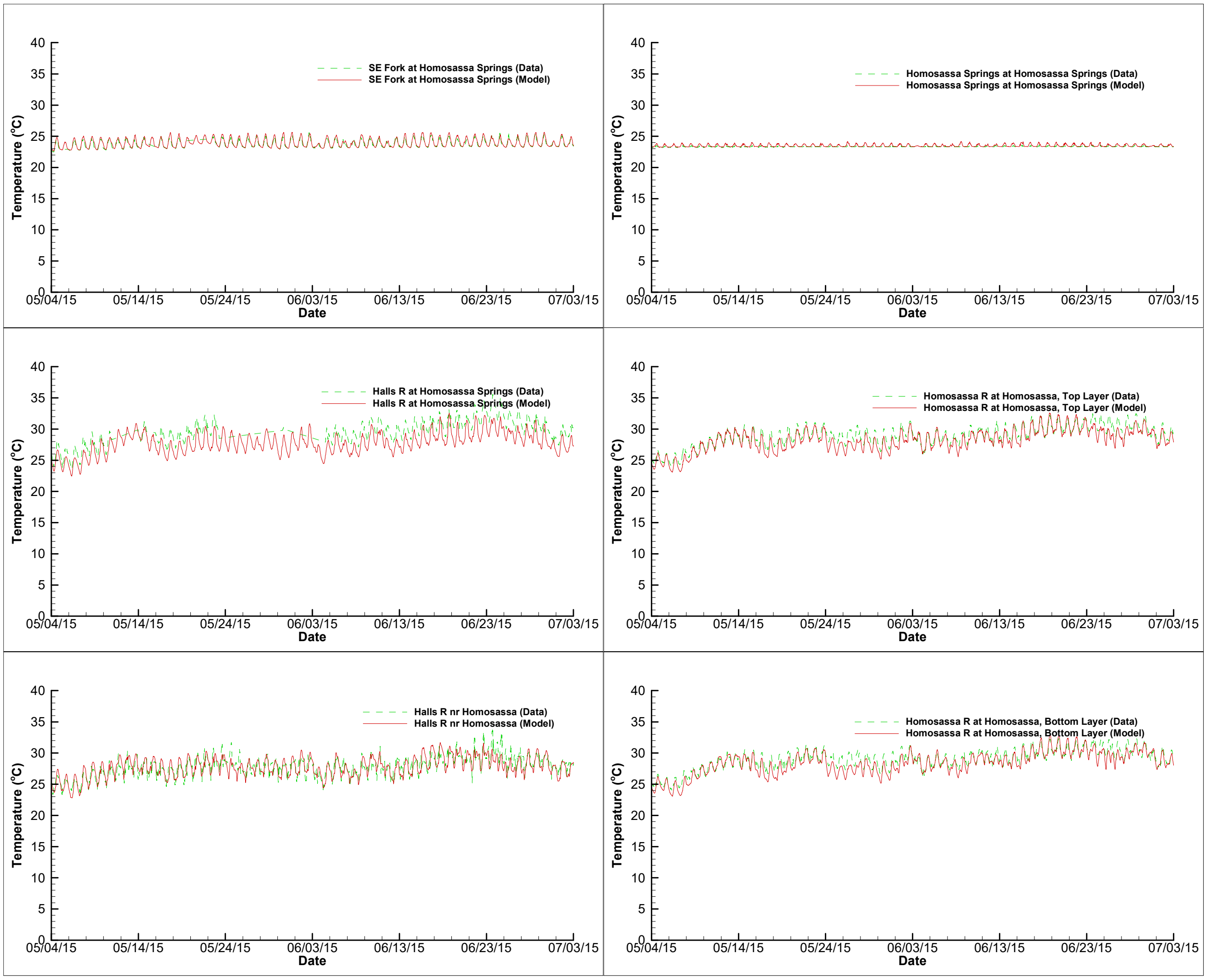

Figure F - 4. Comparisons of simulated (red lines) and measured (dashed green lines) temperatures at SE Fork at Homosassa Spring (top left), Homosassa Springs at Homosassa Springs (top right), Halls River at Homosassa Springs (middle left), Halls River near Homosassa (bottom left), and Homosassa River at Homosassa (middle right for the top layer and bottom right for the bottom layer) stations during 5/4/2015 – 7/3/2015.

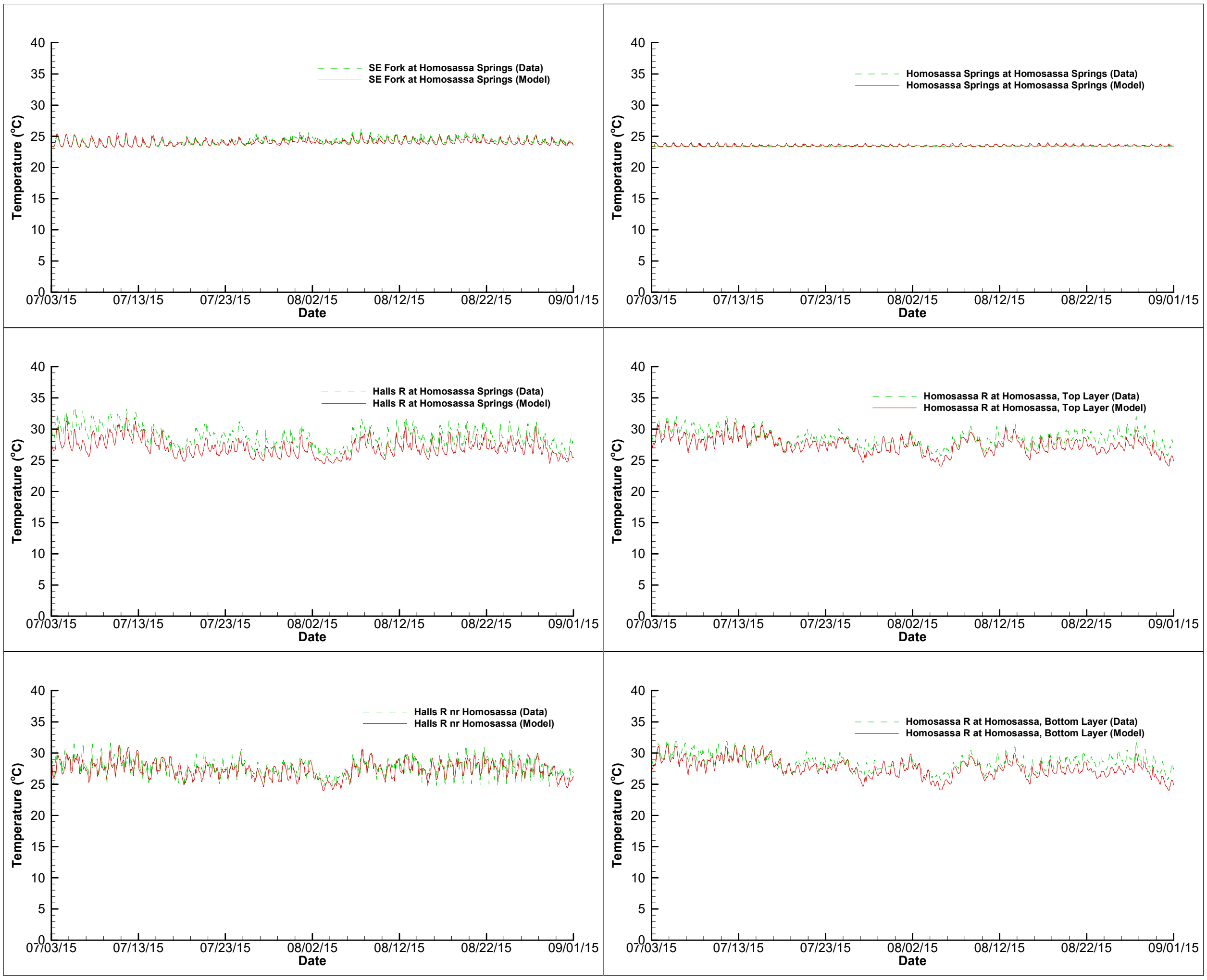

Figure F - 5. Comparisons of simulated (red lines) and measured (dashed green lines) temperatures at SE Fork at Homosassa Spring (top left), Homosassa Springs at Homosassa Springs (top right), Halls River at Homosassa Springs (middle left), Halls River near Homosassa (bottom left), and Homosassa River at Homosassa (middle right for the top layer and bottom right for the bottom layer) stations during 7/3/2015 – 9/1/2015.

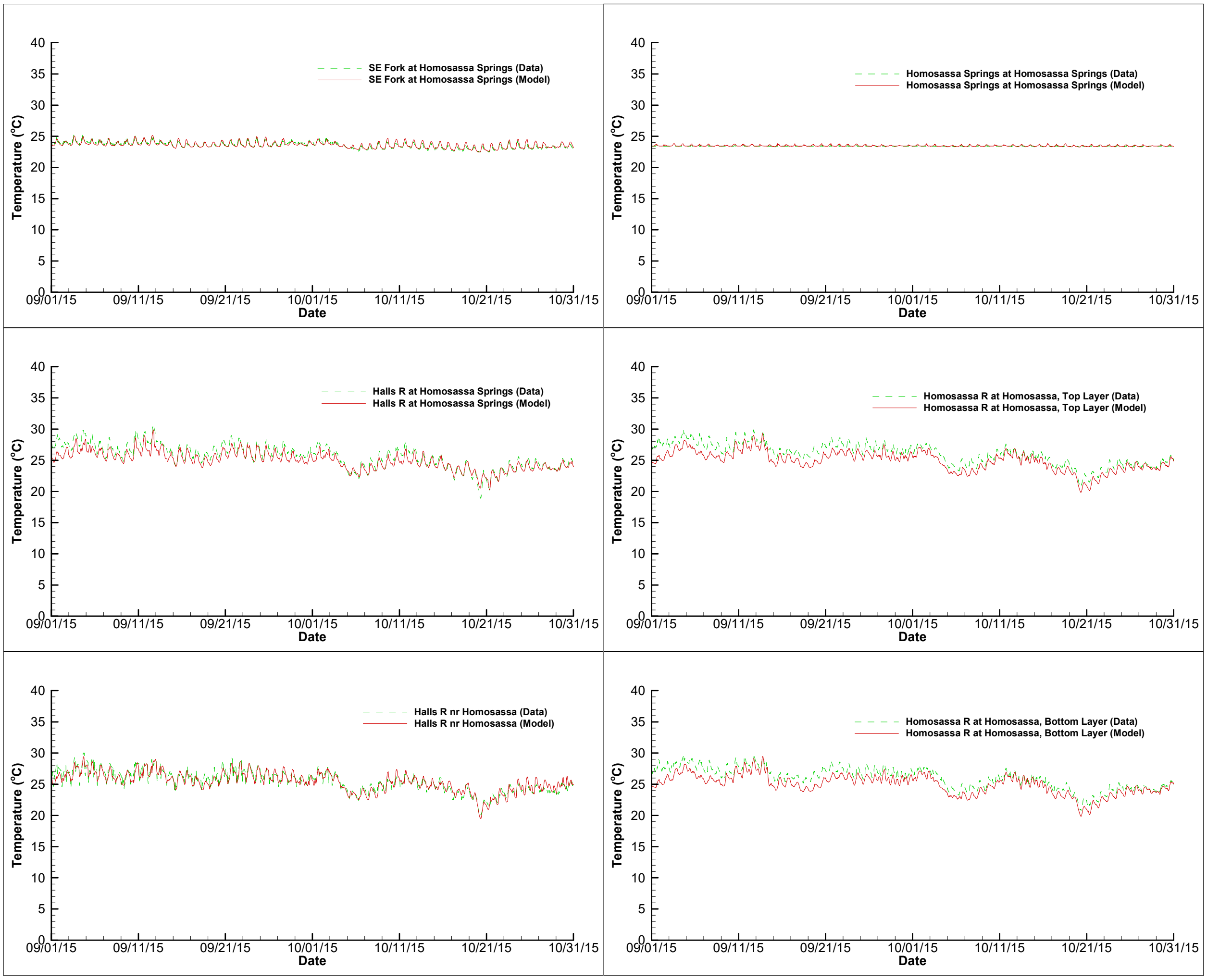

Figure F - 6. Comparisons of simulated (red lines) and measured (dashed green lines) temperatures at SE Fork at Homosassa Spring (top left), Homosassa Springs at Homosassa Springs (top right), Halls River at Homosassa Springs (middle left), Halls River near Homosassa (bottom left), and Homosassa River at Homosassa (middle right for the top layer and bottom right for the bottom layer) stations during 9/1/2015 – 10/31/2015.

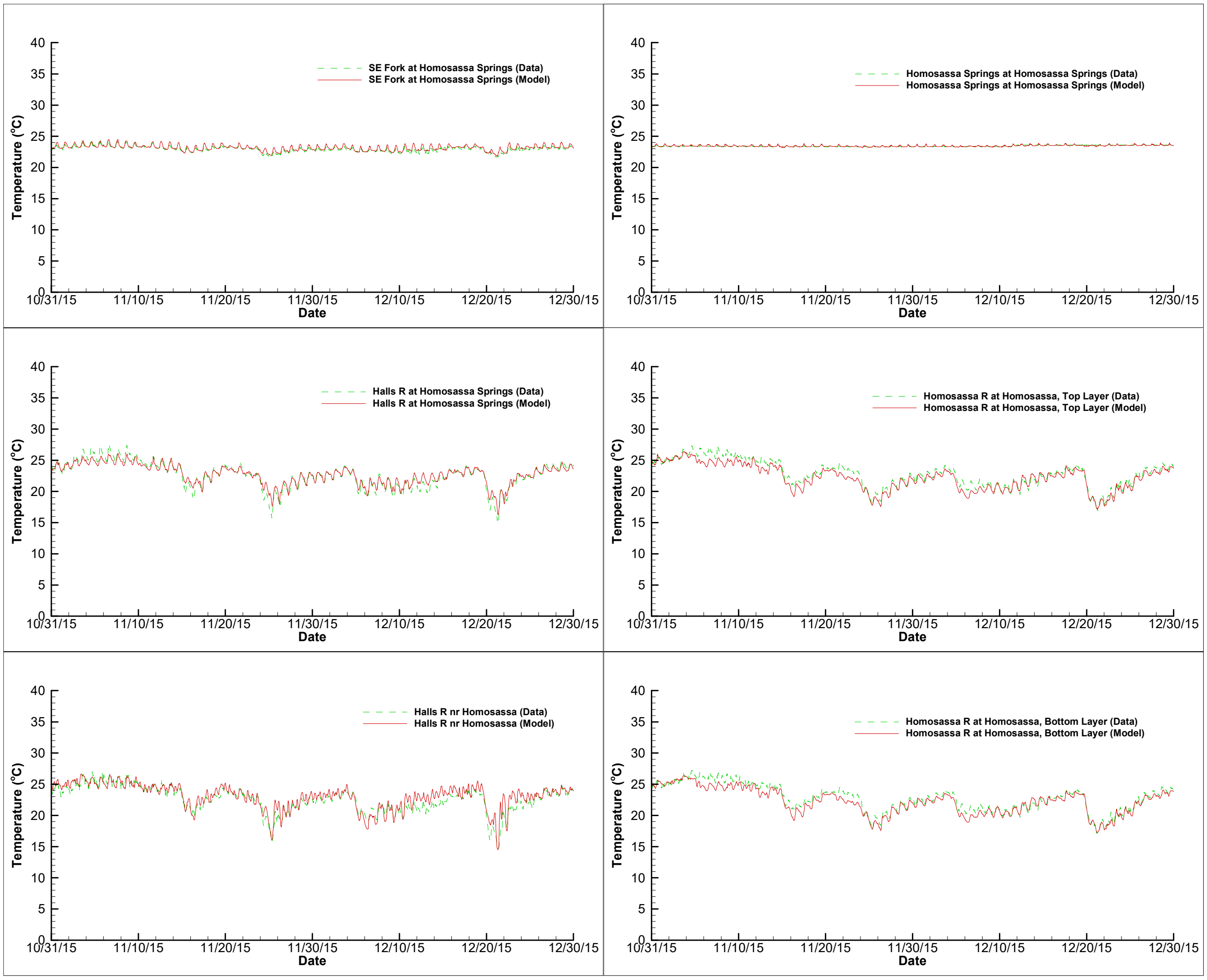

Figure F - 7. Comparisons of simulated (red lines) and measured (dashed green lines) temperatures at SE Fork at Homosassa Spring (top left), Homosassa Springs at Homosassa Springs (top right), Halls River at Homosassa Springs (middle left), Halls River near Homosassa (bottom left), and Homosassa River at Homosassa (middle right for the top layer and bottom right for the bottom layer) stations during 10/31/2015 – 12/30/2015.

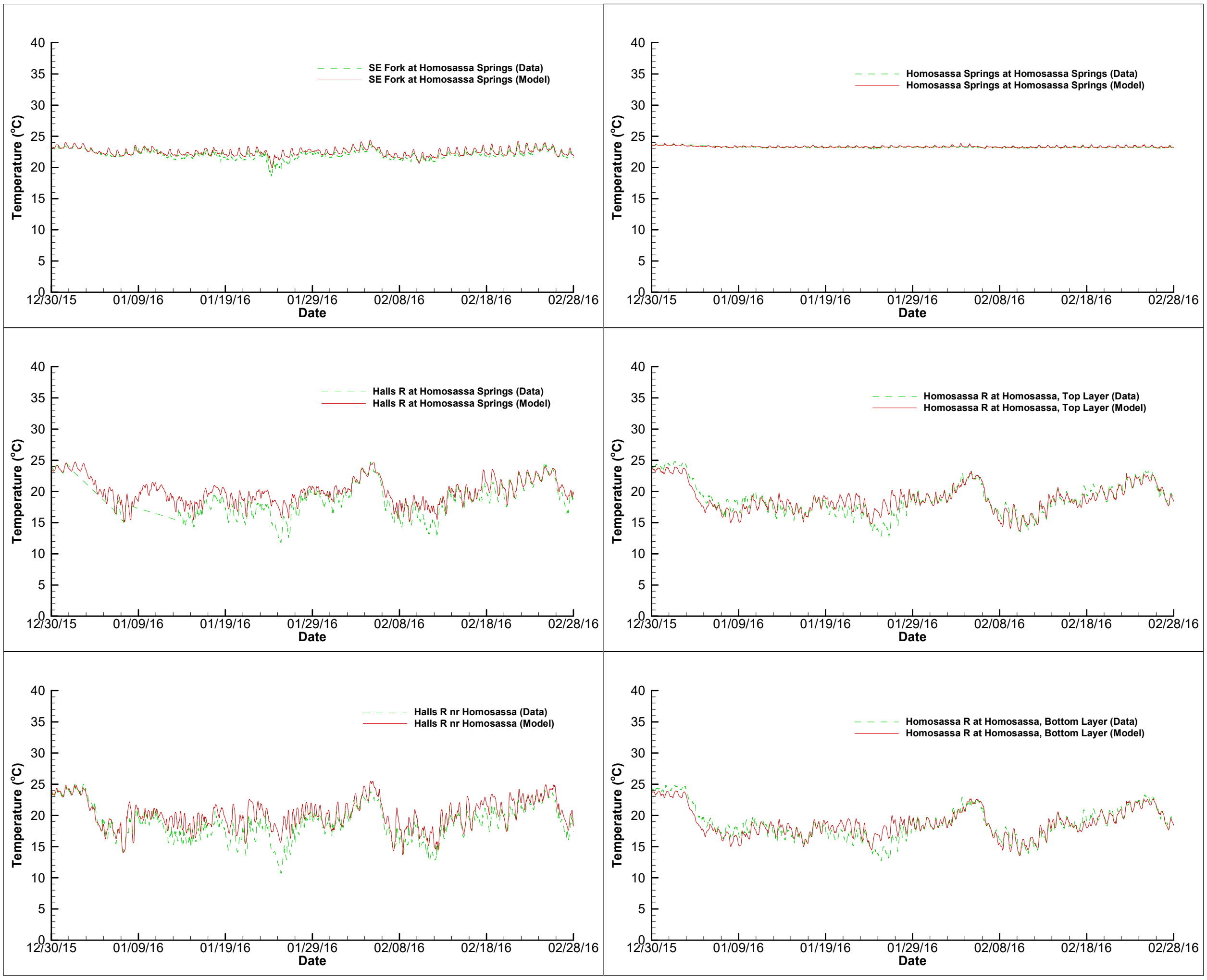

Figure F - 8. Comparisons of simulated (red lines) and measured (dashed green lines) temperatures at SE Fork at Homosassa Spring (top left), Homosassa Springs at Homosassa Springs (top right), Halls River at Homosassa Springs (middle left), Halls River near Homosassa (bottom left), and Homosassa River at Homosassa (middle right for the top layer and bottom right for the bottom layer) stations during 12/30/2015 – 2/28/2016.

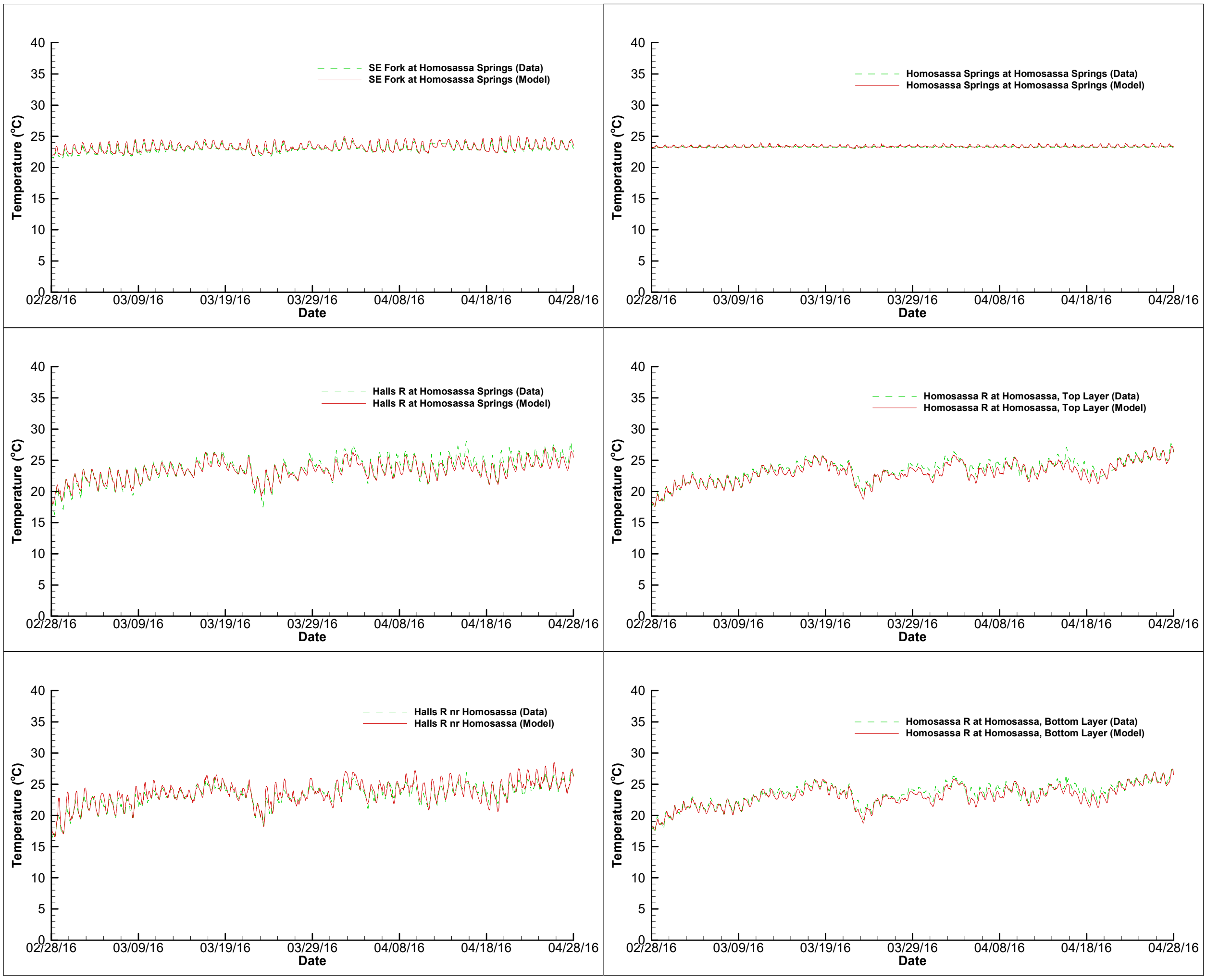

Figure F - 9. Comparisons of simulated (red lines) and measured (dashed green lines) temperatures at SE Fork at Homosassa Spring (top left), Homosassa Springs at Homosassa Springs (top right), Halls River at Homosassa Springs (middle left), Halls River near Homosassa (bottom left), and Homosassa River at Homosassa (middle right for the top layer and bottom right for the bottom layer) stations during 2/28/2016 – 4/28/2016.

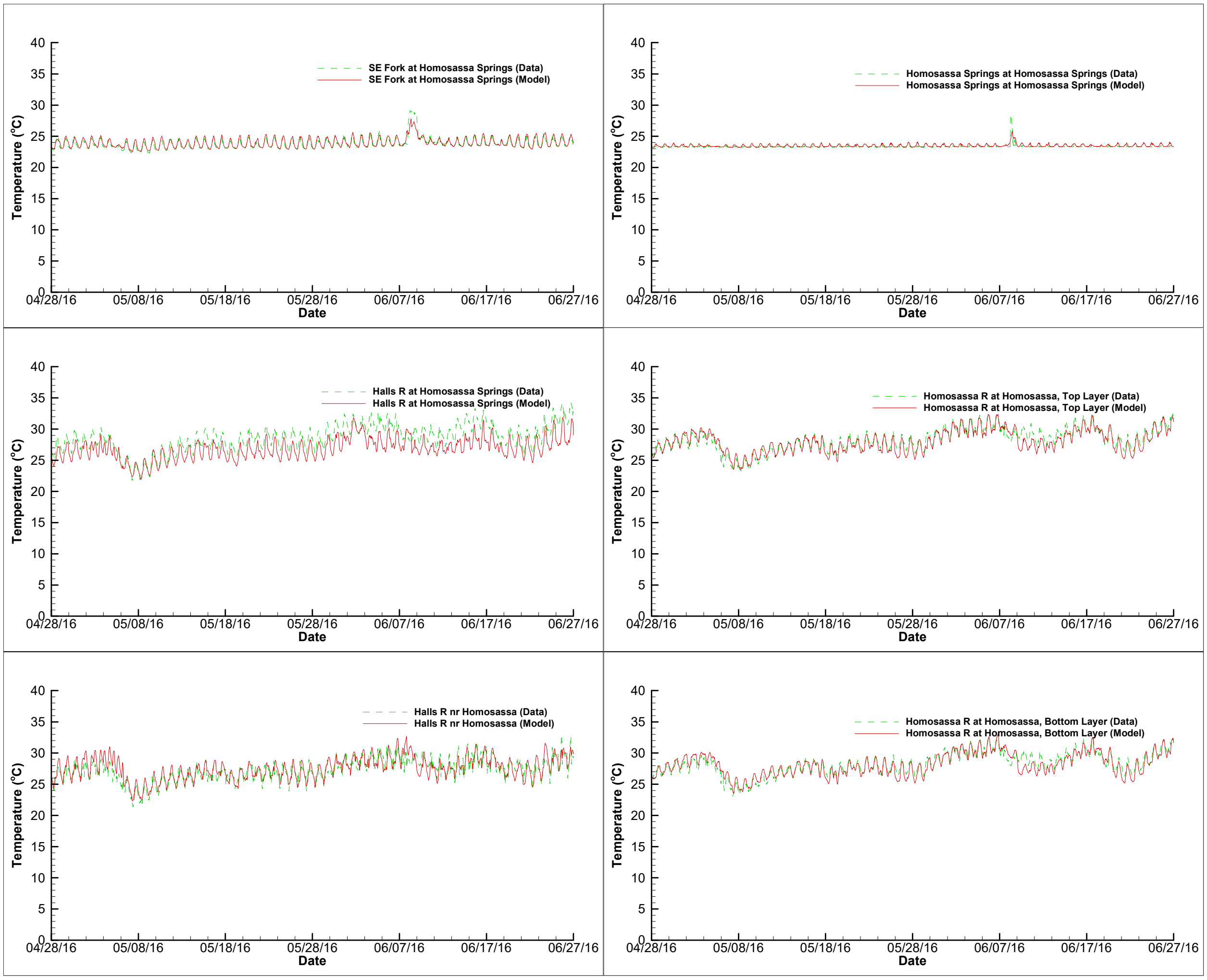

Figure F - 10. Comparisons of simulated (red lines) and measured (dashed green lines) temperatures at SE Fork at Homosassa Spring (top left), Homosassa Springs at Homosassa Springs (top right), Halls River at Homosassa Springs (middle left), Halls River near Homosassa (bottom left), and Homosassa River at Homosassa (middle right for the top layer and bottom right for the bottom layer) stations during 4/28/2016 – 6/27/2016.

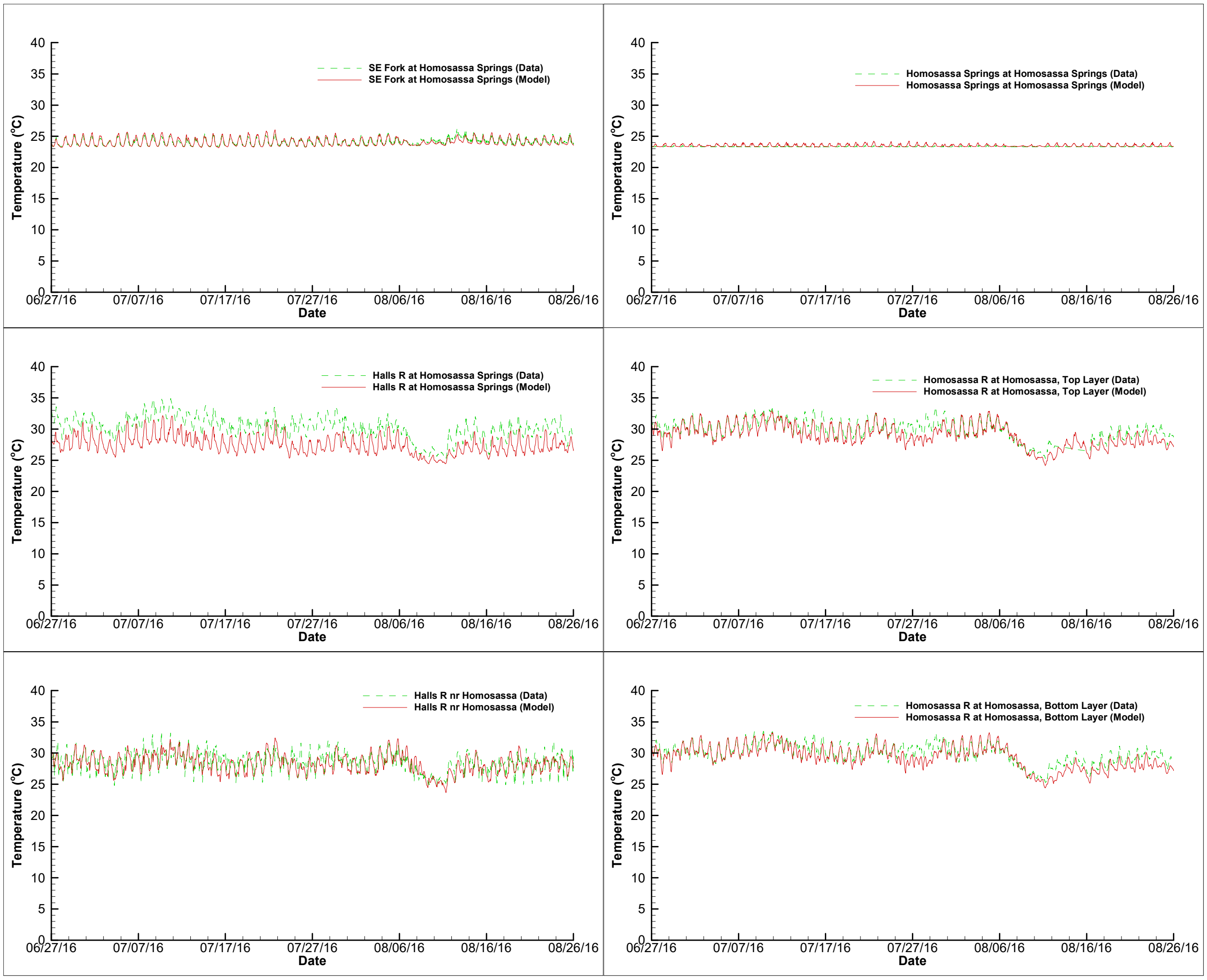

Figure F - 11. Comparisons of simulated (red lines) and measured (dashed green lines) temperatures at SE Fork at Homosassa Spring (top left), Homosassa Springs at Homosassa Springs (top right), Halls River at Homosassa Springs (middle left), Halls River near Homosassa (bottom left), and Homosassa River at Homosassa (middle right for the top layer and bottom right for the bottom layer) stations during 6/27/2016 - 8/26/2016.

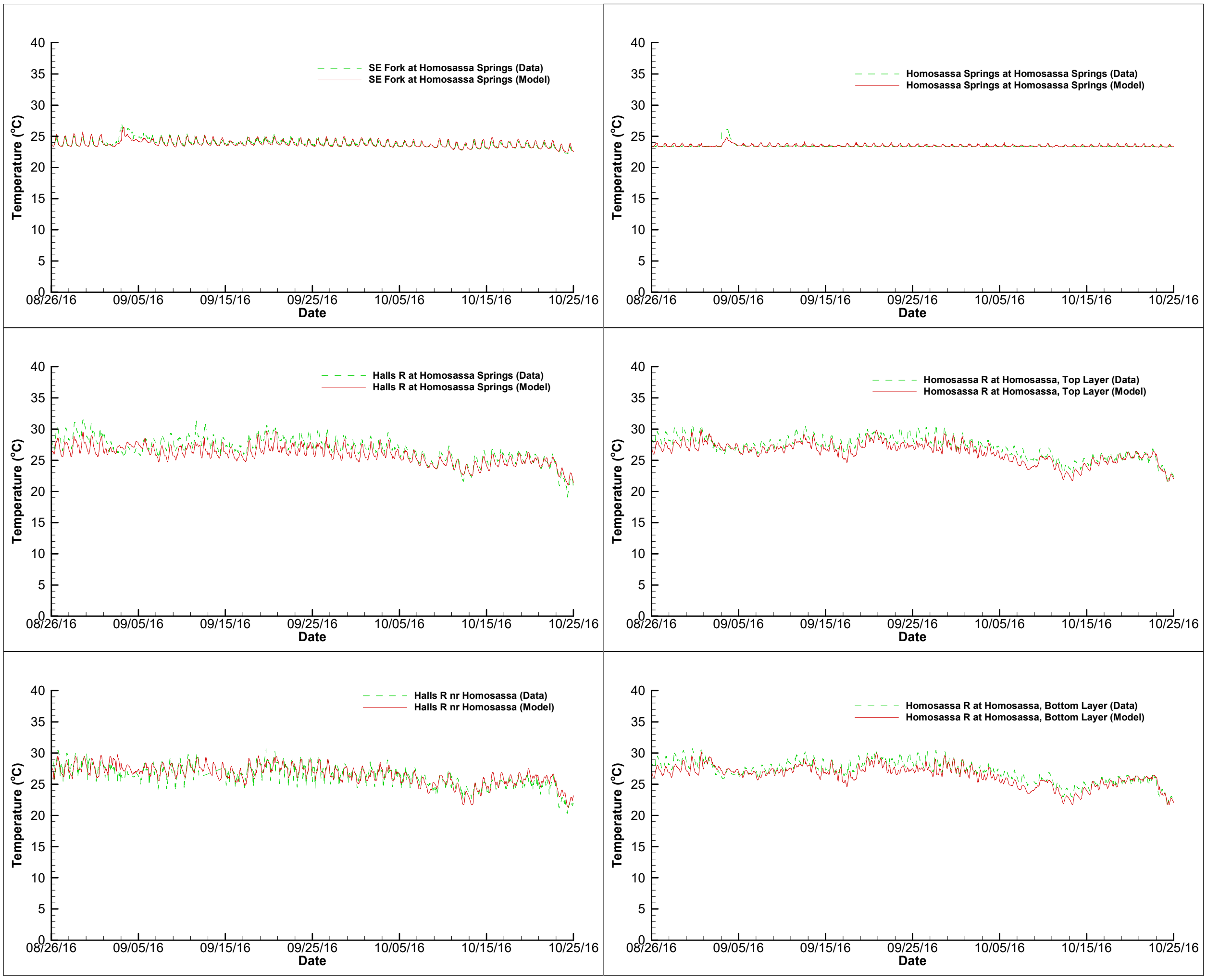

Figure F - 12. Comparisons of simulated (red lines) and measured (dashed green lines) temperatures at SE Fork at Homosassa Spring (top left), Homosassa Springs at Homosassa Springs (top right), Halls River at Homosassa Springs (middle left), Halls River near Homosassa (bottom left), and Homosassa River at Homosassa (middle right for the top layer and bottom right for the bottom layer) stations during 8/26/2016 – 10/25/2016.

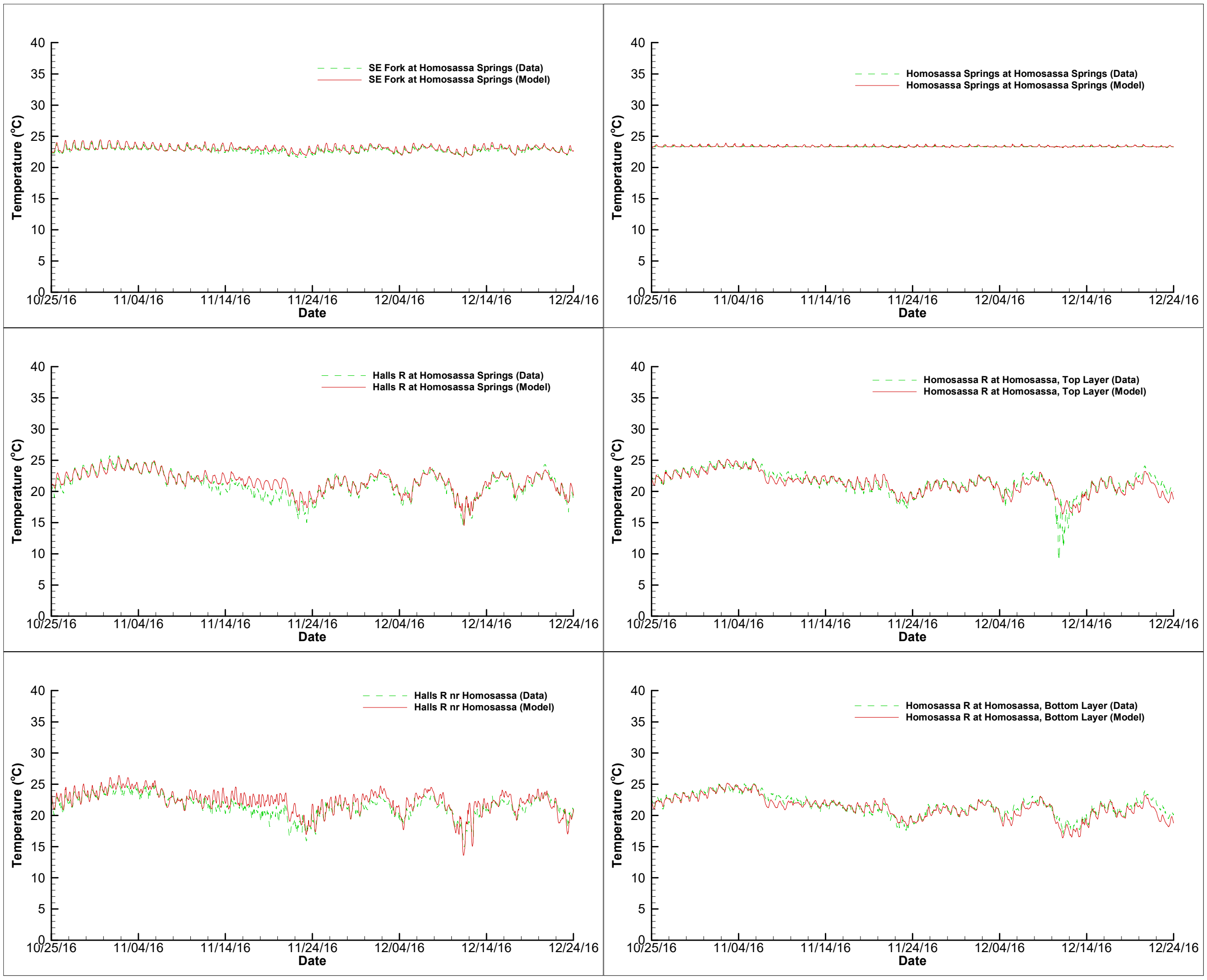

Figure F - 13. Comparisons of simulated (red lines) and measured (dashed green lines) temperatures at SE Fork at Homosassa Spring (top left), Homosassa Springs at Homosassa Springs (top right), Halls River at Homosassa Springs (middle left), Halls River near Homosassa (bottom left), and Homosassa River at Homosassa (middle right for the top layer and bottom right for the bottom layer) stations during 10/25/2016 – 12/24/2016.

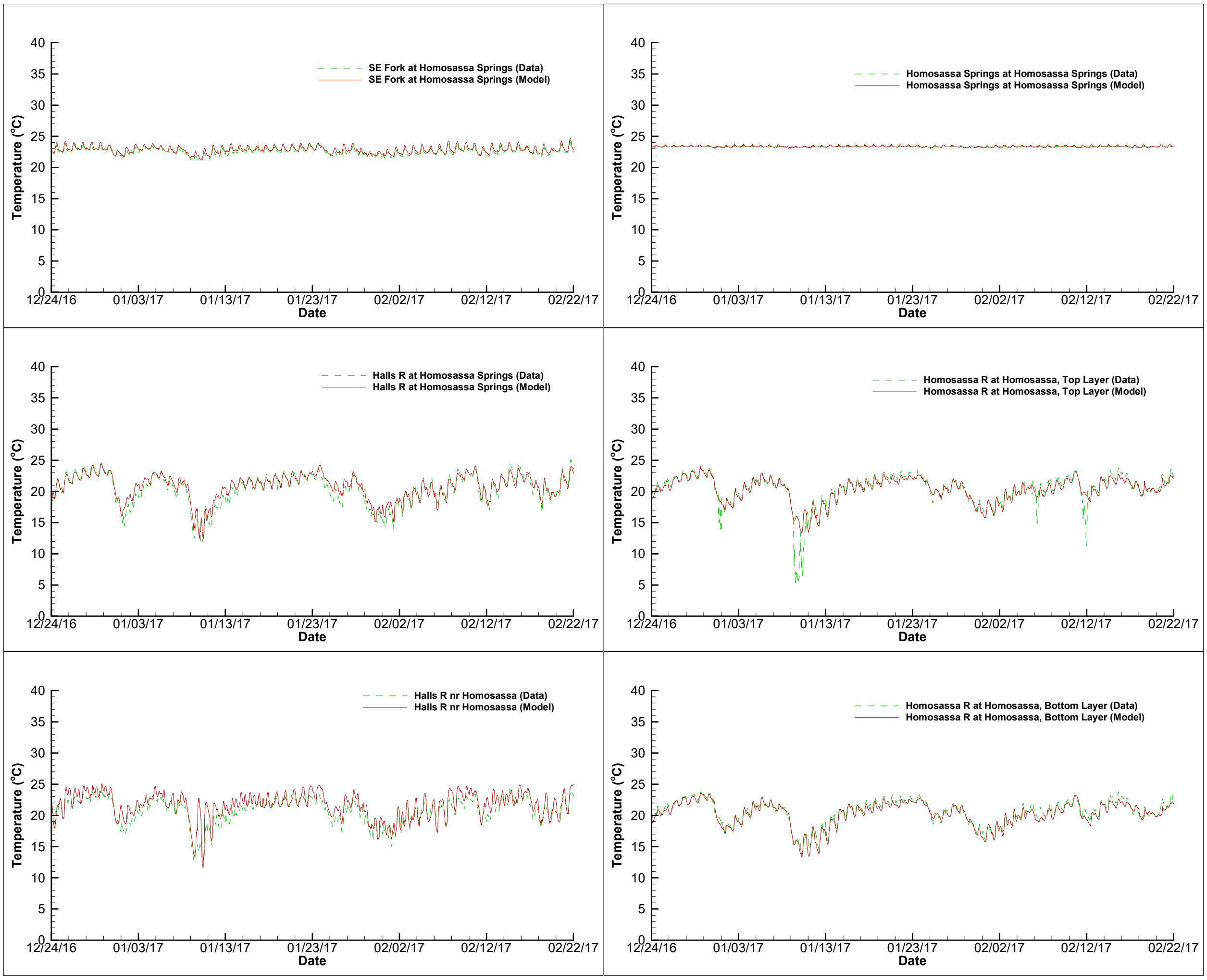

Figure F - 14. Comparisons of simulated (red lines) and measured (dashed green lines) temperatures at SE Fork at Homosassa Spring (top left), Homosassa Springs at Homosassa Springs (top right), Halls River at Homosassa Springs (middle left), Halls River near Homosassa (bottom left), and Homosassa River at Homosassa (middle right for the top layer and bottom right for the bottom layer) stations during 12/24/2016 – 2/22/2017.

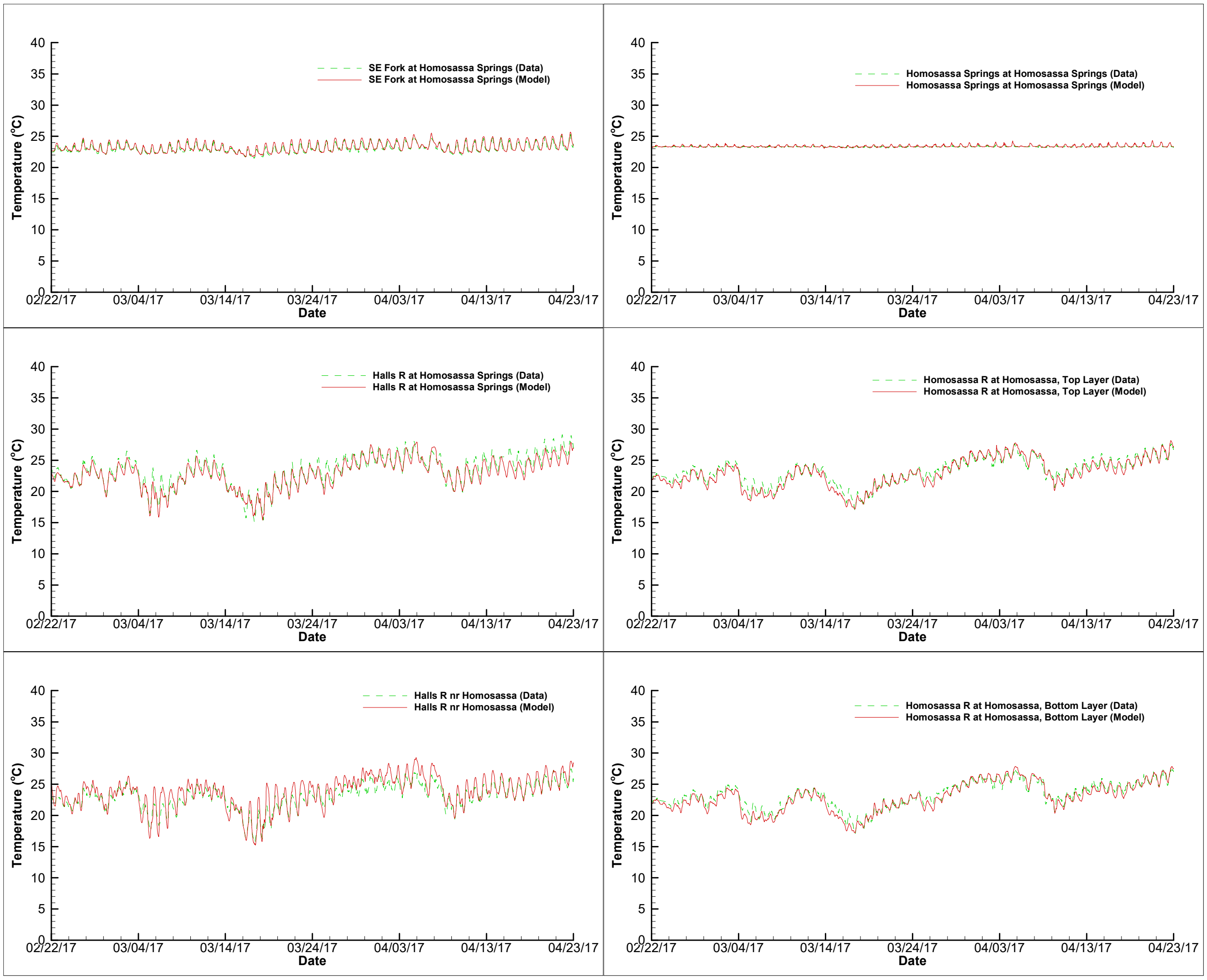

Figure F - 15. Comparisons of simulated (red lines) and measured (dashed green lines) temperatures at SE Fork at Homosassa Spring (top left), Homosassa Springs at Homosassa Springs (top right), Halls River at Homosassa Springs (middle left), Halls River near Homosassa (bottom left), and Homosassa River at Homosassa (middle right for the top layer and bottom right for the bottom layer) stations during 2/22/2017 – 4/23/2017.

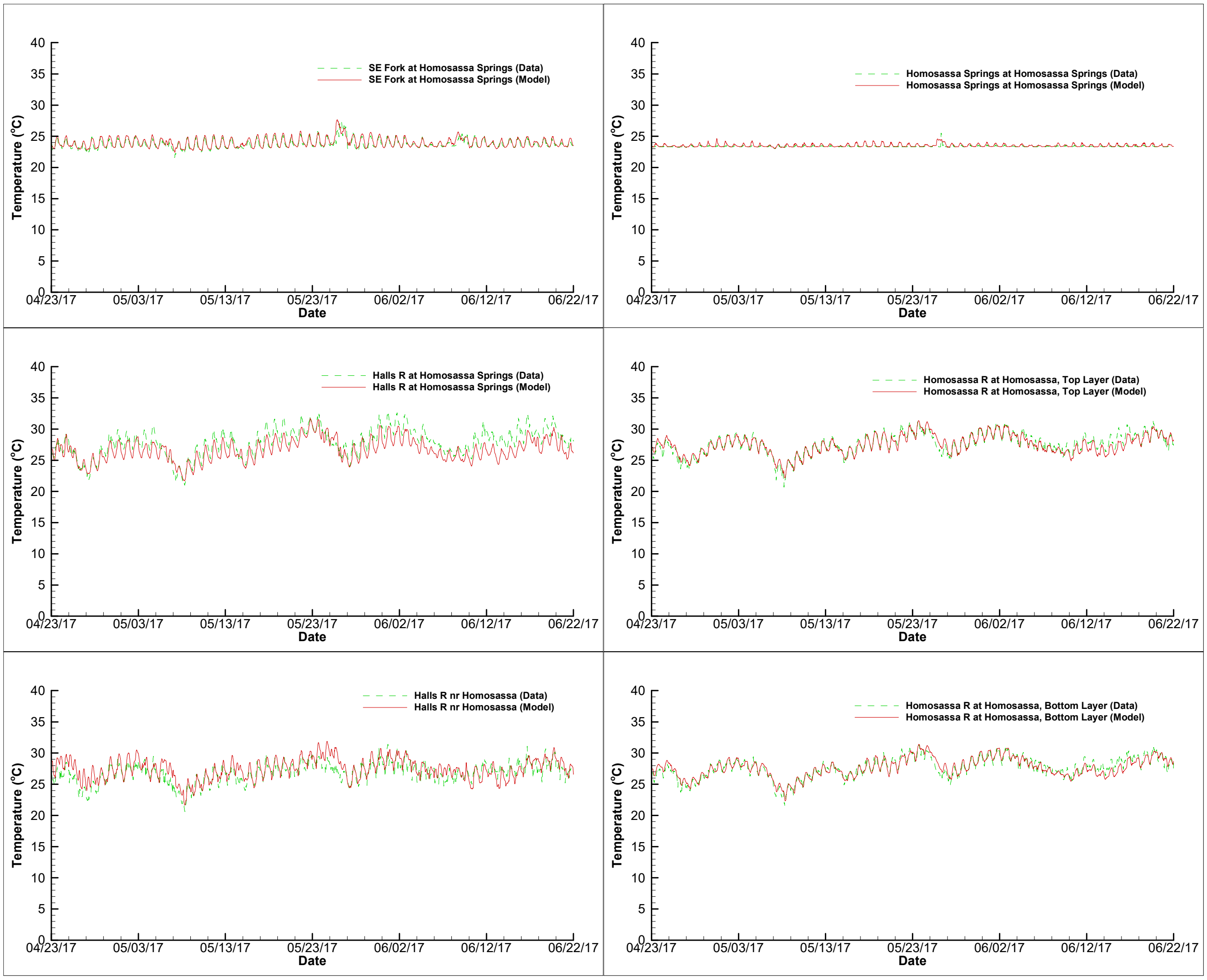

Figure F - 16. Comparisons of simulated (red lines) and measured (dashed green lines) temperatures at SE Fork at Homosassa Spring (top left), Homosassa Springs at Homosassa Springs (top right), Halls River at Homosassa Springs (middle left), Halls River near Homosassa (bottom left), and Homosassa River at Homosassa (middle right for the top layer and bottom right for the bottom layer) stations during 4/23/2017 – 6/22/2017.

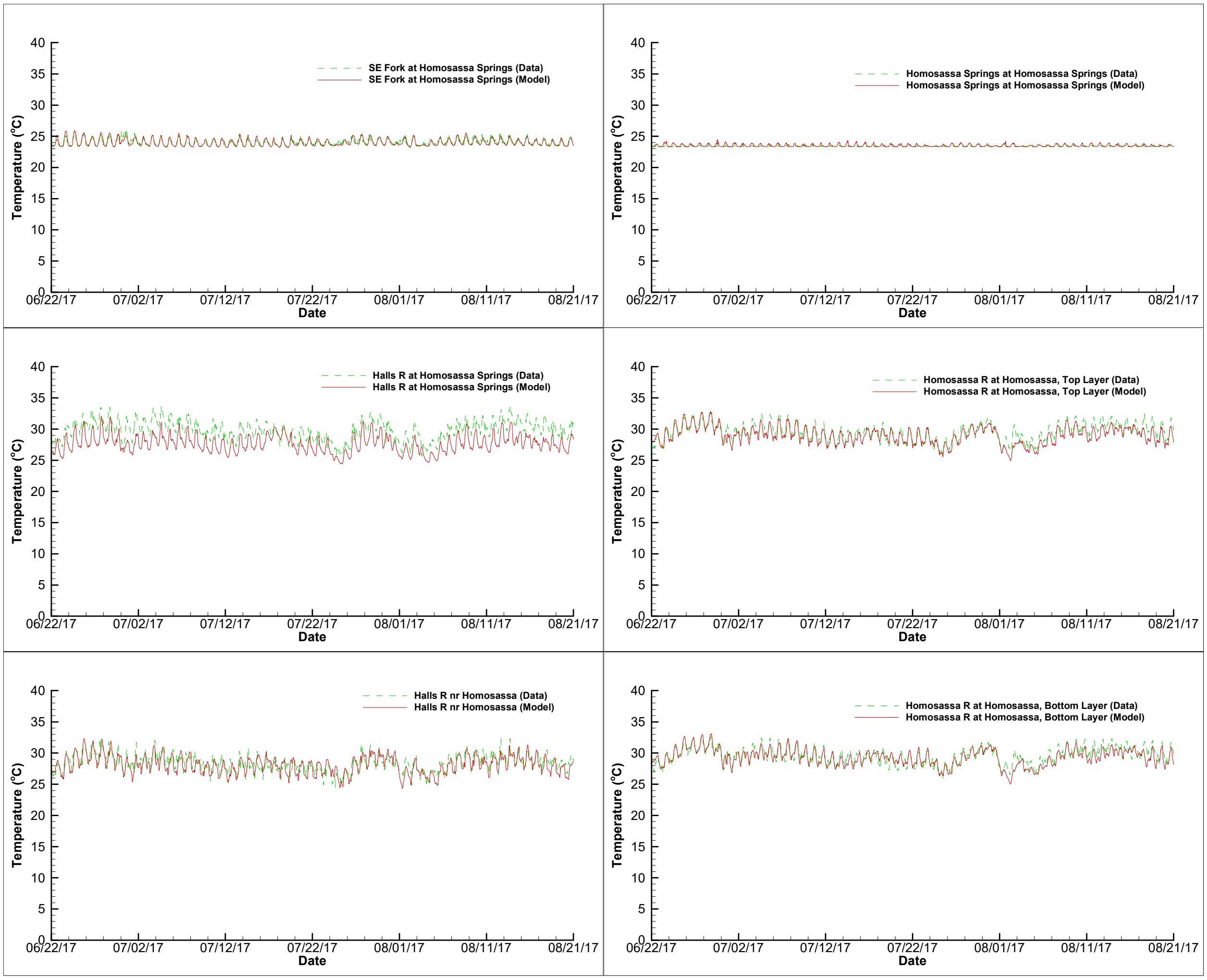

Figure F - 17. Comparisons of simulated (red lines) and measured (dashed green lines) temperatures at SE Fork at Homosassa Spring (top left), Homosassa Springs at Homosassa Springs (top right), Halls River at Homosassa Springs (middle left), Halls River near Homosassa (bottom left), and Homosassa River at Homosassa (middle right for the top layer and bottom right for the bottom layer) stations during 6/22/2017 – 8/21/2017.

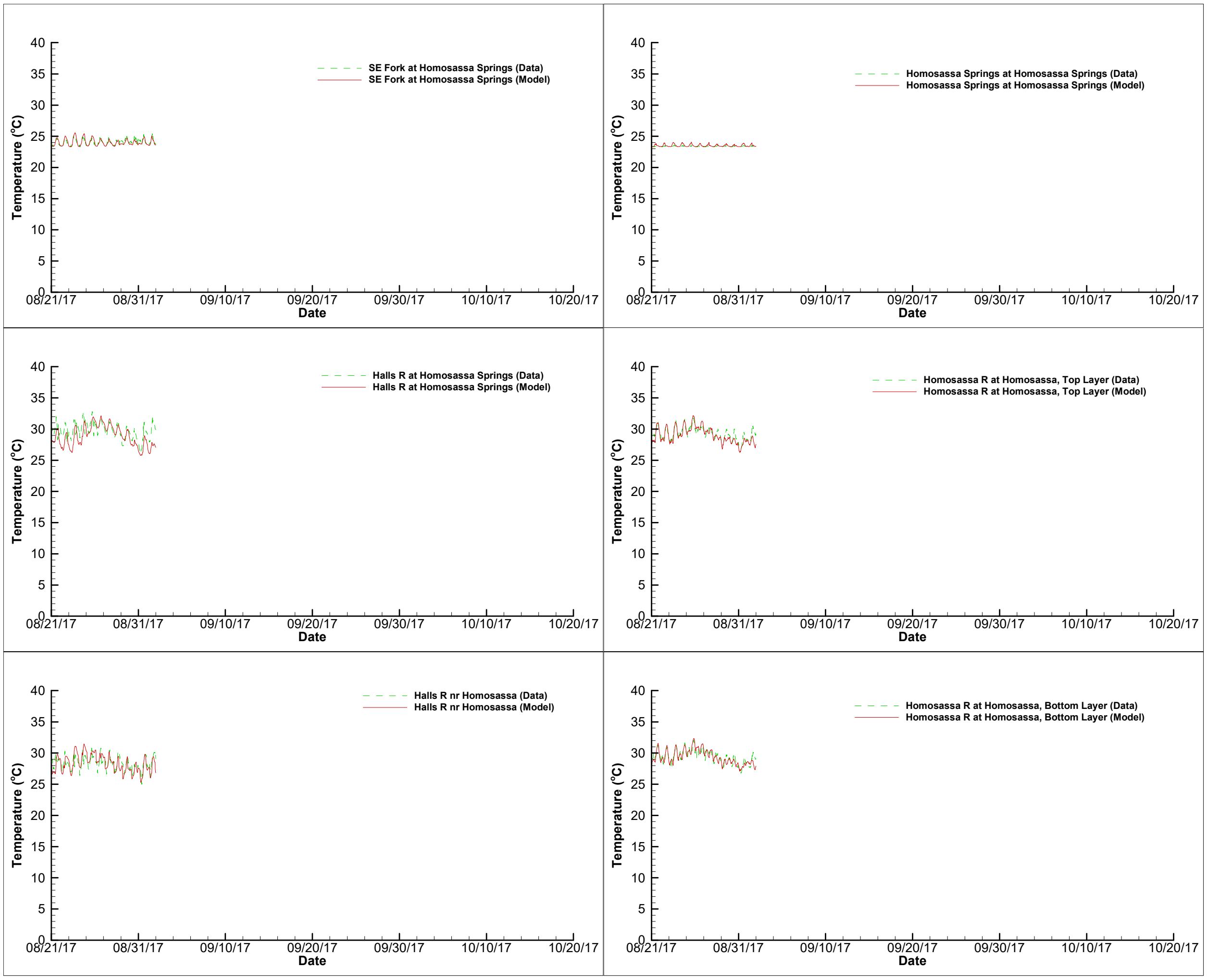

Figure F - 18. Comparisons of simulated (red lines) and measured (dashed green lines) temperatures at SE Fork at Homosassa Spring (top left), Homosassa Springs at Homosassa Springs (top right), Halls River at Homosassa Springs (middle left), Halls River near Homosassa (bottom left), and Homosassa River at Homosassa (middle right for the top layer and bottom right for the bottom layer) stations during 8/21/2017 – 10/20/2017.